JOURNAL OF CAVE AND KARST STUDIES

DEDICATED TO THE ADVANCEMENT OF SCIENCE, EDUCATION, AND EXPLORATION

Front cover: Moonmilk stalatites in Grotta Nera, Italy. See Cacchio et al., in this issue.

FSC
www.fsc.org
MIX
Paper from
responsible sources
FSC® C006300

KARST EVOLUTION OF THE GARRAF MASSIF (BARCELONA, SPAIN): DOLINE FORMATION, CHRONOLOGY AND ARCHAEO-PALAEONTOLOGICAL ARCHIVES

JOAN DAURA[1], MONTSERRAT SANZ[1], JOAN JOSEP FORNÓS[2], ANTONI ASENSIO[3], AND RAMON JULIÀ[4]

Abstract: Karst landscape evolution has been widely studied in recent years on karst plateaus, but the use of dating methods has not usually been possible owing to a lack of data. The intensely karstified Garraf Massif, however, presents large solution dolines and several shafts that contain archaeological and palaentological remains that can be used for determining the chronological framework of the karstification processes. These sites have been dated using various techniques, and the resulting data combined with evidence from previous geomorphological studies. The results allow us to define the pattern and timing of the evolution of karst morphologies in the northeast of the Iberian Peninsula. We propose a simple five-stage geomorphological model of the evolution of the Garraf dolines located on the plateau, between the Middle to Upper Miocene and the Holocene. The study also provides important information for analyzing landscape history in high plateaus of karst regions.

INTRODUCTION

Various models of the geomorphological formation and evolution of dolines have been proposed, based on the study of sedimentary fills (Sauro et al., 2009), host-rock dissolution processes (Zambo and Ford, 1997), and deposit morphology and architecture (Ford and Williams, 2007; Waltham et al., 2005). Solution dolines are the most commonly studied of the karst landforms, having been described in detail since the end of the nineteenth century (Cvijic, 1893), while collapse sinkholes are perhaps the most spectacular, with the *tiankengs* in the karst areas of China providing the best examples (Zhu and Waltham, 2005). Recently, many studies conducted in different karst regions have proposed new models for the full evolutionary sequence of doline development (Gibbard et al., 1986; Bruxelles et al., 2008, 2012; Luzón et al., 2008; Siart et al., 2010).

Chronological approaches to the dating of doline and karst evolution are limited and involve associating these depressions with the archaeological or palaeontological record (Ufrecht, 2008). Sediment-filled depressions, mainly dolines, have been used as promising records for geoarchaeological research (Van Andel, 1998; Bruxelles et al., 2006), especially as part of a multidisciplinary approach (Siart et al., 2010), and have led to a better understanding of the chronological framework. Such studies provide absolute ages of the sediments and the materials preserved in the dolines, which makes it possible to date the doline formation. This has been the case, for example, of the Doline d'Orgnac 3 (Moncel, 2003; Moncel et al., 2005), the doline of Cantalouette (Bourguignon, 2004), the dolines in the Causses region (Quilès et al., 2002), and the doline in Visogliano (Falguères et al., 2008), among others.

More common is the use of these sediment-filled depressions for archaeological and palaeoenvironmental reconstruction (Gibbard et al., 1986, Bruxelles et al., 2008; Siart et al., 2010; Bruxelles et al., 2012). Most of these reconstructions have been conducted in ancient Mediterranean landscapes (Marriner and Morhange, 2007; Fouache et al., 2008), where the abundance of karst regions without running surface water and any associated sediment accumulations has hindered reconstruction owing to the absence of corresponding non-karst archives. These studies emphasize the importance of karst depressions as highly valuable, unique sources of information. These depressions act as traps for eroded soils that may accumulate and be preserved from further erosion, thereby facilitating the analysis of landscape evolution, chronology, and associated palaeoenvironmental phases (Hempel, 1991).

More than three hundred shafts are documented in the central Garraf Massif, and studies of this karst region have a long geological and speleological tradition dating back to the end of the nineteenth century (Font, 1897). Work carried out during the 1940s and 1950s offered an initial model of the Garraf karst's origin and development, providing an initial chronological approach to understanding doline formation (Llopis, 1943, 1947; Montoriol, 1950,

[1] G.R.Q. Grup de Recerca del Quaternari. SERP. Dept. Prehistòria, H. Antiga i Arqueologia. Facultat de Geografia i Història. Universitat de Barcelona. C/ Montalegre, 6. 08001, Barcelona, Spain. grq@ub.edu
[2] Departament de Ciències de la Terra, Universitat de les Illes Balears. Ctra. Valldemossa km 7, 5. 07122 Illes Balears, Spain
[3] S.E.O. del C.E.V. Secció Espeleològica de l'Ordal del Centre Excursionista de Vallirana. C/Major, 402. 08759. Vallirana, Barcelona, Spain
[4] Institut Ciències de la Terra "Jaume Almera". CSIC. C/Lluís Solé Sabarís s/n. 08028, Barcelona, Spain
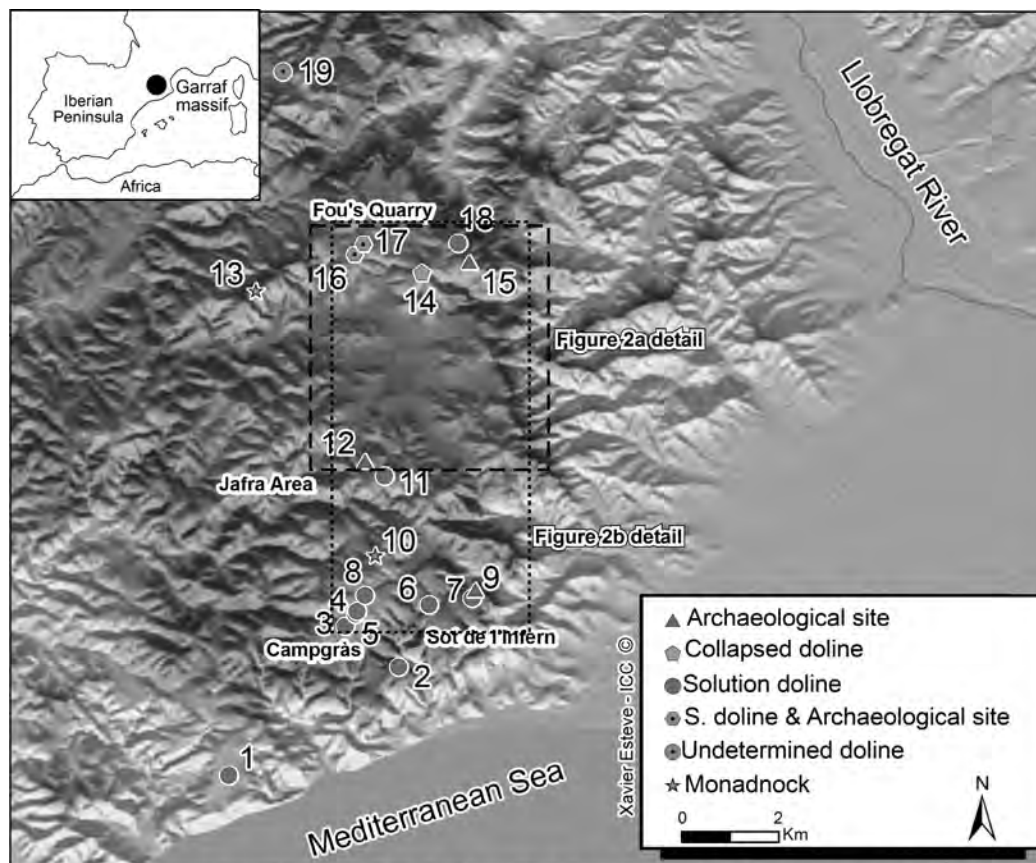
Figure 1. Location of the study area and of the principal dolines and their associated deposits (Source: X. Esteve and ICC, Institut Cartogràfic de Catalunya).

1954; Montoriol and Muntan, 1959, 1961), while more recent studies have focused their attention on other karst features (Freixes, 1989; Custodio et al., 1993). However, the somewhat simplistic and schematic studies undertaken during the 1950s do not provide any direct dating of the region's doline formation. More recently, the Grup de Recerca del Quaternari of the University of Barcelona (GRQ-UB) has initiated sedimentological and archaeological work aimed at obtaining more precise dates for the Pleistocene sedimentary fills in the Garraf karst (Daura, 2008).

The findings from these earlier studies, combined with more recent geomorphological and chronological data, allow us to initiate development of a chronological model that can be extrapolated to other karst massifs in the Iberian Peninsula and the Western Mediterranean and to establish the chronology of doline sedimentation stages. Furthermore, we present the karst cavities of the Garraf Massif as a specific case study that can be used to explain the apparent hiatus in Pliocene and Pleistocene sedimentary fill on karst plateaus.

GEOLOGICAL SETTING AND STUDY AREA

GARRAF MASSIF

Occupying an area of around 500 km^2 (Salas, 1987), the Garraf Massif is a horst located in the northeast of the Iberian Peninsula, 30 km southwest of the city of Barcelona. The massif, composed mainly of Jurassic and Cretaceous limestone and dolostone (Figs. 1 and 2), is a low-relief mountain range that rises to a height of less than 600 m as a result of gentle tilting. On the eastern side of the massif, Palaeozoic (Benet, 1990) and Triassic materials can be found (Marzo, 1979).

Cretaceous carbonate rocks (Andreu et al., 1987; Salas, 1987; Albich et al., 2006; Moreno, 2007) dominate the central part of the massif, where most of the karst landforms have developed (Borràs, 1974; Lloret, 1979; Rubinat, 1981; Asensio, 1993; Rubinat, 2004). The Cretaceous formations consist of limestone with dolomitic intercalations from the Valanginian and Barremian stages. Outcrops of Cretaceous marls and marly limestone (Salas, 1987) of Aptian age (Moreno, 2007) are also found in a few areas.
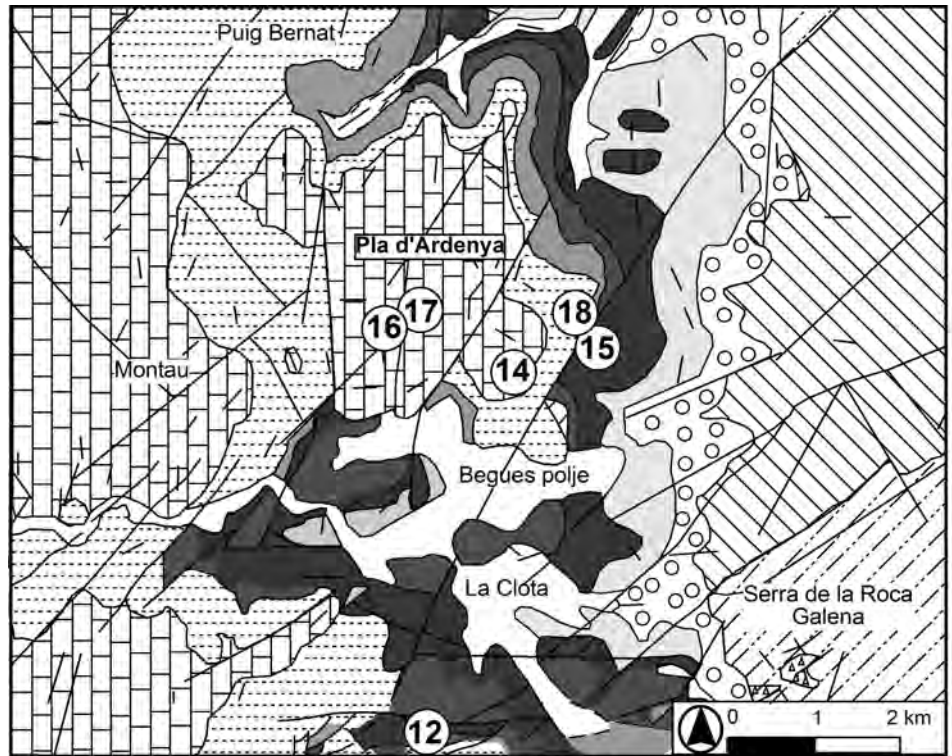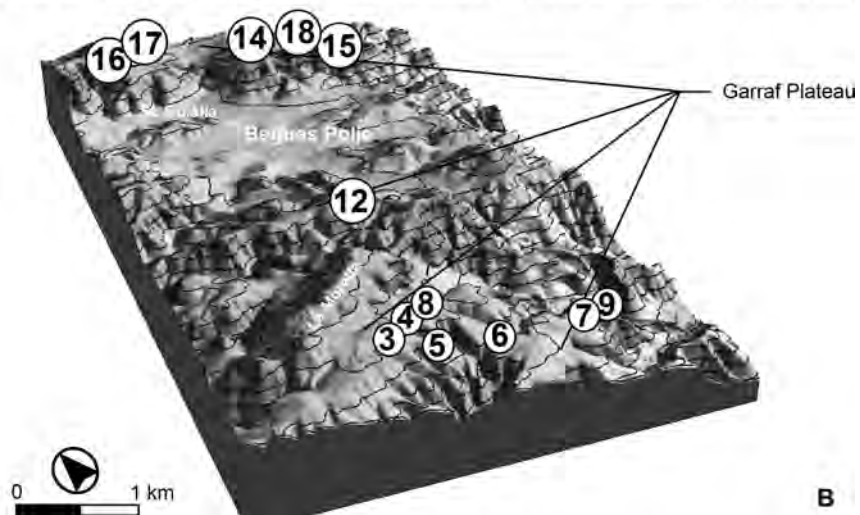
Figure 2. A: Geologic map of the central part of the Garraf Massif with the location of its main dolines and their associated deposits. B: Digital elevation model of the Garraf plateau showing the location of main dolines and shafts.

Garraf karstification is concentrated in the massif's fractured carbonate rocks, and its main karst features include dolines, shafts, and caves containing Pleistocene sedimematry fill (Daura et al., 2005, 2010a,b). Structurally, the limestone massif is an antiform (Bartrina et al., 1992), resulting from a northeast to southwest compression of the alpine orogeny, and a series of fractures trending predominantly northeast to southwest run across the entire complex (Guimerà, 1988). Fractures control almost all the development of shafts in the massif, including those beneath the doline perimeters.

Garraf Dolines and Plateau

Generally, the Garraf dolines are found in Cretaceous rocks. The Jurassic strata in the high plains present less significant karst development and fewer dolines. The Triassic carbonates comprise strata that only crop out in the northeast of the Garraf Massif rim. On the Garraf plateau, several areas (Llopis, 1941) of doline density can be discerned (Fig. 1). The most significant accumulation lies between Campgràs, Puig de l'Olla, and Sot de l'Infern, with a total of thirteen dolines, followed by Coll de l'Ordal-Lledoner, with twelve depressions, and Pla d'Ardenya with four preserved dolines (Fig. 2).

According to the models proposed by Waltham et al. (2005, p. 26 and subseq.) and Ford and Williams (2007, p. 339 and subseq.), these dolines can be classified into two main types. The first includes dolines with higher concavity indices, with no or very scarce sedimentary deposits, and with well-developed shafts in the center. These dolines, for example, the Dolina del Sotarro or the dolines in southeast Campgràs, have previously been described by Montoriol (1950, 1954) and Montoriol and Muntan (1958, 1959) and will not be dealt with here.

The second type includes dolines with low concavity indices and depressions that are associated with undeveloped shafts. These dolines usually present large sedimentary terra-rossa type deposits produced by chemical weathering within their perimeters. Most dolines in the Garraf Massif are of this type, and examples include the dolines in les Alzines, Esquerda de les Alzines, Campgràs, Pla de Querol, Bassot de l'Arbre, Puig de l'Olla, and Serra del Mas among others (Fig. 1).

The dolines of low concavity and their associated shafts in the Garraf plateau present the best morphologies for studying karst-landscape evolution thanks to their sedimentary fill. This plateau (Fig. 2-B) is an erosional surface that, following an episode of uplift during the late Miocene, now lies between 450 and 550 m amsl, as determined by Llopis (1947), and corresponds to a period during the Miocene when the sea level (base level here) was probably stable for a long period. Correlation between the erosional surface of the limestone massif and sea levels have been based on marine deposits (Llopis, 1947) located on the northwest side of the massif. These deposits correspond to the Middle to Upper Miocene (Machpherson, 1994; de Porta and Civis, 1996). During that time most of the littoral range would have been submerged (Gallart, 1980), and while the emerging part of the Garraf Massif was developing an erosional surface, the sunken part of the depression preserved its pre-flooding relief intact, due to its own fossilization. Some of the highest peaks in the massif today are evidence of the aforementioned process of erosion and levelling. Examples such as Morella and Montau (Fig. 1) have been considered monadnocks, i.e., rocky masses that survived the erosion and stand isolated above the general level of the plateau. After Llopis (1947), subsequent authors have considered this karst plain to be a peneplain (Montoriol, 1954; Montoriol and Muntan, 1961).

Today the karst plain is no longer continuous, as faulting has separated it into different blocks. The main faults in the Garraf block are arranged in two orthogonal systems, one aligned with the Garraf Massif (NE-SW) and the other perpendicular to the range (NW-SE) (Fig. 2). Some minor faults also follow this pattern. This group of faults is responsible for the sinking of some blocks and the elevation of others. The most significant case is the Begues plain, where a polje subsequently evolved and divides the two main areas with a high concentration of dolines.

Shafts containing sedimentary fill and located under the Garraf plateau are especially relevant here because they preserve records that can be used to understand the evolution and chronology of the karst plain. These shafts have developed along vertical tectonic fractures, predominantly at the base of the epikarst zone. These shafts, cone- or bell-shaped and blind, reach upwards to near the surface, but many of them have no natural opening to the surface, and those that do, often owe their development to surface activity (tree-root action, speleological works, subsoil corrosion, etc.). None of them has a known accessible connection to an active horizontal cave system.

This morphology, which is common in the Garraf Massif, suggests an upward shaft development formed by ascending erosion (Maucci, 1960; Jennings, 1985; Klimchouk, 2000; Baroň, 2002; Jones et al., 2004); however, neither hypogenetic processes nor up-welling deep waters have been recorded in the Garraf plateau.

Site Description

This study focuses on four sites in the Garraf plateau containing archaeological and palaeontological remains (Fig. 2). The first two sites, site 1, Esquerda de les Alzines and site 2, Alzines, were discovered in 2004 by two of the authors (JD and MS). They are solution dolines (*dolina*) excavated between 2004 and 2009 by the Grup de Recerca del Quaternari, and both contain shafts (*avenc*) below the depression. Besides these dolines, two additional karst formations on the Garraf karst plain, site 3, Avenc Marcel and site 4, the Cave (*Cova*) Bonica, were discovered during speleological work in the twentieth century and are of the

utmost importance when establishing a chronological framework for the first Quaternary sediment deposition at this level of the general erosion surface.

SITE 1: ESQUERDA DE LES ALZINES

Site 1 is the Dolina de Esquerda de les Alzines (DEA) and its subterranean network of shafts (Fig. 3). It is a solution doline located at the convergence of two faults (d1 and d2) extending over approximately 2 km. The doline is located at between 530 and 523.6 m amsl and is elliptical in shape. The depression is 40-m long by 30-m wide, with a maximum depth of 11 m. Its central section has been significantly modified as a consequence of speleological work (GIRES, 1995) carried out during the 1990s.

The site, delimited by the doline perimeter, includes four shafts (Avenc de l'Esquerda de les Alzines, Avenc Gran de l'Esquerda de les Alzines, Avenc dels Arqueòlegs and Avenc Petit de l'Esquerda de les Alzines) that together form a subterranean network that has developed along faults d1 and d2.

Archaeological work undertaken in Layer C and in the mixed sediments of the DEA by the GRQ-UB recovered 1,067 artifacts (Fig. 4). They are characterized by a predominance of flakes from the reduction of cores and artifacts of various morphologies. However, the chronological framework and technological traits identified do not allow the site to be placed within a particular one of the Upper or Middle Palaeolithic tool groups, although the recovery of some artifacts commonly found in Upper Palaeolithic assemblages suggests a connection to this period (Daura et al., 2011).

SITE 2: ALZINES

Site 2, or Alzines, corresponds to a solution doline and its subterranean network of shafts. The doline, known as Dolina II de les Alzines (DA) (Fig. 3), is located 290 m to the northeast of Site 1. Located on the same plateau, between 528.2 and 523.6 m amsl, it is more elliptical in shape than DEA and has also developed on fault d1. Its present day surface has been modified by speleological work carried out in the 1960s by the Grup Exploracions Subterrànies (Montoriol, 1964) and by subsequent work by the Grup d'Investigacions, Recerques i Espeleologia Sesrovires and the Secció Espeleològica Ordal del Centre Excursionista de Vallirana.

Site 2, delimited by the perimeter of DA, contains a significant subterranean network, comprising two main shafts. The first of these, Avenc de les Desil·lusions, also named Avenc Nou de les Alzines (Valdepeñas, 2012), was discovered during GRQ-UB excavations (Daura and Sanz, 2010) and does not contain any Pleistocene remains. The second, Avenc de les Alzines, contains archaeological and palaeontological remains that appear to have entered the shaft from Parets dels Ossos (Table 1).

Large mammal bones have been recovered at the base of the DA in a mass of cemented red breccia. As the site's faunal remains are still being restored, palaeontological analyses are not yet available. Therefore Table 1 only provides a preliminary assignment of bear remains as *Ursus* sp. Collapsed sediments throughout Parets dels Ossos provide rhinoceros remains (*Stephanorhinus etruscus*) corresponding to posterior extremities, isolated hyena teeth and carpals, and a few stone tools (Daura 2008).

SITE 3: AVENC MARCEL

Located in the Triassic (Upper Muschelkalk) dolostone and limestone, Avenc Marcel (Fig. 5) is a complex system of 80 m deep, spindle-shaped shafts, developed as a result of rock fracturing and cliff regression. It was discovered in 1982 during the erection of a transmission tower and explored fully for the first time in 1989 by one of the authors (AA). Palaeontological remains were recovered at the original collapsed entrance during the first exploration (Asensio, 1993) (Table 1). In 2002, a palaeontological excavation by B. Martínez-Navarro, J. Agustí, and M. Llenas from the Institut Català de Paleontologia Miquel Crusafont was carried out in the shaft, but no archaeological or palaeontological remains were found (Martínez-Navarro et al., 2002).

SITE 4: COVA BONICA

Cova Bonica is a small cave chamber containing a vertical shaft near a significant fracture, which is also in contact with the Triassic dolostone and limestone. Sediments have been displaced through the vertical shaft and fissures from an area of the plateau with a high density of dolines. The cave was first explored during the nineteenth century (Font, 1899) and at various times in the twentieth (Montoriol, 1954; Borràs, 1974) by speleologists and geological groups. Studies have been conducted on the palaeontological remains (Table 1), focusing on small mammals (Agustí, 1988; Blain and Bailón, 2006; Blain, 2009) and primates (Delson, 1971, 1973, 1974; Delson and Nicolaescu-Plopsor, 1975; Crusafont-Pairó and Golpe-Posse, 1984).

METHODS

To determine the chronology of doline formation and evolution, a series of field surveys were conducted at sites 1, the dolina de Esquerda de les Alzines, and 2, the Dolina II de les Alzines. Several test pits were dug with a power shovel, reaching a maximum depth of 6 m below the current floor level to where the Mesozoic host rock cropped out. Sections from each test pit were stratigraphically described, and sediment samples were taken to study the fill.

The samples and cores were bagged, numbered, and taken to the Earth Sciences Department at the University of Illes Balears, where they were opened, sectioned lengthwise, photographed, and sampled at different intervals in stratigraphical order, according to the different layers observed. The presence of sedimentary structures, such as laminations, and other general observations were noted.
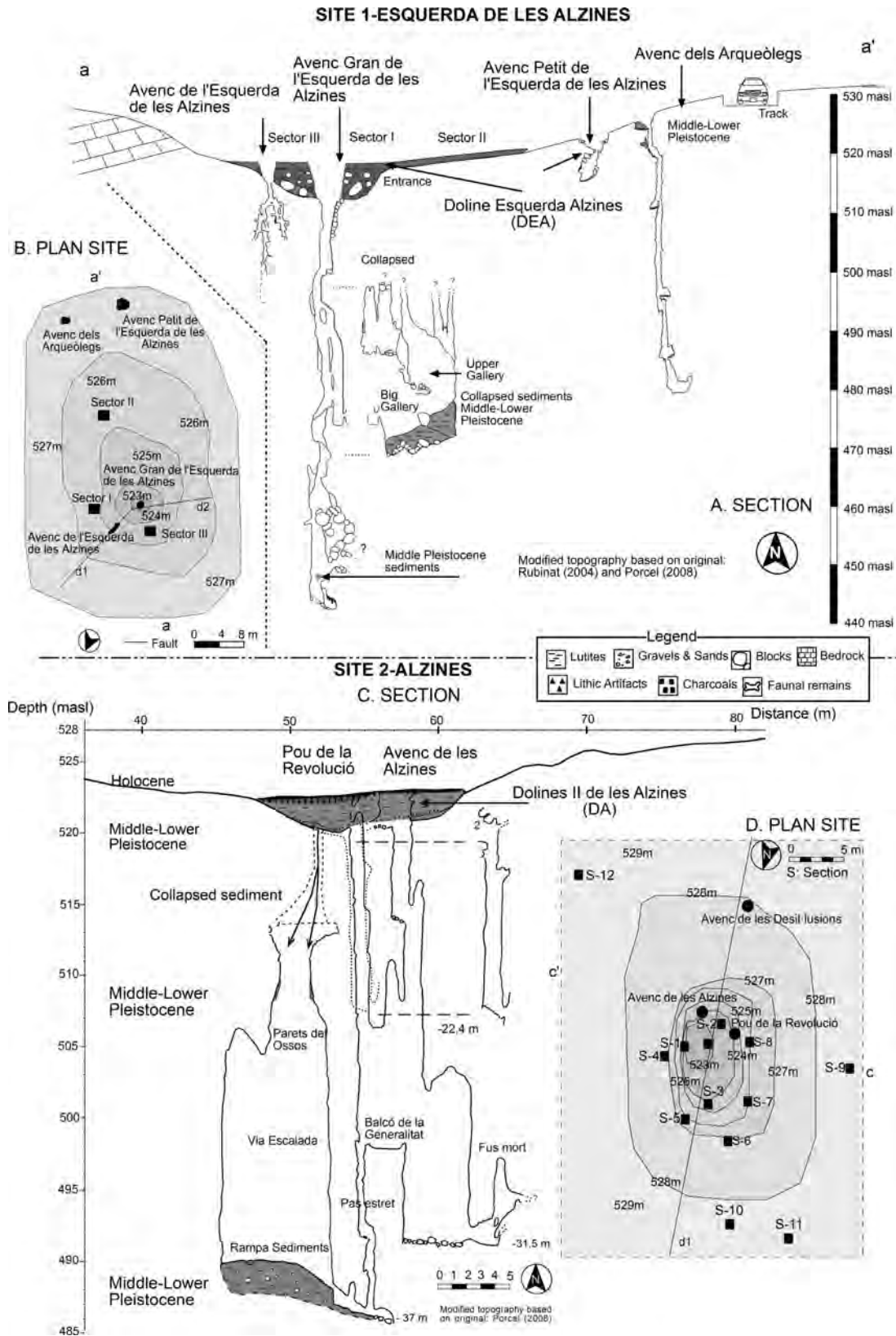
Figure 3. Cross-section (A) and plan (B) of site 1, Esquerda de les Alzines, and Cross-section (C) and plan (D) of site 2, Dolina II de las Alzines.
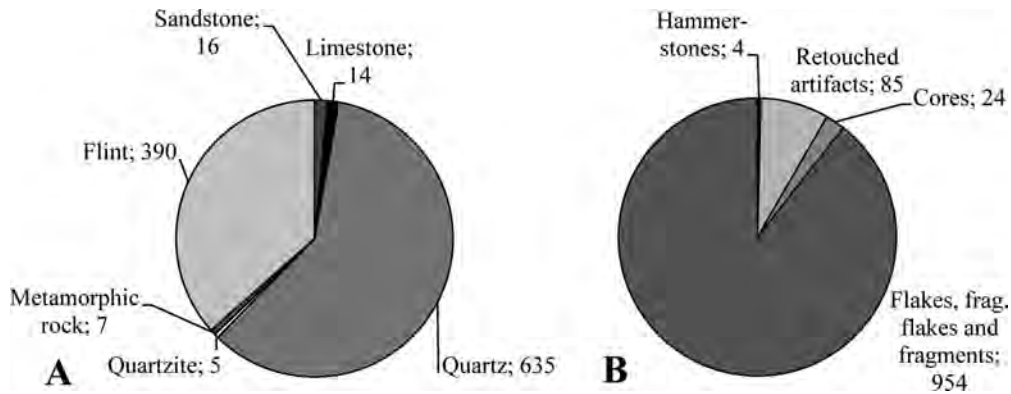
Figure 4. Site 1, Esquerda de les Alzines, raw materials (A) and structural categories (B) of stone artifacts based on Daura et al. (2011).

Archaeo-palaeontological remains were subsequently discovered at sites 1 and 2. At DEA, the excavation focused on a twenty-square-meter area using standard archaeological methods, including three-dimensional plotting of finds and their features. Archaeological remains were mapped in situ prior to removal, and sediments were dry-sieved using superimposed 5 and 0.5 mm mesh screens.

Table 1. Faunal remains recovered from the bases of dolines and inside of shafts, as well as from other caves that have an opening to the Garraf plateau.

Plateau Sites			
Site 2, Alzines	Site 3, Cova Bonica	Site 4, Avenc Marcel	Coll Sostrell
Perissodactyla	Primates	Carnivora	Unidentified[a]
Stephanorhinus etruscus[a]	*Macaca* cf. *sylvanus*[b]	Felidae indet.[e]	
Artiodactyla	*Dolichopithecus arvernensis*[b]	*Megantereon* sp.[e]	
Cervidae sp. I[a]	Lagomorpha	*Lynx* sp.[a]	
Caprinae indet[a]	*Prolagus michauxi*[d]	*Panthera* sp.[a]	
Carnivora	Insectivora	*Homotherium* sp.[e]	
Ursus sp.	*Beremendia fissidens*[d]	*Canis* sp.[e]	
Lynx sp.	Rodentia	*Vulpes* sp.[e]	
	Eliomys intermedius[d]	*Martes* sp.[e]	
	Castillomys crusafonti[d]	Perissodactyla	
	Apodemus mystacinus[d]	*Equus* sp.[e]	
	Apodemus jeanteti[d]	*Stephanorhinus etruscus*[e]	
	Allophaiomys sp.?[d]	Artiodactyla	
	Trilophomys vandeweerdi[d]	Cervidae sp. I[e]	
	Stephanomys donnezani[d]	Cervidae sp. II[e]	
	Mimomys medasensis[d]	Ovibovini indet aff. *Soergelia* sp.[e]	
	Sciurus sp.[d]	Caprinae indet[a]	
	Pliopetaurista pliocaenica[d]	Proboscidea	
	Blackia sp.[d]	*Elephas* sp. ?[e]	
	Pteromys sp.[d]	Testudines	
		Testudo sp.[a]	
		Rodentia	
		Mimomys medasensis[e]	
		Mimomys aff. *tornensis*[e]	
		Apodemus aff. *mystacinus*[e]	

[a] Daura (2008).
[b] Delson (1971; 1973; 1974), Crusafont and Golpe-Posse (1974) and Delson and Plopsor (1975).
[c] Agustí (1988).
[d] Described here for the first time, following the identification currently listed in the collections of the Museu de Geologia de Barcelona (MGB).
[e] Asensio (1993).
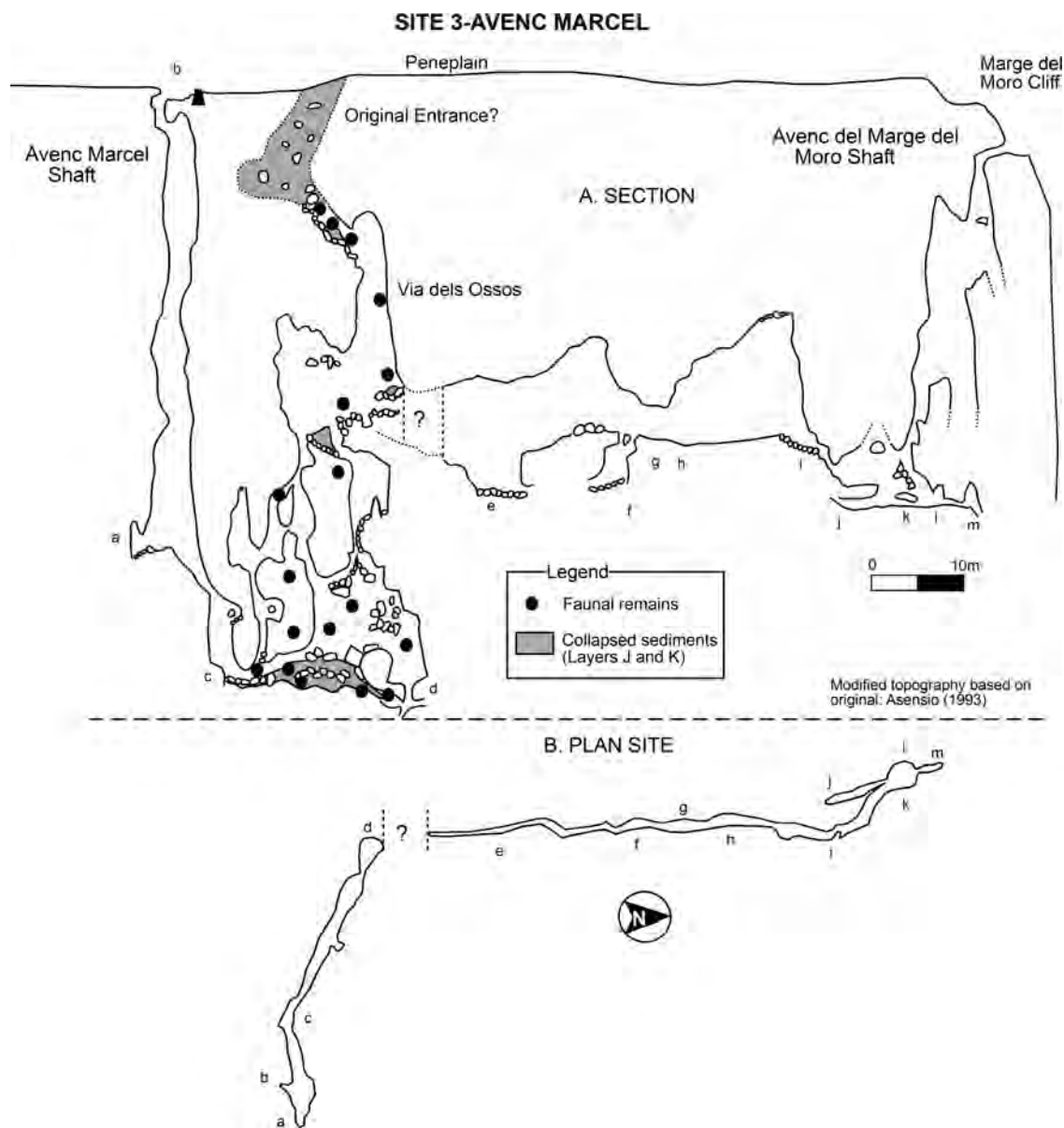
Figure 5. Cross-section (A) and plan (B) of site 3, Avenc Marcel.

At DA, levels presenting palaeontological remains comprise very compact, hard calcareous breccias that are cemented at the doline base. According to the methodological proposals made by Ramos et al. (2008) for sites of this type, excavation should involve the removal of sediment in different blocks. Using hammers and chisels, each recovered block was taken to the archaeological laboratory of the Grup de Recerca del Quaternari at the Seminari d'Estudis i Recerques Prehistòriques (la Guixera) operated by the Castelldefels Town Council, treated, and excavated with a pneumatic microhammer.

At a later date, a speleological expedition was undertaken by the GRQ and the Secció Espeleòlogica de l'Ordal del Centre Excursionista de Vallirana to detect any new cavities (Avenc de les Desil·lusions at site 2 and Avenc

dels Arqueòlegs at site 1; Fig. 3) and to explore caves (Cova Bonica and Avenc Marcel; Fig. 2) and shafts under the Garraf plateau. A topographical and geological study was also carried out to determine the evolution of the doline and karst plain and the relationship between the endokarst and exokarst morphologies.

Sediment dates were analyzed by optically stimulated luminescence and thermoluminescence at the Radiochemistry and Dating Laboratory of the Universidad Autónoma de Madrid using the additive dose method and standard procedures (Fleming, 1970; Zimmerman, 1971; Aitken, 1985; Nambi and Aitken, 1986; Arribas et al., 1990) and by ^{14}C at the Beta Analytic Laboratory, USA. To determine the age of materials beyond the radiocarbon and the OSL dating limits, the palaeonto-

logical records from Avenc Marcel, DEA, Coll Sostrell, and Cova Bonica were also included in the study. The latter are based on previous studies (Delson, 1971, 1973, 1974; Delson and Nicolaescu-Plopsor, 1975; Crusafont-Pairó and Golpe-Posse, 1984; Agustí, 1988; Asensio, 1993; Daura, 2008).

Results

Stratigraphic Setting

Sedimentary fill from site 1, the Dolina de l'Esquerda de les Alzines, is the most significant for stratigraphic reconstruction. Current fieldwork focused on the excavation of five test pits (Fig. 3), two in sectors I, II and III, and one in the Avenc dels Arqueòlegs area (Fig. 6). The results form a single, unified sequence 4.5 m in length, but the correlations between the pits are merely tentative, given the discontinuities between them.

The lowest unit corresponds to highly cemented breccia and conglomerates (layers E, G1 and I), with a reddish, silty matrix formed by decalcification. The coarsest fraction is highly weathered and rounded by dissolution and typically contains sparitic calcite fragments, consisting of large dogtooth spar crystals of unusually high purity and crystallinity. Layer H, above, is composed of non-cemented, compact lutites, separated from the upper part of the sequence by sub-angular boulders.

At the top of the sequence, layers C, C2, D2, B1, D1, B, and D, infillings are typically characterized by deposits up to 2-m thick (Table 2), corresponding to lutites that are occasionally burned, with almost non-existent host rock components, indicative of the high degree of solution activity in the doline formation process. In fact, silt-size grains of quartz are predominant in the samples analysed (84.2 to 90.6%) followed by feldspars (4.9 to 10.6%), while host rock fragments are very scarce (0 to 5.2%). Illite is present in minor amounts (0 to 4.5%).

The uppermost layer, layer 1, contains 10- to 20-cm thick superficial, rounded and sub-angular limestone gravel without lutites and may represent the current soil layer. The stratigraphy is summarized in Table 2 and illustrated in Figure 6.

Site 2 was studied via thirteen test pits (Fig. 3). The idealized schematic profile presented in Figure 6 shows similarities to DEA. Moreover, three broad episodes of sedimentation can be identified. The underlying layer E is composed of cemented breccia and conglomerates with sparitic calcite fragments adhered to the bedrock, representing the earliest deposition found in test pit S-11, which collapsed along Pou de la Revolució into the subterranean network. This unit contains bones of large mammals from the Lower Pleistocene that apparently fell from the Paret dels Ossos. The second package, layer D, is composed mainly of cemented red clay with iron oxides and without a coarse fraction. On top, subsequent layers C and B are dominated by a lutitic matrix without gravels and contain a few small pieces of rubified sediment and sparse Holocene faunal remains. The uppermost 10 cm comprise the current soil layer and contain sub-angular limestone gravels.

Other sites, because they do not present a complete stratigraphic sequence, are less significant to our understanding of the sedimentary fill on the Garraf plateau. However, these units constitute the oldest stratigraphic levels exposed. Sedimentary fills that contain fossil remains have been identified in the subaerial exposure of cemented breccia in Coll Sostrell (layer K); in very highly cemented breccia adhered to external cave walls (layer K) and infiltrated from the Garraf karst plain (layer J) at site 4, Cova Bonica; and in cemented red breccia (layer K) and compacted lutites with iron oxides (layer J) at Site 3, the Avenc Marcel.

Sediment collapses into the underlying cavities are common in the Garraf system. Stratigraphic correlations between the external and internal sediments are tentative, given the major discontinuities, including the Big Gallery in site 1 and the Parets del Ossos in site 2 (Fig. 3).

Dating

Our dating of the doline and shaft fill under the Garraf plateau indicates a chronology ranging between the Pliocene and Holocene. Seven radiometric dates were obtained from test pits, two ^{14}C dates on charcoal and bone and five optically stimulated luminescence dates on sediment. These, along with one thermoluminescesence date, are presented in Table 3 and discussed below. The dating of the doline deposits is hindered by taphonomic and geological processes, the absence or scarcity of organic material, and wildfire disturbance of sediments.

To determine the age of the first sediment accumulation in the plateau, the chronological range of the mammalian species present in Cova Bonica (site 4) and Avenc Marcel (site 3) is clearly diagnostic of Pliocene and Lower Pleistocene contexts (Fig. 7). Avenc Marcel (Fig. 5) developed on this ancient surface, and its sedimentary fill originated from the ancient plateau base, which contains Lower Pleistocene faunal remains. The different species of the genus *Mimomys* found here suggest a chronology between MN17 and MQ1 for this site (Asensio, 1993). Similarly, the Cova Bonica fill originating from the karst plateau includes a richness of small vertebrate species and Cercopithecidae remains. The remains recovered present a two-stage chronology, MN15 and MN17/MQ1 (Delson, 1971, 1973, 1974; Delson and Nicolaescu-Plopsor, 1975; Crusafont-Pairó and Golpe-Posse, 1984; Agustí, 1988; Blain, 2009). Coll Sostrell is a karst fissure associated with the plateau. Its conglomerate and breccia deposits contain faunal remains from the Lower Pleistocene (Daura, 2008). Finally, rhinoceros remains assigned preliminarily to *Stephanorhinus etruscus* from Pou de la Revolució at site 2 date the site from MN16 to the beginning of the Middle Pleistocene (Guérin, 1980; van der Made, 2010; van der Made and Grube, 2010).

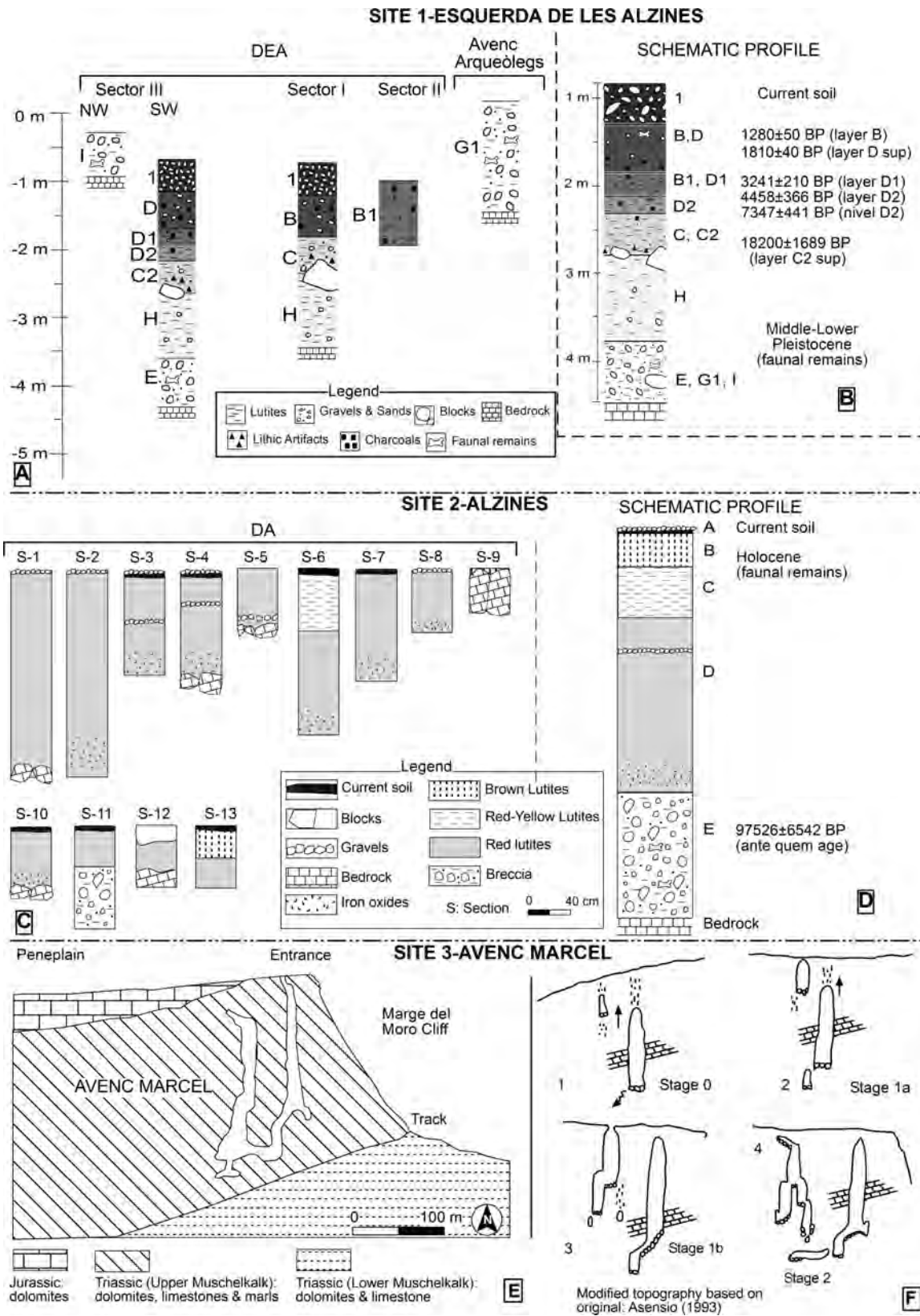Figure 6. Site 1, Esquerda de les Alzines: A, stratigraphy of individual locations; B, assembled schematic profile with suggested chronology. Site 2, Alzines: C, stratigraphic test pits dug; D, assembled schematic profile with suggested chronology. Site 3, Avenc Marcel: E, shaft geological cross-section of the plateau; F, proposed evolutionary model for the formation of the site during Pliocene and Lower Pleistocene stages.

Table 2. Main layers identified in the dolines and shafts on the Garraf plateau.

Stage	Plateau Sites[a]					Description
	Site 1, DEA[b]	Site 2, DA[c]	Coll Sostrell	Site 3, Bonica	Site 4, Avenc Marcel	
4 Current Soil	1	A	•••			Ongoing erosion process.
						Rounded and sub-angular Mesozoic limestone gravel without lutites. Current doline soil is not added. Lower contact is clean and clear. Thickness: ~5–10 cm.
3	B	B				Compact lutites and few gravels. Thickness: About 50 cm. Holocene faunal remains.
	B1					Compact lutites and few gravels. Thickness: About 50 cm.
						Lutites with few pebbles and combustion signals. Bronze Age pottery.
	D	D-top				Not very compacted lutites with few gravels. Thickness: 50 cm.
	D1					Reddish, yellow-reddish and yellow burnt lutites with large charcoal accumulation. Gravel is altered and the colour varies from whitish to light grey or blue due to combustion. Thickness: 1 m.
	D2					Mildly burnt lutites and subrounded pebbles. Thickness: 50 cm.
2	C2					Non-cemented lutites without gravels. Located in DEA -Sector III, is equivalent to layer C but it is not possible to demonstrate complete stratigraphic continuity across Avenc Gran. Steep SW-NE slope with large blocks at the base. Middle Palaeolithic artifacts. Soil affected by wildfire.
	C					Non-cemented lutites without gravels. Located in DEA-Sector I and rather thin (ca. 10 cm), it contains Middle Palaeolithic stone tools. Soil affected by wildfire.
1b	H					Compacted lutites and subrounded gravels. Upper contact with layer C and lower contact with layer F. Slopes steeply towards the entrance of Avenc Gran de les Alzines. Thickness: 1 m.
1a	E	E	E	J	J	Reddish compacted lutites with iron oxides infiltred through karstic fissures. Faunal remains in Cova Bonica and Avenc Marcel have been documented.
			K	K	K	Reddish cemented breccia. Coarse fraction is predominant (30%) with sub-angular morphologies and dog-tooth spar. Pliocene and Plistocene faunal remains in DEA, Coll Sostrell, Cova Bonica and Avenc Marcel.
	G1					Cemented breccia recorded in Avenc dels Arqueòlegs. Thickness: 7 m. Present at the entrance and partly collapsed inside the cavity. Faunal remains are removed inside shaft.
1a	I	I	I			Highly cemented breccia with few pebbles. DEA-Sector III has lateral contact with sediments of layers D and D2. Faunal remains are recovered in DEA and DA. Thickness: ca. 30 cm

[a] Letter symbols refer to infilling layers.
[b] Dolina de l'Esquerda de les Alzines.
[c] Dolina II de les Alzines.

Table 3. ^{14}C and optically-stimulated-luminescence ages for layers B, C2, D, D1 and D2 from the Dolina de l'Esquerda de les Alzines and layer E from the Dolina II de les Alzines.

Site[a]	Layer	Material	Lab #	$^{13}C/^{12}C$ ratio	Archeolological dose (Gy)	Annual dose (mGy/Year)	U (ppm)	Th (ppm)	K$_2$0 (%)	H$_2$0 (%)	Measured ^{14}C age BP (1σ)	^{14}C age BP (1σ)	Years ago (1σ)
DEA	B	Antler (*Cervus elaphus*)	Beta 216702	−20.5‰							1280±50	1212±56[b/d]	
DEA	C	Burnt flint	MADN-5989BIN		171.58	7.59	9.96	2.88	0.01	1.2			22744 ± 1605
DEA	C2 top	Sediment (2–10μ)	MAD-4959		62.72	3.55	0.17	12.55	1.74	13.59			18200±1689[e]
DEA	D top	Charcoal (*Quercus ilex/coccifera*)	Beta-210946	−26.8‰							1810±40	1754±50[c/d]	
DEA	D1	Sediment (2–10μ)	MAD-4566		10.58	3.77	1.17	12.7	0.6	3.4			3241±210[e]
DEA	D2	Sediment (2–10μ)	MAD-5693rBIN		29.16	6.54	4.29	11.58	1.54	11.34			4458±366[e]
DEA	D2 base	Sediment (2–10μ)	MAD-5291SDA		25.35	3.45	0.01	18.85	1.84	13.55			7347±441[e]
DA	E	Sediment: Neocarbonates (2–10μ)	MAD-5807		488.71	5.01	3.81	6.56	1	1.8			97526±6542[e]

[a] DEA: Site 1-Dolina Esquerda de les Alzines; DA: Site 2-Dolina II de les Alzines.
[b] cal AD 738±56.
[c] cal AD 196±50.
[d] CalPal program (Weninger et al., 2008) and the Hulu age model (Weninger and Jöris, 2008) was used to convert conventional ^{14}C ages into the calendar time scale.
[e] Sediment dates were obtained by OSL at the Radiochemistry and Dating Laboratory of the Universidad Autónoma de Madrid, using the additive dose method and standard procedures (Fleming, 1970; Zimmerman, 1971; Aitken, 1985; Nambi and Aitken, 1986; Arribas et al., 1990).
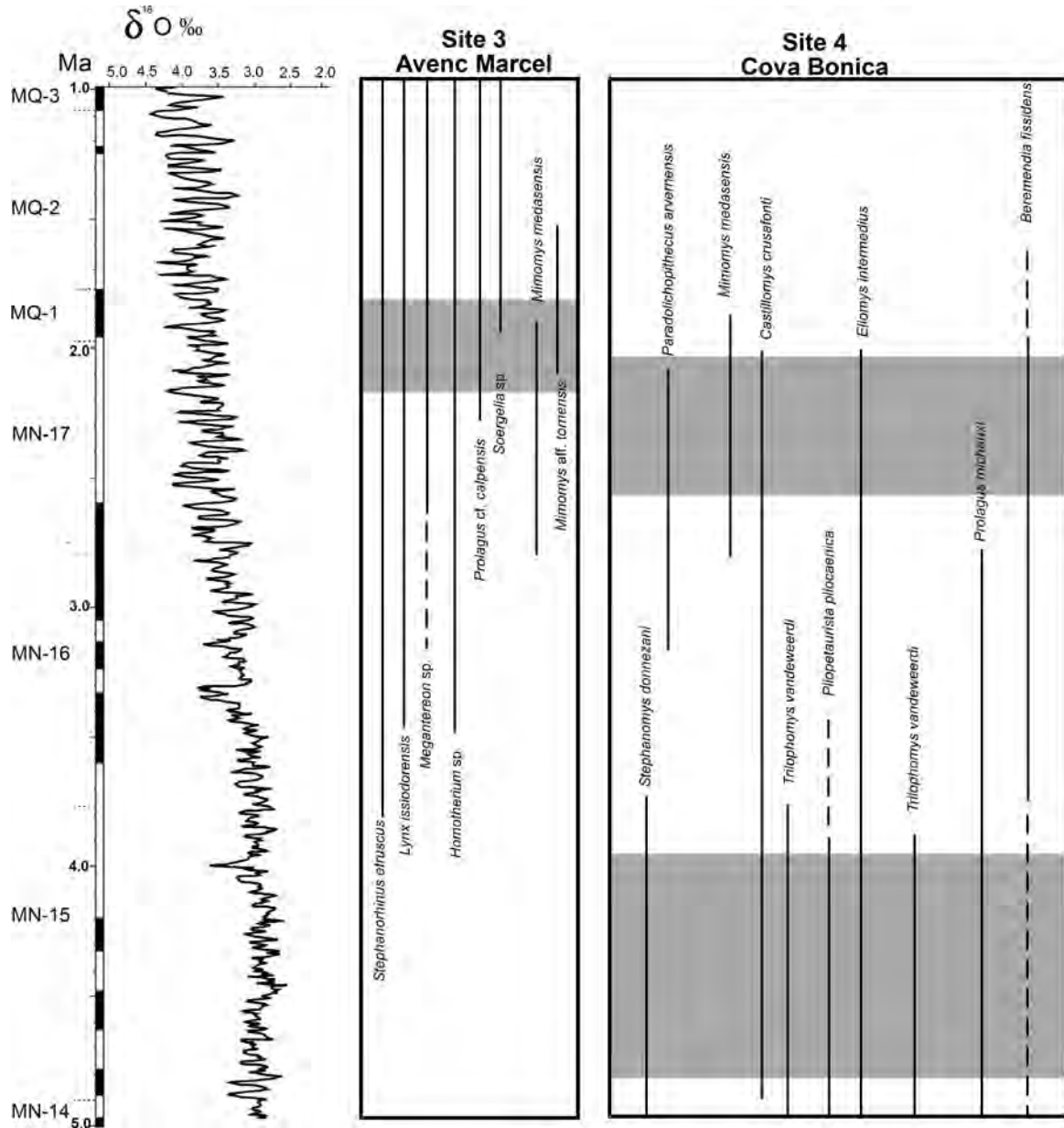
Figure 7. Vertical distribution of the main taxa identified at site 3, Avenc Marcel (Asensio, 1993; Daura 2008), and site 4, Cova Bonica. Small mammals from Cova Bonica are described here for the first time, following the identification currently listed in the collections of the Museu de Geologia de Barcelona and Agustí, (1988) whereas the Cercopithecidae have been previously described (Delson, 1971, 1973, 1974; Delson and Nicolaescu-Plopsor, 1975; Crusafont-Pairó and Golpe-Posse, 1984). Age in millions of years (Ma), Mammal Neogene Units (MN) (Agustí, 2001) and oxygen isotope curve (Shackleton et al., 1995) on the left. The vertical lines highlight the chronological ranges based on current literature for large mammals (Pickford and Morales, 1994; van der Made, 2005; Martínez-Navarro et al., 2010; Rook and Martínez-Navarro, 2010) and micromammals (Minwer-Barakat et al., 2004; de Marfà, 2009; Furió, 2007; García-Alix et al., 2007; Minwer-Barakat et al., 2008). Gray rectangle indicates the chronostratigraphic range proposed for the site.

The oldest absolute date for the sediments at the base of the dolines was found in layer E of the Dolina II de les Alzines (site 2). A multi-grain OSL average date of 97526±6542 BP was obtained. However, the result should be treated with some caution given, the method used (not single-grain) and the taphonomy of the sediments.

More recent layers have been Dated using other techniques. Layers C and C2 at the the Dolina de l'Esquerda de les Alzines (site 1) contain lithic artifacts that are chronologically dated to the Middle or Upper Palaeolithic techno-complex (Daura et al., 2011). A thermoluminescence date for burnt flint from layer C gives

an age of 22744±1605 BP, and an OSL date is 18200±1689 BP for sediment from the top of layer C2.

The DEA continued to be filled throughout the Upper Pleistocene and Holocene, from >22.7 ka until the present. However, several wildfires occurred during this time, affecting different layers and altering the sediments. As a result, reliable direct OSL dates are not easily obtained, as fires can make sediment appear younger, especially because of burnt tree stumps. Nonetheless, these dates (Table 3) are indicative of an *ante quem* age for the fill that is older than the dates obtained both by OSL (7 ka to 3 ka) and radiocarbon dating (cal AD 738±56 and 196±50). The presence of Bronze and Iron Age pottery in Layers B1 and D1 provide an approximate chronology for the accumulation of these deposits in accordance with OSL results.

A Model of Landscape Development and Karstification

Attempts were made to correlate the various dolines and shafts on the basis of their layers, stratigraphic position, and chronology. This correlation remains tentative because of the discontinuities between the various deposits and the shortcomings presented by each deposit. Our stratigraphic study identifies five stages or episodes resulting in the formation of a single unified sequence (Fig. 8). Its backbone is formed by the sediments preserved in the Dolina de l'Esquerda de les Alzines and the Dolina II de les Alzines, while the Cova Bonica, Avenc Marcel, and Coll Sostrell sites represent significant deposits for determining the ancient stage of the Garraf plateau.

Stage 0 corresponds to the formation of the Garraf plateau during the Upper Miocene that resulted in the horizontal modelling of the landscape (Llopis, 1943, 1947; Montoriol, 1950, 1954; Montoriol and Muntan, 1959, 1961). As such, the conditions required to trigger the doline formation process were present during this stage, despite the fact that no sediment had yet accumulated. The result of this stage is the presence of some monadnock-shaped standing remains.

Stages 1a and 1b correspond to the oldest sediment accumulations in the plateau, dating from between the Pliocene and Lower Pleistocene. The process of doline and shaft fill is confirmed by the presence of the most ancient deposits located at the base of the dolines and the sediments collapsed into the shafts. In the earlier part of the stage (1a), the first layer (G1) of sediments in the DEA lies at the base of the Avenc dels Arqueòlegs area and has partially collapsed into the subterranean network. The lower contact is irregular and overlies the Cretaceous limestone. In the latter part of the stage (1b), layers are also found in the Avenc (shaft) de l'Esquerda de les Alzines (layer I) and in Sector III-W at the base of the doline's center (layer E), as well as in the DA, which contains

mammal bones. In this case, deposits are located near Pou de la Revolució (Fig. 3), and part of the fill collapsed into the shaft through the Parets dels Ossos.

Infilling of similar material that probably originated from a collapsed surface deposit is found adhered to the walls in Via del Ossos of the Avenc Marcel shaft. The fill contains mammal bones and has been scattered throughout the subterranean network from which palaeontological remains were recovered. Finally, the Cova Bonica fill originates from sediment infiltration from the plateau through a combination of karst fissures and karren.

Stages 2 and 3 correspond to the second layers of deposits to accumulate. After the oldest sediment, those of stage 1 (layers E, G1, and I) developed, parts of these sediments were altered by the evolutionary process undergone by the depression. In some areas, fill from stage 1 was cemented and preserved at the rim of the doline or inside its shafts, as well as in layer E of the DEA (Fig. 3 and 6) and the base of the DA. In other cases, shafts received part of the collapsed sediment, as is the case in the DA (Fig. 6).

Stage 1 sediments found at the doline base are always capped by stage 2 layers. The most significant examples of stage 2 are layers C and C2 in the DEA. They contain Upper Palaeolithic artifacts such as burins, denticulates, and scrapers, among others.

The final sediment layer (stage 3) is characterized by highly compact lutites with few pebbles and gravels. These have been altered by wildfire combustion in sectors I, II, and III-SW in the DEA, a distortion in this area that is only limited by a gentle slope. Layers B, B1, and D1 of this unit contain prehistoric pottery. One layer, composed mainly of rounded sub-angular limestone gravels, corresponds to the current doline soil.

Stage 4 corresponds to the ongoing erosion process in which the dolines are being continuously transformed by agricultural or speleological activities.

Discussion and Conclusions

The results obtained from the Garraf case study coincide with proposals made for other European karst massifs (Piccini et al., 2003; Ufrecht, 2008) that the primary karst development appears to have taken place at the end of the Tertiary and the beginning of the Lower Pleistocene. The main karst features around the western Mediterranean were probably inherited from the end of the Miocene (Messinian period), when the sea level dropped dramatically due to the closing of the Atlantic connection and the subsequent desiccation of the Mediterranean sea (Krijgsman et al., 1999). The depths and altitudes of several conduits and galleries in karst areas around the western Mediterranean that do not match known Quaternary glacio-eustatic sea levels are linked to the erosive features observed during the Miocene and the Pliocene (Audra et
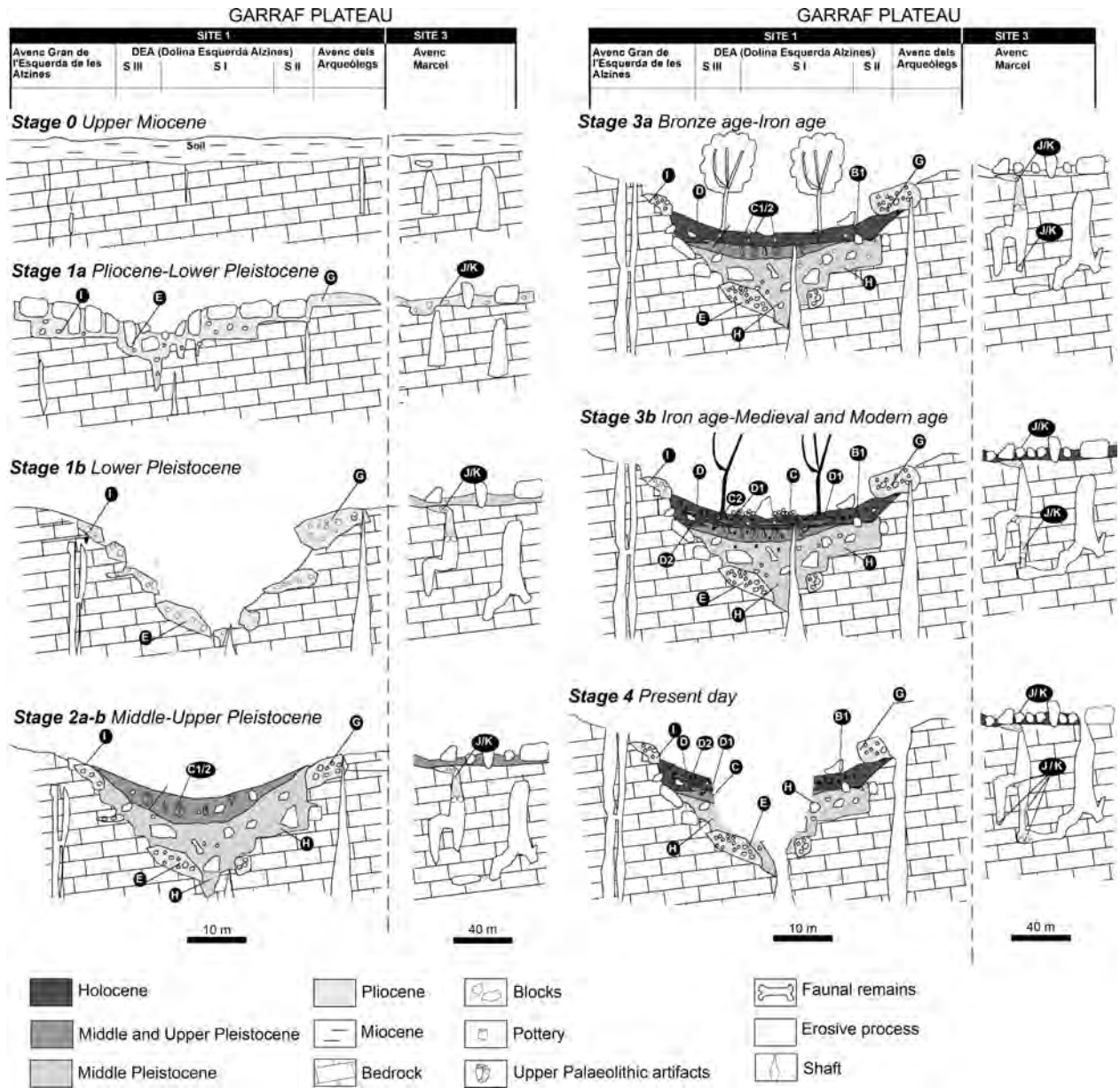
Figure 8. Characteristic stages of Garraf doline evolution, according on hypothesis based data obtained at the different dolines and shafts studied and applied to various parts of site 1, Dolina Esquerda de les Alzines, and site 3, Avenc Marcel. The labels on the sediment levels are those in Figure 6 and the text.

al., 2004). These karst paleo-galleries evolved after the subsequent Pliocene sea level rise and transgression, flooding the former karst system. Later oscillations of the water table, forced by the Quaternary eustatic sea-level changes, favored the evolution of the karst depressions and the sedimentary infill of the former karst system above the water table.

Previous research has argued in favor of a general Miocene age for the Garraf plateau (Llopis, 1943, 1947; Montoriol, 1950, 1954; Montoriol and Muntan, 1959, 1961). Based on the sediments preserved, we can confirm that the doline and shaft infill originating from the Garraf

plateau can be dated to the beginning of the Pliocene (stage 1) and, hence, earlier karstification processes must have taken place during the Miocene (stage 0), when conditions were suited to triggering the doline-formation process. The Garraf deep karst system was probably formed during the Messinian period (-5.96 to -5.32 Ma) and was reflooded during the Pliocene when the Mediterranean salinity crisis terminated (Audra et al., 2004). In fact, the discharge point for water draining out of the Garraf massif is La Falconera shaft, at least 81 m below the present sea level, suggesting that karstification occurred during this period of lower sea level (Montoriol, 1966; Custodio, 1975; Cardona, 1990).

Palaeopalynological studies (Suc and Cravatte, 1982; Suc et al., 1995; Fauquette et al., 1999) emphasize a subtropical climate for the northwestern Mediterranean during the Pliocene, and these environmental conditions could have accelerated karstification.

Palaeontological remains from stage 1 indicate an age of MN15 and MN17 (Delson, 1971, 1973, 1974; Delson and Nicolaescu-Plopsor, 1975; Crusafont-Pairó and Golpe-Posse, 1984; Agustí, 1988; Asensio, 1993; Daura, 2008). Today, sediments from this stage are located within the deepest inner part of the Garraf karst and have been eroded from their original position in the Garraf plateau. In this sense, the Canal Negre-1 (Guillén, 2010) assemblage could represent the earlier sediment accumulation, from stage 1 to the Upper Miocene (MN13).

The species richness at the paleontological sites Cova Bonica, Avenc Marcel, and Canal Negre-1 and the results of the pollen analyses (Suc and Cravatte, 1982; Suc et al., 1995; Fauquette et al., 1999) point to ecological optima in the Garraf plateau during the Pliocene, a different scenario from the current habitability of this area. Thus, dolines and collapsed cavities under the plateau are a useful record for Quaternary paleoenvironmental studies.

During the Middle-Upper Pleistocene (stage 2), significant sediment deposits accumulated in the dolines and shafts of the Garraf karst plateau. Infill of the same chronology is common beyond the plateau in other karst landforms, including the caves of Cova del Gegant (Daura et al., 2010a), Cova del Rinoceront (Daura et al., 2005), and Cova del coll Verdaguer (Daura et al., 2010b). However, in the karst plateau sediment has collapsed down into the subterranean network, suggesting that archaeological and paleontological records must be sought in the deeper levels of the karst system. This conclusion is supported by a large number of sites in the Iberian Peninsula, including the Almonda system in the Maciço Calcário Estremenho (Zilhão et al., 1993; Hoffmann et al., 2013), El Sidrón in Surco Oviedo-Infiesto (Rosas et al., 2006), the Sierra de Atapuerca (Rosas et al., 2001), and Cueva del Ángel in the Sierra de Araceli (Barroso Ruíz et al., 2011), among others.

A marked gap should be noted between the Pliocene–Lower Pleistocene and the Middle-Upper Pleistocene, with sedimentary deposits from this period being unknown in the Garraf plateau and in other caves and shafts of the Garraf Massif. There are three possible explanations for this: the sediments collapsed into the inner karst system through vertical shafts, no sedimentary processes occurred, or the phase has yet to be documented. However, we speculate that the sediments accumulated at the Big Gallery of Avenc Gran de les Alzines in site 1 and at the base of Rampa Sediments in site 2 could be dated to this period.

The Garraf Massif and the five stages identified here in its evolution point to the importance of karst development and sediment displacement for archaeological and paleontological studies, especially for the detection and evaluation of the viability of a karst plateau as an area of hominid presence (Bourguignon, 2004; Mosquera et al., 2007) because of its faunal or water resources.

Our results, based on geomorphologic arguments and sediment dating, are more accurate, we believe, than the previously proposed estimates of the age of Garraf doline and karst landforms (Llopis, 1943, 1947; Montoriol, 1950, 1954; Montoriol and Muntan, 1959, 1961). We have been able to construct a model of the geomorphic evolution of the Garraf Massif dolines that resulted in a single and unified sequence (Fig. 8). This sequence spans the Pliocene to the Holocene and constitutes the first chronological proposal for the Garraf karst. Our study has provided new examples and important data regarding the speleogenetic processes and the chronology of western Mediterranean dolines, shafts and karst plateaus.

ACKNOWLEDGEMENTS

REFERENCES

Agustí, J., 1988, Els cordats [excepte els primats humínids], *in* Gallemí, J., cord., Registre Fòssil. Història Natural dels Països Catalans: Barcelona, Fundació Enciclopèdia Catalana, v. 15, p. 389–427.

Agustí, J., 2001, Defining MN-units and magnetobiostratigraphic correlation of the Spanish sections, *in* Latal, C., and Pillar, W.E., eds., Environmental and Ecosystem Dynamics of the Eurasian Neogene (EEDEN); Stratigraphy & Paleogeography Workshop March 15–18 2001, Graz, Austria: Graz, Berichte des Institutes für Geologie und Paläontologie der Karl-Franzens-Universität Graz, no. 4, p. 23–26.

Agustí, J., Cabrera, L., Garcés, M., Krijgsman, W., Oms, O., and Parés, J.M., 2001, A calibrated mammal scale for the Neogene of Western

Europe. State of the art: Earth-Science Reviews, v. 52, p. 247–260. doi:10.1016/S0012-8252(00)00025-8.

Aitken, M.J., 1985, Thermoluminescence Dating. London, Academy Press, 359 p.

Albich, S., Bernaus, J.M., Boix, C., Caus, E., Martín-Closas, C., Salas, R., Vicedo, V., and Villalonga, R., 2006, Caracterización bioestratigráfica y paleoambiental del Cretácico inferior (Berraisiense-Barremiense) del Macizo del Garraf (Cadena Costera Catalana): Revista Española de Micropaleontología, v. 38, no. 2-3, p. 429–451.

Andreu, A., Calvet, F., Font, X., and Viladevall, M., 1987, Las mineralizaciones de Pb-Zn-Ba en el Muschelkalk inferior de los Catalánides: Cuadernos de Geología Ibérica, v. 11, p. 779–795.

Arribas, J.G., Millán, A., Sibilia, E., and Calderón, T., 1990, Factores que afectan en la determinación del error asociado a la datación absoluta por TL: Fábrica de ladrillos: Boletín de la Sociedad Española de Mineralogía, v. 13, p. 141–147.

Asensio, T., 1993, Cavidades del Pla del Marge del Moro: Nuevos descubrimientos en el Avenc Marçel: Passamà, v. 1, p. 27–42.

Audra, P., Mocochain, L., Camus, H., Gilli, E., Clauzon, G., and Bigot, J.-Y., 2004, The effect of the Messinian Deep Stage on karst development around the Mediterranean Sea. Examples from Southern France: Geodinamica Acta, v. 17, no. 6, p. 389–400. doi:10.3166/ga.17.389-400.

Baroň, I., 2002, Speleogenesis along sub-vertical joints: A model of plateau karst shaft development: A case study: the Dolný Vrch Plateau (Slovak Republic): Cave and Karst Science, v. 29, no. 1, p. 5–12.

Barroso Ruíz, C., Botella Ortega, D., Caparrós, M., Moigne, A.M., Celiberti, V., Testu, A., Barsky, D., Notter, O., Riquelme Cantel, J.A., Pozo Rodríguez, M., Carretero León, M.I., Monge Gómez, G., Khatib, S., Saos, T., Gregoire, S., Bailón, S., García Solano, J.A., Cabral Mesa, A.L., Djerrab, A., Hedley, I.G., Abdessadok, S., Batalla LLasat, G., Astier, N., Bertin, L., Boulbes, N., Cauche, D., Filoux, A., Hanquet, C., Milizia, C., Moutoussamy, J., Rossoni, E., Verdú Bernejo, L., and de Lumley, H., 2011, The Cueva del Angel (Lucena, Spain): An Acheulean hunters habitat in the South of the Iberian Peninsula: Quaternary International, v. 243, no. 1, p. 105–126. doi:10.1016/j.quaint.2011.02.021.

Bartrina, M.T., Cabrera, L., Jurado, M.J., Guimerà, J., and Roca, E., 1992, Evolution of the central Catalan margin of the Valencia trough (western Mediterranean): Tectonophysics, v. 203, p. 219–247. doi:10.1016/0040-1951(92)90225-U.

Benet, I., 1990, El Paleozoico de la parte NE del Macizo del Garraf (Cadenas Costeras Catalanas): Acta Geológica Hispánica, v. 25, no. 1-2, p. 133–139.

Blain, H.-A., 2009, Contribution de la paléoherpétofaune (Amphibia et Squamata) à la connaissance de l'évolution du climat et du paysage du Pliocène supérieur au Pléistocène moyen d'Espagne: Treballs del Museu de Geologia de Barcelona, v. 16, p. 39–170.

Blain, H.-A., and Bailon, S., 2006, Catalogue of Spanish Plio-Pleistocene amphibians and squamate reptiles from the Museu de Geologia de Barcelona: Treballs del Museu de Geología de Barcelona, v. 14, p. 61–80.

Borràs, J., 1974, Catálogo Espeleológico del Macizo del Garraf: Barcelona, Ed. Limonograph, 3 vols.

Bourguignon, L., Ortega, I., Sellami, F., Brenet, M., Grigoletto, F., Vigier, S., Daussy, A., Deschamps, J.-F., and Casagrande, F., 2004, Les occupations paléolithiques découvertes sur la section Nord de la déviation de Bergerac: résultats préliminaires obtenus à l'issue des diagnostics: Préhistoire du Sud-Ouest, v. 11, no. 2, p. 155–172.

Bruxelles, L., Colonge, D., and Salgues, T., 2006, Morphologie et remplissage des dolines de Causse de Martel d'après les observations réalisées au cours du diagnostic archéologique de l'aérodrome de Brive-Souillac (Corrèze et Lot): Karstologia, v. 47, p. 21–32.

Bruxelles, L., Colonge, D., Jarry, M., and Pons, F., 2008, Climate change and human impacts: the dolines fillings of limestone plateaus of the south western of France, in: The Fifth International Conference, Climate Change: Karst Record. School of Geographical Sciences, Southwest University, Chongqing, China, Abstract Volume, 106 p.

Bruxelles, L., Colonge, D., and Salgues, T., 2012, Les dolines du Causse de Martel (Corrèze et Lot): études des remplissages et implications paléoenvironnementales: Géologues, v. 173, p. 23–27.

Cardona, F., 1990, Grans cavitats de Catalunya. El sistema mediterrani i la depressió central: Barcelona, Espeleoclub de Gràcia, 484 p.

Crusafont-Pairó, M., and Golpe-Posse, J.M., 1984, Nuevo hallazgo de macaco en Cova Bonica (Gavà): Acta Geológica Hispánica, v. 19, no. 1, p. 29–32.

Custodio, E., 1975, Metodología y resultados del estudio hidrogeológico del macizo kárstico de Garraf, Barcelona: Boletín Geológico y Minero, v. 86, no. 1, p. 31–44.

Custodio, E., Bayo, A., Pascual, M., and Bosch, X., 1993, Results from studies in several karst formation in southern Catalonia (Spain), in Proceedings of the Antalya Symposium and Field Seminar, October, 1990, IAHS Publ. no. 207, p. 295–326.

Cvijić, J., 1893, Das Karstphänomen. Versuch einer morphologichen Monographie: Geographische Abhandlungen heruasgegeben von Prof. Dr. A. Penck, v. 5, no. 3, p. 218–329.

Daura, J., 2008, Caracterització arqueològica i paleontològica dels jaciments plistocens del massís del Garraf-Ordal i curs baix del riu Llobregat [Ph. D. thesis]: Barcelona, Universitat de Barcelona, 674 p.

Daura, J., and Sanz, M., 2010, Memòria de les intervencions arqueològiques a la Dolina II de les Alzines-Can Pau de la Figuera (Begues-Vallirana, Baix Llobregat): Unpublished Archaeological Report, Barcelona, Servei d'Arqueologia i Paleontologia, Departament de Cultura i Mitjans de Comunicació, Generalitat de Catalunya, 85 p.

Daura, J., Sanz, M., Pike, A.W.G., Zilhão, J., Subirà, M.E., Fornós, J.J., Fullola, J.M., and Julià, R., 2010a, Stratigraphic context and direct dating of the Neandertal mandible from Cova del Gegant (Sitges, Barcelona): Journal of Human Evolution, v. 59, no. 1, p. 109–122. doi:10.1016/j.jhevol.2010.04.009.

Daura, J., Sanz, M., Rosell, J., and Julià, R., 2010b, La Cova del Coll Verdaguer (Cervelló, Barcelona): Un cubil de hiena y osos con presencia de humana durante del Paleolítico Medio, in Baquedano, E., and Rosell, J., eds., Proceedings of the I Reunión de científicos sobre cubiles de hienas (y otros grandes carnívoros) en los yacimientos arqueológicos de la Península Ibérica: Zona Arqueológica, v. 13, p. 502–507.

Daura, J., Sanz, M., and Vaquero, M., 2005, El Pleistoceno de la Cova del Rinoceront (Castelldefels, Barcelona), in Ferreira-Bicho, N., ed., O Paleolítico. Proceedings of the IV Congresso de Arqueologia Peninsular: Faro, Universidade do Algarve, Promontoria Monográfica, v. 2, p. 217–227.

Daura, J., Sanz, M., Vaquero, M., and Fullola, J.M., 2011, La Dolina de l'Esquerda de les Alzines (Macizo del Garraf, Barcelona): un yacimiento del Pleistoceno superior al aire libre con industria lítica paleolítica: Trabajos de Prehistoria, v. 68, no. 2, p. 353–367. doi:10.3989/tp.2011.11074.

Delson, E., 1971, Estudio preliminar de unos restos de simios pliocénicos procedentes de "Cova Bonica" (Gavà), (Prov. Barcelona): Acta Geológica Hispánica, v. 6, no. 2, p. 54–57.

Delson, E., 1973, Fossil Colobine Monkeys of the circum-mediterranean region and the revolutionary history of the Cercopithecidae (Primates, Mammalia) [Ph. D. thesis]: New York, Columbia University, 856 p.

Delson, E., 1974, Preliminary review of Cercopithecid distribution in the Circum Mediterranean Region: Mémoires du Bureau de Récherches Géologiques et Minières, v. 78, no. 1, p. 131–135.

Delson, E., and Nicolaescu-Plopsor, D., 1975, Paradolichopithecus, a large terrestrial monkey (Cercopithecidae, primates) from the Plio-Pleistocene of southern Europe and its importance for mammalian biochronology, in Proceedings of the 6th Session, Regional Committee on Mediterranean Neogene Stratigraphy: Bratislava, Slovak Academy of Sciences, p. 91–96.

Falguères, C., Bahain, J.-J., Tozzi, C., Boschian, G., Dolo, J.-M., Mercier, N., Valladas, H., and Yokoyama, Y., 2008, ESR/U-series chronology of the Lower Palaeolithic palaeoanthropological site of Visogliano, Trieste, Italy: Quaternary Geochronology, v. 3, no. 4, p. 390–398. doi:10.1016/j.quageo.2008.01.007.

Fauquette, S., Suc, J.-P., Guiot, J., Diniz, F., Feddi, N., Zheng, Z., Bessais, E., and Drivaliari, A., 1999, Climate and biomes in the West Mediterranean area during the Pliocene: Palaeogeography, Palaeoclimatology, Palaeoecology, v. 152, no. 1-2, p. 15–36. doi:10.1016/S0031-0182(99)00031-0.

Fleming, S.J., 1970, Thermoluminescent dating: refinement of the quartz inclusion method: Archaeometry, v. 12, no. 2, p. 133–143. doi:10.1111/j.1475-4754.1970.tb00016.x.

Font, N., 1897, Catalech Espeleologich de Catalunya: Butlletí del Centre Excursionista de Catalunya, no. 24, p. 8–20; no. 25, p. 79–84; no. 26,

p. 107–112; no. 27, p. 141–149; no. 29, p. 197–202; no. 31, p. 235–238; no. 32, p. 249–253; no. 33, p. 266–274; no. 35, p. 311–323.

Font, N., 1899, Sota Terra, Excursió espeleológica a la Baronia d'Aramprunyà, Conferencia llegida'l dia 30 de Desembre de 1898: Butlletí del Centre Excursionista de Catalunya, v. 9, no. 57–58, p. 233–252.

Fouache, E., Ghilardi, M., Vouvalidis, K., Syrides, G., Styllas, M., Kunesch, S., and Stiros, S., 2008, Contribution on the Holocene reconstruction of Thessaloniki Coastal Plain, Greece: Journal of Coastal Research, v. 24, no. 5, p. 1161–1173. doi:10.2112/06-0786.1.

Ford, D.C., and Williams, P.W., 2007, Karst Hydrology and Geomorphology: Chichester, John Wiley and Sons Ltd, 562 p.

Freixes, A., 1989, El karst en las Cordilleras Costeras Catalanas, in Durán, J.J., and López-Martínez, J., eds., El karst en España, Sociedad Española de Geomorfologia, Monografia, v. 4, p. 145–149.

Furió, M., 2007, Los insectívoros (Soricomorpha, Erinaceomorpha, Mammalia) del Neógeno superior del Levante Ibérico [Ph. D. thesis]: Bellaterra, Universitat Autònoma de Barcelona, 299 p.

Gallart, F., 1980, Estudi geomorfològic del Penedès, sector Anoia i Riudebitlles [Ph. D. thesis]: Barcelona, Universitat de Barcelona, 247 p.

García-Alix, A., Minwer-Barakat, R., Martín-Suárez, E., and Freudenthal, M., 2007, New data on Mio-Pliocene Sciuridae (Rodentia, Mammalia) from southern Spain: Comptes Rendus Palevol, v. 6, p. 269–279. doi:10.1016/j.crpv.2007.02.001.

Gibbard, P.L., Bryant, I.D., and Hall, A.R., 1986, A Hoxian interglacial doline infilling at Slade Oak Lane, Denham, Buckinghamshire, England: Geological Magazine, v. 123, no. 1, p. 27–43. doi:10.1017/S0016756800026510.

GIRES (Grup d'Investigacions i Recerques Espeleològiques Sesrovires), 1995, Avenc Gran de les Alzines, Pla d'Ardenya, Vallirana: Speleological Unpublished Report, Barcelona, Centre Excursionista de Vallirana, 16 p.

Guérin, C., 1980, Les Rhinoceros (Mammalia, Perissodactyla) au Pléistocène Superieur en Europe Occidentale; Comparasion avec les Espèces Actuelles: Documents des Laboratoires de Géologie de Lyon no. 79, 1185 p.

Guillén, J., 2010, Canal Negre 1, jaciment càrstic de vertebrats del Miocè, Pliocè i Pleistocè de Catalunya: Exploracions, no. 19, p. 7–87.

Guimerà, A., 1988, Estudi estructural de l'enllaç entre la Serralada Ibèrica i la Serralada Costanera Catalana [Ph. D. thesis]: Barcelona, Universitat de Barcelona, 600 p.

Hempel, L., 1991, Forschungen zur physische Geographie der Insel Kreta im Quartär. Ein Beitrag zur Geoökologie des Mittelmeerraumes: Göttingen, Vandenhoeck und Ruprecht, Abhandlungen der Akademie der Wissenschaften in Göttingen, no. 42, 171 p.

Hoffmann, D., Pike, A.W.G., Wainer, K., and Zilhão, J., 2013, New U-series results for the speleogenesis and the Palaeolithic archaeology of the Almonda karstic system (Torres Novas, Portugal): Quaternary International, v. 294, p. 168–182. doi:10.1016/j.quaint.2012.05.027.

Jennings, J.N., 1985, Karst Geomorphology: Oxford, Basil Blackwell, 293 p.

Jones, W.K., Culver, D.C., and Herman, J.S., eds., 2004, Epikarst. Proceedings of the Symposium Held October 1 through 4, 2003, Sheperdstown, West Virginia, USA: Charles Town, West Virginia, Karst Waters Institute, Special Publication 9, 160 p.

Klimchouk, A., 2000, The formation of epikarst and its role in vadose speleogenesis, in Klimchouk, A., Ford, D., Palmer, A.N., and Dreybrodt, W., eds., Speleogenesis. Evolution of Karst Aquifers: Huntsville, National Speleological Society, p. 91–99.

Krijgsman, W., Hilgen, F.J., Raffi, I., Sierro, F.J., and Wilson, D.S., 1999, Chronology, causes and progression of the Messinian salinity crisis: Nature, v. 400, no. 6745, p. 652–655. doi:10.1038/23231.

Llopis, N., 1941, Morfología y hidrología subterránea de la parte oriental del macizo cárstico de Garraf (Barcelona): Estudios Geográficos, v. 2, p. 413–466.

Llopis, N., 1943, Estudio tectomorfológico de la terminación meridional de la depresión Prelitoral catalana: Estudios Geográficos, v. 4, p. 31–111.

Llopis, N., 1947, Contribución al Conocimiento de la Morfoestructura de los Catalánides: Barcelona, CSIC-Instituto Lucas Mallada, 372 p.

Lloret, J., 1979, Catálogo espeleológico del pla d'Ardenya, Tomo 1: Barcelona, by the author, 106 p.

Luzón, A., Pérez, A., Soriano, M.A., and Pocoví, A., 2008, Sedimentary record of Pleistocene paleodoline evolution in the Ebro basin (NE Spain): Sedimentary Geology, v. 205, no. 1–2, p. 1–13. doi:10.1016/j.sedgeo.2008.01.004.

Macpherson, I., 1994, Revisión bioestratigráfica de los depósitos marinos del Mioceno medio en la cuenca del Penedès: Acta Geológica Hispánica, v. 29, no. 2-4, p. 123–132.

Marfà, R. de, 2009, Els lagomorfs (O. Lagomorpha, Cl. Mammalia) del Pliocè i el Pleistocè europeus [Ph. D. thesis]: Barcelona, Universitat de Barcelona, 206 p.

Marriner, N., and Morhange, C., 2007, Geoscience of ancient Mediterranean harbours: Earth-Science Reviews, v. 80, no. 3-4, p. 137–194. doi:10.1016/j.earscirev.2006.10.003.

Martínez-Navarro, B., 2010, Early pleistocene faunas of Eurasia and hominin dispersals, in Fleagle, J.G., Shea, J.J., Grine, F.E., Baden, A.L., and Leakey, R.E., eds., Out of Africa I: The First Hominin Colonization of Eurasia: Dordrecht, Springer, Vertebrate Paleobiology and Paleoanthropology Series, p. 207–224. doi:10.1007/978-90-481-9036-2_13.

Martínez-Navarro, B., Llenas, M., and Agustí, J., 2002, Estudio de las brechas fosilíferas del Avenc Marcel, Pla del Marge del Moro (Vallirana-Begues, Baix Llobregat): unpublished archaeological report, Barcelona, Servei d'Arqueologia i Paleontologia, Departament de Cultura i Mitjans de Comunicació, Generalitat de Catalunya, 4 p.

Marzo, M., 1979, El Buntsandstein de los Catalánides: estratigrafía y procesos de sedimentación [Ph. D. thesis]: Barcelona, Universitat de Barcelona, 317 p.

Maucci, W., 1960, La speleogenesi nel Carso Triestino: Bollettino della Società Adriatica di Scienze Naturali in Trieste, v. 51, p. 233–254.

Minwer-Barakat, R., García-Alix, A., Martín-Suárez, E., and Freudenthal, M., 2004, Arvicolidae (Rodentia) from the Pliocene of Tollo de Chiclana (Granada, SE Spain): Geobios, v. 37, p. 619–629. doi:10.1016/j.geobios.2004.05.001.

Minwer-Barakat, R., García-Alix, A., Martín-Suárez, E., and Freudenthal, M., 2008, The latest Ruscinian and early Villanyian Arvicolinae from southern Spain re-examined: biostratigraphical implications: Journal of Vertebrate Paleontology, v. 28, no. 3, p. 841–850. doi:10.1671/0272-4634(2008)28[841:TLRAEV]2.0.CO;2.

Moncel, M.-H., 2003, L'exploitation de l'espace et la mobilité des groupes humains au travers des assemblages lithiques à la fin du Pléistocène moyen et au début du Pléistocène supérieur. La moyenne vallée du Rhone entre Drôme et Ardèche: Oxford, Archaeopress, BAR (British Archaeological Reports) International Series 1184, 179 p.

Moncel, M.-H., Moigne, A.-M., and Combier, J., 2005, Pre-Neandertal behaviour during isotopic stage 9 and the beginning of stage 8. New data concerning fauna and lithics in the different occupation levels of Orgnac 3 (Ardèche, South-East France): occupation types: Journal of Archaeological Science, v. 32, no. 9, p. 1283–1301. doi:10.1016/j.jas.2005.03.014.

Montoriol, J., 1950, El campo de dolinas del Plá de Campgrás (macizo del Garraf, Barcelona): Speleon, v. 1, no. 2, p. 23–39.

Montoriol, J., 1954, La hidrología kárstica del Pla de les Basses y sus relaciones con la de otras zonas del macizo del Garraf (Barcelona): Speleon, v. 5, no. 1–2, p. 55–104.

Montoriol, J., 1964, Estudio de las formas kársticas hipogeas desarrolladas en los bordes del polje de Begues (Macizo del Garraf, Barcelona): Speleon, v. 15, no. 1–4, p. 3–38.

Montoriol, J., 1966, Las surgencias de las Costas del Garraf (Barcelona), in Akten des Dritter Internationaller Kongress für Spelaologie, vol. 5: Viena, Verband österreichischer Höhlenforscher, p. 43–49.

Montoriol, J., and Muntan, L., 1958, Sobre la evolución del Fondo de les Tarradelles (nota complementaria): Speleon, v. 9, no. 3–4, p. 61–74.

Montoriol, J., and Muntan, L., 1959, Resultados de nuevas investigaciones en el campo de dolinas del Plá del Campgrás (Macizo del Garraf, Barcelona): Speleon, v. 10, no. 3–4, p. 127–152.

Montoriol, J., and Muntan, L., 1961, Resultados de las nuevas investigaciones sobre el karst del pla de les Bases (Macizo del Garraf, Barcelona): Speleon, v. 12, no. 1–2, p. 35–55.

Moreno, J.A., 2007, Bioestratigrafía del Aptiense del macizo del Garraf (NE de la Península Ibérica): Geogaceta, v. 41, p. 131–134.

Mosquera, M., Ollé, A., Pérez-González, A., Rodríguez, X.P., Vaquero, M., Vergès, J.Mª., and Carbonell, E., 2007, Valle de las Orquídeas: un yacimiento al aire libre del Pleistoceno superior en la sierra de

Atapuerca (Burgos): Trabajos de Prehistoria, v. 64, no. 2, p. 143–155. doi:10.3989/tp.2007.v64.i2.113

Nambi, K.S.V., and Aitken, M.J., 1986, Annual dose conversion factors for TL and ESR dating: Archaeometry, v. 28, no. 2, p. 202–205. doi:10.1111/j.1475-4754.1986.tb00388.x.

Piccini, L., Drysdale, R., and Heijnis, H., 2003, Karst morphology and cave sediments as indicators of the uplift history in the Alpin Apuane (Tuscany, Italy): Quaternary International, v. 101–102, p. 219–227. doi:10.1016/S1040-6182(02)00104-0.

Pickford, M., and Morales, J., 1994, Biostratigraphy and palaeobiogeography of East Africa and the Iberian Peninsula: Palaeogeography, Palaeoclimatology, Palaeoecology, v. 112, p. 297–322. doi:10.1016/0031-0182(94)90078-7.

Porcel, E., 2008, Els avencs de les Alzines, dels Arqueòlegs, dels Llambrics, de l'Emili Sabaté i Petit Pasant: Cavernes, v. 27, p. 36–47.

Porta, J. de, and Civis, J., 1996, La sucesión bioestratigráfica del Mioceno marino en el Penedès y en el horst de Tarragona-Bonastre (Neógeno del Sistema Mediterráneo): Geogaceta, no. 19, p. 97–100.

Quilès, D., Rohr, V., Joly, K., Lhuillier, S., Ogereau, P., Martin, A., Baziles, F., and Vernet, J.L., 2002, Les feux préhistoriques holocènes en montagne sub-méditerranéene: premiers résultats sur les Causse Méjean (Lozère, France): Comptes Rendus Palevol, v. 1, no. 1, p. 59–65. doi:10.1016/S1631-0683(02)00010-6.

Ramos, J., Bernal, D., Domínguez-Bella, S., Calado, D., Ruiz, B., Gil, M.J., Clemente, I., Durán, J.J., Vijande, E., and Chamorro, S., 2008, The Benzú rockshelter: a middle Palaeolithic site on the North African coast: Quaternary Science Reviews, v. 27, no. 23–24, p. 2210–2218. doi:10.1016/j.quascirev.2008.08.030.

Rook, L., and Martínez-Navarro, B., 2010, Villafranchian: The long story of a Plio-Pleistocene European large mammal biochronologic unit: Quaternary International, v. 219, p. 134–144. doi:10.1016/j.quaint.2010.01.007.

Rosas, A., Martínez-Maza, C., Bastir, M., García-Tabernero, A., Lalueza-Fox, C., Huguet, R., Ortiz, J.E., Julià, R., Soler, V., de Torres, T., Martínez, E., Cañaveras, J.C., Sánchez-Moral, S., Cuezva, S., Lario, J., Santamaría, D., de la Rasilla, M., and Fortea, J., 2006, Paleobiology and comparative morphology of a late Neanderthal simple from El Sidrón, Asturias, Spain: Proceedings of the National Academy of Sciences of the United States of America, v. 103, no. 51, p. 19266–19271. doi:10.1073/pnas.0609662104.

Rosas, A., Pérez-González, A., Carbonell, E., van der Made, J., Sánchez, A., Laplana, C., Cuenca-Bescós, G., Parés, J.M., and Huguet, R., 2001, Le gisement pléistocène de la "Sima del Elefante" (Sierra de Atapuerca, Espagne): L'Anthropologie, v. 105, no. 2, p. 301–312. doi:10.1016/S0003-5521(01)80018-2.

Rubinat, F., 1981, Catàleg espeleològic del massís del Garraf. Unitat septentrional. Sector 10: Gours, no. 8, p. 45–78.

Rubinat, F., 2004, Catàleg Espeleològic del Massís de l'Ordal: Barcelona, Centre Excursionista Àliga, EspeleoSie Monogràfic, 118 p.

Salas, R., 1987, El Malm i el Cretaci inferior entre el massís del Garraf i la serra d'Espadà. [Ph. D. thesis]: Barcelona, Universitat de Barcelona, 345 p.

Sauro, U., Ferrarese, F., Francese, R., Miola, A., Mozzi, P., Rondo, G.Q., Trombino, L., and Valentini, G., 2009, Doline fills. Case study of the Faverghera plateau (Venetian Pre-Alps, Italy): Acta Carsologica, v. 38, no. 1, p. 51–63.

Shackleton, N.J., Hall, M.A., and Pate, D., 1995, Pliocene stable isotope stratigraphy of site 846, in Pisias, N.G., Mayer, L.A., Janecek, T.R., Palmer-Julson, A., and van Andel, T.H., eds., Proceedings of the Ocean Drilling Program, Scientific Results, v. 138: College Station Texas (Ocean Drilling Program), p. 337–355. doi:10.2973/odp.proc.sr.138.117.1995.

Siart, C., Hecht, S., Holzhauer, I., Altherr, R., Meyer, H.P., Schukraft, G., Eitel, B., Bubenzer, O., and Panagiotopoulos, D., 2010, Karst depressions as geoarchaeological archives: The palaeoenviromental reconstruction of Zominthos (Central Crete), based on geophysical prospection, sedimentological investigations and GIS: Quaternary International, v. 216, no. 1–2, p. 75–92. doi:10.1016/j.quaint.2009.06.020.

Solé, L.L., 1964, Geología de los alrededores de Barcelona, in: Publicacionesde la Dirección General de Enseñanza Media. Colección "la Nueva Geografía". Ministerio de Educación Nacional, Madrid, no. 379, p. 67–72.

Suc, J.-P., and Cravatte, J., 1982, Etude palynologique du Pliocène de Catalogne (Nord-est de l'Espagne): Paléobiologie Continentale, v. 13, no. 1, p. 1–31.

Suc, J.-P., Diniz, F., Leroy, S., Poumot, C., Bertini, A., Dupont, L., Clet, M., Bessais, E., Zheng, Z., Fauquette, S., and Ferrier, J., 1995, Zanclean (~Brunssumian) to early Piacenzian (~early-middle Reuverian) climate from 4° to 54° north latitude (West Africa, West Europe and West Mediterranean areas): Mededelingen Rijks Geologische Dienst, v. 52, p. 43–56.

Ufrecht, W., 2008, Evaluating landscape development and karstification of the Central Schwäbische Alb (Southwest Germany) by fossil record of karst fillings: Zeitschrift für Geomorphologie, v. 52, no. 4, p. 417–436. doi:10.1127/0372-8854/2008/0052-0417.

Valdepeñas, P., 2012, L'Avenc Nou de les Alzines: EspeleoCat, v. 9, p. 34–36.

Van Andel, T.H., 1998, Paleosols, red sediments, and the Old Stone Age in Greece: Geoarchaeology, v. 13, no. 4, p. 361–390. doi:10.1002/(SICI)1520-6548(199804)13:4<361::AID-GEA2>3.0.CO;2-0.

Van der Made, J., 2005, La fauna del Pleistoceno europeo, in Carbonell, E., coord., Homínidos: Las Primeras Ocupaciones de los Continentes: Barcelona, Ariel, p. 394–432.

Van der Made, J., 2010, The rhinos from the Middle Pleistocene of Neumark-Nord (Saxony-Anhalt), in Mania, D., and Meller, H., eds., Ein interglaziales Ökosystem des mittelpaläolithischen Menschen: Halle (Saale), Landesmuseum für Vorgeschichte, Veröffentlichungen des Landesamtes für Denkmalpflege und Archäologie Sachsen-Anhalt no. 62, 433–527.

Van der Made, J., and Grube, R., 2010, The rhinoceroses from Neumark-Nord and their nutrition, in Meller, H., ed., Elefantenreich – eine Fossilwelt in Europa: Halle (Saale), Landesmuseum für Vorgeschichte, Begleithefte zu Sonderausstellungen 2, p. 383–398.

Waltham, T., Bell, F.G., and Culshaw, M.G., 2005, Sinkholes and Subsidence: Karst and Cavernous Rocks in Engineering and Construction: Chichester, Springer Praxis Publishing Ltd, 382 p.

Weninger, B., and Jöris, O., 2008, A ^{14}C age calibration curve for the last 60 ka: the Greenland-Hulu U/Th timescale and its impact on understanding the Middle to Upper Paleolithic transition in Western Eurasia: Journal of Human Evolution, v. 55, no. 5, p. 772–781. doi:10.1016/j.jhevol.2008.08.017.

Weninger, B., Jöris, O., and Danzeglocke, U., 2008, CalPal-2007. Cologne Radiocarbon Calibration and Palaeoclimate Research Package: http://www.calpal.de/ [accessed 10 February 2012].

Zambo, L., and Ford, D.C., 1997, Limestone dissolution processes in Beke doline Aggtelek National Park, Hungary: Earth Surface Processes and Landforms, v. 22, no. 6, p. 531–543. doi:10.1002/(SICI)1096-9837(199706)22:6<531::AID-ESP711>3.0.CO;2-I.

Zhu, Xuewen, and Waltham, T., 2005, Tiankengs: definition and description: Cave and Karst Science, v. 32, no. 2–3, p. 75–80.

Zilhão, J., Maurício, J., and Souto, P., 1993, Jazidas arqueológicas do sistema cársico da nascente do Almonda: Nova Augusta, v. 7, p. 35–54.

Zimmerman, D.W., 1971, Thermoluminescence dating using fine grains from pottery: Archaeometry, v. 13, no. 1, p. 29–52. doi:10.1111/j.1475-4754.1971.tb00028.x.

BIOGENICITY AND CHARACTERIZATION OF MOONMILK IN THE GROTTA NERA (MAJELLA NATIONAL PARK, ABRUZZI, CENTRAL ITALY)

Paola Cacchio[1], Gianluca Ferrini[2], Claudia Ercole[1], Maddalena Del Gallo[1], and Aldo Lepidi[1]

Abstract: Observations and hypotheses on the possible influence of unidentified calcifying bacteria on moonmilk speleothem formation in the Grotta Nera are reported for the first time. The Majella Massif hosts a complex karst system of several caves; the accessible Grotta Nera is the most interesting one. Despite its name, the cave is characterized by particularly abundant ivory-white deposits of moonmilk. Two samples of moonmilk were analyzed to determine the geochemistry, fabric, depositional setting, and extent of biogenicity. For this, we combined geochemical, scanning electron microscopic, microbiological, and *in vitro* precipitation studies. X-ray diffraction of the moonmilk deposits gave clear evidence for the presence of calcite. Scanning electron microscopy showed that moonmilk in the Grotta Nera consists of a network of calcite fibers oriented in all directions, resembling a felted mat. The cultivation on specific medium of moonmilk and drip-water samples showed the presence of fungi, actinomycetes, and other bacteria, but the dominant cultivable microorganisms were bacteria, which produced significant crystallization. Examination of Gram-stained smears taken from the fifteen different colony types showed that the majority (66.7%) of the bacterial isolates were Gram-negative. Single small rods and rod chains were the most common bacteria isolated from the Grotta Nera. None of the molds isolated from the Grotta Nera samples were able to precipitate $CaCO_3$ crystals, suggesting a major bacterial contribution to moonmilk deposition in the cave. Bacteria were capable of precipitating $CaCO_3$ on B-4 solid medium at 15 (cave temperature), 22, and 32 °C. The calcifying bacteria isolated from the Grotta Nera showed a greater capability to solubilize $CaCO_3$ than those associated with consolidated stalactites sampled from previously studied caves. The electron microscopy and microbiological evidences, together with the geochemistry and environmental data, allowed us to postulate the biogenic nature of the moonmilk in the Grotta Nera Cave.

INTRODUCTION

Moonmilk is a whitish material described as soft and pasty, resembling cream-cheese, when wet, and crumbly and powdery, like chalk, when dry (Fisher, 1988; Hill and Forti, 1997; Northup and Lavoie, 2001; Cañaveras et al., 2006). On aging, the moonmilk becomes dry and more rigid and compact, but the external morphology stays unchanged (Gradziñsky et al., 1997). It is a microcrystalline aggregate, typically found on the ceilings, floors, and walls of carbonate caves and on speleothems. Moonmilk deposits have been reported in numerous caves worldwide, in a variety of different countries and in climates from alpine to tropical (Onac and Ghergari, 1993; Hill and Forti, 1997; Chirienco, 2002; Lacelle et al., 2004; Ford and Williams, 2007; Blyth and Frisia, 2008; Richter et al., 2008; Curry et al., 2009). Frequently, moonmilk is the only speleothem present in cold, high-altitude or high-latitude caves, where massive calcite speleothems such as stalagmites do not form (Onac and Ghergari, 1993; Hill and Forti, 1997; Borsato et al., 2000; Lacelle et al., 2004). Moonmilk is composed of water and small

crystals of minerals such as $CaCO_3$ polymorphs (calcite, aragonite, vaterite), monohydrocalcite ($CaCO_3 \cdot H_2O$), magnesite ($MgCO_3$), hydromagnesite ($Mg_5(OH)_2(CO_3)_4 \cdot 4H_2O$), dolomite ($CaMg(CO_3)_2$), nesquehonite ($MgCO_3 \cdot 3H_2O$), huntite ($Mg_3Ca(CO_3)_4$), and gypsum ($CaSO_4 \cdot 2H_2O$) (Onac and Ghergari, 1993; Hill and Forti, 1997; Northup and Lavoie, 2001; Lacelle et al., 2004). This array of minerals relates to various host lithologies (Gradziñski et al., 1997) and water chemistries associated with each cave.

About 95% of moonmilk deposits are carbonatic, and its most common type is calcite moonmilk with greater than 90% calcite in its solid phase (Fisher, 1992, 1993). The water content of active moonmilk varies considerably. Under its hydrated phase, its water content ranges from 40 to 70% by weight (Hill and Forti, 1997; Lacelle et al., 2004). According to Istvan et al. (1995), the water retaining

[1] Department of Life, Health & Environmental Sciences, Microbiology Laboratory, University of L'Aquila, Coppito, 67010 L'Aquila, Italy paolacacchio@yahoo.it
[2] Department of Life, Health & Environmental Sciences, Geology Laboratory, University of L'Aquila, Coppito, 67010 L'Aquila, Italy

capacity of active moonmilk can be attributed to its porous network of calcite fibers.

The morphology of moonmilk is as varied as its composition (Curry et al., 2009). Microscopically, the most diagnostic calcitic moonmilk feature is needle-shaped or fibrous crystal morphology that appears as unstructured aggregates of micrometer- to nanometer-sized crystals with no apparent preferred orientation (Onac and Ghergari, 1993; Gradziñski et al., 1997; Hill and Forti, 1997; Borsato et al., 2000; Cañaveras et al., 2006). Moonmilk that is biologically active also contains significant amounts of cells, filaments, and apparent biofilms (Gradziñski et al., 1997; Boston et al., 2001; Curry et al., 2009). The origin of moonmilk has long been discussed, and many hypotheses for its genesis have been proposed since its first description was made by Nicolas Langh in 1708 (Bernasconi, 1976). Biotic and abiotic processes have been postulated (Gradziñsky et al., 1997; Borsato et al., 2000; Forti, 2001; Northup and Lavoie, 2001). Some evidences of microbial activities related with calcite moonmilk deposits have been reported (Bertouille, 1972; James et al., 1982; Callot et al., 1985; Gradziñski et al., 1997; Barton and Northup, 2007; Braissant et al., 2012). Moonmilk is the cave deposit most commonly associated with biogenic calcite precipitation, either by direct precipitation by microorganisms (fungi, algae, bacteria, and archaea) (Castanier et al., 1999; Barton and Northup, 2007; Ercole et al., 2012) or by passive precipitation in which microorganisms themselves act as nucleation surfaces on which minerals precipitate (Jones and Kahle, 1993; Blyth and Frisia, 2008). There is an ongoing debate about the extent of the microbial role in the formation of moonmilk. Some researchers have claimed to have identified microbial structures associated with the crystal matrix, including calcified cells and filaments (Gradziñsky et al., 1997; Cañaveras et al., 2006), whereas others, citing the lack of unequivocal evidence of bioprecipitation, have attributed moonmilk formation to predominantly inorganic processes (Bernasconi, 1961; Mélon and Bourguignon, 1962; Gèze, 1976; Onac and Ghergari, 1993; Hill and Forti, 1997; Moore and Sullivan, 1997; Borsato et al., 2000). In addition to being precipitated inorganically or by microbes, moonmilk can also be formed by speleothem weathering (Sweeting, 1973; Hill and Forti, 1997). This process is also thought to be biologically mediated; for example, it can result from biochemical corrosion of bedrock by organic acids produced by microrganisms (Caumartin and Renault, 1958). More recently, moonmilk has been attributed to a combination of both physico-chemical and biogenic processes (Onac and Ghergari, 1993; Basillais, 1997).

To determine the role of calcifying bacteria as geological agents in the genesis of moonmilk speleothems from the Grotta Nera in the Abruzzi Region of Italy, a combination of studies have been carried out: microscopic, microbiological, *in vitro* precipitation, and geochemical investigations. Because DNA analysis of bacteria provides no information on the metabolism, the physiology, the ecology, the biochemistry, or the geomicrobiology of a strain, laboratory-based culture experiments and geochemical techniques were used to determine their ability to alter the chemistry of their microenvironment and produce biominerals. This paper reports the results of a preliminary identification and characterization of microorganisms isolated from moonmilk and drip-water samples from the Grotta Nera, Gram staining and cell morphology analysis by light microscopy, chemical analysis by X-ray diffraction and scanning electron miscroscopy of moonmilk and calcium carbonate crystals obtained *in vitro* in the presence of bacterial isolates, and *in vitro* solubilization tests of calcium carbonate by the calcifying bacteria. The results provide additional arguments for the significant role of bacteria as geochemical agents.

SITE AND ENVIRONMENTAL PARAMETERS

Grotta Nera (129A in Catasto Grotte Abruzzo, source of these data)
Elevation: m 1380 a.s.l.
Total length: 110 m Vertical extent: 10 m
Maps: Carta d'Italia Istituto Geografico Militare (1:25000) sheet 147 III NE (Pennapiedimonte), geological map of Abruzzi (1:100,000) (Vezzani and Ghisetti, 1993)

The Grotta Nera is not only one of the most famous and peculiar caves in the Abruzzi region in central Italy (Fig. 1), but it also has the most impressive examples of moonmilk speleothems that have been described in Italy (Forti and Rossi, 2003). It is located in the heart of the Majella National Park, in the Feudo Ugni Natural Reserve, a dense mixed-deciduous forest characterized by large seasonal temperature variations and relatively high precipitation. This park was established in part to protect this peculiar high-altitude karst landscape. In this area, surface karst features have been affected by important signs of glacial erosion. The Majella Massif hosts a complex karst system of several caves (Burri, 2003), some of which are show caves, the most famous of which is the Grotta del Cavallone.

Access to the Grotta Nera has been strictly regulated for many years and is only allowed for scientific purposes to preserve the peculiar concretions for which the cave is famous. The cave is characterized by a wide entrance (Fig. 1). This opens directly on the cliff and is accessible by a rocky route that is made easier by a few cut steps and a safety wire rope. This trail leads into a large room with its floor completely covered by collapsed material, including angular boulders, some of them covered by the remains of broken stalactites (Figs. 1 and 2). This first large space leads on to a narrow passage that is lined with stalagmite columns and protected by a gate. This is the entrance to the main room of the cave, where its peculiar speleothems are concentrated (Figs. 3 and 4a,b,c). In this inner, bell-shaped room, extensive ivory-white deposits of moonmilk as

Figure 1. Grotta Nera entrance from inside. In the foreground a fallen big boulder clutters the passage. In the inset, the red dot shows the approximate location of the cave.

stalactites, stalagmites, and cave pearls cover the whole cavity (Fig. 4). Really impressive stalactites hang from the 10-m high ceiling and show a peculiar shape characterized by an apex diameter that is larger than that of the root and a development not vertical (Fig. 3). These beautiful rounded stalactites are concentrated mostly in a small portion of the room (Fig. 2b) and are huge, with an average length of about 1.5 m. Their size, and consequently their weight, play a key role in their general development. In fact, in the center of the room there is a buildup of broken or fallen stalactites that have been re-cemented by flows of coating material (Fig. 4g). Numerous active gours with growing pisolites inside are also present on the flowstone floor (Fig. 4i).

These peculiar moonmilk formations were described by Forti and Rossi (2003) as *trays* whose development was inferred to be related to strong evaporation caused by complex air flows within the room (Forti and Rossi, 2003; Savini, 2004). Trays are flat-bottomed speleothems that

end in a flat, horizontal surface (Hill and Forti, 1986). The mechanism of their formation is still not well understood. Martini (1986) was the first to speculate on the abiotic origin of carbonate (calcite-aragonite) trays. Calaforra and Forti (1994) have proposed an abiotic mechanism for the growth of gypsum trays. Biogenic trays were found in the submarine cave Lu Lampiùne, one of the most complex and largest caves in the Salento coast of southeastern Italy. Those structures hang abundantly from the roof and lateral walls of the cave, where they show a slanted, non-vertical orientation (Onorato et al., 2003). The trays in the Grotta Nera (Fig. 3) are the biggest so far described in Italy; they have an asymmetric enlargement at the bottom and are similar to a tongue (Forti and Rossi, 2003).

As clearly exposed in the geological map of the cave (Figs. 2, 5), the development of the cave was strongly controlled by several variously oriented faults. One of these faults controls the shape of the room where the moonmilk trays grow and where a clear fault plane is outcropping
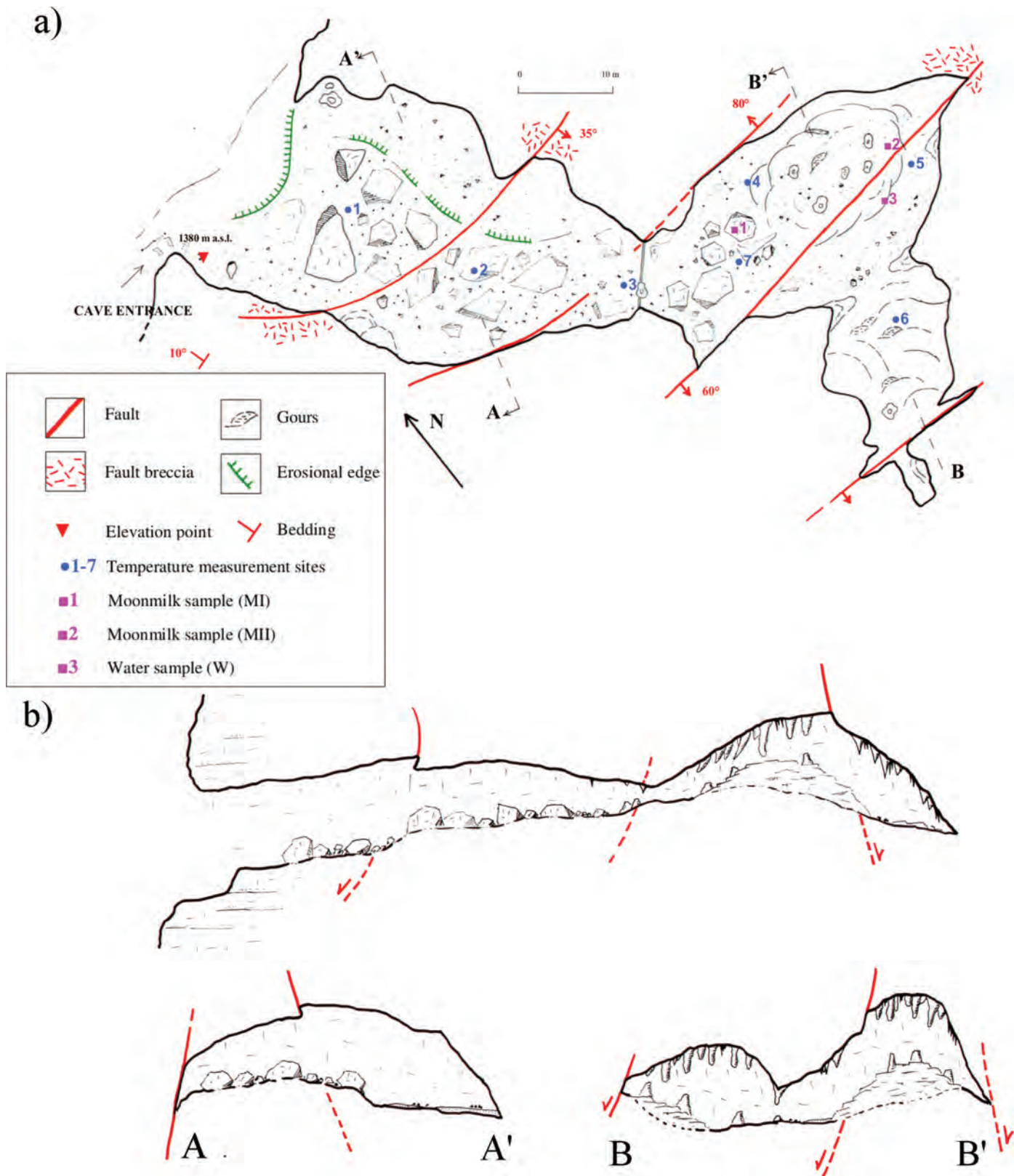
Figure 2. Map and geology of Grotta Nera (Abruzzi, central Italy). Based on a first survey in 1969 by E. Burri, E. Bevilacqua, and G. Di Iorio drawn by E. Burri and a second survey in 2005 by G. Di Prinzio and G. Ferrini drawn by G. Ferrini.

Figure 3. Moonmilk stalactites (trays) hanging from the ceiling of the inner room of the Grotta Nera. Note the peculiar shape and the development differing from the vertical axis.

(Fig. 2b); several plant roots are leaning along the fault plane, showing that the ceiling is relatively thin.

From a speleogenesis point of view, the cavity can be seen as a relict gallery undergoing an important gravity reshaping, especially in the great entrance antechamber; here the big boulders cluttering the passage could be related to collapse linked to the last Holocene glacial period. To date, no water flows or water-transported deposits have been reported in the cave; only a moderate dripping in the inner portion has been noted.

A preliminary survey of air-temperature distribution was carried out to highlight the relationship between the cave and the outside temperatures, measure any thermal gradients inside the cave and their influence on air movement in the cave, and the cave's microclimate. In late
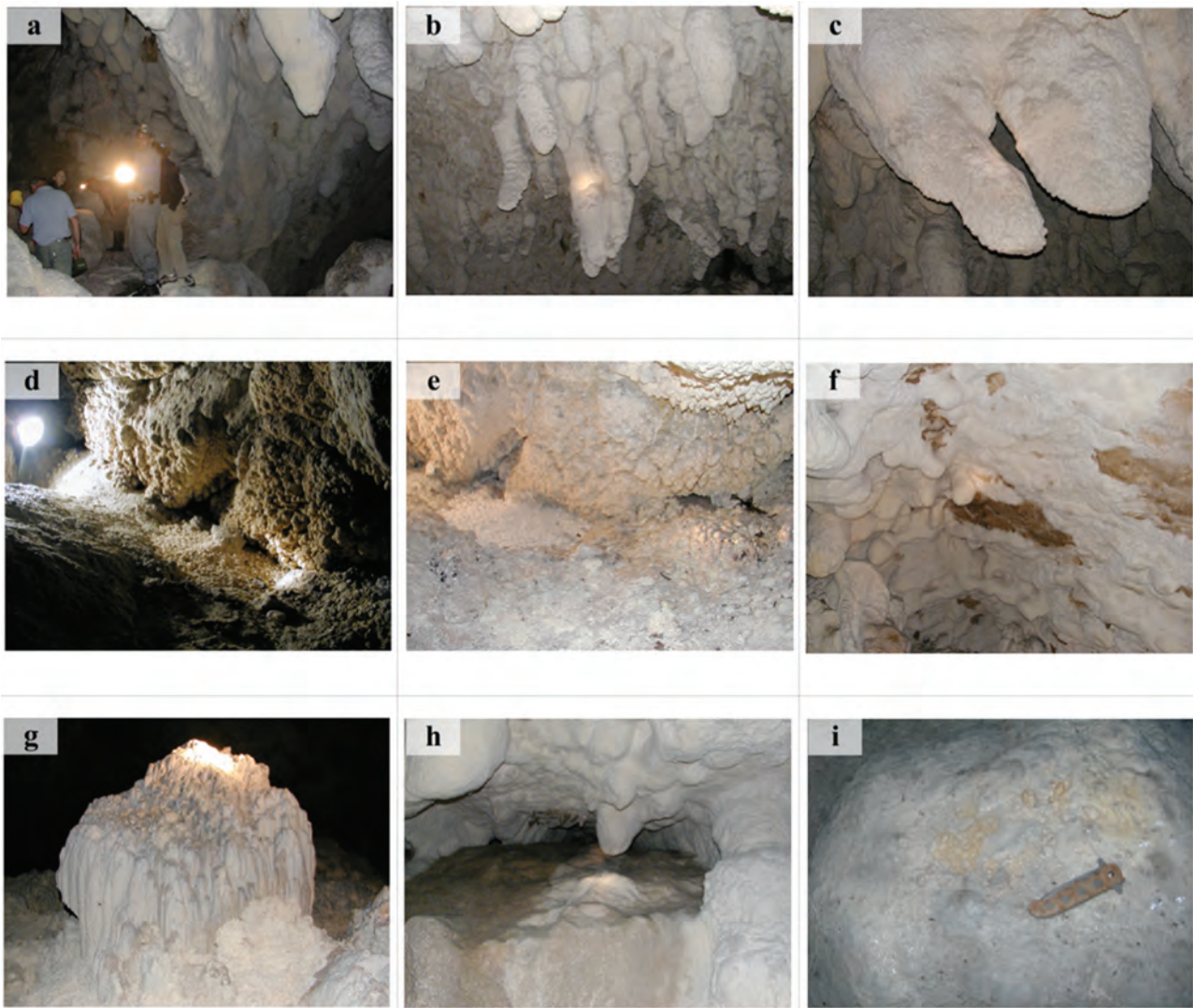
Figure 4. Moonmilk decorating the ceiling (a, b, c), the walls (d, e, f) and the floor (g, h, i) of the inner room of Grotta Nera. Note the huge moonmilk stalactites with an average height of about 1.5 m (a), round and smooth in their form (a, b, c), with a non-vertical development (b,c); a mound formed by fallen stalactites (g); the presence of a bat (h); the presence of pisolites (i).

Figure 5. Temperature distribution in Grotta Nera in late autumn.

spring, early summer, and autumn the air temperature was monitored in seven sites, three in the first room and four in the inner one (Fig. 2a). The collected data showed that the air temperature inside the large entrance room is strongly affected by the climatic conditions outside, which are characterized by strong seasonal variability. The situation is quite different for the inner room. Regardless of the season, a temperature pattern showed relatively small diff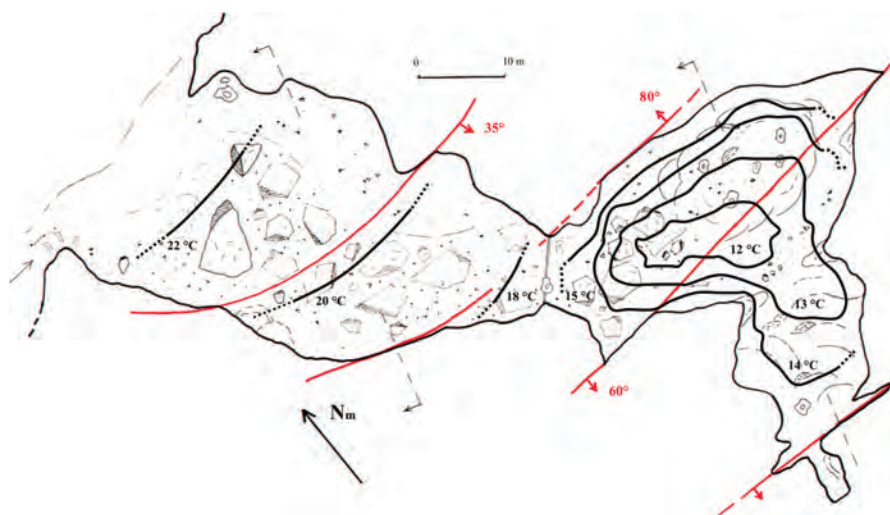erences across the inner room. It was noted that for most of the year the temperatures recorded (an average of 15 °C) were higher than those on the outside. The high temperature measured in the inner room could be due to a low or lack of water circulation during the last period of the cave's evolution and to the geometry of the cave. The Grotta Nera is an ascending cavity with a single input, the entrance being in the lower part of the cave, suggesting that its inner room may behave as a hot trap where air is trapped during the winter (Crammer, 1899). During the summer in a hot trap, the air, which is colder than the outside atmosphere, flows downward, whereas in the winter, the cave air, which is warmer than the outside atmosphere, remains in equilibrium, and there is only a limited circulation at the entrance (Crammer, 1899).

Airflows within the inner room of the Grotta Nera were assessed by smoke movement, and by the three-dimensional pattern of temperatures (Fig. 5) at varying distances in the cave and at varying heights above the cave floor. Circulation inside the inner room seems not to be linked to changes in barometric pressure, which has no influence on the insignif-icant total volume of the cave, but it might possibly be due to an internal convective flow generated by temperature gradients and by exchanges with external air. During the summer, hot air comes in from outside and flows into the inner room, thereby activating a circulation. During the cold season, cold air penetrates in from the exterior through the thin ceiling and generates the same type of air circulation.

In conclusion, the inner room has its own microclimate that, in general, is typical of the hot trap with the peculiarities that are caused by the presence of a very thin layer of upper soil so that the internal circulation in this room of the cave is not limited to the entrance, according to Crammer (1899) but is a more complex circulation (Forti and Rossi, 2003).

Materials and Methods

Sample Location and Sampling

The studied samples were collected in the inner room of the Grotta Nera (Fig. 2a). Two moonmilk samples (MI and MII) were collected respectively from site 1, located 74 m from the entrance, and site 2, located in a more distant portion of the cave (96 m); a sample of percolating water (W) was taken in a sterile tube at site 3. Moonmilk samples were taken aseptically in sterile tubes from small stalactites approximately 15 to 20 cm in length and 3 to 4 cm in diameter. MI was a portion of a white solid stalactite without an internal feeding tube. MII was taken from a stalactite, colored brown due to plant roots, with a large internal tube. The moonmilk and percolating water samples were stored at room temperature (18 °C) for about 18 hours before microbiological analysis was carried out.

Moonmilk Physicochemical Analyses

Moonmilk samples were analyzed by X-ray diffraction and X-ray fluorescence. X-ray diffraction was used to determine the minerals in the moonmilk deposits and the crystals deposited *in vitro*. Measurements were made by using a two-circle θ/2θ diffractometer with a Cu radiation source, secondary graphite monochromator, and scintilla-tion detector (Seifert MZ IV). The supply voltage of the X-ray tube was set at 50 kV and 30 mA. The 2θ-scan range was between 22 and 50°; each scan was done at steps of

0.05°. Depending on the sample density, a counting time between one and ten seconds per step was selected. The crystalline phases were identified using database cards from the International Center for Diffraction Data.

X-ray fluorescence spectroscopy is a non-destructive analysis technique from which it is possible to obtain the elemental composition of a sample through the study of fluorescence radiation. We performed fluorescence spectroscopy on both samples of moonmilk taken in the Grotta Nera at sites 1 and 2 utilizing a SPECTRO (mod. XEPOS 2000) spectrophotometer. Four grams of moonmilk powder were ground down to < 100 µm, well homogenized with 0.9 g of Hoechst wax, and then pressed with 12 tons to a 32-mm pellet.

Isolation and Characterization of Cultivable Heterotrophic Calcifying Bacteria

To isolate the cultivable heterotrophic bacterial microflora that is associated with the moonmilk samples from the Grotta Nera, 10 g of each solid sample was ground to a powder using a sterile mortar and pestle. This powder was then suspended in 90 mL of saline solution (0.9% NaCl). Triplicate B-4 agar plates (Boquet et al., 1973) were inoculated with moonmilk sample dilutions ranging from 10^{-1} to 10^{-6}. The drip-water sample was similarly plated, undiluted or diluted to 10^{-5}. Solid B4 medium was composed (per liter) of 2.5-g calcium acetate, 4.0-g yeast extract, 10.0-g glucose, and 18.0-g agar. The final pH was adjusted, after sterilization, to 8.0 using NaOH. The inoculated plates were incubated at 22 °C, a higher temperature than in the cave from where the samples were obtained, for four weeks in order to isolate slowly growing strains. Previous studies have demonstrated that colonies from cave samples grow very slowly at cave temperature and that the diversity of the cultivable genera observed was similar whether the bacteria were grown at 13 °C (cave temperature) or at 28 °C (Groth et al., 2001; Laiz et al., 2003). Individual colonies were selected and purified by streaking on B-4 agar. The relative abundance of each isolate, with respect to the total cultivable bacterial microflora, was determined by direct counts on B-4 agar plates. For short-term preservation, the isolates were streaked on B-4 agar slants and stored at 4 °C, but for long-term maintenance, pure calcifying isolates were stored in liquid nitrogen at −196 °C. Cell and aggregate morphology was studied under a light microscope (Leitz-Biomed), and Gram-staining was performed with the Color Gram 2 kit (bioMérieux, Marcy-l'Etoile, France).

Calcium Carbonate Precipitation and Dissolution by Calcifying Bacteria

We assessed the calcite production of isolates by culturing them on B-4 agar plates, as described above. The bacterial isolates were spread in triplicate on the surface of agar plates and were then incubated aerobically at 15, 22, or 32 °C. For up to 30 days after inoculation, to follow crystal production,

all plates were examined daily under a light microscope (Leitz-Biomed). With respect to negative controls, we checked for the presence of crystals in a sterile medium and in a medium inoculated with autoclaved bacteria.

Since it has been established that microbially mediated reactions can generate considerable amounts of H^+ ions that can dissolve the cave walls or the speleothems and that moonmilk can also be formed by speleothem decay (Sweeting, 1973; Hill and Forti, 1997), the ability of calcifying bacteria to dissolve calcium carbonate was also tested. Calcifying isolates were grown on Deveze-Bruni medium (pH 6.8) containing 0.14 or 2.5% $CaCO_3$ at 15 °C (Normal Commision, 1990). Carbonate solubilization after 7, 15, and 30 days was quantified by measuring the diameter of the clear halo that surrounded each colony in response to decreased pH (Martino et al., 1992).

SEM Analysis

Morphological characteristics were studied by scanning electron microscopy. Cultured solid media samples were dried at 37 °C; agar medium was cut into flat blocks, gold-shadowed, and observed with a Philips scanning electron microscope XL30CP.

For crystallite-poor samples, the method of Rivadeneyra et al. (1998) was applied. The crystals produced by cultured bacteria were removed from the medium by cutting out agar blocks and placing them in boiling water until the agar dissolved. The supernatants were decanted and the sediment was resuspended and washed in distilled water until the crystals were free of impurities. The washed crystals were air-dried at 37 °C and then used for SEM analysis. To observe the inner portion of the bioliths, crystals were first powdered by using a mortar and pestle.

Results and Discussion

Moonmilk Physicochemical Analyses

X-ray diffraction revealed that both samples of moonmilk taken at the Grotta Nera consist of a single mineral phase of calcium carbonate, i.e., calcite. On the other hand, according to previous literature, moonmilk is usually composed of calcite (Fisher, 1992, 1993), even though the presence of other carbonates, as well as sulfates and phosphates in moonmilk, has been reported by several authors (Onac and Ghergari, 1993; Hill and Forti, 1997; Moore and Sullivan, 1997; Borsato et al., 2000; Lacelle et al., 2004). X-ray fluorescence analysis showed that the moonmilk consists primarily of CaO (60.87% at site 1, sample MI, and 60.18% at site 2, sample MII), while other constitutive elements such as MgO and Al_2O_3 never reached 1% (Table 1).

Microbial Cultures from Moonmilk and Dripping Water

The cultures from both moonmilk deposits and dripping water yielded a visible growth for common soil

Table 1. Chemical contents of moonmilk from site 1 (sample MI) and site 2 (sample MII) in Grotta Nera.

Mineral Constituent	Sites	
	Site 1	Site 2
CaO	60.87	60.18
MgO	< 0.83	< 0.83
Al_2O_3	< 0.19	< 0.19
P_2O_5	0.18	0.19
SiO_2	0.05	0.06
SO_3	0.05	0.04
Fe_2O_3	0.01	0.02
MnO	0.01	0.01
K_2O	< 0.01	< 0.01

microflora groups (fungi, bacteria, and actinomycetes bacteria) (Fig. 6), but the dominant cultivable microorganisms were bacteria that caused significant crystallization. A wide range of microbes, particularly bacteria and streptomycetes bacteria, but also fungi, algae, and protozoa, can also be cultured from moonmilk, often in very high densities (Northup et al., 2000).

By using the traditional cultivation techniques, an abundant cultivable heterotrophic bacterial microflora from the moonmilk samples MI (2.1×10^4 colony-forming units per gram of dry weight) and MII (6.0×10^4 cfu/g d.w.) was isolated, suggesting that bacteria presence was probably not accidental. A similar bacterial density has been reported by Baskar et al. (2011) for moonmilk deposits from Krem Mawmluh Cave, India. A similar bacterial density for the calcareous speleothems from the Stiffe and Cervo Caves and also for an unusual newly

described calcite speleothem from Grave Grubbo Cave were reported in our previous studies (Cacchio et al., 2003, 2004, 2012). The higher bacterial density in sample MII may be related to a greater presence of organic matter released from plant roots and to a greater water content. The active moonmilk samples taken from the Grotta Nera had a water content of 74% (MI) and 78% (MII) in summer.

Based on the cell and colony morphologies of the isolates (Table 2), it was concluded that the sample MI contained nine cultivable microbial strains (eight bacterial isolates numbered from M1 to M8 and one mold), while the moonmilk sample named MII contained eight cultivable microbial strains (four bacterial isolates numbered from M9 to M12 and four molds). The cultivable heterotrophic bacterial density found in the sample of percolating water, was of two orders of magnitude lower than that found in moonmilk (4.1×10^2 cfu/mL). However, the dripping water contained a considerable number of bacteria, and they could not have filtered through the thin layer of rock that covers the cave, due to the fact that the Grotta Nera is in a mixed-deciduous forest. From this sample four strains were isolated, three bacterial strains named from W1 to W3 and one mold.

RELATIVE ABUNDANCE AND PRELIMINARY
CHARACTERIZATION OF BACTERIAL ISOLATES

The most abundant strains were the following: isolate M8 from the moonmilk sample MII, isolate M9 from the moonmilk sample MII, and the W2 strain from the drip-water sample. These bacterial strains represented 40.00%, 73.12%, and 68.05% of their samples' respective bacterial populations. The strains M2 and M3 represented 22.90%
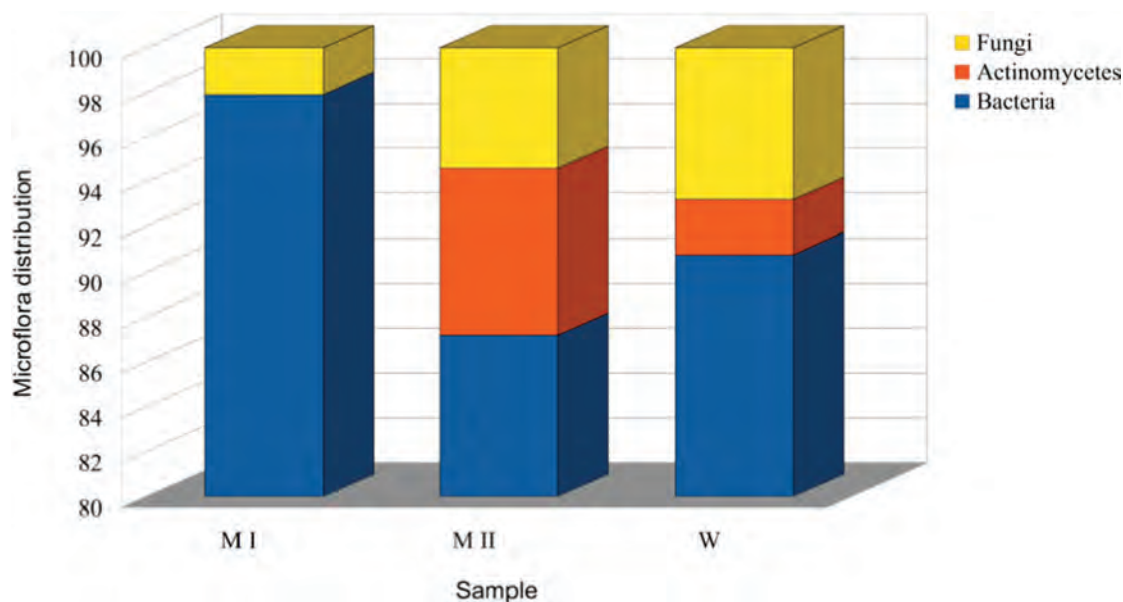

Figure 6. Distribution of actinomycetes, other bacteria, and fungi (percentage of strains) in the cultivable heterotrophic microflora from moonmilk (MI and MII) and percolating water (W) samples collected from Grotta Nera.

Table 2. Bacterial strains isolated from moonmilk and water samples collected from Grotta Nera, Abruzzi, Italy, with their colony and cell morphologies, Gram result, and relative abundances.

Isolate	Colony Morphology	Cell Morphology	Gram	Relative Abundance
MI Moonmilk Sample				
M1	Medium creamy	Rod chain	G−	2.13
M2	Medium creamy	Single rod	G−	22.90
M3	Medium white	Single rod	G−	17.89
M4	Punctiform creamy	Single rod	G−	2.18
M5	Big creamy	Single rod	G−	4.26
M6	Big white	Rod chain	G+	4.26
M7	Medium yellowish	Single rod	G−	6.38
M8	Medium white	Single rod	G−	40.00
MII Moonmilk Sample				
M9	Punctiform pink	Rod chain	G−	73.12
M10	Medium black	Actinom.	G+	7.42
M11	Small creamy	Rod chain	G−	14.13
M12	Big creamy	Rod chain	G+	5.33
Water Sample				
W1	Punctiform creamy	Single rod	G+	29.51
W2	Small yellowish	Single rod	G−	68.05
W3	Punctiform white	Actinom.	G+	2.44

and 17.89% of the MI moonmilk bacterial population, respectively. The strain M11 represented 14.13% of the MII sample, while the strain W1 represented 29.51% of the bacterial population in the percolating water sample. The contributions of the remaining isolates to the overall respective bacterial population ranged from 2.13% to 7.42%.

The actinomycetes component did not exceed 7.42% of the total bacterial population in the MII moonmilk sample, taken in the presence of plant roots, and 2.44% in the drip-water sample. In sample MI from the fully moonmilk speleothem, the actinomycetes component was absent (Table 2). Actinomycetes are common in caves, where their growth is related not only to particular environmental conditions, such as temperature ranging from 10 to 15 °C and high relative humidity, but also to the input of refractory organic matter in dripping water (Groth and Saiz-Jimenez, 1999). Dissolved organic matter from soil, which is the origin of the organic carbon found in dripping waters, contains aliphatic organic acids and phenolic compounds produced by lignocellulose degradation (Guggenberg et al., 1994; Saiz-Jimenez and Hermosin, 1999). Both lignocellulose and humic materials are almost selectively degraded by actinomycetes, which are well known for their ability to grow on very poor media and to use recalcitrant organic matter (Crawford et al., 1983; McCarthy, 1987; Groth and Saiz-Jimenez, 1999). The findings of this research not only confirm the importance of temperature and relative humidity to determine actinomycetes colonization and long-term growth on cave surfaces, but also underlines the role of recalcitrant organic

matter that, according to our results, seems to be the main determining factor. In fact, the proportion of actinomycetes among the bacterial microflora is higher in the sample MII, which receives organic matter from percolating water and plant roots, than in the drip-water sample, and they disappear entirely in the stalactite of moonmilk that does not receive organic matter from dripping water and root exudates.

These results are interesting, but may not reflect the actual microbial activity taking place in the speleothem because cultivation techniques are thought to greatly underestimate microbial diversity due to the non-culturability of the large majority of microorganisms (Dojka et al., 2000). In this study, single small rods and rod chains predominate in the strains isolated (Table 2). An examination of Gram-stained smears taken from the fifteen different colony types from moonmilk deposits and drip-water showed that the majority (66.7%) of the isolated strains were Gram-negative (Table 2). The relative abundances of each isolate with respect to the total cultivable bacterial microflora showed that (Fig. 7 and Table 2) the most abundant strains (M2 and M8 strains in the MI sample, M9 and M11 strains in the MII sample) in both the studied moonmilk samples were Gram-negative, as previously found by some authors elsewhere (Danielli and Edington, 1983; Mulec et al., 2002). The Grotta Nera is located in a mixed-deciduous forest, and it is known from previous literature that Gram-negative bacteria tend to be more abundant in rhizosphere soil compared to the bulk soil (Schlegel, 1993; Steer and Harris, 2000): Gram-negative bacteria biomass increases when rapidly decomposable
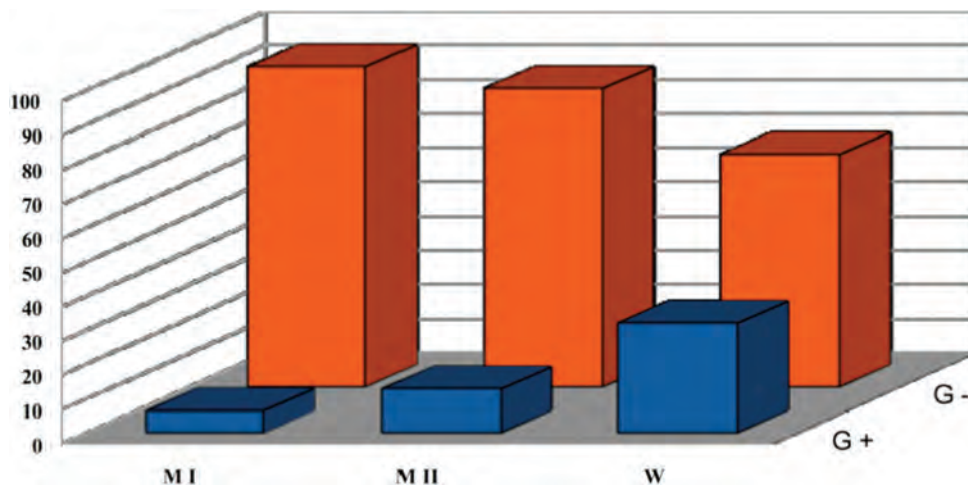
Figure 7. Gram-negative/Gram-positive proportions in the cultivable heterotrophic bacterial microflora of moonmilk (M I and M II) and percolating water (W) samples collected from Grotta Nera, by relative abundance (see Table 2).

carbon compounds, such as sugars and organic and amino acids, are available (Marilley and Aragno, 1999), whereas higher proportions of Gram-positive bacteria are usually found in resource limited areas (Atlas and Bartha, 1998; Kourtev et al., 2002). In fact, the ratio of Gram-negative to Gram-positive bacteria in moonmilk samples MI (95.74%) and MII (87.25%) was significantly higher than in previously studied consolidated calcareous speleothem and soil samples (Cacchio et al., 2003, 2004, 2012) from which nearly all strains isolated were Gram-positive. A high proportion (68.05%) of Gram-negative bacteria was also found in the percolating water sample. In general, cultivable bacterial communities from groundwater have low proportions of Gram-positive bacteria (Laiz et al., 1999). No attempts were made to identify the various bacterial species present, as attention was directed on the processes of carbonate deposition rather than on taxonomy.

In Vitro Bacterial Precipitation and Dissolution of Calcium Carbonate

Since all the molds isolated from moonmilk and water samples were incapable of precipitating $CaCO_3$ crystals, this suggests a major participation of bacteria in the biomineralization processes involved in the moonmilk stalactite formation. Some previous studies have suggested fungi as the major participants in the process (Callot et al., 1985), although more recent investigations have proposed bacteria as the major inducers of carbonate deposition forming moonmilk in caves (Cañaveras et al., 2006; Barton and Northup, 2007; Portillo and Gonzales, 2011). Bacterial $CaCO_3$ precipitation on B-4 solid medium occurred at all the temperatures tested, 15 °C (cave temperature), 22 °C, and 32 °C. Under laboratory conditions, it was found that all of the bacterial isolates associated with the hollow stalactite (sample MII) and the drip-water sample were capable of forming crystalline calcium carbonate. This confirms the hypothesis that in appropriate conditions, especially in carbonate-rich environments such as limestone caves, many bacteria can form calcium carbonate crystals (Boquet et al., 1973; Cacchio et al., 2003, 2004, 2012). Not all of the bacterial strains isolated from the solid moonmilk stalactite (sample MI) were calcifying; the high relative abundance (40%) of strain M8, which was not capable of precipitating crystals, is consistent with the less intense calcification of this stalactite. This is consistent with our previous hypothesis (Cacchio et al., 2004), according to which drip-water may select calcifying bacteria, and hence the intensity of calcifying activity is greater in younger stalactites. It is worth noting that in tubular stalactites, calcification also takes place in the inner surface, giving rise to filling of the space (Moore and Sullivan, 1997). By using a knock-out in the *cha*A calcium antiporter protein, Banks et al. (2010) have suggested that calcium toxicity provides both the physiological basis and selection pressure for the calcification phenotype. All the Gram-positive strains isolated from the Grotta Nera were capable of depositing crystals on B4 agar plates at all the studied temperatures. The comparison of the percentages of calcifying bacteria isolated from the previously studied caves (Cacchio et al., 2003, 2004, 2012) has shown that the temperature factor plays a key role in the extent of calcium carbonate deposition by bacteria. In fact, in Stiffe and Cervo Caves, the temperature ranges from 10 to 12 °C, whereas in Grave Grubbo Cave, located in south Italy, where the range is 14 to 15 °C the biogenic activity is, as in the Grotta Nera, much more impressive. Hence, it can be suggested that 15 °C is the threshold of two biologically different calcification environments.

Carbonate precipitation by calcifying isolates at 22 and 32 °C started with some delay compared to that at 15 °C. All the calcifying bacteria began to precipitate carbonate after three days at 15 °C, after one week at 22 °C, and after
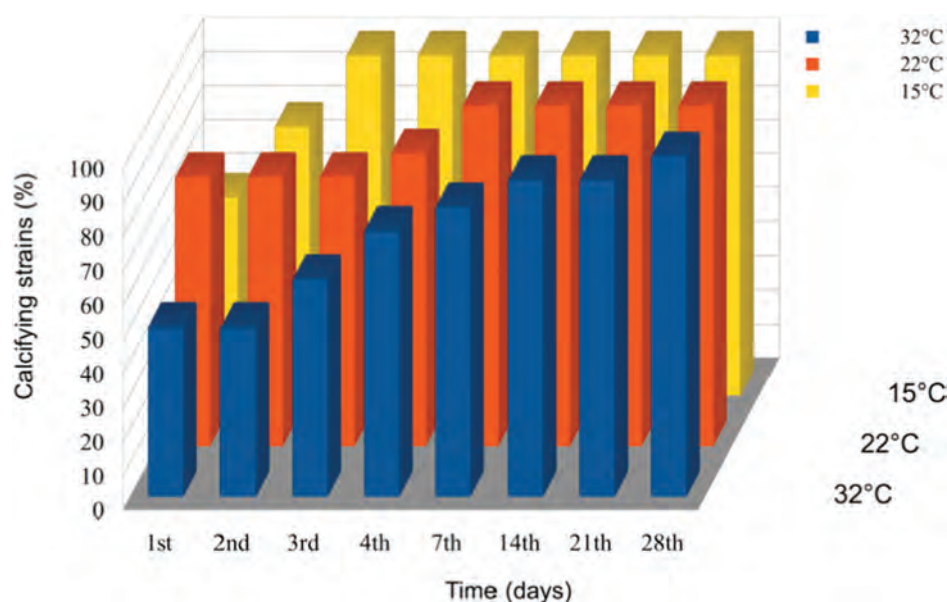
Figure 8. Relationship between percentage of calcifying strains showing production of calcite by the indicated duration of culturing on B-4 agar cultures at 15 °C, 22 °C, and 32 °C. Note non-linear X axis.

four weeks at 32 °C (Fig. 8). In our previous studies, it was found that calcification took place more quickly at 32 °C than at lower temperatures, including the temperature of the studied caves (Cacchio et al., 2003, 2004, 2012). In fact, the bacteria isolated from moonmilk deposits are much more rapid in the process of calcification in the cave than the strains isolated from cave speleothems not consisting of moonmilk (Cacchio et al., 2003, 2004, 2012). To explain this significant difference, a working hypothesis is adopted that microbes inhabiting the Grotta Nera have been exposed to a longer period of evolution at a constant temperature of 15 °C, hence strengthening their calcification capability at such a temperature. In the other studied caves, which have running water, the temperature tends to change throughout the year according to the discharge changes and periods of drought.

The calcite nature of the crystals deposited on B4 agar plates was confirmed by X-ray diffraction analysis. No carbonate precipitation took place in the controls since metabolic activity is necessary for precipitation.

The corrosion behavior of the calcifying isolates was also studied showing that 13% of the calcifying bacteria isolated from the MII moonmilk speleothem solubilized calcium carbonate when grown on agar plates containing 0.14% and 2.5% $CaCO_3$ after two weeks at 15 °C. This percentage increased to 32% for the calcifying bacteria isolated from the dripping water. With respect to the solubilization activity of the calcifying bacteria associated with the MI moonmilk speleothem, this was at least 32% after one week at 15 °C. However, the calcifying bacteria isolated from the Grotta Nera Cave showed a greater ability to dissolve calcium carbonate than those associated

with consolidated stalactites sampled from previously studied caves (Cacchio et al. 2003, 2004 and 2012).

SEM ANALYSIS

Scanning electron micrographs of the crystals deposited on B-4 agar plates revealed significant amounts of bacterial cells on the inner surface of the crystals (Fig. 9a,b), calcified bacterial cells (Fig. 9e,f) and their imprints (Fig. 10c,d,e,f); newly formed (Fig. 9a,b,c,d) or calcified biofilms (Fig. 9e,f) cementing the carbonate grains; and the presence of crystals that vary in size and shape (Fig. 10a,b). SEM studies of the extensive moonmilk deposits in the Grotta Nera revealed that they were mainly composed of a network of fiber calcite crystals and filaments (Fig. 10g,h). The results of SEM examination point toward a significant bacterial influence in the genesis of moonmilk in the Grotta Nera.

CONCLUSIONS

Caves are extreme and specialized habitats for terrestrial life that sometimes contain moonmilk. There are many caves around the world with impressive amounts of moonmilk (Onac and Farcas, 1992; Chirienco, 2002). In Italy, calcite moonmilk is found in many caves in the Italian Alps (Borsato et al., 2000). The Cesare Battisti Cave contains moonmilk deposits up to 0.5 m thick and 120 m long that developed under several seepages (Borsato et al., 2000) and a moonmilk flowstone on the wall of the Cripta Chamber that has developed to a thickness of 40 to 50 cm. In the Bus del Toni Cave, there are extensive curtains of moonmilk (Miorandi and Borsato, 2005)
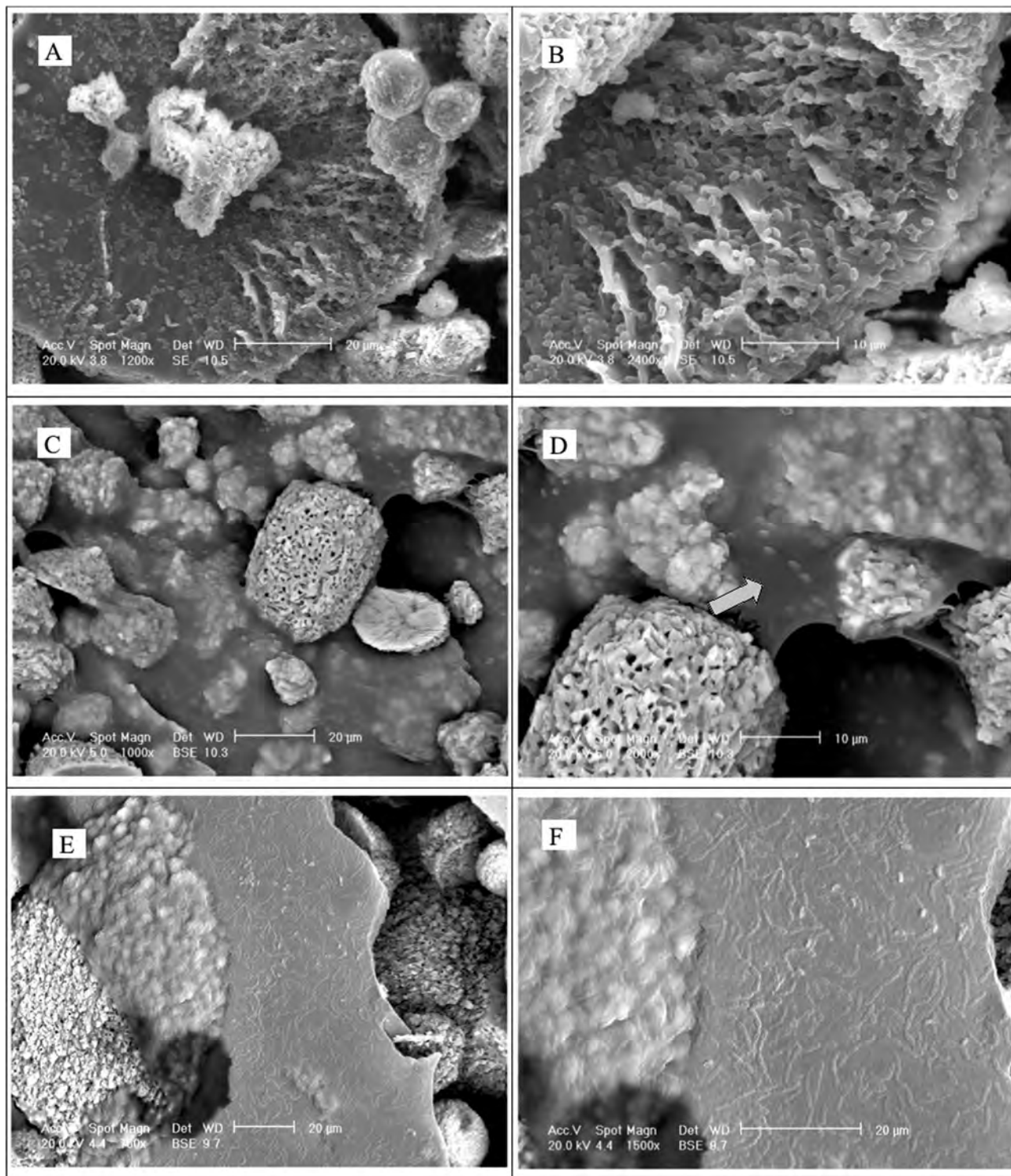
Figure 9. Scanning electron micrographs: (a) Calcifying bacterial cells isolated from moonmilk collected from Grotta Nera of the unidentified strain M5 on the inner surface of a CaCO$_3$ crystal precipitated on B-4 agar, after 30 days at 22 °C; scale bar 20 μm. (b) Higher magnification view of (a); scale bar 10 μm. Observe the significant number of bacterial cells and the presence of biofilm. (c) Bacterial cells included in a biofilm that bridges calcite crystals deposited on B-4 agar plates after 30 days of incubation at 32 °C of the strain W1 isolated from a sample of drip-water collected in Grotta Nera; scale bar 20 μm. (d) Higher magnification view of (c); arrow points to some of the cells. Scale bar 10 μm. (e) Cemented biofilms that incorporate the calcifying cells of the M9 strain isolated from moonmilk collected in Grotta Nera, observed after 30 days of incubation on B-4 agar at 32 °C; scale bar 20 μm. (f) Higher magnification view of (e); scale bar 20 μm. Observe the significant thickness of the calcium carbonate layer produced by M9, the most abundant strain in the MII moonmilk sample; compare with (c).
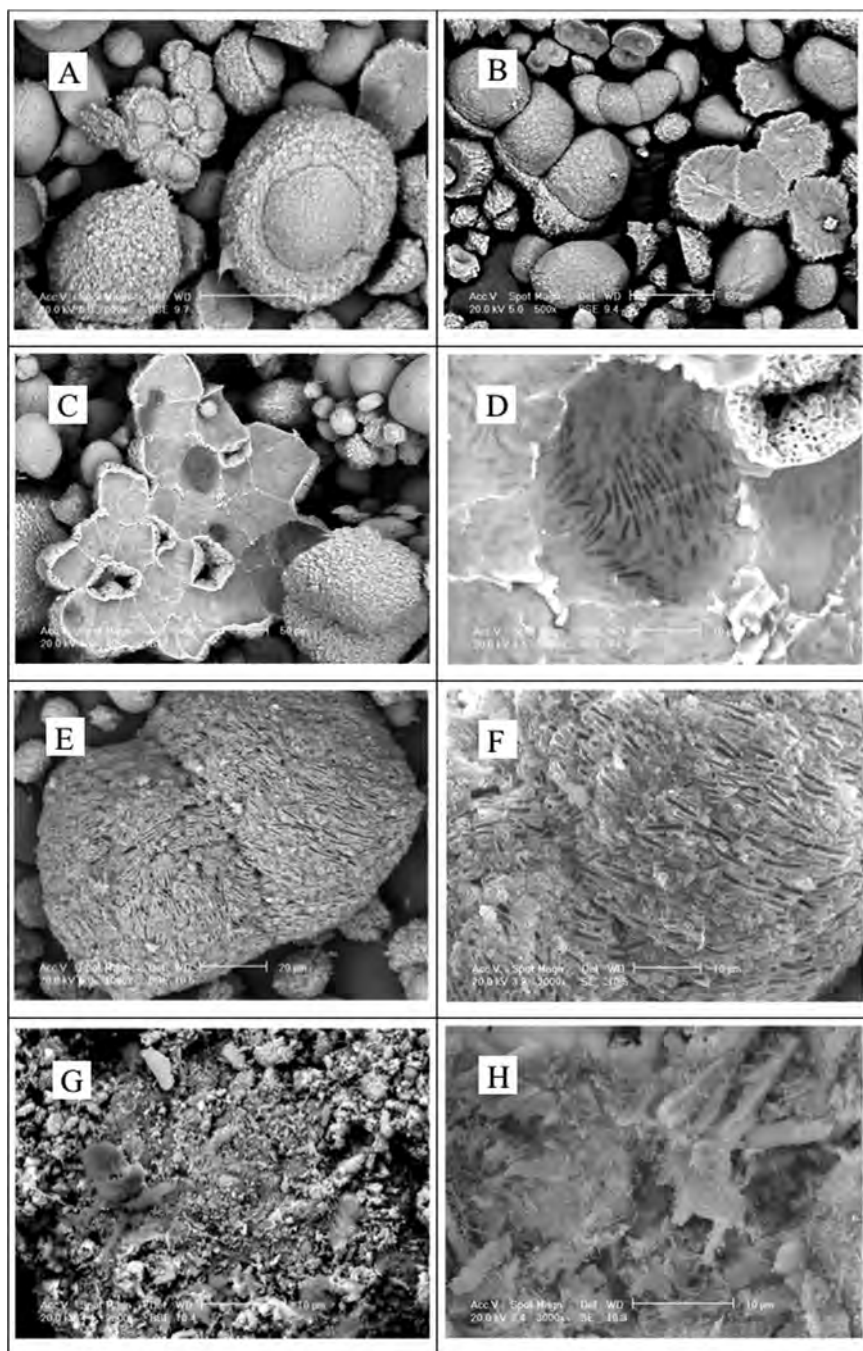
Figure 10. Scanning electron micrographs of CaCO₃ deposited on B4 agar plates by the strain M9, isolated from moonmilk sample MII collected in Grotta Nera. Spherulite crystals and calcite aggregates; (a) scale bar 50 μm, (b) scale bar 50 μm. Bacterial imprints in the inner portion of the crystals; (c) scale bar 50 μm, (d) scale bar 10 μm, (e) scale bar 20 μm, (f) scale bar 10 μm. Calcite moonmilk fiber; (g) scale bar 10 μm, (h) scale bar 10 μm.

In the Grotta Nera, moonmilk entirely covers the walls, the ceiling, and the floor of the room, generating exceptional examples of decorations, including stalactites, stalagmites, and cave pearls. Even though in Italy it is not common to find extensive moonmilk deposits, the extraordinary scientific importance of this cave is mainly linked to the presence of unusual speleothems classified as *trays* whose size has no equal in other caves in Italy (Forti and Rossi, 2003).

Our preliminary study of cultivable microbial populations in two samples of moonmilk and one of dripping water from Grotta Nera was carried out to estimate the concentration of colony-forming units; no identification of genera and species was provided. This study revealed high

cultivable heterotrophic population densities and a diverse microbial community, including filamentous bacteria, associated with the moonmilk. Moonmilk and drip-water bacterial communities tend to have low proportions of Gram-positive bacteria and are mainly composed of Gram-negative single rods and rod chains. This can be ascribed to the fact that Gram-positive bacteria are likely to be more successful in resource-limited areas, suggesting that the association of moonmilk with Gram-negative bacteria is at least partially driven by the characteristics of the soil and overlying vegetation. Most of the bacteria isolated have the ability to precipitate calcite crystals when cultured using B-4 agar, and due to their metabolic activity this probably happens also in natural habitats. In carbonate caves, the metabolism of microorganisms can alter their microenvironment, if products of microbial activity result in a pH increase in the environment. An increase in metabolic end products, such as carbonate ions, can increase precipitation of calcium carbonate in caves (Braissant et al., 2002; Barton and Northup, 2007; Portillo et al., 2009). The different morphologies of the precipitates formed by the different calcifying isolates confirmed that crystal morphology was species-specific, and this suggests that the bacteria play a major role in the precipitation process. When examined by scanning electron microscope, the Grotta Nera moonmilk samples exhibited a felted mat of fibers; X-ray diffraction analysis of the speleothems gave clear evidence for calcite.

The electron microscopic and microbiological evidences, together with the geochemistry and environmental data obtained in this study, indicate that moonmilk from the Grotta Nera stalactites is of biogenic origin. It is therefore possible to infer that there are two different bacterial contributions to the biogenic moonmilk hosted in the Grotta Nera, active precipitation of moonmilk by bacteria and bacterial biochemical corrosion of the bedrock by organic acid, as suggested by the presence of non-calcitic mineral inclusions into the moonmilk and by the solubilization activity of the calcifying bacterial strains.

The extensive presence of biogenic moonmilk in Grotta Nera may be related to the peculiar $CaCO_3$ precipitation environment, i.e., its middle elevation, mixed-deciduous vegetation cover, and local microclimate. Therefore a conclusion of this study is that microbial activity at a constant and optimum temperature appears to be a key factor promoting calcite precipitation and moonmilk formation in Grotta Nera.

References

Atlas, R.M., and Bartha, R., 1998, Microbial Ecology: Fundamentals and Applications, 4th edition: San Francisco, Benjamin Cummings, 640 p.

Banks, E.D., Taylor, N.M., Gulley, J., Lubbers, B.R., Giarrizo, J.G., Bullen, H.A., Hoehler, T.M., and Barton, H.A., 2010, Bacterial calcium carbonate precipitation in cave environments: a function of calcium homeostasis: Geomicrobiology Journal, v. 27, p. 444–454. doi:10.1080/01490450903485136.

Barton, H.A., and Northup, D.E., 2007, Geomicrobiology in cave environments: past, current and future perspectives: Journal of Cave and Karst Studies, v. 69, p. 163–178.

Basillais, A., 1997, Dégradation des parois de grotte en milieu souterrain: Mémoire de DEA, Centre de Recherche sur la Matière Divisée, Université d'Orléans, France, 24 p., plates.

Baskar, S., Baskar, R., and Routh, J., 2011, Biogenic evidences of moonmilk deposition in the Mawmluh Cave, Meghalaya, India: Geomicrobiology Journal, v. 28, p. 252–265. doi:10.1080/01490451.2010.494096.

Bernasconi, R., 1961, L'evolution physico-chimique du mondmilch: Rassegna Speleolog Italiana Memoire, v. 5, p. 75–100.

Bernasconi, R., 1976, The physio-chemical evolution of moonmilk: Cave Geology, v. 1, p. 63–88. (English translation of Bernasconi, 1961.)

Bertouille, H., 1972, Le mondmilch, repère climatique?: Annales de Spéléologie, v. 27, p. 609–623.

Blyth, A.J., and Frisia, S., 2008, Molecular evidence for bacterial mediation of calcite formation in cold high-altitude caves: Geomicrobiology Journal, v. 25, p. 101–111. doi:10.1080/01490450801934938.

Boquet, E., Boronat, A., and Ramos-Cormenzana, A., 1973, Production of calcite (calcium carbonate) crystals by soil bacteria is a general phenomenon: Nature, v. 246, p. 527–529. doi:10.1038/246527a0.

Borsato, A., Frisia, S., Jones, B., and Van Der Borg, K., 2000, Calcite moonmilk: Crystal morphology and environment of formation in caves in the Italian Alps: Journal of Sedimentary Research, v. 70, p. 1171–1182. doi:10.1306/032300701171.

Boston, P.J., Spilde, M.N., Northup, D.E., Melim, L.A., Soroka, D.S., Kleina, L.G., Lavoie, K.H., Hose, L.D., Mallory, L.M., Dahm, C.N., Crossey, L.J., and Schelble, R.T., 2001, Cave biosignature suites: Microbes, minerals, and Mars: Astrobiology, v. 1, p. 25–55. doi:10.1089/153110701750137413.

Braissant, O., Bindschedler, S., Daniels, A.U., Verrecchia, E.P., and Cailleau, G., 2012, Microbial activities in moonmilk monitored using isothermal microcalorimetry (Cave of Vers Chez le Brandt, Neuchatel, Switzerland): Journal of Cave and Karst Studies, v. 74, no. 1, p. 116–126. doi:10.4311/2011JCKS0213.

Braissant, O., Verrecchia, E.P., and Aragno, M., 2002, Is the contribution of bacteria to terrestrial carbon budget greatly underestimated?: Naturwissenschaften, v. 89, p. 366–370. doi:10.1007/s00114-002-0340-0.

Burri, E., 2003, Gli ambienti naturali, in Latini, M.L., and Burri, E., eds., Parco Nazionale della Majella. La montagna dei lupi, degli orsi e dei santi eremiti: Pescara, Italy, Carsa Edizioni, 272 p.

Cacchio, P., Contento, R., Ercole, C., Cappuccio, G., Preite Martinez, M., and Lepidi, A., 2004, Involvement of microorganisms in the formation of carbonate speleothems in the Cervo Cave (L'Aquila-Italy): Geomicrobiology Journal, v. 21, p. 497–509. doi:10.1080/01490450490888109.

Cacchio, P., Ercole, C., Cappuccio, G., and Lepidi, A., 2003, Calcium carbonate precipitation by bacterial strains isolated from limestone cave and from a loamy soil: Geomicrobiology Journal, v. 20, p. 85–98. doi:10.1080/01490450303883.

Cacchio, P., Ercole, C., Contento, R., Cappuccio, G., Preite Martinez, M., Del Gallo, M., and Lepidi, A., 2012, Involvement of bacteria in the origin of a newly described speleothem in the gypsum cave of Grave Grubbo (Crotone-Italy): Journal of Cave and Karst Studies, v. 74, no. 1, p. 7–18. doi:10.4311/2010MB0136R.

Calaforra, J.M., and Forti, P., 1994, Two new types of gypsum speleothems from New Mexico: gypsum trays and gypsum dust: Bulletin of the National Speleological Society, v. 56, p. 32–37.

Callot, G., Mousain, D., and Plassard, C., 1985, Concentrations de carbonate de calcium sur les parois del hyphes mycéliens: Agronomie, v. 5, p. 143–150.

Cañaveras, J.C., Cuezva, S., Sanchez-Moral, S., Lario, J., Laiz, L., Gonzales, J.M., and Saiz-Jimenez, C., 2006, On the origin of fiber calcite crystals in moonmilk deposits: Naturwissenschaften, v. 93, p. 27–32. doi:10.1007/s00114-005-0052-3.

Castanier, S., Le Métayer-Levrel, G., and Perthuisot, J.-P., 1999, Ca-carbonates precipitation and limestone genesis—the microbiogeologist point of view: Sedimentary Geology, v. 126, p. 9–23. doi:10.1016/S0037-0738(99)00028-7.

Caumartin, V., and Renault, P., 1958, La corrosion biochimique dans un réseau karstique et la genèse du mondmilch: Notes biospéleologiques, v. 13, p. 87–109.

Chirienco, M., 2002, Calcite moonmilk in the Humpleu Cave system (Romania): the relationship between crystal morphology and cave topoclimate: Cave and Karst Science, v. 29, no. 3, p. 101–104.

Crammer, H., 1899, Eishöhlen- und Windröhren-Studien: Vienna, Abhandlungen der Kaiserlich-Königlichen Geographischen Gesellschaft in Wien, no. 1, p. 19–76.

Crawford, D.L., Pometto, A.L. III, and Crawford, R.L., 1983, Lignin degradation by *Streptomyces viridosporus*: isolation and characterization of a new polymeric lignin degradation intermediate: Applied and Environmental Microbiology, v. 45, p. 898–904.

Curry, M.D., Boston, P.J., Spilde, M.N., Baichtal, J.F., and Campbell, A.R., 2009, Cottonballs, a unique subaqueous moonmilk, and abundant subaerial moonmilk in Cataract Cave, Tongass National Forest, Alaska: International Journal of Speleology, v. 38, no. 2, p. 111–128.

Danielli, H.M.C., and Edington, M.A., 1983, Bacterial calcification in limestone caves: Geomicrobiology Journal, v. 3, p. 1–16. doi:10.1080/01490458309377780.

Dojka, M.A., Harris, J.K., and Pace, N.R., 2000, Expanding the known diversity and environmental distribution of an uncultured phylogenetic division of bacteria: Applied and Environmental Microbiology, v. 66, no. 4, p. 1617–1621. doi:10.1128/AEM.66.4.1617-1621.2000.

Ercole, C., Bozzelli, P., Altieri, F., Cacchio, P., and Del Gallo, M., 2012, Calcium carbonate mineralization: involvement of extracellular polymeric materials isolated from calcifying bacteria: Microscopy and Microanalysis, v. 18, no. 4, p. 829–839. doi:10.1017/S1431927612000426.

Fisher, H., 1988, Etymology, terminology, and an attempt of definition of mondmilch: NSS Bulletin, v. 50, p. 54–58.

Fisher, H., 1992, Type locality of mondmilch: Cave Science, v. 19, p. 59–60.

Fisher, H., 1993, Mondmilchloch: la cavité type du mondmilch (Obwalden, Suisse): Karstologia, no. 21, p. 56–58.

Ford, D., and Williams, P., 2007, Karst Hydrogeology and Geomorphology: Chichester, John Wiley and Sons, 562 p.

Forti, P., 2001, Biogenic speleothems: an overview: International Journal of Speleology, v. 30A, p. 39–56.

Forti, P., and Rossi, A., 2003, Le straordinarie concrezioni della Grotta Nera di Pennapiedimonte, in Latini, M.L., and Burri, E., eds., Parco Nazionale della Majella. La montagna dei lupi, degli orsi e dei santi eremiti: Pescara, Italy, Carsa Edizioni, 272 p.

Gèze, B., 1976, Actual status of the question of moonmilk: Cave Geology, v. 1, p. 57–62.

Gradziński, M., Szulc, J., and Smyk, B., 1997, Microbial agents of moonmilk calcification, in Jeannin, P.-Y., ed., Proceedings of the 12th International Congress of Speleology, vol 1: La Chaux-de-Fonds, Swiss Speleological Society, p. 275–278.

Groth, I., and Saiz-Jimenez, C., 1999, Actinomycetes in hypogean environments: Geomicrobiology Journal, v. 16, p. 1–8. doi:10.1080/014904599270703.

Groth, I., Schumann, P., Saiz-Jimenez, C., Laiz, L., Sanchez-Moral, S., Cañaveras, C.J., and Saiz-Jimenez, C., 2001, Geomicrobiological study of the Grotta dei Cervi, Porto Badisco, Italy: Geomicrobiology Journal, v. 18, p. 241–258. doi:10.1080/01490450152467778.

Guggenberg, G., Zech, W., and Schulten, H.-R., 1994, Formation and mobilization pathways of dissolved organic matter: evidence from chemical structural studies of organic matter fractions in acid forest floor solutions: Organic Geochemistry, v. 21, p. 51–66. doi:10.1016/0146-6380(94)90087-6.

Hill, C.A., and Forti, P., 1986, Cave Minerals of the World: Huntsville, National Speleological Society, 238 p.

Hill, C.A., and Forti, P., 1997, Cave Minerals of the World, second edition: Huntsville, National Speleological Society, 463 p.

Istvan, D., Manescu, S., and Jurca, M., 1995, Study on moonmilk from Pestera Mare, Piatra Molosnaia (Repedea, Maramures Mountains, Romania): Theoretical and Applied Karstology, v. 8, p. 69–74.

James, J.M., Jennings, J.N., and Dyson, H.G., 1982, Mineral decoration and weathering of the caves, in Dyson, H.J., Ellis, R., and James, J.M., eds., Wombeyan Caves: Sydney, Sydney Speleological Society, p. 121–136.

Jones, B., and Kahle, C.F., 1993, Morphology, relationship, and origin of fiber and dendritic calcite crystals: Journal of Sedimentary Petrology, v. 63, p. 1018–1031. doi:10.1306/D4267C85-2B26-11D7-8648000102C1865D.

Kourtev, P.S., Ehrenfeld, J.G., and Häggblom, M., 2002, Exotic plant species alter the microbial community structure and function in the soil: Ecology, v. 83, p. 3152–3166. doi:10.1890/0012-9658(2002)083[3152:EPSATM]2.0.CO;2.

Lacelle, D., Lauriol, B., and Clark, I.D., 2004, Seasonal isotopic imprint in moonmilk from Caverne de l'Ours (Quebec, Canada): implications for climatic reconstruction: Canadian Journal of Earth Sciences, v. 41, p. 1411–1423. doi:10.1139/e04-080.

Laiz, L., Gonzalez-Delvalle, M., Hermosin, B., Ortiz-Martinez, A., and Saiz-Jimenez, C., 2003, Isolation of cave bacteria and substrate utilization at different temperatures: Geomicrobiology Journal, v. 20, p. 479–489. doi:10.1080/713851125.

Laiz, L., Groth, I., Gonzales, I., and Saiz-Jimenez, C., 1999, Microbiological study of the dripping waters in Altamira cave (Santillana del Mar, Spain): Journal of Microbiological Methods, v. 36, p. 129–138. doi:10.1016/S0167-7012(99)00018-4.

Marilley, J., and Aragno, M., 1999, Phylogenetic diversity of bacterial communities differing in degree of proximity of *Lolium perenne* and *Trifolium repens* roots: Applied Soil Ecology, v. 13, p. 127–136. doi:10.1016/S0929-1393(99)00028-1.

Martini, J., 1986, The tray: an example of evaporation-controlled speleothems: Bulletin of the South African Speleological Association, v. 27, p. 46–51.

Martino, T., Salamone, P., Zagari, M., and Urzì, C., 1992, Adesione a substrati solidi e solubilizzazione del CaCO₃ quale misura della capacità deteriorante di batteri isolati dal marmo Pentelico: Italian Society of General Microbiology and Microbial Biotechnology (SIMGBM) XI Meeting, Gubbio, p. 249–250.

McCarthy, A.J., 1987, Lignocellulose-degrading actinomycetes: FEMS Microbiology Letters, v. 46, p. 145–163. doi:10.1016/0378-1097(87)90061-9.

Mélon, J., and Bourguignon, P., 1962, Étude de mondmilch de quelques grottes de Belgique: Bulletin de la Société Française de Minéralogie et Cristallographie, v. 85, p. 234–421.

Miorandi, R., and Borsato, A., 2005, Ambiente di formazione di tufo calcareo e latte di monte in grotte del Trentino con particolare riferimento al Gruppo di Brenta e Paganella: Studi Trentini di Scienze Naturali Acta Geologica, v. 82, p. 225–237.

Moore, G.W., and Sullivan, N., 1997, Speleology: Caves and the Cave Environment: St. Louis, Cave Books, 176 p.

Mulec, J., Zalar, P., Hajna, N.Z., and Rupnik, M., 2002, Screening for culturable microorganisms from cave environments (Slovenia): Acta Carsologica, v. 31, no. 2, p. 177–187.

NORMAL Commission, 1990, NORMAL 9/88 recommendations. Autotrophic and heterotrophic microflora: isolation in culture: Rome, CNR/ICR.

Northup, D.E., Dahm, C.N., Melim, L.A., Spilde, M.N., Crossey, L.J., Lavoie, K.H., Mallory, L.M., Boston, P.J., Cunningham, K.I., and Barns, S.M., 2000, Evidence for geomicrobiological interactions in Guadalupe caves: Journal of Cave and Karst Studies, v. 62, p. 80–90.

Northup, D.E., and Lavoie, K.H., 2001, Geomicrobiology of caves: a review: Geomicrobiology Journal, v. 18, p. 199–222. doi:10.1080/01490450152467750.

Onac, B.P., 1995, Mineralogical data concerning moonmilk speleothems in few caves from Northern Norway: Acta Carsologica, v. 24, p. 429–437.

Onac, B.-P., and Ghergari, L., 1993, Moonmilch mineralogy in some Romanian and Norwegian Caves: Cave Science, v. 20, p. 107–111.

Onac, B.P., and Farcas, T., 1992, Le moonmilk des grottes de Trollkjerka et de Reshellarn (Lavangsmarka, Nordland, Norvège): Travaux de l'Institute de Spéologie "Emile Recovitza", v. 31, p. 133–138.

Onorato, R., Forti, P., Belmonte, G., Poto, M., and Costantini, A., 2003, La Grotta sottomarina *lu Lampiùne*: novità esplorative e prime indagini ecologiche: Thalassia Salentina, v. 26 Suppl., p. 55–64.

Portillo, M.C., and Gonzales, J.M., 2011, Moonmilk deposits originate from specific bacterial communities in Altamira Cave (Spain): Microbial Ecology, v. 61, p. 182–189. doi:10.1007/s00248-010-9731-5.

Portillo, M.C., Porca, E., Cuezva, S., Cañaveras, J.C., Sanchez-Moral, S., and Gonzales, J.M., 2009, Is the availability of different nutrients a critical factor for the impact of bacteria on subterraneous carbon budgets?: Naturwissenshaften, v. 96, p. 1035–1042. doi:10.1007/s00114-009-0562-5.

Richter, D.K., Immenhauser, A., and Neuser, R.D., 2008, Electron backscatter diffraction documents randomly orientated c-axes in moonmilk calcite fibres: evidence for biologically induced precipitation: Sedimentology, v. 55, p. 487–497. doi:10.1111/j.1365-3091.2007.00915.x.

Rivadeneyra, M.A., Delgado, G., Ramos-Cormenzana, A., and Delgado, R., 1998, Biomineralisation of carbonates by *Halomonas eurihalina* in solid and liquid media with different salinities: crystal formation sequence: Research in Microbiology, v. 149, p. 277–287. doi:10.1016/S0923-2508(98)80303-3.

Saiz-Jimenez, C., and Hermosin, B., 1999, Thermally assisted hydrolysis and methylation of dissolved organic matter in dripping waters from the Altamira Cave: Journal of Analytical and Applied Pyrolysis, v. 49, p. 337–347. doi:10.1016/S0165-2370(98)00112-0.

Savini, N., 2004, Le Grotte della Montagna Sacra: Il Forestale, no. 25, 28 p.

Schlegel, H.G., 1993, General Microbiology, seventh edition: Cambridge, Cambridge University Press, 655 p.

Steer, J., and Harris, J.A., 2000, Shifts in the microbial community in rhizosphere and nonrhizosphere soils during the growth of *Agrostis stolonifera:* Soil Biology and Biochemestry, v. 32, p. 869–878. doi:10.1016/S0038-0717(99)00219-9.

Sweeting, M.M., 1973, Karst Landforms: New York, Columbia University Press, 362 p.

Vezzani, L., and Ghisetti, F., 1993. Carta geologica dell'Abruzzo. Regione Abruzzo-Settore urbanistica, beni ambientali e cultura. S.E.L.C.A., Firenze.

ADAPTATIONS OF INDIGENOUS BACTERIA TO FUEL CONTAMINATION IN KARST AQUIFERS IN SOUTH-CENTRAL KENTUCKY

Tom D. Byl[1,2]*, David W. Metge[3], Daniel T. Agymang[2], Mike Bradley[1], Gregg Hileman[1], and Ron W. Harvey[3]

Abstract: The karst aquifer systems in southern Kentucky can be dynamic and quick to change. Microorganisms that live in these unpredictable aquifers are constantly faced with environmental changes. Their survival depends upon adaptations to changes in water chemistry, taking advantage of positive stimuli and avoiding negative environmental conditions. The U.S. Geological Survey conducted a study in 2001 to determine the capability of bacteria to adapt in two distinct regions of water quality in a karst aquifer, an area of clean, oxygenated groundwater and an area where the groundwater was oxygen depleted and contaminated by jet fuel. Water samples containing bacteria were collected from one clean well and two jet fuel contaminated wells in a conduit-dominated karst aquifer. Bacterial concentrations, enumerated through direct count, ranged from 500,000 to 2.7 million bacteria per mL in the clean portion of the aquifer, and 200,000 to 3.2 million bacteria per mL in the contaminated portion of the aquifer over a twelve month period. Bacteria from the clean well ranged in size from 0.2 to 2.5 μm, whereas bacteria from one fuel-contaminated well were generally larger, ranging in size from 0.2 to 3.9 μm. Also, bacteria collected from the clean well had a higher density and, consequently, were more inclined to sink than bacteria collected from contaminated wells. Bacteria collected from the clean portion of the karst aquifer were predominantly (~95%) Gram-negative and more likely to have flagella present than bacteria collected from the contaminated wells, which included a substantial fraction (~30%) of Gram-positive varieties. The ability of the bacteria from the clean portion of the karst aquifer to biodegrade benzene and toluene was studied under aerobic and anaerobic conditions in laboratory microcosms. The rate of fuel biodegradation in laboratory studies was approximately 50 times faster under aerobic conditions as compared to anaerobic, sulfur-reducing conditions. The optimum pH for fuel biodegradation ranged from 6 to 7. These findings suggest that bacteria have adapted to water-saturated karst systems with a variety of active and passive transport mechanisms.

INTRODUCTION

Approximately 40% of the United States east of the Mississippi River is considered karst terrain (Quinlan, 1989). Over 55% of Tennessee and Kentucky is underlain by carbonate rocks and exhibits classic karst features such as sinkholes, disappearing streams, and cave systems (Wolfe et al., 1997; Florea et al., 2002). The karst conduit systems provide habitat to a diverse fauna (Schneider and Culver, 2004) and can be an important source of water for humans (Hutson, 1995) and the ecosystem. Despite the common occurrence and importance of karst aquifers, very little is reported in the scientific literature about the adaptations of indigenous bacteria found in water-saturated karst conduits (Byl et al., 2002). Karst aquifers provide distinct hydrologic and chemical environments compared to unconsolidated sandy aquifers. For example, karst conduits typically offer much smaller surface areas for biofilm development per volume of water relative to

granular aquifers. It is therefore reasonable to assume that there are different adaptations and distributions in karst microbial communities as compared to those reported for sandy aquifers (Haack et al., 2012; Harvey et al., 1984; Harvey et al., 1997; Kölbel-Boelke et al., 1988; Barton and Northup, 2007).

There are different types of karst systems throughout the United States and the world (White, 2002). The karst aquifers of north-middle Tennessee and southern Kentucky may trap large volumes of water in fractures along bedding planes and other features isolated from active groundwater flowpaths (Wolfe et al., 1997). In essence, there are dissolution openings with actively flowing waters, as well as stagnant water-filled openings with substantially longer

---

* Corresponding Author: tdbyl@usgs.gov
[1] U.S. Geological Survey, Nashville, TN, 37211
[2] Tennessee State University, Civil & Environmental Engineering Dept., Nashville, TN, 37209
[3] U.S. Geological Survey, Boulder, CO, 80303

residence times. In these stagnant areas isolated from the major groundwater flowpaths, the bacteria and water may reside long enough to have a substantial effect on the geochemistry in that part of the aquifer (Byl and Williams, 2000; Byl et al., 2001). The geochemistry in these conduits can range from aerobic to anaerobic and is affected by recharge events.

The potential for contamination to enter and spread rapidly through a karst-conduit system is high, but the response of indigenous bacteria to dissolved contaminants in these water-filled conduit systems is poorly understood. Barton (2006) mentions a bacterium identified in Carlsbad Caverns, New Mexico, that can degrade complex aromatic compounds like benzothiazole and benzenesulfonic acid. Other bacteria, collected in Lechuguilla Cave, New Mexico, possess the ability to fix nitrogen, metabolize complex aromatic compounds, turn over lipids, and scavenge scarce nutrients (Barton and Jurado, 2007). Northrup and Lavoie (2001) conducted a study that showed bacteria thrive in karst systems under a variety of redox conditions, thus demonstrating that they have adapted to using a variety of terminal electron acceptors. In a previous study in south-middle Tennessee, Byl and Williams (2000) demonstrated that bacteria in a karst aquifer can biodegrade trichloroethylene by reductive dechlorination. It is clear that karst bacteria have adapted to biodegrade a variety of compounds under a broad range of geochemical conditions.

The karst aquifers of southern Kentucky are known for being hydrologically responsive to rain events (Ryan and Meimen, 1996; Vesper and White, 2006). Consequently, it would be expected that some of the evolutionary adaptations within the native microbial communities would facilitate coping with sudden changes. In 2001, the U.S. Geological Survey conducted a study to examine adaptations of the indigenous bacteria found in water-filled karst conduit systems by monitoring bacterial response to jet fuel contamination and pH changes. The scope of the study included the collection of bacterial communities from clean and fuel contaminated portions of the same aquifer and the comparison of their population sizes, buoyant densities, Gram types, and average cell sizes. This paper examines adaptations, size and quantity of bacteria, and rates of fuel biodegradation under both aerobic and anaerobic conditions.

Study Area Description

Three wells located near an airfield in south-central Kentucky were selected for this study because they represented two distinct areas of water quality in the karst aquifer: an area containing uncontaminated groundwater and an area where the groundwater had been contaminated by jet fuel (Fig. 1a and 1b). Two fuel-contaminated bedrock wells (MW-1 and MW-2) were located down-gradient from an uncontaminated bedrock monitoring well (MW-3) located approximately 100 feet upgradient from

MW-1 and 150 feet upgradient from MW-2 (Fig. 1a). Quarterly sampling had detected no petroleum hydrocarbons in the clean well during the previous 10 years (Dames and Moore, Inc., 2001). The airfield had several reported fuel leaks over several decades of intensive use. Wells drilled and screened in the bedrock during the 1980s confirmed the presence of dissolved fuels in specific areas of the karst aquifer (Ewers et al., 1992). The pH fluctuated between 6.4 and 7.8 in the clean well and contaminated well MW-2. The wells were cased with 4-inch PVC pipe and screened in the upper bedrock at 120 to 136 feet below ground surface (Fig. 1b).

Methods and Materials

Water samples for this study were collected in May, June, September, and December of 2001 from wells MW-3 and MW-1. Well MW-2 was added after a sudden increase in pH was observed in MW-1. The pH change from approximately 7 to 12 was due to the over-drilling of a 31-m (100-ft) deep well filled with ash material that was initially designed to be used as an anode to reduce fuel-pipe corrosion around the airfield (Fig. 1a). The anode well was converted to an extraction well, but in the process of over-drilling and grouting the new well, the pH of the surrounding aquifer jumped to 12. This extreme increase in pH provided a unique opportunity to observe how the bacteria in the pH-altered part of the aquifer would respond to a sudden and prolonged change from neutral to strongly alkaline conditions. The pH in the alternate wells MW-2 and MW-3 did not increase above pH 7.8, and it appeared to be unaffected by the pH-altering activities close to well MW-1.

Collection of Groundwater and Bacteria

Water samples were collected by lowering the intake of a cleaned, decontaminated Grundfos jet pump in the wells to specified depths equivalent to the conduit openings (Any use of trade, firm, or product names is for descriptive purposes only and does not imply endorsement by the U.S. Government). For example, in well MW-3, the pump intake was lowered to 40 m below the top of casing because geophysical logging indicated there was a 5 cm water-filled conduit opening at this level. The water was pumped at a rate of 1.5 to 3 L min^{-1} until specific conductance and temperature remained steady for fifteen minutes or more. The purging generally took thirty to forty minutes. Water levels in the well did not fluctuate during pumping, indicating that the water being collected was primarily drawn from the bedrock openings and not from the stagnant well-casing water. The groundwater collected ranged from clear to slightly turbid, with a steady temperature of 14.7 °C. The specific conductance ranged from 340 to 440 µS cm^{-1} in the clean well and 340 to 600 µS cm^{-1} in the contaminated wells, depending on recent rain events.
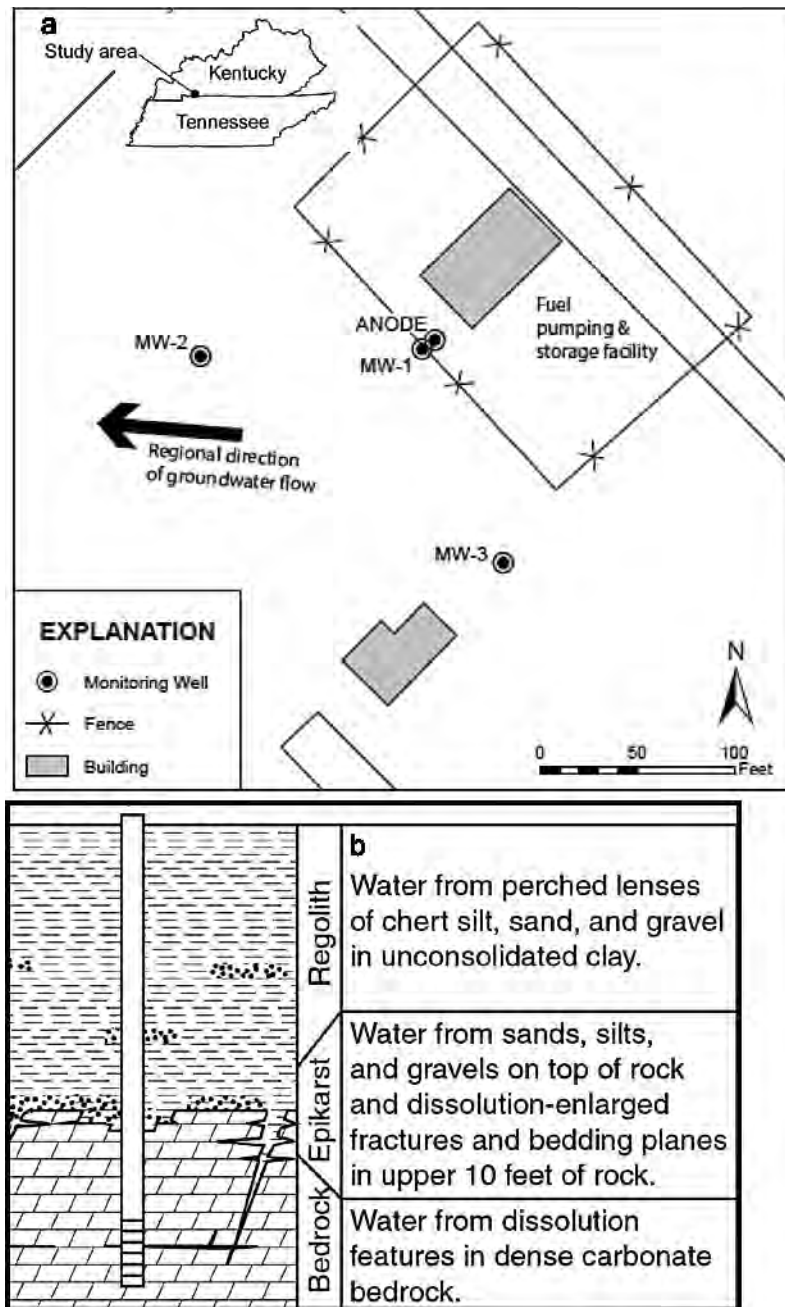
Figure 1. Map of site investigation area, plan view (a), and a conceptual cross section of the wells used in the study (b). Well MW-2 was polluted with fuel, and well MW-3 was clean. The water in well MW-1 changed during the study due to the drilling of nearby well ANODE.

The jet pump used to collect water samples was relatively new and had a Teflon hose. Between uses, the pump was cleaned with a weak 0.3% bleach solution and rinsed with heat-sterilized distilled water to remove hypochlorite residue. Quality control tests conducted on the decontaminated pump system found less than 10 bacteria per L water, indicating there was insignificant microbial cross-contamination due to the pump system. The groundwater samples for geochemical and bacterial analyses were collected in clean, sterile, 1 L brown glass bottles. Samples for analysis of volatile organic compounds (VOCs) were collected in clean, 40 mL brown glass bottles. All bottles were over-filled to avoid headspace and prevent sample volatilization and sealed with a sterile cap. The bottles were placed on ice and transferred to the laboratory at Tennessee State University in Nashville, Tennessee, for microbial, VOC, and geochemical analysis. VOC analysis was done on a Syntex gas chromatograph equipped with a

purge-and-trap system, 30 m by 0.32 mm, 1.8 µm silica-film capillary column, argon carrying gas, and micro-argon ionization detector. The lower detection limit for toluene and benzene on this GC was 0.5 microgram per liter (µg L^{-1}). Every fourth sample was either a duplicate sample or a standard of known toluene concentration. A complete calibration curve of benzene, toluene, ethylbenzene, and xylenes was run prior to and after the microcosm samples. Benzene and toluene were the only mono-aromatic ring compounds identified in the water. Additional unidentified peaks were present in the samples. Results of the VOC analysis were organized and graphed on a spreadsheet. Bacterial samples that were analyzed for buoyant density, size, and microscope direct counts were packed on ice and shipped overnight to the USGS laboratory in Boulder, Colorado.

Bacterial Quantification, Flagella, and Average Size

Two methods were used to quantify the bacteria, a direct count on the microscope and a liquid culturing method. The direct count method counts all bacteria, even those that are dormant, whereas the liquid culturing method provides a population estimate based on the bacteria that are actively dividing and growing. Additional microscopic examination was done to assess the presence or absence of flagella and the Gram-staining characteristics of the bacteria. Traditional Gram staining was conducted, and the result was viewed under a bright-field microscope (Beveridge, 2001). Bacteria flagella staining and viewing was done as described in Grossart et al. (2000).

Direct count and size frequency analyses of free-living bacteria were done using a Nikon Optiphot II epifluorescence microscope and an ITC image processor connected to a personal computer, a Dage SIT66 black and white camera, and a Sony black and white monitor. The image system was optimized to analyze and calculate length, width, area, and perimeter of fluorescent-stained (acridine orange) bacteria in samples previously analyzed for bacterial abundance. Measurements from the image system were standardized using fluorescent-stained 0.45, 0.95, and 1.07 µm microspheres in order to convert pixel measurements to micrometers. All analyses were performed at microscope magnifications of 788 to 1260.

Biological Active Reaction Tests (BART) were conducted to estimate the culturable heterotrophic aerobic bacteria in the groundwater. The BART assays use selective media to grow particular groundwater bacterial types (DBI, 2004). Twenty mL of groundwater were transferred from a sample bottle, having been vigorously shaken to re-suspend the bacteria, into the BART vials, sealed, and incubated in the dark at 22 °C for 7 days. The vials were checked every 24 hours for visible signs of bacteria growth, which was evident by dye-color changes and cloudiness, as described by Cullimore (2008, chapter 9). Growth patterns were recorded and compared to the growth charts to establish an estimate of the culturable bacterial concentration in the groundwater. Results were reported as bacteria per mL.

Buoyant-Density and Density-Gradient Determinations

Buoyant-density determinations were performed using the method described by Harvey et al. (1997). Approximately 2 L of uncontaminated groundwater or 1 L of contaminated groundwater was filtered through 47 mm (diameter), 0.2 µm (pore size) polycarbonate membrane filters at −0.3 atmosphere transmembrane pressure. Bacteria retained by the filters were gently washed with sterile saline solution (2 mM NaCl, pH 6.8) and resuspended in sterile 0.15 M NaCl to provide a cloudy suspension consisting of 1 to 400 cells per mL. Microscopic examination revealed that the vast majority of bacteria were single and not attached to particles. Few non-bacterial colloids were observed. Density gradients were created within transparent, 50-mL Oak Ridge or 10 mL polycarbonate centrifuge tubes using Percoll I solution (1.131 g cm^{-3}, Sigma Chemical Company, St. Louis, Missouri), a colloidal silica suspension, diluted with 0.15 M NaCl. The tubes were then spun for 30 minutes at 15,000 G in a Sorvall RC-5B refrigerated centrifuge. The resulting gradient formed symmetrically on either side of the starting density of 1.100 g cm^{-3}. Brightly colored density marker beads obtained from Sigma Chemical Company were used to indicate specific buoyant-density values along the longitudinal axis of the tubes. Aliquots (2.5 mL) of the bacterial suspensions were carefully layered on the top of the pre-formed gradients. Gradient tubes containing the bacteria were spun at 15,000 G for 1 hour. The equilibrium positions of the bacterial populations were observed as distinct translucent bands. The buoyant densities of the populations were indicated by the position of the bacterial bands relative to those of the marker beads. The band thickness (in mm) provided a semi-quantitative measure of the microbial population corresponding to a particular buoyant density. The total thickness of the bands equals 100 percent, and each band represents a subset or percentage of that total band thickness.

Batch Microcosms for Biodegradation Studies

The rate at which the cultured bacteria degraded fuels under aerobic or anaerobic conditions and under different pH conditions was the subject of microcosm studies. Stagnant batch microcosms were established using raw, unfiltered water collected from either well MW-3 or well MW-2. Water from well MW-3 was used to set up the aerobic microcosms because the waters consistently had dissolved oxygen readings of 3 mg L^{-1} or higher. Anaerobic microcosms were established using water from well MW-2, which consistently had less than 0.5 mg L^{-1} dissolved oxygen. The microcosms consisted of 300-mL brown, biological-oxygen-demand (BOD) glass bottles
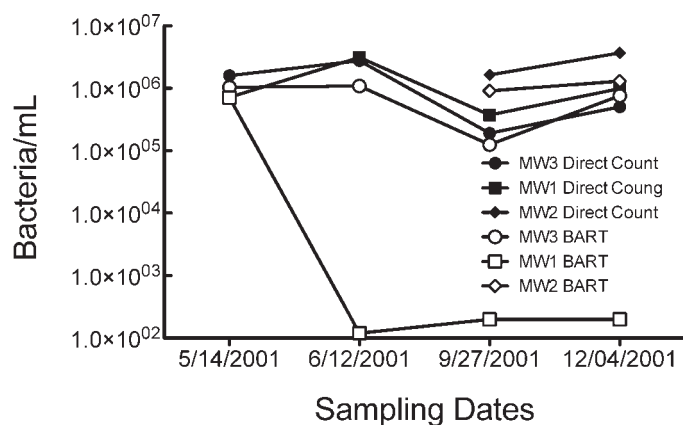
Figure 2. Bacteria quantified in waters collected from three wells intersecting a water-filled conduit in south-central Kentucky, as measured by microscope counting and by BART analyses. The pH of well MW-3 changed following May 2001.

incubated at 25 °C, which is approximately 10 degrees warmer than natural conditions in the conduit. Microcosms were sampled at five different harvest times with three replicates per harvest, aerobic and anaerobic conditions, for a total of thirty microcosms. Aerobic microcosms were harvested on days 0, 1, 3, 5, and 7. Anaerobic microcosms were harvested on days 0, 2, 5, 7, and 10. The dissolved oxygen levels were measured in each microcosm upon harvest to confirm aerobic and anaerobic conditions using YSI-5100 BOD meters. The data from the fifth harvest for the aerobic microcosms were not used because the oxygen had been consumed, and the microcosms had gone anaerobic. Additional sterile and pH-altered microcosms were established for comparison. The pH was adjusted from 6.85 with sodium hydroxide or hydrochloric acid to achieve pH of 2, 5, 7, 9, and 12.

RESULTS

BACTERIAL QUANTIFICATION, FLAGELLA, SIZE, AND BUOYANT DENSITY

The microbial population in the three sampled wells ranged from 200,000 to almost 4,000,000 bacteria per mL (Fig. 2). Population growth measured by direct counts and BART assays had a similar pattern with the exception of contaminated well MW-1. As mentioned earlier, the pH in MW-1 increased from 7 to 12 as a result of nearby drilling activities in late May, between the first and second sampling events. Alkaline conditions will often hamper microbial metabolism and promote detachment of bacteria from aquifer surfaces (Harvey et al., 2010). The sharp increase in pH at MW-1 resulted in an increase in bacteria using the direct-count method in the June 2001 sample, but a 99.99% drop in viable bacteria determined by the BART method. Enumerating environmental bacteria using tradi-

tional culturing techniques, such as agar media plates, can result in questionable bacterial counts due to a low cultivatable percentage (Barton et al., 2004). But the BART tests, which are also growth-based assays, did provide important information concerning the viability of the bacteria. Using the direct count method alone would have provided a false sense that this part of the karst aquifer had 3-million bacteria per mL in June, when the viable bacteria count really dropped from ~1 million to ~100 bacteria per mL.

With the exception of the pH-shocked well (MW-1), there was generally good agreement between the direct counts and the BART estimates. There was a rise and fall in bacteria numbers during the sampling period. Unfortunately, there were insufficient data to conclude whether population flux was due to seasonal patterns or recent weather events. It is clear, however, that bacterial concentrations in the karst conduit water can fluctuate an order of magnitude over several months. The BART method generally provided lower population estimates than the direct count method, indicating that some bacteria types did not grow, and were not measured. However, the BART bacterial estimates were closer to the direct counts than traditional heterotrophic plate counts, which were in the hundreds to thousands of colony forming units per mL (data not shown). The BART assay is different from conventional plate-count methods in several aspects. The BART system allows the water-borne bacteria to remain free-living in the water or to attach to a surface and maintain symbiotic associations. The BART vials provide nutrient and oxygen gradients in the test waters, which offer different types of bacteria their optimal habitat zones.

Microbial samples were Gram stained and viewed using bright-field microscopy. Gram stain has traditionally been used by microbiologists to help identify bacteria based on cell-wall make-up. Aquifer bacteria can alter their cell-wall chemistry under different environmental conditions (Harvey et al., 2011), thereby affecting their ability to hold the Gram stain (Beveridge, 2000). Thus, the objective of this Gram staining effort was to provide information about relative differences in the average composition of the cell envelope in clean versus contaminated conduits. Bacteria collected from the clean well, MW-3, were approximately 95% Gram-negative rods, whereas bacteria collected from MW-1 and MW-2 were 68% Gram-negative. The increase in Gram-positive bacteria in the presence of fuel has been observed by other investigators (Fahy et al., 2008; Ramos et al., 2002). They found Gram-positive bacteria were better competitors than Gram-negative organisms at high benzene concentrations, which suggests that some Gram-positive bacteria are tolerant of high fuel concentrations and can play a role in the natural attenuation of fuel. Segura et al. (1999) list three mechanisms used by Gram-positive bacteria tolerant to aromatic hydrocarbons, metabolizing the toxic hydrocarbons, which can contribute to their transformation into non-toxic compounds, rigid-
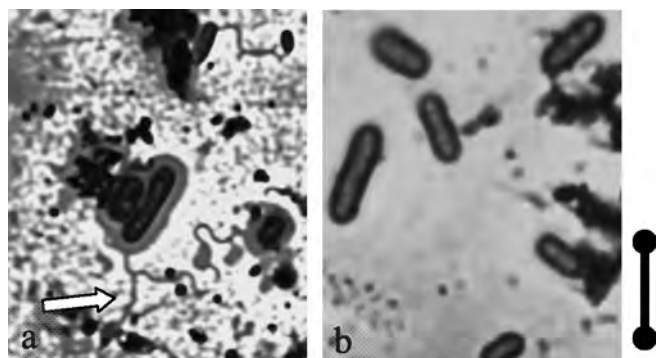
Figure 3. Rod-shaped bacteria from clean well MW-3 with polar flagella (arrow) (a), and rod-shaped bacteria from contaminated well MW-1 or MW-2 (b). Original magnification 1000×; line is 1 μm long.

ifying the cell membrane by altering the composition of phospholipids, and secreting the toxic compound in an energy-dependent process.

Groundwater bacteria have been known to use different methods of locomotion. Groundwater bacteria may use directed locomotion in the presence of chemical gradients (chemotaxis) to actively pursue energy sources, thus facilitating biodegradation (Ford and Harvey, 2007). Many aquatic bacteria propel themselves using flagella (Harschey, 2003), glide by one of several methods (McBride, 2001), or modify their buoyant density and float with the groundwater (Harvey et al., 1997). The use of flagella for locomotion is energy intensive and may be limited in anaerobic environments, where rapid expenditure of energy is costly to the organism. Alternatively, modifying the organism's buoyant density, thereby allowing the bacterium to float in the water-filled conduit openings, would be a low-energy method of locomotion. This study took a simple look at bacteria flagella and buoyancy mechanisms collected from the clean and fuel-contaminated parts of the aquifer. Gliding mechanisms were not part of this study.

Flagella are difficult to observe because they are small and bacteria have developed mechanisms to rapidly drop their flagella when environmental conditions change (Ford and Harvey, 2007; Harschey, 2003). Nonetheless, we observed a reasonable number of flagella attached to bacteria collected from clean well MW-3 (Fig. 3a). Detached flagella were also observed. By comparison, there were no flagella observed, attached or detached, to the bacteria collected from fuel-contaminated wells (Fig. 3b). These results were not quantitative, but they do suggest that a discernable fraction of the bacteria in MW-3 use flagella to move in the water column. Alternatively, these findings suggest that flagella are not a common mode of motility in the fuel-contaminated part of the aquifer likely because of the anaerobic environment, which is not conducive to the oxygen-dependent phosphorylation energy pathway.

Bacteria living in water from wells MW-1 or MW-2 appear to avoid motility mechanisms that require oxygen-dependent respiration because the aquifer was dissolved-oxygen poor (less than 1 mg L^{-1} throughout the year-long study). The part of the aquifer intersected by well MW-3 had dissolved-oxygen levels ranging from 3 to 8 mg L^{-1}. It is reasonable to assume the bacteria from oxygen-poor parts of the karst aquifer have adapted a more passive method to move about in their environment.

An important property governing microbial mobility in groundwater environments is buoyant density, also known as specific gravity. Figure 4 depicts the buoyant-density distribution of the bacteria from each well as a relative percentage derived from the bacteria band thickness after the density-gradient certifugation. One hundred percent of the bacterial population collected from MW-1 on May 14 had a very light specific gravity of 1.02 to 1.03 g cm^{-3}. This microbial population would be relatively buoyant and inclined to float in the water column. The construction of a well nearby in the last week of May, subsequently raising the pH to 12, coincided with a shift in buoyant density. The bacteria became denser and apt to descend in the water column. The microbial population in well MW-2 had a slightly lighter buoyant density (1.02 to 1.04 g cm^{-3}) compared to the bacteria collected from clean well MW-3. Bacteria collected from MW-3 had a moderate buoyant density throughout the sampling period. The data generated by this method were not suitable for statistical analysis.

The size distribution of the collected bacteria from wells MW-1 and MW-3 (Fig. 5) ranged from 0.2 to 4.0 μm. There was a subtle excess in length in the bacteria collected from MW-1 prior to the pH shift when compared to bacteria collected from MW-3. The median length of the bacteria collected from MW-3 was 0.6 μm. The median bacterial length found in MW-1 was 0.8 μm. However, because there was a large range of bacterial sizes in the clean and contaminated wells, an analysis of variance F-test did not find the median lengths to be significantly different.

Batch Microcosms for Biodegradation Studies

Bacteria collected from the wells in this study appear to have adaptations that permit them to swim in clean waters and float in anaerobic fuel-contaminated waters. These adaptations allow the bacteria to overcome the limited surface area for biofilm development. Because they have adapted mechanisms that enhance their abilities to live unattached to rock surfaces, there is also increased opportunity for bacteria to consume dissolved constituents such as benzene and toluene in the water column. Results from the microcosm study in the laboratory indicated that the aerobic and anaerobic biodegradation rates of benzene and toluene were pseudo-first order as exponential equations. The first-order rate constant for aerobic biodegradation (Fig. 6) was 0.64 for benzene ($R^2 = 0.97$) and 1.03 for toluene ($R^2 = 0.93$). Under aerobic conditions,
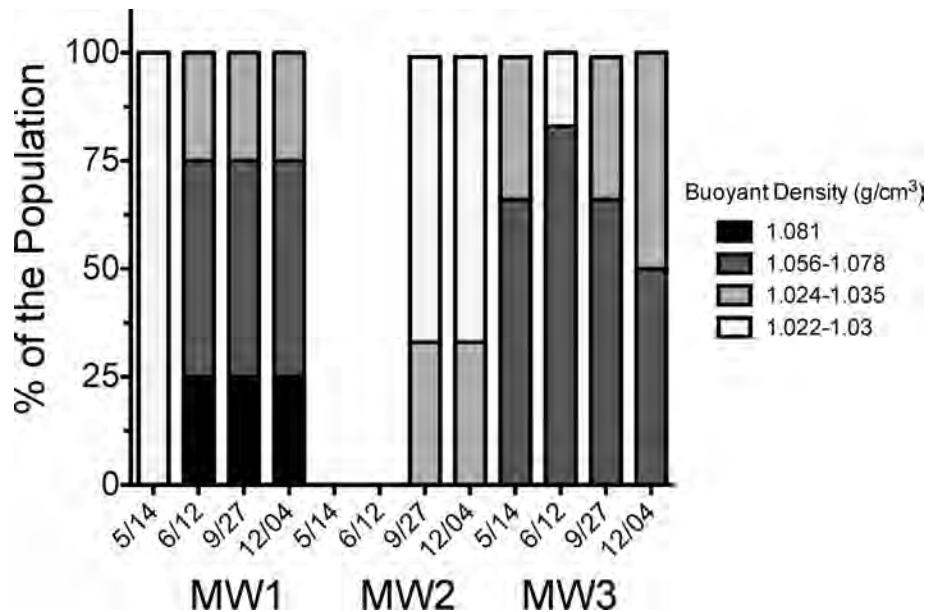
Figure 4. Buoyant densities of bacteria collected from the three karst wells shown as a percent of the total population at sample dates in 2001. MW-1, fuel-contaminated well that experienced pH shift to 12 prior to June; MW-2, fuel-contaminated well added to the study after June; MW-3, clean reference well.

toluene was biodegraded slightly faster than the benzene (Fig. 6), but there was not a statistically significant difference. The sterile controls lost less than 3% over the same time period.

The first-order anaerobic rate constants for degradation of benzene and toluene were essentially the same, 0.027 and 0.031, respectively ($R^2 = 0.98$ for both) (Fig. 7), which demonstrated that bacteria collected from the three wells in this study are capable of biodegrading fuel compounds under aerobic and anaerobic conditions. We documented both aerobic and anaerobic conditions in the bedrock aquifer at this site. Conditions in wells MW-1 and MW-2 were anaerobic, with less than 1 mg L^{-1} dissolved oxygen, which was probably due to use of oxygen as the final electron acceptor during the consumption of the dissolved fuel.

OPTIMUM pH FOR FUEL BIODEGRADATION

All enzymes, including those involved in biodegradation of fuels, have an optimum pH. Some enzymes can function in a broad range of pH values. Others require a narrow and
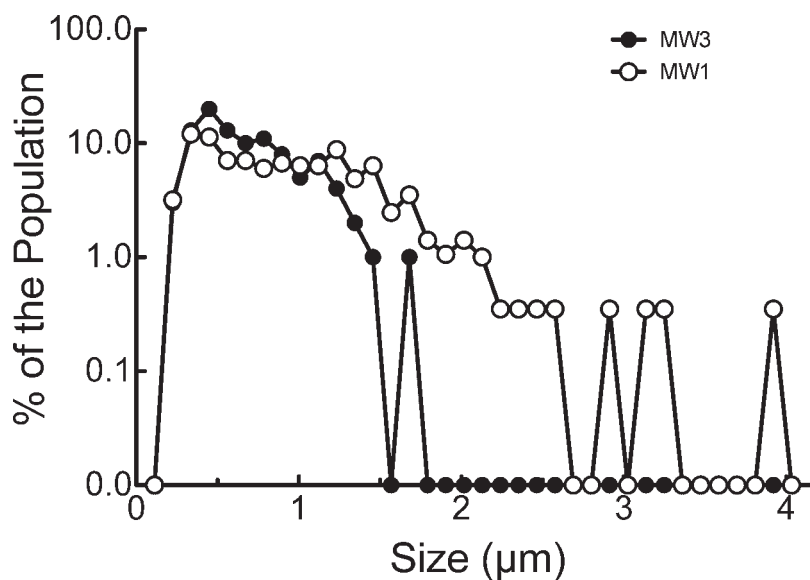

Figure 5. Bacterial size distribution for microbes collected from a clean (MW-3) and fuel-contaminated (MW-1) karst aquifer in southern Kentucky. Note logarithmic scale. The difference in the medians is not statistically significant.
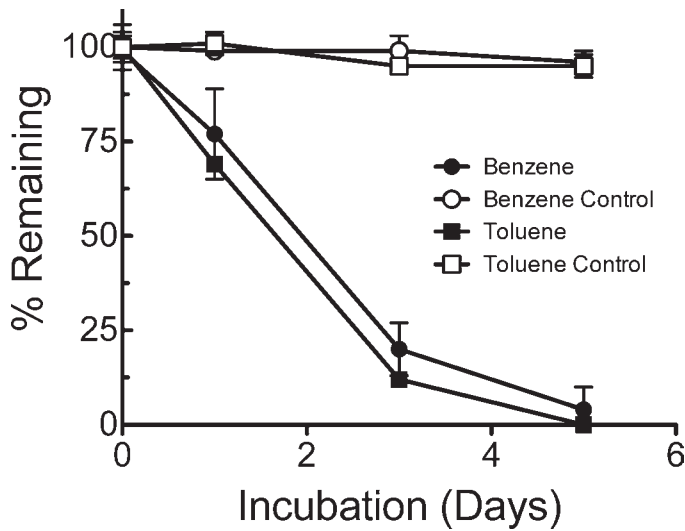
Figure 6. Aerobic biodegradation of mono-aromatic fuel compounds benzene and toluene by bacteria collected from clean well MW-3, compared to sterile control samples. Error bars are one standard deviation of three replicates.

controlled pH range in order to function. Aerobic samples from clean well MW-3 were treated with benzene and toluene levels of 4.8 and 15.3 µg L^{-1} and had pH adjusted to various levels as described in the methods section. Results from this microcosm study show that the microcosms with pH 2 and 12 had no noticeable consumption of dissolved oxygen over a 12-day period; whereas the other microcosms (pH values of 5, 7, and 9) became anaerobic around day 5 (Fig. 8).

The benzene and toluene in the microcosms were measured and the data were transformed to percent
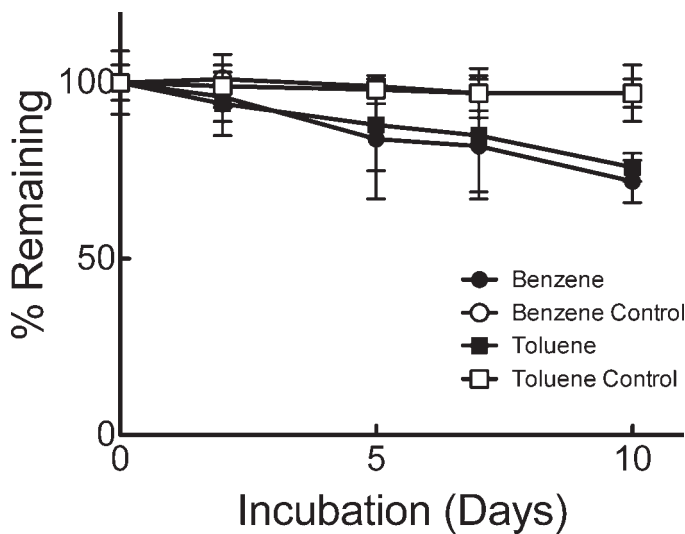

Figure 7. Anaerobic biodegradation of mono-aromatic fuel compounds benzene and toluene by bacteria collected from polluted well MW-2, compared to sterile control samples. Error bars are one standard deviation of three replicates.
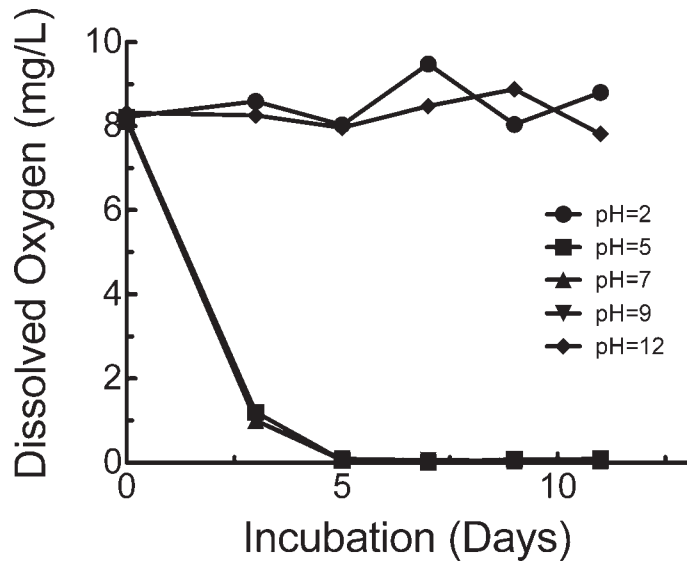
Figure 8. Dissolved oxygen levels in the static microcosms incubated over a 12-day period established using raw water from well clean well MW-3 with adjusted pH. Samples with near-neutral pH were anaerobic by day 5.

benzene and toluene remaining on day 5 (Fig. 9). The two microcosm treatments with pH 2 and 12 water did not have any toluene or benzene removal over the five-day period. The greatest amount of removal was found in microcosms with neutral pH, which indicated that the optimum pH for aerobic toluene or benzene biodegradation was between pH 6 and 7.

DISCUSSION

In spite of the austere conditions present in karst aquifers in south-central Kentucky, this study showed that these environments can harbor large numbers of bacteria, from 200,000 to 3,000,000 bacteria per mL. Many of the bacteria in the clean, oxygenated groundwater possessed flagella for motility, whereas bacteria from the oxygen-depleted, fuel-contaminated zones were less likely to have flagella and more likely to alter their buoyant density to facilitate their advective transport. A microorganism's buoyant density affects its frequency of collision with conduit surfaces because it affects the rate of settling. Buoyant density of bacteria collected in these three wells ranged from light (1.02 g cm^{-3}) to dense (1.08 g cm^{-3}). A similar difference in size and buoyant densities of groundwater bacteria observed in pristine versus contaminated zones of a sandy aquifer in Cape Cod, Massachusetts, resulted in an estimated 64-fold difference in their settling rates (Harvey et al., 1997). However, the relationship between bacteria shape, size, and sedimentation velocity is not fully understood, and other factors may affect sedimentation rate. The bacteria in the fuel-contaminated parts were, on average, larger than those

Figure 9. Aerobic biodegradation of benzene and toluene in microcosms with adjusted pH using raw water from well MW-3. The y-axis displays the percent benzene or toluene remaining in the microcosms after 5 days. No degradation of the organic compounds was observes at the extremes of pH. Sterile controls lost less than 2% over the 5 days of incubation. Three replicates per treatment; error bars represent coefficient of variation.
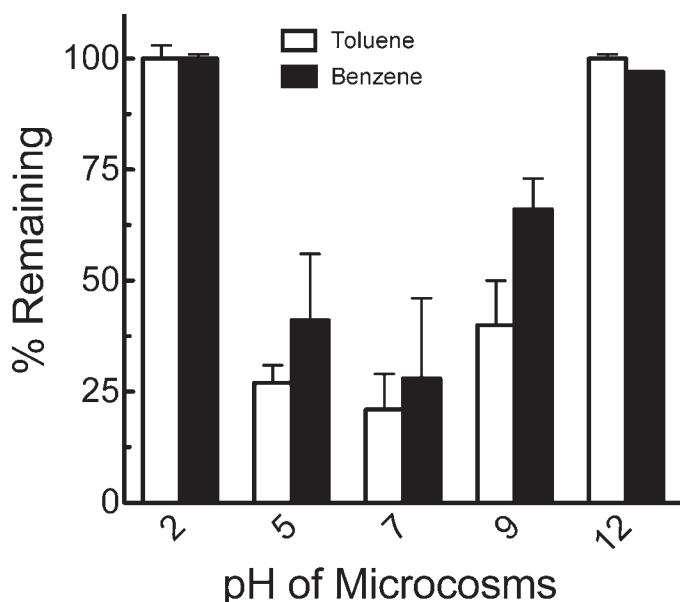
collected from a clean part of the aquifer. However, the median difference in size was not statistically significant due to the wide range of sizes in both clean and fuel-contaminated parts of the aquifer.

Bacteria from the clean, aerobic section and the anaerobic, fuel-contaminated section of the aquifer were able to biodegrade benzene and toluene. The half-lives for aerobic benzene and toluene biodegradation at 25 °C were 1.1 and 0.7 days, respectively. The aquifer in this study was a steady 14.7 °C over the course of this study. Assuming the Arrhenius principle applies to the biodegradation kinetics, which states that for every 10 °C increase there is an approximate doubling of the reaction rate (Laidler, 1984), the half-life of benzene and toluene *in situ* should be closer to 1.5 to 3 days. By comparison, under anaerobic conditions, the benzene and toluene had laboratory half-lives of 23 to 26 days, which should be closer to 50 days in the natural anaerobic aquifer environment. The optimum pH observed in the laboratory microcosms under aerobic conditions was between 6 and 7. This pH range is reasonable, considering this aquifer system generally had a pH ranging from 6.4 to 7.8, with the exception of well MW-1, which was influenced by development of a new well in close proximity. The pH in well MW-1 was initially pH ~7 but increased to pH 12. This study showed that there are large numbers of bacteria in the water-saturated karst

conduits of south-central Kentucky that are adapted to their environment and fully capable of degrading light fuels.

References

Barton, H.A., Taylor, M.R., and Pace, N.R., 2004, Molecular phylogenetic analysis of a bacterial community in an oligotrophic cave environment: Geomicrobiology Journal, v. 21, p. 11–20. doi:10.1080/01490450490253428.

Barton, H.A., 2006, Introduction to cave microbiology: A review for the non-specialist: Journal of Cave and Karst Studies, v. 68, no. 2, p. 43–54.

Barton, H.A., and Jurado, V., 2007, What's up down there? Microbial diversity in caves: Microbe, v. 2, no. 3, p. 132–138.

Barton, H.A., and Northup, D.E., 2007, Geomicrobiology in cave environments: past, current and future perspectives: Journal of Cave and Karst Studies, v. 69, no. 1, p. 163–178.

Beveridge, T.J., 2001, Use of the Gram stain in microbiology: Biotechic & Histochemistry, v. 76, no. 3, p. 111–118.

Byl, T.D., and Williams, S.D., 2000, Biodegradation of chorinated ethenes at a karst site in Middle Tennessee: U.S. Geological Survey Water-Resources Investigations Report 99-4285, 58 p.

Byl, T.D., Hileman, G.E., Williams, S.D., and Farmer, J.J., 2001, Geochemical and microbial evidence of fuel biodegradation in a contaminated karst aquifer in southern Kentucky, June 1999, *in* Kuniansky, E.L., ed., U.S. Geological Survey Karst Interest Group Proceedings, St. Petersburg, Florida, February 13–16, 2001: U.S. Geological Survey Water-Resources Investigations Report 01-4011, p. 151–156.

Byl, T.D., Hileman, G.E., Williams, S.D., Metge, D.W., and Harvey, R.W., 2002, Microbial strategies for degradation of organic contaminants in karst, *in* Aikens, G.R., and Kuniansky, E.L., eds., U.S. Geological Survey Artificial Recharge Workshop Proceedings, Sacramento, California, April 2–4, 2002: U.S. Geological Survery Open-File Report 02-89, p. 61–62.

Cullimore, D.R., 2008, Practical Manual of Groundwater Microbiology, second edition: Boca Raton, Florida, Taylor and Francis Group, 376 p.

Dames and Moore, Inc., 2001, Remedial Investigations Report, Fort Campbell, Kentucky: prepared for U.S. Army Toxic and Hazardous Materials Agency, Aberdeen Proving Ground, Maryland, contract number 15-88-D-0008, 2 volumes.

DBI, 2003, BART User Manual, 2004 edition, Droycon Bioconcepts Inc, Regina, Saskatchewan, 54 p., http://www.dbi.ca/BARTs/Docs/Manual.pdf [accessed March 1, 2013]

Ewers, R.O., Duda, A.J., Estes, E.K., Idstein, P.J., and Johnson, K.M., 1992, The transmission of light hydrocarbon contaminants in limestone karst aquifers, *in* Proceeding of the Third Conference on Hydrogeology, Ecology, Monitoring, and Management of Ground Water in Karst Terranes: Dublin, Ohio, Water Well Journal Publishing, p. 287–306.

Fahy, A., Ball, A.S., Lethbridge, G., McGenity, T.J., and Timmis, K.N., 2008, High benzene concentrations can favour Gram-positive bacteria in groundwaters from a contaminated aquifer: FEMS Microbiolial Ecology, v. 65, p. 526–533. doi:10.1111/j.1574-6941.2008.00518.x.

Florea, L.J., Paylor, R.L., Simpson, L., and Gulley, J., 2002, Karst GIS advances in Kentucky: Journal of Cave and Karst Studies, v. 64, no. 1, p. 58–62.

Ford, R.M., and Harvey, R.W., 2007, Role of chemotaxis in the transport of bacteria through saturated porous media: Advances in Water Resources, v. 30, p. 1608–1617. doi:10.1016/j.advwatres.2006.05.019.

Grossart, H.-P., Steward, G.F., Martinez, J., and Azam, F., 2000, A simple, rapid method for demonstrating bacterial flagella: Applied

and Environmental Microbiology, v. 66, p. 3632–3636. doi:10.1128/AEM.66.8.3632-3636.2000.

Haack, S.K., Metge, D.W., Fogarty, L.R., Meyer, M.T., Barber, L.B., Harvey, R.W., LeBlanc, D.R., and Kolpin, D.W., 2012, Effects on groundwater microbial communities of an engineered 30-day in-situ exposure to the antibiotic sulfamethoxazole: Environmental Science and Technology, v. 46, no. 14, p. 7478–7486. doi:10.1021/es3009776.

Harschey, R.M., 2003, Bacterial motility on a surface: many ways to a common goal: Annual Review of Microbiology, v. 57, p. 249–273. doi:10.1146/annurev.micro.57.030502.091014.

Harvey, R.W., Smith, R.L., and George, L., 1984, Effect of organic contamination upon microbial distributions and heterotrophic uptake in a Cape Cod, Mass., aquifer: Applied and Environmental Microbiology, v. 48, p. 1197–1202.

Harvey, R.W., Metge, D.W., Kinner, N., and Mayberry, N., 1997, Physiological considerations in applying laboratory-determined buoyant densities to predictions of bacterial and protozoan transport in groundwater: Results of in-situ and laboratory tests: Environmental Science and Technology, v. 31, p. 289–295. doi:10.1021/es960461d.

Harvey, R.W., Metge, D.W., Barber, L.B., and Aiken, G.R., 2010, Effects of altered groundwater chemistry upon the pH-dependency and magnitude of bacterial attachment during transport within an organically contaminated sandy aquifer: Water Research, v. 44, p. 1062–1071. doi:10.1016/j.watres.2009.09.008.

Harvey, R.W., Metge, D.W., Mohanram, A., Gao, Xiaodong, and Chorover, J., 2011, Differential effects of dissolved organic carbon upon re-entrainment and surface properties of groundwater bacteria and bacteria-sized microspheres during transport through a contaminated, sandy aquifer: Environmental Science and Technology, v. 45, p. 3252–3259. doi:10.1021/es102989x.

Hutson, S.S., 1995, Ground-water Use by Public-Supply Systems in Tennessee in 1990: U.S. Geological Survey Open-File Report 94-483, 1 sheet.

Kölbel-Boelke, J., Anders, E.-M., and Nehrkorn, A., 1988, Microbial communities in the saturated groundwater environment, II. Diversity of bacterial communities in a Pleistocene sand aquifer and their in vitro activities: Microbial Ecology, v. 16, p. 31–48. doi:10.1007/BF02097403.

Laidler, K., 1984, The development of the Arrhenius equation: Journal of Chemical Education, v. 61, p. 494–498. doi:10.1021/ed061p494.

McBride, M.J., 2001, Bacterial gliding motility: multiple mechanisms for cell movement over surfaces: Annual Review of Microbiology, v. 55, p. 49–75. doi:10.1146/annurev.micro.55.1.49.

Northup, D.E., and Lavoie, K.H., 2001, Geomicrobiology of caves: a review: Geomicrobiology Journal, v. 18, p. 199–222. doi:10.1080/01490450152467750.

Quinlan, J.F., 1989, Ground-water monitoring in karst terranes: recommended protocols and implicit assumptions: Las Vegas, Nevada, U.S. Environmental Protection Agency, Environmental Monitoring Systems Laboratory, EPA/600/X-89/050, 88 p.

Ramos, J.L., Duque, E., Gallegos, M.-T., Godoy, P., Ramos-González, M.I., Rojas, A., Terán, W., and Segura, A., 2002, Mechanisms of solvent tolerance in Gram-negative bacteria: Annual Review of Microbiology, v. 56, p. 743–768. doi:10.1146/annurev.micro.56.012302.161038.

Ryan, M., and Meimen, J., 1996, An examination of short-term variations in water quality at a karst spring in Kentucky: Ground Water, v. 34, no. 1, p. 23–30. doi:10.1111/j.1745-6584.1996.tb01861.x.

Schneider, K., and Culver, D.C., 2004, Estimating subterranean species richness using intensive sampling and rarefaction curves in a high density cave region in West Virginia: Journal of Cave and Karst Studies, v. 66, p. 39–45.

Segura, A., Duque, E., Mosqueda, G., Ramos, J.L., and Junker, F., 1999, Multiple responses of Gram-negative bacteria to organic solvents: Environmental Microbiology, v. 1, no. 3, p. 191–198. doi:10.1046/j.1462-2920.1999.00033.x.

Vesper, D.J., and White, W.B., 2006, Comparative storm response of contaminants in a carbonate aquifer, Fort Campbell, Kentucky-Tennessee, in Harmon, R.S., and Wicks, C., eds., Perspectives on Karst Geomorphology, Hydrology, and Geochemistry—A Tribute Volume to Derek C. Ford and William B. White: Geological Society of America Special Paper 404, p. 267–274. doi:10.1130/2006.2404(22).

White, W.B., 2002, Karst hydrology; recent developments and open questions: Engineering Geology, v. 65, p. 85–105. doi:10.1016/S0013-7952(01)00116-8.

Wolfe, W.J., Haugh, C.J., Webbers, A., and Diehl, T.H., 1997, Preliminary conceptual models of the occurrence, fate, and transport of chlorinated solvents in karst aquifers of Tennessee: U.S. Geological Survey Water-Resources Investigations Report 97-4097, 80 p.

AEROSOLIZED MICROBES FROM ORGANIC RICH MATERIALS: CASE STUDY OF BAT GUANO FROM CAVES IN ROMANIA

DANIELA R. BORDA[1], RUXANDRA M. NĂSTASE-BUCUR[1*], MARINA SPÎNU[2], RALUCA URICARIU[2], AND JANEZ MULEC[3]

Abstract: Cave air, bat guano, and swabs of bat fur from caves with bat guano in Romania were analyzed by using RIDA®COUNT cultivation plates and standard selective media for *Staphylococcus* and *Streptococcus*. The samples of guano varied in concentration of cultivable chemoheterotrophic bacteria (max. 1.9×10^{10} CFU/g), coliforms (max. 2.2×10^8 CFU/g), *Escherichia coli* (max. 1.0×10^8 CFU/g), and yeasts and molds (max. 1.7×10^7 CFU/g). The gravity-settling principle was applied to sample airborne microorganisms, and a new method was developed for evaluation of aerosolization potential. In cave air, the concentration of total bacteria was higher than yeast and molds. In addition to coliforms, enterobacteria, *E. coli*, and unidentified cultivable bacteria in the air samples, we also identified *Chryseomonas luteola*, *Klebsiella pneumoniae*, *Micrococcus*, *Salmonella*, *Staphylococcus*, and *Streptococcus*. In the experiment that provoked microbial aerosolization from guano, 3.35% of total cultivable fungi were aerosolized, up to 0.10% of bacteria, and 0.00% of *E. coli*. The concentration of *Staphylococcus* in the air exceeded counts of *Streptococcus*. The highest concentrations of airborne microorganisms were on the ground level. Using cultivation plates as a robust method we demonstrated that the relative proportion of microbial subgroups in the air remained constant in different seasons, with lower concentrations of airborne microbiota in the autumn. Caves as simplified natural systems demonstrated complex relationships between atmospheric parameters and microorganisms. Bats introduce into caves varying, but not negligible, concentrations of microbes on their fur. Caves with guano had relative high concentration of airborne microbes that may represent a biohazard for animals and humans.

INTRODUCTION

Air is an important habitat for metabolically active and reproducing microbes (Womack et al., 2010) and a vehicle for the transport of different microorganisms. When airborne, microorganisms can travel reasonable distances. For some microbes certain air conditions, such as desiccation, extreme temperature, UV radiation, or chemical and radioactive stressors, can be lethal.

Aerosolization, the production of an aerosol, results in a fine mist or spray containing minute particles that contain biological particles. There are different types of bioaerosol formation caused by wind, animals and humans, or splashing water (Mulec et al., 2012c). It occurs in natural and man-made environments. Human exposure to aerosols of organic-rich materials generates a potential risk and can cause different types of infection. The health hazards of poor air quality can be associated with airborne microbes, and exposure to elevated concentrations of microorganisms can lead to numerous respiratory and dermatological infections, allergies, and other problems (Fabian et al., 2005).

The study of bioaerosols in controlled lab conditions provides valuable information, but trials under natural conditions provide a better insight into the fate of minute biological particles. Due to changeable atmospheric conditions and interrelated environmental stressors such as wind, UV, and humidity, some natural outdoor environments provide complex study conditions. A natural system that is low in environmental stressors and rich in organic material is karst caves harboring piles of bat guano. Caves are generally natural light-free environments connected with the outside by one or more entries, and with high relative air humidity, constant temperature, and low or negligible air movements (Simon, 2012; White and Culver, 2012). Poulson and Lavoie (2000) considered bat guano one of the most important energy inputs for caves in temperate climate zones. Guano is an important habitat, a source for microbial aerosolization, and a biohazard factor for humans and bats, e.g. *Histoplasma capsulatum* (Alteras, 1966; Jülg et al., 2008).

The objectives of this study were to define the relations between atmospheric parameters and airborne microorganisms that derive from *in situ* organic matter in caves.

* Corresponding author: ruxandra.nastase.bucur@academia-cj.ro
[1] "Emil Racoviță" Institute of Speleology, Department of Cluj-Napoca, Romanian Academy, Clinicilor St. 5, POBox 58RO-400006 Cluj-Napoca, Romania
[2] University of Agricultural Science and Veterinary Medicine, Faculty of Veterinary Medicine, Calea Mănăștur 3-5, RO-400372 Cluj-Napoca, Romania
[3] Karst Research Institute, Research Centre of the Slovenian Academy of Sciences and Arts, Titov trg 2, SI-6230 Postojna, Slovenia

Table 1. Caves studied, with abbreviations used in the figures. The distance from the cave entrance to the most remote bioaerosol sampling site is included. Lithology after Bandrabur and Radu, 1994, Bleahu et al., 1976, and Todoran and Onac 1987; biogeographical regions after ANPM, 2013.

Cave	Biogeographical Region	Entrance a.s.l. (m)	Lithology	Studied Distance / Length of Cave (m)
Adam Cave, AC	Continental	295	Jurassic / Cretaceous limestone	25 / 169
Cheile Turzii Cave, CT	Alpine	552	Jurassic limestone	36 / 120
Fuşteica Cave, FC	Continental	200	Jurassic / Cretaceous limestone	47 / 1270
Gura Dobrogei Cave, GD	Steppe	46	Jurassic limestone	125 / 500
Meziad Cave, MC	Alpine	440	Triassic limestone	375 / 4750
Răstoci Cave, RC	Continental	319	Eocene / Oligocene limestone	87 / 507
Topolniţa Cave, TC	Continental	434	Jurassic / Cretaceous limestone	320 / 20500

Caves in Romania with bat guano were studied to observe seasonal and air-stratification effects on concentration of bioaerosols, as well as to estimate the level of aerosolized microbes from guano and the role of bats as vectors for microbial transmission. To estimate the percentage of aerosolization, a new method to induce aerosolization was developed and tested in caves. Results from the study are useful for comparison with other organic-rich environments that contain biohazard microbes, such as farms, landfills, and wastewater or compost treatment plants.

MATERIALS AND METHODS

STUDY SITES

Seven caves that are rich in guano deposits and populated by bats in three biogeographic and climate regions in Romania were selected: Avenul lui Adam (Adam Cave), Peştera Cetăţeaua Mare din Cheile Turzii (Cetă-ţeaua Mare Cave from Gorges of Turda, referred to in the text and tables as Cheile Turzii Cave), Peştera Fuşteica (Fuşteica Cave), Pestera Liliecilor de la Gura Dobrogei (Bat Cave from Gura Dobrogei, referred to as Gura Dobrogei Cave), Peştera Meziad (Meziad Cave), Peştera de la Răstoci/ Peştera Măgurici (Răstoci Cave), and Peştera Topolniţa (Topolniţa Cave) (Table 1). Apart from Cheile Turzii Cave, which contains a maternity roost, the other caves host bats all year round, including maternity and hibernation colonies. The most prevalent bat species and number of species in each cave are presented in Table 2.

Adam Cave is located in Băile Herculane area in the Domogled-Cerna Valley National Park, which has 700 to 750 mm of annual precipitation (Munteanu, 2011). The cave entrance is vertical, starting with an 11 m shaft. Temperature is constant year round, with an average of 27 °C that is attributed to intermittent steam vapors; water

Table 2. Bats in studied caves; data from Borda, 2002a, b; Borda et al., 2004; Burghele-Bălăcescu and Avram, 1966; Carbonnel et al., 1996; Coroiu et al., 2007; Pocora and Pocora, 2011.

Cave	Presence	Number of Individuals	Number of Bat Species	Main Guano Contributors
Adam Cave	All year	5000	8	*Miniopterus schreibersii* *Myotis capacinii* *Myotis myotis* *Rhinolophus euryale*
Cheile Turzii Cave	Summer	1500	3	*Miniopterus schreibersii* *Myotis myotis / M. oxygnathus*
Fuşteica Cave	All year	1500	7	*Miniopterus schreibersii* *Myotis capacinii* *Myotis myotis / M. oxygnathus*
Gura Dobrogei Cave	All year	300	10	*Miniopterus schreibersii* *Myotis daubentonii* *Myotis myotis / M. oxygnathus*
Meziad Cave	All year	5000–7000	10	*Miniopterus schreibersii* *Myotis myotis / M. oxygnathus*
Răstoci Cave	All year	200	5	*Myotis myotis / M. oxygnathus*
Topolniţa Cave	All year	1500	10	*Miniopterus schreibersii* *Myotis myotis / M. oxygnathus*

temperature is around 42 °C and bursts of vapor at 44.5 to 53 °C (Povară et al., 1972). Because of these particularities, the Adam Cave is unique in Romania, being a tropical-type cave, distinct from all other caves from Romania. Due to the intermittent steam emissions, air mixing is caused by the ascending warm and descending colder air. The air circulation is more obvious in the winter, when temperature differences between cave and external air are more pronounced. The warm air accumulating in the cave becomes a perfect shelter for maternity colonies of bats. The largest guano heap in the Guano Gallery is up to 2.5 m high (Carbonnel et al., 1996).

Cheile Turzii Cave is a small cave located on the right slope of Hașdate Valley in the Trascău Mountains where the average annual precipitation is around 600 mm (Beldean, 2005). In the past, the cave offered shelter for the local people against invasions. The entrance still contains part of a fortification wall that partially obstructs normal air ventilation.

Fușteica Cave is located in the Vîlcan Mountains where the annual average precipitation is approximately 800 mm (Costache, 2011). This is an active cave with large guano deposits that are partially flushed away by an intermittent subterranean stream that drains to the Isvarna River (Burghele-Bălăcescu and Avram, 1966). Both maternity and hibernation bat colonies are sheltered in the cave.

Gura Dobrogei Cave is located in Dobrogea in southeastern Romania. Annual precipitation in the region is 350 to 450 mm (Lungu, 2008). In the Fossils Gallery there are large quantities of old and fresh deposits of guano.

Meziad Cave is partly a tourist cave and is located in the Pădurea Craiului Mountains, part of the Apuseni Mountains. The annual average of precipitation in the area is 720 mm (Moza, 2008). The cave is a big subterranean cavity developed on three levels, the main gallery, the first floor, and the second floor. Meziad Cave was included in the study because of big maternity and mating colonies of bats and important fresh guano deposits. During our research activities there has been no electrification and no construction of new trails; this resulted in minimal human visits and preservation of the bat population. The cave has a front gate embedded in an artificial stone wall three meters high.

Răstoci Cave is one of the main caves of the Someșan Plateau of Transylvania, and it is the only cave in that area that shelters a considerable number of bats. The annual average precipitation in the Someșan area for the last hundred years is 635 mm (Sorocovschi and Vodă, 2009).

Topolnița Cave is a large cave located in the Mehedinți Mountains where precipitation is between 900 and 1,000 mm per year (Robu, 2009). The gallery network of the cave is developed on four levels, two dry (one lower and one upper), one semi-active, and the lowest one active. We investigated only the upper inactive part of the cave, where *H. capsulatum* was detected for the first time in Europe (Alteras, 1966). A gate installed in 1960s restricted the

access of bats in this part of the cave and probably induced changes in atmospheric conditions. In 1996 two new openings for bats were cut in the wall, which allowed for re-colonization by bats.

Microbiological Media and Reading Results

Due to the proven versatility of RIDA®COUNT cultivation plates in caves (Mulec et al., 2012a, b) and in organic-rich environments (Oarga et al., 2012), the following varieties of this product were used: for total bacterial counts (RIDA®COUNT Total Aerobic Count), for *Escherichia coli* and coliforms (RIDA®COUNT E. coli/Coliform), for enterobacteria (RIDA®COUNT Enterobacteriaceae), and for yeast and molds (RIDA®COUNT Yeast&Mold Rapid). After 24 and 48 hours of cultivation at 37 °C, readings of bacterial growth were scored. For yeasts and molds, readings were taken after 48 and 72 hours of cultivation at the temperature of 25 °C. The counts of bacteria after 48 and for fungi after 72 hours were considered for statistical analyses. Prolonged incubation for 24 hours gives a more realistic view of the microbial communities, as some cave microbes have demonstrated slow growth on RIDA®COUNT media (Mulec et al., 2012a). Isolates that exhibited ß-D-glucuronidase and ß-D-galactosidase biochemical activities on RIDA®COUNT E. coli/Coliform plates were considered indicative of E. coli (R-Biopharm AG, Germany).

To supplement RIDA®COUNT readings with additional indicators of potential pathogenic microbes, we used the standard selective media for *Streptococcus* (Azide bloodagar medium; Holmes and Lermit, 1955) and *Staphylococcus* (Mannitol salt agar medium; Chapman, 1945). Open Petri plates with these media were placed parallel to RIDA®COUNT plates in Meziad Cave and Cheile Turzii Cave. The plates were incubated at 37 °C, and colonies were counted after 24 and 48 hours. This approach is frequently used in Romania to quantify airborne microbiota in organic-rich environments such as domestic farms (Drăghici et al., 2002), zoos (Borda et al., 2012), and caves with bat guano (Borda et al., 2004; 2009; Borda and Borda, 2004).

For subsequent identification of bacterial isolates from Adam Cave and Topolnița Cave, the morphologically distinct colonies developed on Total Aerobic RIDA®COUNT were plated on glucose nutrient agar (Oxoid, UK) and MacConkey agar (Sigma-Aldrich). After Gram staining, API® strips (Biomérieux, France) were used to identify isolates, API20E for enteric bacteria, API20NE for non-enteric Gram-negative bacteria, and APIStaph for identification of staphylococci and micrococci. The results were interpreted using APIweb software.

Sampling Procedure and Atmospheric Parameters

Four different types of samples were analyzed: bat guano, cave air, cave air inoculated with guano by our *in situ* aerosolization procedure, and swabs of bats' fur. For

air samples, results are reported as colony-forming units (CFU) per surface in a definite period of sampling, e.g., $CFU/20\ cm^2/20\ min$, for guano as CFU per gram (w/v), and for swabs as CFU per surface, e.g. $CFU/20\ cm^2$.

Fresh guano and guano accumulated in caves in previous years were included in the study. For microbiological analysis, guano heaps were aseptically sampled with a spoon in a range from 0 to 5 cm depth. After sampling, characteristics of guano heaps were measured: volume, surface area, and pH. pH was measured at the site using pH indicator strips (EMD Chemicals, Germany) after a sample of guano was homogenized with an equal part of sterile deionised water. Samples for microbiological analyses were transported in a cool box to the lab as soon as possible. After establishing the weight of a guano samples, generally around 2 g, 15 mL of sterile physiological saline was added to the samples and rigorously vortexed. This mixture was serially diluted up to 10^{-8}. One milliliter of these serial dilutions was applied onto RIDA®COUNT test plates. Microbial counts were expressed as colony-forming-units per gram.

To sample airborne microorganisms the gravity-settling method was adopted. Open plates with media were exposed to the cave atmosphere for 20 minutes and, after cultivation in laboratory conditions, microbial counts were expressed as CFU per surface unit (Borda et al., 2004; Mulec, 2008; Mulec et al., 2012a, b). In caves, bioaerosol was sampled on the ground floor at different distances from the cave entrance and guano heaps. Besides the horizontal gradient sampling, a vertical gradient of bioaerosols was also sampled by using a 1.5-m standing rack. To diminish the influence of researchers' presence upon the air quality, sampling was performed consecutively; the first sample was taken at the cave entrance, and the next ones later at previously selected sites, up to the last sampling sites at a guano heap in the cave. If cave morphology at a particular site allowed, sampling was performed in duplicate or triplicate, and the average CFU value was used in subsequent analyses. After sampling was finished, the distances from the cave entrance and guano heap for each individual sampling site was measured. In some caves (Adam Cave, Fuşteica Cave, Gura Dobrogei Cave, Răstoci Cave, Topolniţa Cave) aerosols were sampled once per year, while in Cheile Turzii Cave and Meziad Cave we also sampled in different periods of the year in order to observe seasonal variability. The summer investigations in these two caves took place once the fresh guano was deposited.

In selected caves (Cheile Turzii Cave, Gura Dobrogei Cave, and Meziad Cave) we performed artificially induced aerosolization to estimate the maximum numbers of cultivable microorganisms from aerosols. A spoon of guano was aseptically transferred to a sterile beaker (diameter 7 cm, height 9 cm, with total volume of 0.346 liter). To provoke *in situ* aerosolization of microbes in guano, the beaker with guano was temporary sealed with a plastic bag and manually shaken for ten seconds. Big particles of guano were shaken off and removed from the beaker, and the beaker was placed with the opening over the RIDA®COUNT media for 20 minutes, so the airborne microbes could settle (Fig. 1). The inoculated RIDA® COUNT media was later transferred in the laboratory and incubated as previously described.

During natural aerosol sampling we measured atmospheric parameters, temperature, relative humidity (RH), and air pressure with a Kestrel 4500 Pocket Weather Tracker. The carbon dioxide concentration in the atmosphere was measured with a MI70 Vaisala CO_2 meter.

Swabs of bat coats were sampled to get an idea of how many cultivable microbes bats host on their body surfaces and how much bats contribute to spreading of microbes. A moistened sterile cotton swab was used to swab the body of a bat. The cotton swab was placed into a tube with 4 mL of physiological saline and thoroughly shaken. Finally, one mL of the suspension was spread on RIDA®COUNT test plates (Total Aerobic Count, *E. coli*/Coliform, Yeast& Mold Rapid). Cultivation conditions were as described above. Microbial counts from the fur coat were expressed as CFU per surface. Two individuals of *Rhinolophus ferrumequinum* and *R. hipposideros* were swabbed at the beginning of hibernation (October-November 2010).

Statistical Evaluations

Canonical correspondence analysis was used to correlate data of abundance of all cultivable microbial groups, *E. coli* (EC), non-*E. coli* coliforms (NECCO), non-coliform bacteria (NCOBA), and yeasts and molds (Y&M) with environmental variables. The NECCO count was calculated as the number of *E. coli* colonies subtracted from the total coliform counts, and the NCOBA count represented all bacteria excluding coliforms (Oarga et al., 2012). Parametric multivariate analysis was run by the program package CANOCO 4.5 (ter Braak and Šmilauer, 2002). The significance of environmental variables in the analysis was tested by a Monte Carlo permutation test. No transformations of the environmental data were applied.

Results and Discussion

Bat Guano

Animal excrement is an important source of nutrients, including bat guano in caves (Deharveng, 2005). Guano contains diverse microbiota (Chroňaková et al., 2009) and is a source for microbial aerosolization, which represents a potential biohazard for humans and bats, (e.g., Alteras, 1966; Jülg et al., 2008). Fresh guano is basic, and older guano becomes acidic (Moulds, 2006). Based on macroscopic observation and pH measurements, guano samples were assigned as fresh if they were up to one season old and neutral to alkaline. No correlations were observed between physical guano parameters (pH, volume, surface) and
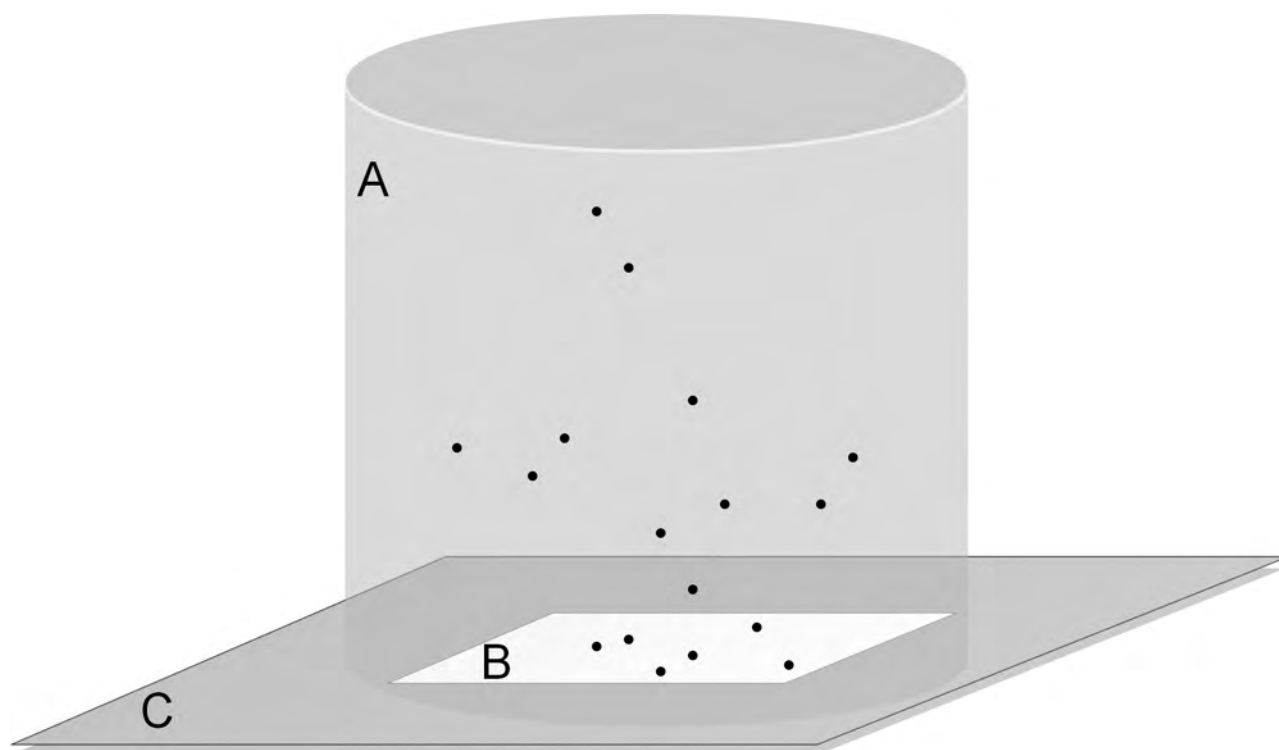
Figure 1. Schematic representation of aerosolization experiment. A, beaker with minute particles represented as dots; B, RIDA®COUNT microbiological medium; C, flexible support with attached microbiological medium.

microbial groups. The biggest guano heap was in Adam Cave (Table 4). The samples of guano varied in concentration of bacteria (up to 1.9×10^{10} CFU/g), coliforms (up to 2.2×10^8 CFU/g), *E. coli* (up to 1.0×10^8 CFU/g), and yeasts and molds (up to 1.7×10^7 CFU/g). The concentrations of fungi varied considerably; interestingly no isolates were retrieved from old guano samples from Gura Dobrogei Cave (Table 5). Coliforms and *E. coli* were not detected in old and dry guano samples from Gura Dobrogei Cave and Topolniţa Cave. All guano samples positive on *E. coli*-RIDA®COUNT specific plate were fresh, a few weeks or a few months old. By using the API identification scheme, *Chryseomonas luteola* (99.9% ID) and *Burkholderia cepacia* (99.9% ID) were identified in fresh guano from Adam Cave, and in addition, *B. cepacia* was present in old guano from Topolniţa Cave. In a previous study of microbial quantification from guano from Topolniţa Cave, Hodorogea (1972) showed approximately a 150-fold decrease in number of bacteria in the 10–20 cm layer compared with the surface layer (1–5 cm), and fungal concentration was approximately 100-fold higher in the lower layer compared to the guano surface (Hodorogea, 1972).

ATMOSPHERIC CONDITIONS IN CAVES

The highest temperature differences among sampling sites in the same cave were observed in Meziad Cave during sampling in October 2011 (6.6 °C), and in Cheile Turzii Cave in July 2011 (4.1 °C) (for temperature ranges see Table 3). In both caves, even in colder months, slightly higher temperatures were observed in the sectors with the biggest guano heaps. Temperature differences between sampling sites were high in Meziad Cave also during sampling in November 2010, 2.7 °C, and in Fuşteica Cave in October 2010, 2.1 °C. In other caves, temperature differences were smaller. The highest air temperatures were measured in Adam Cave (26.0 to 27.3 °C), with a difference of 1.3 °C between sampling sites. The biggest differences in relative humidity among sites in the same cave were in Meziad Cave in October 2011 at 27.5% and in November 2010 at 14.4%. The next higher differences among sites were in Fuşteica Cave (20%), followed by Cheile Turzii Cave (8.4%); this cave had also the lowest measured relative humidity (42.8 to 51.2%). When CO_2 concentration was measured, the biggest differences among sampling sites were in Meziad Cave during November 2010 sampling (175 ppm), followed by Răstoci Cave (133 ppm) and Adam Cave (103 ppm). In Adam Cave, the concentration was the highest among all caves, ranging between 1,307 and 1,410 ppm (Table 3).

AIRBORNE MICROBES

Except in Fuşteica Cave and Meziad Cave, the total concentration of airborne bacteria was higher than the total concentration of airborne yeast and molds (Fig. 2). In Adam Cave, the concentration of airborne bacteria was the

Table 3. Ranges of atmospheric parameters during sampling.

Cave	Date (mm/dd/yy)	Temperature (°C)	Relative Humidity (%)	CO_2 (ppm)
Adam Cave	10/29/10	26.0–27.3	96.4–99.8	1307–1410
Cheile Turzii Cave	07/15/11	14.8–18.9	…	…
	10/16/11	8.4–9.3	42.8–51.2	410–470
Fuşteica Cave	10/28/10	8.2–10.3	80.0–100.0	421–423
Gura Dobrogei Cave	10/23/11	11.0–12.8	…	…
Meziad Cave	11/02/10	11.5–14.2	84.3–98.7	397–572
	07/26/11	13.3–14.6	…	…
	10/17/11	7.5–14.1	62.9–90.4	370–416
Rastoci Cave	10/25/10	8.1–8.8	96.0–100.0	418–551
Topolniţa Cave	10/30/10	12.7–13.6	96.0–100.0	488–557

highest compared to other caves, probably due to the large volume and contact surface of guano (Table 4). High temperature and high humidity (96.5% to 99.8%) in combination with vaporized compounds from guano that can serve as nutrients for microbial multiplication create an excellent air habitat for microbes. In addition, intermittent thermal emanations in this cave can introduce additional compounds into cave atmosphere and enhance the aerosolization effect. The lowest concentration of airborne microbes was in Fuşteica Cave, where guano heaps were located along both sides of the riverbed. The low concentration can be related to the permanent flow of the underground river that constantly washes the central part of the guano deposit and creates continual water saturation of the air, so that aerosol particles settle relatively quickly.

Airborne microorganisms had previously been studied in Romanian caves (Borda and Borda, 2004; Borda et al., 2004) with different ranges of cultivable aerobic bacteria (56 to 1,021 CFU/m^3) and fungi (52 to 22,373 CFU/m^3). When caves were rich in guano, total aerobic bacteria of up to 11,317 CFU/m^3 were detected. A direct comparison with this study is not appropriate due to the use of different sampling methods and cultivation media; in this study RIDA®COUNT cultivation plates were used and results are reported as CFU/20 cm^2/20 min.

Coliform bacteria and *E. coli*, representative of fecal enterobacteria and common sources of enteric infections (Guentzel, 1996), were screened to observe microbial load that probably originated from feces. Concentrations of airborne coliforms varied reasonably. Typical *E. coli* colonies on RIDA®COUNT *E. coli*/Coliform plates were not detected in the air in Adam Cave, Cheile Turzii Cave, and Fuşteica Cave (Fig. 3). Furthermore, despite high concentration of airborne coliforms and total bacteria in Adam Cave and Cheile Turzii Cave, no typical *E. coli* colonies were retrieved on the media, which indicates that *E. coli* is short-lived when airborne and its presence in the cave air is more or less random. Additionally, the results of *in situ* aerosolization showed that *E. coli* is hard to find in aerosols (Fig. 6). *E. coli* does not survive generally more than two or three weeks in low-nutrient environments in a viable and cultivable state (Neidhardt et al., 1996), and indications of its presence in nutrient-poor cave habitats should be carefully examined (Barton and Pace, 2005). Airborne fecal coliforms generally do not survive long outdoors, so the probability of causing infections for wildlife and humans is low (Hughes, 2003). Similar conclusion could be drawn for the underground environment.

Distinct bacterial colonies from Adam Cave and Topolniţa Cave that developed on the RIDA®COUNT Total Aerobic were identified using API as *Klebsiella pneumoniae* ssp. *ozaenae*, *Salmonella arizonae*, and *Salmonella* spp. The source of these microbes is very likely bats' intestines (e.g., Adesiyun et al., 2009; Di Bella et al., 2003). These microbes are also present in human intestines (Guentzel, 1996). In the air in Topolniţa Cave, a non-Enterobacteriaceae isolate, *Chryseomonas luteola* (99.9% ID), was also found.

Table 4. Physical characteristics of studied guano heaps in the investigated caves.

Cave	Studied Guano Heaps	pH	Volume, m^3	Surface, m^2
Adam Cave	1	4.4	32.710	43.90
Cheile Turzii Cave	1	5.8–8.5	0.010–0.400	0.25–4.00
Fuşteica Cave	3	4.0–6.5	0.001–0.058	0.30–1.00
Gura Dobrogei Cave	4	4.8–7.2	0.001–0.610	0.09–3.51
Meziad Cave	2	4.7–7.8	0.015–1.360	1.54–6.60
Răstoci Cave	1	4.5	0.049	0.98
Topolniţa Cave	2	4.0–6.8	0.375–9.600	3.75–40.00

Table 5. Microbial counts in guano samples expressed as colony-forming units per gram after 48 hours of incubation for bacteria and 72 hours for yeasts and molds.

Cave	Bacteria (CFU/g)	Coliforms (CFU/g)	E.coli (CFU/g)	Yeast and Molds (CFU/g)
Adam Cave	2.1×10^8–2.1×10^8	3.37×10^5–6.5×10^5	1.4×10^4–2.2×10^5	2.5×10^6–1.7×10^7
CheileTurzii Cave	6.5×10^7–1.9×10^{10}	1.7×10^6–2.0×10^8	1.2×10^6–1.0×10^8	5.9×10^3–1.7×10^7
Fuşteica Cave	8.8×10^4–1.7×10^6	1.8×10^3–3.8×10^4	0.0	1.0×10^5–2.3×10^6
Gura Dobrogei Cave	9.3×10^3–7.9×10^5	0.0–9.3×10^4	0.0–6.1×10^3	0.0–3.4×10^4
Meziad Cave	3.1×10^5–2.2×10^8	3.9×10^3–9.8×10^7	0.0–3.1×10^6	7.2×10^1–3.6×10^6
Răstoci Cave	1.2×10^5	2.2×10^3	0.0	6.8×10^4
Topolniţa Cave	3.6×10^3–1.1×10^9	0.0–2.2×10^8	0.0–8.3×10^4	9.2×10^4–8.9×10^5

Screening for the presence of *Streptococcus* and *Staphylococcus* was performed; they are an important part of indoor atmospheres (Mandal and Brandl, 2011; Hospodsky et al., 2012). *Staphylococcus* is usually used as an indicator for microbiota from skin and mucous membranes (Aydogdu et al., 2005; Schulz et al., 2004), and *Streptococcus* indicates oral, pharyngeal, and skin bacterial biota and even faecal soil pollution (Kibbey et al., 1978). Except for sampling in Meziad Cave in July 2011, the concentration of *Staphylococcus* in the air exceeded counts of *Streptococcus* (Fig. 4). Concentration of staphylococci and streptococci are frequently elevated in the proximity of guano heaps during the summer when bats are active and fly in their underground roosts (Borda et al., 2004). The biochemical profile of two isolates from Adam Cave atmosphere revealed *Staphylococcus* and *Micrococcus* (99.8% ID). Micrococci are not as common as staphylococci; however, both are frequently present in bat guano (Mohod, 2011; Vandžurová et al., 2013). This group of

microbes can survive in the air for a long time; for example, *Staphylococcus aureus* can survive several months on fabric or dust particles (Mitscherlich and Marth, 1984). Under natural cave conditions airborne *Staphylococcus* and *Streptococcus* are expected to be viable much longer than *E. coli.*

In caves with bat guano, elevated concentrations of airborne bacteria, and to a lesser extent, fungi were detected in our study. We identified *Chryseomonas luteola*, *E. coli*, *Klebsiella pneumoniae* ssp. *ozaenae*, *Micrococcus*, *Salmonella*, *Staphylococcus*, and *Streptococcus*, as well as unidentified cultivable bacteria, coliforms, and enterobacteria. All these microbes can be indicative for bats and guano, and in caves, they might represent a biohazard because they can survive longer as airborne there than in other organic-rich environments with more environmental stressors. High microbial concentrations in guano did not always correspond to high concentration of airborne microbes at the same guano heap (compare Fig. 2 and Table 5).
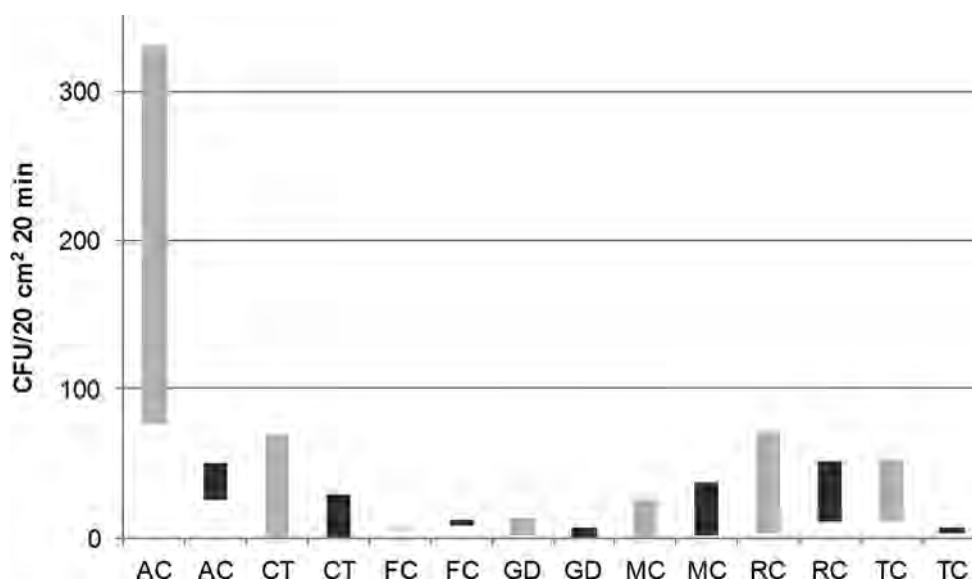

Figure 2. Ranges of concentrations of airborne microbes (grey, total bacteria; black, yeasts and molds) in the air of Adam Cave (AC), Fuşteica Cave (FC), Meziad Cave (MC), Răstoci Cave (RC), and Topolniţa Cave (TC) in autumn of 2010, and in Cheile Turzii Cave (CT), Gura Dobrogei Cave (GD), and Meziad Cave (MC) in autumn of 2011.
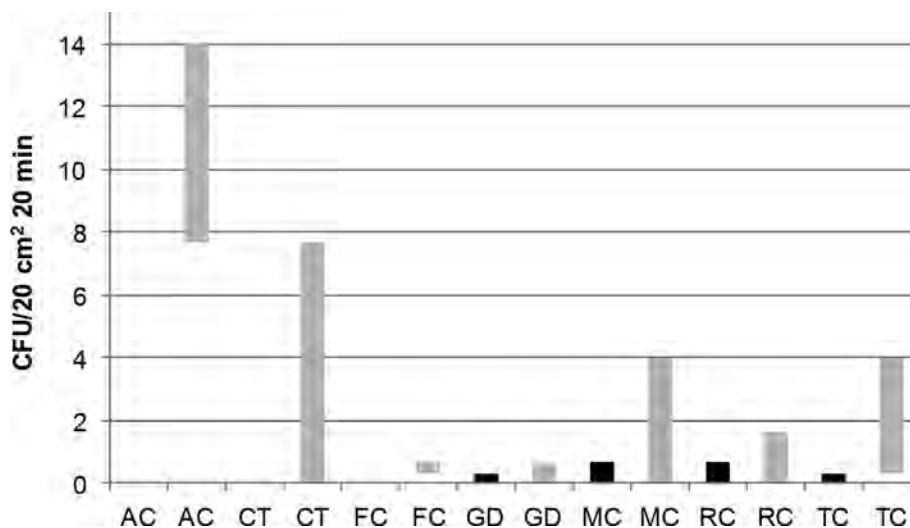
Figure 3. Ranges of concentrations of coliforms (grey) and *E. coli* (black) in the air of Adam Cave (AC), Fuşteica Cave (FC), Meziad Cave (MC), Răstoci Cave (RC), and Topolniţa Cave (TC) in autumn of 2010, and in Cheile Turzii Cave (CT), Gura Dobrogei cave (GD), and Meziad Cave (MC) in autumn of 2011.

AIRBORNE MICROBES AND ATMOSPHERIC PARAMETERS

Canonical correspondence analysis was performed on the basis of six variables, if available: temperature, relative humidity, air pressure, CO_2, distance to the cave entrance from each individual sampling site, and distance to the guano heap from each individual sampling site. Only a small portion of measured environmental variables explained the variances (Table 6). Measured physical parameters explained the highest variance in the structure of microbial communities in the autumn in Gura Dobrogei Cave (October 2011) by 0.31 and in Meziad Cave (November 2011) by 0.12. In other caves in autumn and also in summer they explained less than 0.09. Temperature had a significant impact ($p<0.05$) on the bioaerosol

abundance in Meziad Cave in November 2011 and RH in Topolniţa Cave in October 2010.

In a study from Postojna Cave, Slovenia, (Mulec et al., 2012c) where the impacting sampling method was used, in the transition periods, i.e., spring and autumn, physical parameters explained variances less (winter 0.62, spring 0.25, summer 0.49, autumn 0.08). The sampling method used in this study is based on gravity settling and is not directly comparable. The method based on settling is very sensitive to any air disturbances that can cause the particles to deviate from their vertical settling route. Other factors that influence settling behavior, in addition to air movements, pressure, temperature, and human and animal movements, are characteristics of an individual particle,
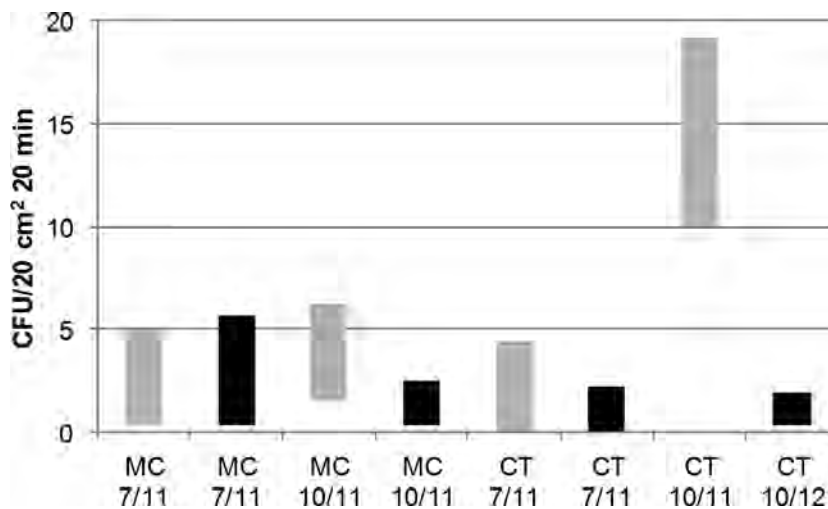

Figure 4. Ranges of concentrations of airborne *Staphylococcus* (grey) and *Streptococcus* (black) in Meziad Cave (MC) and Cheile Turzii Cave (CT) in July (7) and October (10) of 2011.

Table 6. Summary of canonical correspondence analysis analysis using forward selection for explanation of variance by selected variable. Dist_Ent, distance from the closest cave entrance; Dist_Gua, distance to the closest guano heap. AC, Adam Cave; CT, Cheile Turzii Cave; FC, Fuşteica Cave; GD, Gura Dobrogei Cave; MC, Meziad Cave; RC, Răstoci Cave; TC, Topolniţa Cave. In bold, $p<0.05$.

Parameter	Cave / Period									
	AC / Oct 10	CT / Jul 11	CT / Oct 11	FC / Oct 10	GD / Oct 11	MC / Nov 10	MC / Oct 11	MC / Oct 11	RC / Oct 10	TC / Oct 10
Temperature										
p	1.00	1.00		1.00	0.24	0.05	1.00	0.14	1.00	1.00
var.	0.08	0.02		0.01	0.02	0.10	0.02	0.05	0.01	0.00
Relative Humidity										
p						1.00		1.00		**0.03**
var.						0.01		0.00		0.06
Pressure										
p			0.171					0.43	0.37	
var.			0.05					0.02	0.03	
CO_2										
p									0.38	0.12
var.									0.02	0.00
Dist_Ent										
p							0.22			0.36
var.							0.05			0.03
Dist_Gua										
p		0.35			0.09	0.20	0.43			
var.		0.02			0.29	0.01	0.01			
Variance explained	0.09	0.04	0.05	0.01	0.31	0.12	0.08	0.07	0.06	0.09
Sum of all eigen values	0.08	0.05	0.05	0.01	0.31	0.12	0.08	0.07	0.06	0.09

such as its size and mass, and morphological characteristics of a space that, for example, enables creating of air gaps. Interestingly, distances from guano did not always contribute to the common variance during autumn samplings, but during both summer samplings in Cheile Turzii Cave and in Meziad Cave they did. This can be attributed as a seasonal effect connected with the presence of bats and very fresh guano droppings and its aerosolization. In that period, a pronounced gradient of airborne microbes can be formed radiating from a site of a bat colony and its guano heap, but more data are needed to confirm that. Nevertheless, conditions in cave atmospheres are complex and dynamic and become more complicated when other factors are involved, such as aerosolized microbes/particles from animal excrements. Sampling position in the space has also very important influence on the detection of bioaerosol signals.

Vertical Microbial Gradient and Effect of Seasonality

Concentration of airborne microorganisms at different heights above the ground varied, indicating that selection of bioaerosols sampling positions is important and should be clearly reported (Fig. 5). The concentration of airborne microorganisms was generally higher when bioaerosols were sampled at the ground level, in Cheile Turzii Cave on average 3.4 orders of magnitude and in Meziad Cave on average 1.3 orders. In both Cheile Turzii Cave and Meziad Cave, the total microbial counts were higher in summer than in autumn. Total microbial counts were defined as a sum of counts of *E. coli* (EC), non-*E. coli* coliforms (NECCO), non-coliform bacteria (NCOBA), and yeasts and molds (Y&M) (Fig. 5). Coliform bacteria other than *E. coli* were detected in both caves in the summer period. In addition, in Meziad Cave *E. coli* was detected airborne on *E. coli*-specific plates, while in Cheile Turzii Cave these bacteria were not observed in the air at all. Sampling site MC2 in Meziad Cave is located in a big chamber (Pyramid Room, approx. 220,000 m³) with 0.015 m³ of guano, and sampling site MC3 is located in a smaller chamber (Bat Room, approx. 37,500 m³) with a greater quantity of guano ($\sim$1.36 m³) that is more scattered in the space. The Bat Room, which had a higher concentration of airborne microbes, shelters from May to August a big nursery colony of about five to seven thousand individuals of *Myotis myotis*/*M. oxygnathus* mixed with *Miniopterus schreibersii*.
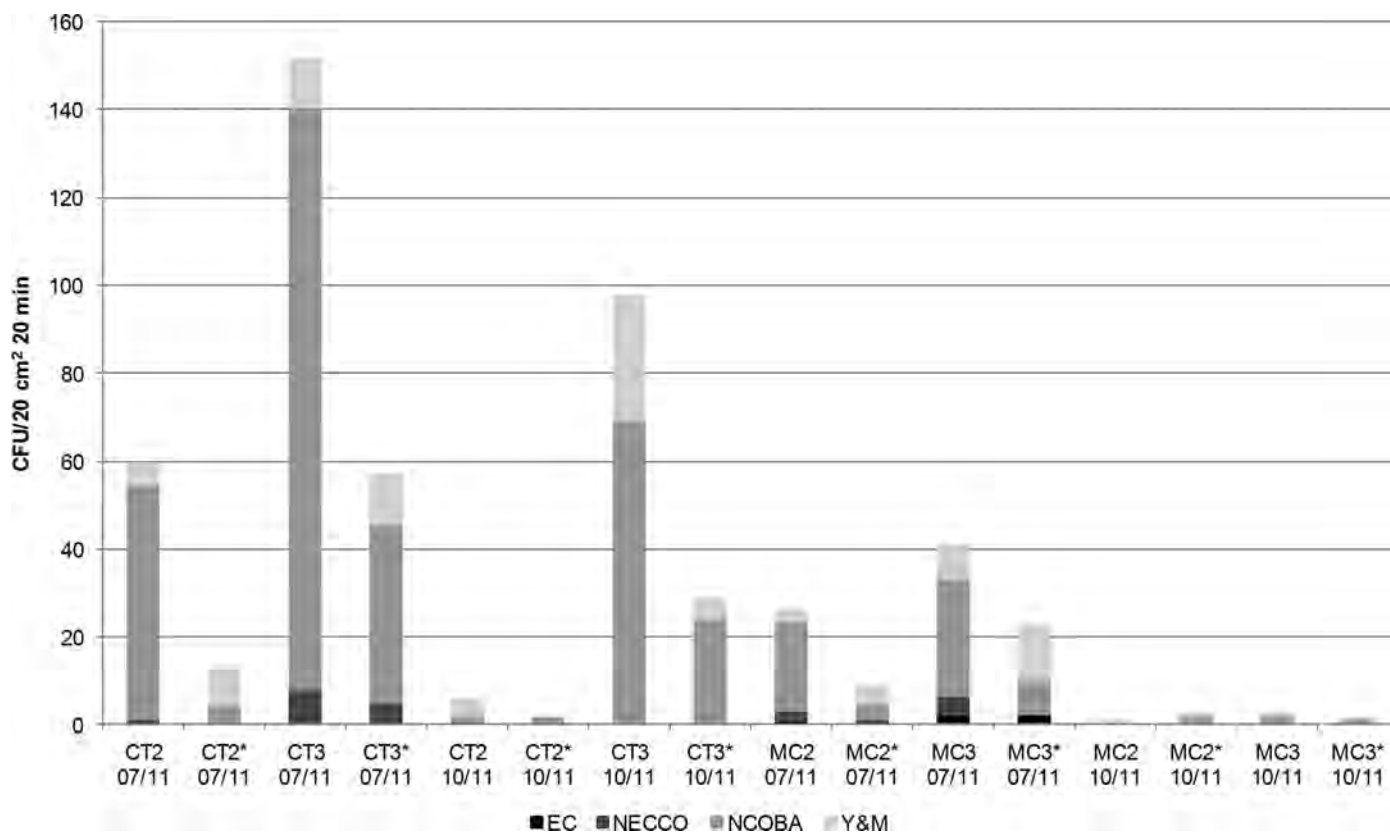
Figure 5. Effect of season and sampling position on concentration of airborne microbes at Cheile Turzii Cave (CT) sampling sites 2 and 3 and at Meziad Cave (MC) sample sites 2 and 3. Sampling was performed in July (7) and October (10) 2011. Samples taken 1.5 meters above the ground are designated by an asterisk; other samples were taken at ground level. EC, *E. coli*; NECCO, other coliforms; NCOBA, non-coliform bacteria; Y&M, yeasts and molds.

The proportion of microbial subgroups seems to be the same at each tested site, with generally smaller concentrations in the autumn when air changes with the subsurface are suppressed and maternity colonies of bats are dispersed. The concentrations of airborne fungi were rather low compared to bacteria (Fig. 5). It is important to underline that sampling at 1.5 m above the ground was chosen as the level of human breathing to point out the possibility of getting in contact with bioaerosols.

AEROSOLIZATION OF MICROBES FROM GUANO

Percentage of aerosolized microbial groups from samples from Cheile Turzii Cave, Gura Dobrogei Cave, and Meziad Cave are summarized in Figure 6. Total bacterial counts ranged from 0.00 to 0.10%, coliforms from 0.00 to 0.16%, *E. coli* 0.00%, enterobacteria from 0.00 to 0.03%, and yeasts and molds from 0.00 to 3.35%. In the three independent sampling campaigns, aerosolization of *E. coli* was unsuccessful, although concentration of this microbe in different tested guanos varied from 0.0 to 1.7×10^7 CFU/g (Table 5). On the other hand, successful aerosolization of coliform bacteria and enterobacteria indicated that aerosolization of *E. coli* may be possible. Transmission of *E. coli* via cave air is probably quite limited.

Artificially induced aerosolization resulted in a large amount of aerosolized fungi from guano. Aerosolization of microbes in caves can be easily enhanced by disturbing guano surfaces while walking. From other microbes-rich materials in different environments, aerosolization can also be caused by wind and animals. Due to their small size, microbes can persist long in the air. For example, droplets more than 5 μm in diameter sediment more quickly on the ground than droplets that are less than 5 μm, which can remain suspended in the air for a long time (D'arcy et al., 2012). As bat guano in Topolniţa Cave was already reported to be the source of *H. capsulatum* (Alteras, 1966), the estimation that more than 3% of cultivable fungi may be aerosolized gives an important warning to avoid contact with potential fungal pathogens from guano. High aerosolization potential of fungal spores from guano can be the answer for many cases of guano-associated histoplasmoses reported in landfill, bridge, and wagon-train workers (Gustafson et al., 1981; Huhn et al., 2005), during home renovations (Schoenberger et al., 1988), or among cavers (Ashford et al., 1999).

BATS AS VECTORS FOR MICROORGANISMS

Bats were swabbed to get an estimation on transmission of microbes on their bodies. Swabbing of *Rhinolophus*
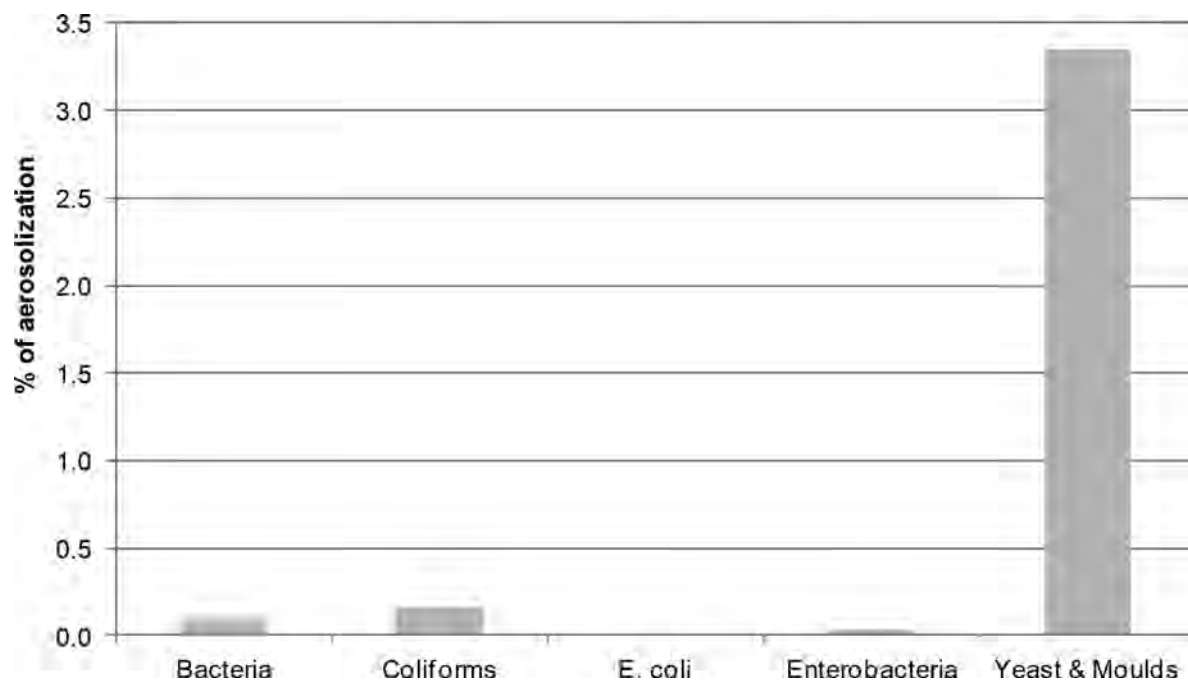
Figure 6. Percentage of aerosolised microbial groups from bat guano.

ferrumequinum coats produced higher numbers of microorganisms than *R. hipposideros* coats (Table 7). Although their body sizes are quite different, *R. ferrumequinum* being almost twice that of *R. hipposideros* (57 to 71 mm versus 37 to 45 mm head and body; 350 to 400 mm versus 192 to 254 mm wingspan), it is possible that behavior is more important for microbial contamination of cave air. In the sampling period at the beginning of November, individuals of *R. hipposideros* were already prepared to hibernate and their daily torpor was already very deep, in contrast to *R. ferrumequinum*, which were still active. Social behavior of bats could also play an important role in spreading of microorganisms; solitary bats rarely get in contact with other bats. *R. hipposideros* usually hang free as isolated individuals and during hibernation wrap themselves completely in their wings, but individuals of *R. ferrumequinum* hibernate in big clusters, where bats coats get in contact because of incomplete wing wrapping. The role of bat species in the propagation and spread of fungi is already known. On one hand their feces serve as a source of

nutrients for microbes, and on the other hand they can be active disseminators of fungi in the environment (Hoff and Bigler, 1981).

CONCLUSIONS

Elevated concentrations of bacteria, including those of enteric origin and to a lesser extent of fungi, were detected in, and around, bat guano. Favorable atmospheric conditions for microbial multiplication, such as high temperature and vaporized compounds from organic matter, produced the highest counts of airborne microorganisms. A cave rich with guano, with high relative humidity, and with a flowing river had the lowest concentrations of airborne microbes. Concentrations of airborne microorganisms were higher at ground level compared to the concentrations at 1.5 m above the ground. Coliform bacteria were frequently detected in air in areas with high organic matter and animal excrements. *E. coli* was rarely found in air, and its successful aerosolization

Table 7. Swab analyses of fur coat of *Rhinolophus* from Meziad Cave expressed as CFU/20 cm² after 48 hours of plate incubation for bacteria and 72 hours for yeast and molds.

Bat Species	Total Bacteria (CFU/20 cm²)	*E.coli* (CFU/20 cm²)	Coliforms (CFU/20 cm²)	Yeast and Molds (CFU/20 cm²)
R. ferrumequinum 1	821	0	0	1067
R. ferrumequinum 2	2005	0	135	1030
R. hipposideros 1	0	0	0	21
R. hipposideros 2	5	0	0	7

was not achieved. Microbial aerosolization rate from guano was for bacteria up to 0.10%, and for fungi up to 3.35%. *Staphylococcus* and *Streptococcus* were found in air close to bat guano. In the summer, microbial load in the cave air was elevated, which we attribute to the presence of bats. The proportion of microbial groups was preserved in the summer and autumn periods. Bats and especially their social behavior are crucial for introduction and spread of airborne microbes. Airborne microbes indicative of bats and guano and especially a high potential of fungal aerosolization represent a biohazard for animals and humans in caves. Activities that lead to aerosol formation from animal excrements should be avoided. In comparison to other external environments, caves provide a simplified system of studying bioaerosols, although even in caves complex relationships between atmospheric and microbiological parameters co-exist.

REFERENCES

Adesiyun, A.A., Stewart-Johnson, A., and Thompson, N.N., 2009, Isolation of enteric pathogens from bats in Trinidad: Journal of Wildlife Diseases, v. 45, no. 4, p. 952–961. doi:10.7589/0090-3558-45.4.952.

Alteras, I., 1966, First Romanian isolation of *Histoplasma capsulatum* from the soil: International Journal of Dermatology, v. 5, no. 2, p. 69–71. doi:10.1111/j.1365-4362.1966.tb05188.x.

ANPM, 2013, Agenţia naţională pentru protecţia mediului: Harta delimitării regiunilor geografice (map of Romanian geographic regions), http://www.anpm.ro/upload/12561_Anexa2_harta_regbiogeografice.pdf [accessed May 15, 2013].

Ashford, D.A., Hajjeh, R.A., Kelley, M.F., Kaufman, L., Hutwagner, L., and McNeil, M.M., 1999, Outbreak of histoplasmosis among cavers attending the National Speleological Society Annual Convention, Texas, 1994: The American Journal of Tropical Medicine and Hygiene, v. 60, no. 6, p. 899–903.

Aydogdu, H., Asan, A., Otkun, M.T., and Ture, M., 2005, Monitoring of fungi and bacteria in the indoor air of primary schools in Edirne City, Turkey: Indoor and Built Environment, v. 14, p. 411–425. doi:10.1177/1420326X05057539.

Bandrabur, G., and Radu, R., 1994, Recherches hydrogéologiques dans la zone de Tureni-Petreştii de Sus (Roumanie). Utilisation de l'électrométrie en hydrogéologie: Theoretical and Applied Karstology, no. 7, p. 109–114.

Barton, H.A., and Pace, N.R., 2005, Discussion: persistent coliform contamination in Lechuguilla cave pools: Journal of Cave and Karst Studies, v. 67, no. 1, p. 55–57.

Beldean, P.-V., 2005, Ecological Studies on the Coreoidea (Heteroptera, Insecta) in the Nature Reserve Cheile Turzii (Cluj County): Studia Universitatis Babeş-Bolyai, Studia Biologia, v. 50, no. 1, p. 3–10.

Bleahu, M., Decu, V., Negrea, Ş., Pleşa, C., Povară, I., and Viehmann, I., 1976, Peşteri din România: Bucureşti, România, Editura Ştiinţifică şi Enciclopedică, 415 p.

Borda, C., and Borda, D., 2004, Airborne microorganisms in show caves from Romania: Travaux de L' Institut de Spéologie "Émile Racoviza", v. 43–44, p. 65–74.

Borda, C., Popescu, S., and El Mahdy, I.C., 2012, Seasonal evolution of the microclimate factors level in a zoo: Bulletin of University of Agricultural Sciences and Veterinary Medicine Cluj-Napoca, Veterinary Medicine, v. 69, no. 1–2, p. 49–53.

Borda, D., 2002a, Chiropterele, *in* Racoviţă, G., Moldovan, O., and Onac, B.P., eds., Monografia carstului din Munţii Pădurea Craiului: Cluj-Napoca, Presa Universitară, p. 172–182.

Borda, D., 2002b, The distribution of bats in Romanian caves (I): Travaux de L' Institut de Spéologie "Émile Racoviza", v. 37–38, p. 223–230.

Borda, D., Borda, C., and Tămaş, T., 2004, Bats, climate and air microorganisms in a Romanian cave: Mammalia, v. 68, no. 4, p. 337–343. doi:10.1515/mamm.2004.033.

Borda, D., Năstase-Bucur, R., Borda, C., and Gorban, I., 2009, The assessment of the airborne microorganismes in subterranean environment—preliminary data: Bulletin of University of Agricultural Sciences and Veterinary Medicine Cluj-Napoca, Veterinary Medicine, v. 66, no. 1, p. 236–242.

Burghele-Bălăcescu, A., and Avram, S., 1966, Peşteri cercetate în Oltenia, între valea Motrului şi Valea Tismanei: Travaux de L' Institut de Spéologie "Émile Racoviza", v. 5, p. 21–42.

Carbonnel, J.-P., Decu, V., Olive, P., Povara, I., and Gheorghiu, V., 1996, Première datation par C14 du remplissage de guano d'une grotte des Carpates Meridionales: Peştera lui Adam (Roumanie) : Travaux de L' Institut de Spéologie "Émile Racoviza", v. 35, p. 145–154.

Chapman, G.H., 1945, Determination of the Chromogenic Property of Staphylococci: Journal of Bacteriology, v. 50, no. 2, p. 201–203.

Chroňáková, A., Horák, A., Elhottová, D., and Krištůfek, V., 2009, Diverse archaeal community of a bat guano pile in Domica Cave (Slovak Karst, Slovakia): Folia Microbiologica, v. 54, p. 436–446. doi:10.1007/s12223-009-0061-2.

Coroiu, I., David, A., and Borda, D., 2007, Bats hibernacula in Meziad Cave: Miscellanea Chiropterologica, v. 1, p. 77–81.

Costache, I., 2011, Flora şi vegetaţia bazinului Hidrografic inferior al râului Motru, v. I. Flora: Craiova, Romania, Ed. Universitară, 215 p.

D'Arcy, N., Canales, M., Spratt, D.A., and Lai, Ka Man, 2012, Healthy schools: standardisation of culturing methods for seeking airborne pathogens in bioaerosols emitted from human sources: Aerobiologia, v. 28, no. 4, p. 413–422. doi:10.1007/s10453-012-9251-5.

Deharveng, L., 2005, Diversity patterns in the tropics, *in* Culver, D.C., and White, W.B., eds., Encyclopedia of Caves: Burlington, Massachusetts, Elsevier/Academic Press, p. 166–170.

Di Bella, C., Piraino, C., Caracappa, S., Fornasari, L., Violani, C., and Zava, B., 2003, Enteric microflora in Italian chiroptera: Journal of Mountain Ecology, no. 7 (Suppl.), p. 221–224.

Drăghici, C., Popescu, S., Borda, C., and Kallay, Z., 2002, Density and quality of air micro-organisms in poultry houses for broiler chicken: Buletinul Universităţii de Ştiinţe Agricole şi Medicină Veterinară Cluj-Napoca, Seria Medicină Veterinară, v. 57–58, p. 555–560.

Fabian, M.P., Miller, S.L., Reponen, T., and Hernandez, M.T., 2005, Ambient bioaerosol indices for indoor air quality assessments of flood reclamation: Aerosol Science, v. 36, p. 763–783. doi:10.1016/j.jaerosci.2004.11.018.

Guentzel, M.N., 1996, *Escherichia, Klebsiella, Enterobacter, Serratia, Citrobacter*, and *Proteus*, *in* Baron, S., ed., Medical Microbiology, 4th edition: University of Texas Medical Branch at Galveston; Chapter 26, http://www.ncbi.nlm.nih.gov/books/NBK8035/, [accessed May 15, 2013].

Gustafson, T.L., Kaufman, L., Weeks, R., Ajello, L., Hutcheson, R.H., Wiener, S.L., Lambe, D.W., Sayvetz, T.A., and Schaffner, W., 1981, Outbreak of acute pulmonary histoplasmosis in members of a wagon train: American Journal of Medicine, v. 71, p. 759–765.

Hodorogea, P., 1972, Recherches microbiologiques dans la grotte de Topolniţa (Roumanie). Première note: Travaux de L' Institut de Spéologie "Émile Racoviza", v. 11, p. 335–342.

Hoff, G.L., and Bigler, W.J., 1981, The role of bats in the propagation and spread of histoplasmosis: A review: Journal of Wildlife Diseases, v. 17, no. 2, p. 191–196.

Holmes, M.C., and Lermit, A., 1955, Transport and enrichment media in the isolation of haemolytic streptococci from the upper respiratory tract: Monthly Bulletin of the Ministry of Health and the Public Health Laboratory Service, v. 14, p. 97–103.

Hospodsky, D., Qian, J., Nazaroff, W.W., Yamamoto, N., Bibby, K., Rismani-Yazid, H., and Peccia, J., 2012, Human occupancy as a source of indoor airborne bacteria: PLoS ONE, v. 7, no. 4, e34867. http://www.plosone.org/article/info%3Adoi%2F10.1371%2Fjournal.pone.0034867, [accessed May 15, 2013]. doi:10.1371/journal.pone.0034867.

Hughes, K.A., 2003, Influence of seasonal environmental variables on the distribution of presumptive fecal Coliforms around an Antarctic research station: Applied and Environmental Microbiology, v. 69, no. 8, p. 4884–4891. doi:10.1128/AEM.69.8.4884-4891.2003.

Huhn, G.D., Austin, C., Carr, M., Heyer, D., Boudreau, P., Gilbert, G., Eimen, T., Lindsey, M.D., Cali, S., Conover, C.S., and Dworkin, M.S., 2005, Two outbreaks of occupationally acquired histoplasmosis: more than workers at risk: Environmental Health Perspectives, v. 113, no. 5, p. 585–589. doi:10.1289/ehp.7484.

Jülg, B., Elias, J., Zahn, A., Köppen, S., Becker-Gaab, C., and Bogner, J., 2008, Bat-associated histoplasmosis can be transmitted at entrances of bat caves and not only inside the caves: Journal of Travel Medicine, v. 15, p. 133–136. doi:10.1111/j.1708-8305.2008.00193.x.

Kibbey, H.J., Hagedorn, C., and McCoy, E.L., 1978, Use of fecal streptococci as indicators of pollution in soil: Applied and Environmental Microbiology, v. 35, no. 4, p. 711–717.

Lungu, M., 2008, Resurse şi riscuri climaticed in Dobrogea [PhD Thesis]: Universitatea Bucureşti, 279 p.

Mandal, J., and Brandl, H., 2011, Bioaerosols in indoor environment - a review with special reference to residential and occupational locations, The Open Environmental and Biological Monitoring Journal, v. 4, p. 83–96. doi:10.2174/1875040001104010083.

Mitscherlich, E., and Marth, E.H., 1984, Microbial Survival in the Environment—Bacteria and Rickettsiae Important in Human and Animal Health: Berlin, Springer-Verlag, 802 p. doi:10.1007/978-3-642-69974-0.

Mohod, R.S., 2011, Studies on thermostable alkaliphilic extracellular lipase producing halo-alkaliphilic bacteria from bat guano of Lonar Lake: International Journal of Advance Pharmaceutical and Biological Sciences, v. 1, no. 1, p. 24–29.

Moulds, T.A., 2006, The seasonality, diversity and ecology of cavernicolous guano dependent arthropod ecosystems in southern Australia. [PhD. Thesis]: Adelaide, Australia, The University of Adelaide, 260 p. http://hdl.handle.net/2440/37815 [accessed May 15, 2013].

Moza, A.C., 2008, Aspects regarding the mean annual quantities of rainfall in the Crişul Repede hydrographic basin: Analele Universităţii din Oradea, Seria Geografie, v. 18, p. 74–80.

Mulec, J., 2008, Microorganisms in hypogeon: examples from Slovenian karst caves: Acta Carsologica, v. 37, no. 1, p. 153–160.

Mulec, J., Krištůfek, V., and Chroňáková, A., 2012a, Comparative microbial sampling from eutrophic caves in Slovenia and Slovakia using RIDA®COUNT test kits: International Journal of Speleology, v. 41, no. 1, p. 1–8. doi:10.5038/1827-806X.41.1.1.

Mulec, J., Krištůfek, V., and Chroňáková, A., 2012b, Monitoring of microbial indicator groups in caves through the use of RIDA® COUNT kits: Acta Carsologica, v. 41, no. 2–3, p. 287–296.

Mulec, J., Vaupotič, J., and Walochnik, J., 2012c, Prokaryotic and eukaryotic airborne microorganisms as tracers of microclimatic changes in the underground (Postojna Cave, Slovenia): Microbial Ecology, 2012, v. 64, no. 3, p. 654–667. doi:10.1007/s00248-012-0059-1.

Munteanu, C., 2011, Bãile Herculane Resort: Balneo-Research Journal, English Edition, v. 2, no. 3, p. 17–23. doi:10.12680/balneo.2011.1020.

Neidhardt, F.C., Curtis, III, R., Ingraham, J.L., Lin, E.C.C., Low, K.B., Magasanik, B., Reznikoff, W.S., Riley, M., Schaechter, M., and Umbarger, H.E., 1996, Escherichia coli and Salmonella, Cellular and Molecular Biology: Washington, D.C., American Society for Microbiology Press, 2822 p.

Oarga, A., Griessler Bulc, T., Jenssen, P.D., and Mulec, J., 2012, Monitoring of microbial indicator groups in organically heavily loaded wastewater treatment systems by using RIDA®COUNT kits: Fresenius Environmental Bulletin, v. 21, no. 12a, p. 3886–3893.

Pocora, I., and Pocora, V., 2011, Bat communities in four dobrogean caves (Romania): Analele Ştiinţifice ale Universităţii ''Alexandru Ioan Cuza'' din Iaşi, Biologie animală, v. 57, p. 107–124.

Poulson, T.L., and Lavoie, K.H., 2000, The trophic basis of subsurface ecosystems, in Wilkins, H., Culver, D.C., and Humphreys, W.F., eds., Subterranean Ecosystems: Amsterdam, Elsevier Press, Ecosystems of the World 30, p. 231–249.

Povară, I., Diaconu, G., and Goran, C., 1972, Observations préliminaries sur les grottes influences par les eaux thermo-minérales de la zone Băile Herculane: Travaux de L' Institut de Spéleologie "Émile Racoviza", v. 11, p. 355–366.

Robu, M., 2009, Groundwater vulnerability assessment in the Motru Sec karst area, Mehedinţi Mountains: Travaux de L' Institut de Spéleologie "Émile Racoviza", v. 48, p. 69–81.

Schoenberger, C.I., Weiner, J.H., Mayo, F.J., Spellman, J., and Waltersdorff, R.G., 1988, Acute pulmonary histoplasmosis outbreak following home renovation: Maryland Medical Journal, v. 37, no. 6, p. 457–460.

Schulz, J., Hartung, J., Seedorf, J., and Formosa, L.C., 2004, Staphylococci as an indicator for bacterial emissions from a broiler house, in Madec, F., and Clement, G., eds., Proceeedings of In Between Congress of The International Society for Animal Hygiene, Animal production in Europe: The way forward in a changing world, Sant-Maolo, France, Oct. 2004, v. 1, p. 75–78.

Simon, K.S., 2012, Cave ecosystems, in White, W.B., and Culver, D.C., eds., Encyclopedia of Caves, 2nd ed.: Amsterdam, Academic Press, p. 99–102.

Sorocovschi, V., and Vodă, M., 2009, The study of drought phenomena in the Transylvania plain using the analysis of the non-periodical variations of precipitations, in Proceedings of the 4th IASME/WSEAS International Conference on Water, Resources, Hydraulics and Hydrology (WHH'09), Cambridge, UK, Feb. 2009: WSEAS Press, p. 163–167.

ter Braak, C.J.F., and Šmilauer, P., 2002, CANOCO Reference Manual and CanoDraw for Windows User's Guide: Software for Canonical Community Ordination (version 4.5). Ithaca, NY, USA (www.canoco.com): Ithaca, New York, Microcomputer Power, 500 p.

Todoran, V., and Onac, B., 1987, La morphologie de l'exo- et de l'endokarst du plateau de Purcăreţ-Mesteacăn (Plateau du Someş): Theoretical and Applied Karstology, v. 3, p. 127–131.

Vandžurová, A., Bačkor, P., Javorský, P., and Pristaš, P., 2013, Staphylococcus nepalensis in the guano of bats (Mammalia): Veterinary Microbiology, v. 164, no. 1–2, p. 116–121. doi:10.1016/j.vetmic.2013.01.043.

White, W.B., and Culver, D.C., 2012, Cave, Definition of, in White, W.B., and Culver, D.C., eds., Encyclopedia of Caves, 2nd ed.: Amsterdam: Academic Press, p. 103–107.

Womack, A.M., Bohannan, B.J.M., and Green, J.L., 2010, Biodiversity and biogeography of the atmosphere: Philosophical Transactions of the Royal Society B, Biological Sciences, v. 365, p. 3645–3653. doi:10.1098/rstb.2010.0283.

GLACIAL LAKE SCHOHARIE: AN INVESTIGATIVE STUDY OF GLACIOLACUSTRINE LITHOFACIES IN CAVES, HELDERBERG PLATEAU, CENTRAL NEW YORK

Jeremy M. Weremeichik and John E. Mylroie

Department of Geosciences, Mississippi State University, MS 39762-5448, USA, jmw868@msstate.edu

Abstract: The glacially deranged karst topography of the Helderberg Plateau, central New York, contains glaciolacustrine lithofacies deposited at the end of the Wisconsin glaciation. Eight pre-glacial caves (Barrack Zourie Cave, McFail's Cave, Howe Caverns, Secret Caverns, Bensons Cave, Gage Caverns, Schoharie Caverns, and Caboose Cave), containing a unique sediment section, are located within the footprint of Glacial Lake Schoharie, Schoharie County. The lithofacies consist of three individual facies, stratigraphically uniform, with the middle facies in sharp contact with the facies directly above and below. This assemblage displays a similar stratigraphic sequence from bottom to top: tan/white to light-grey, very thinly bedded, silts and clays, rich in calcite, overlain by poorly sorted, matrix-supported gravels, in turn overlain by dark-brown very thinly bedded silts and clays. A post-glacial cave within the lake's footprint (Westfall Spring Cave) and a nearby pre-glacial cave outside the footprint (Knox Cave) were found to lack these lithofacies. The tan/white to light-grey sediment facies is interpreted to be a glacial rock flour deposited under stagnant lake conditions that limited fine-grained calcite particle dissolution. The overlying gravel facies were emplaced during lake termination and reestablishment of turbulent epigenic flow in the eight stream caves. The more recent dark-brown facies is perhaps soil-loss deposition following European settlement. Initial interpretations hypothesized that the deposits were laid down under ice-cover conditions, but similar deposits were not found in other glaciated cave settings in New York. The results presented here explain why the unusual tan/white and light-grey glaciolacustrine facies are not found in other caves in the glaciated central New York region, as those areas were not subject to inundation by glacial lake water.

INTRODUCTION

As glaciers advanced and retreated across northeastern USA during the late Pleistocene, sediment and exposed bedrock were stripped from the cave-rich Helderberg Plateau in central New York State (Fig. 1) and subsequently covered by allochthonous glacial sediment. The sediment was deposited on the surface of the plateau and in caves within the plateau. The glacial sediment deposited within the caves has been sheltered from surficial weathering and erosion, perhaps allowing for a more accurate record to be preserved. Interpretation and analysis of cave-sediment samples can assist in reconstructing the glacial surficial environment. In most glacially deranged landscapes, surficial deposits can be scarce and difficult to identify; this study focused and relied on samples collected from within caves. Specific horizons of sediment found within the caves in the area are thought to be associated with the existence of a glacial event (Mylroie, 1984; Palmer et al., 1991; Palmer et al., 2003). The work presented here re-interprets those earlier studies and classifies the unique cave sediments as being the result of a glacial lake inundating the caves. This lake, referred to as Glacial

Lake Schoharie, is believed to have existed during the Late Wisconsin glacial period approximately 23.0–12.0 ka in the present-day Schoharie Valley in central New York (e.g., Dineen, 1986).

To determine the nature of the surficial environment in the Schoharie Valley during the Late Wisconsin glacial period, multiple research trips were taken to select caves located in the Helderberg Plateau. From west to east, the caves in this study include: Barrack Zourie Cave (1 in Fig. 1), McFail's Cave (2), Howe Caverns (3), the Secret-Benson Cave System (4 and 5), Gage Caverns (6), Westfall Spring Cave (7), Schoharie Caverns (8), Caboose Cave (9), and Knox Cave (10) (Figs. 1 and 2). As documented by Lauritzen and Mylroie (2000), U/Th dating of stalagmites demonstrates that the caves of the Schoharie Valley are older than the onset of the most recent glaciation and, in some cases, several glaciations reaching back 350 ka.

The purpose of this study was to reconstruct the paleo-environment of a proglacial lake, Glacial Lake Schoharie, located primarily within Schoharie County, New York. The glacial lake is thought to have endured at least four readvances of the Mohawk and Hudson glacial lobes during the Woodfordian Substage of the Late Wisconsin
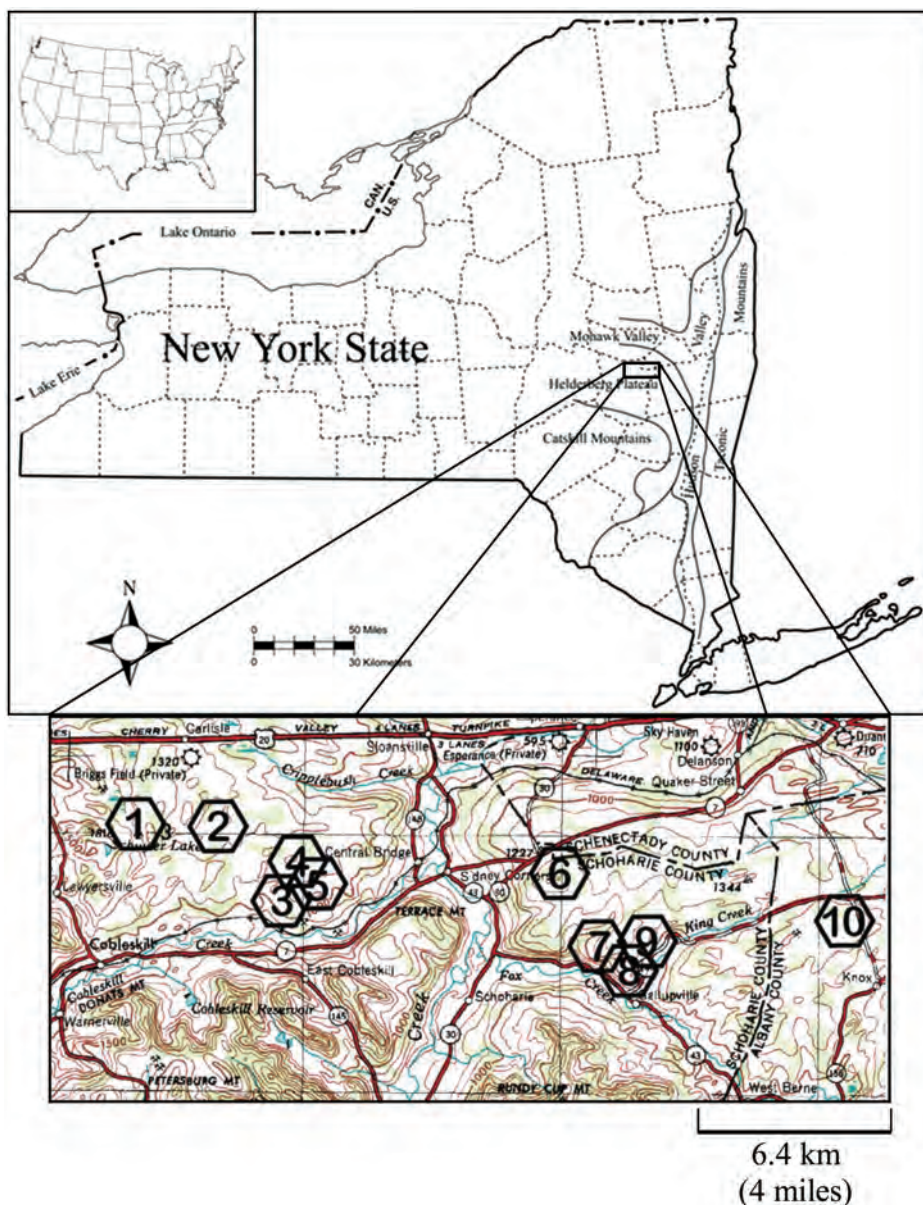
Figure 1. Map showing the general location of the Helderberg Plateau in east-central New York as well as the locations of the caves included in this study. 1 = Barrack Zourie Cave, 2 = McFail's Cave, 3 = Howe Caverns, 4 = Secret Caverns, 5 = Benson's Cave, 6 = Gage Caverns, 7 = Westfall Spring Cave, 8 = Schoharie Caverns, 9 = Caboose Cave, 10 = Knox Cave. Re-drawn and modified from Dineen (1986). The topographic map is a USGS Digital Raster Graphic of the Binghamton Quadrangle (1:250,000 scale).

glaciation; see Dineen (1986) for more detail on the nature of the readvances. The multiple readvances caused the shoreline of the lake, and hence its footprint, to be modified multiple times throughout its existence. The caves selected for investigation were chosen because of the known or suspected existence of what had been presumed to be glacially deposited clastics, in particular a characteristic white or tan clay that is sometimes varved (e.g., Mylroie, 1984; Dumont, 1995) (Figs. 3 and 4). It was also the purpose of this study to determine the composition

of the "white" clay horizon, as well as the composition of other associated sediment horizons (Fig 4).

Initial interpretation of Mylroie (1984) was that the sediments found in the caves were caused by stagnant sub-ice conditions during the last glacial maximum. Under these conditions, Mylroie (1984) thought that the stagnant water would soon saturate with $CaCO_3$ and that any further fine-grained particulate $CaCO_3$ introduced to the caves would not dissolve and could collect as a sediment deposit. There was no disagreement in the literature about
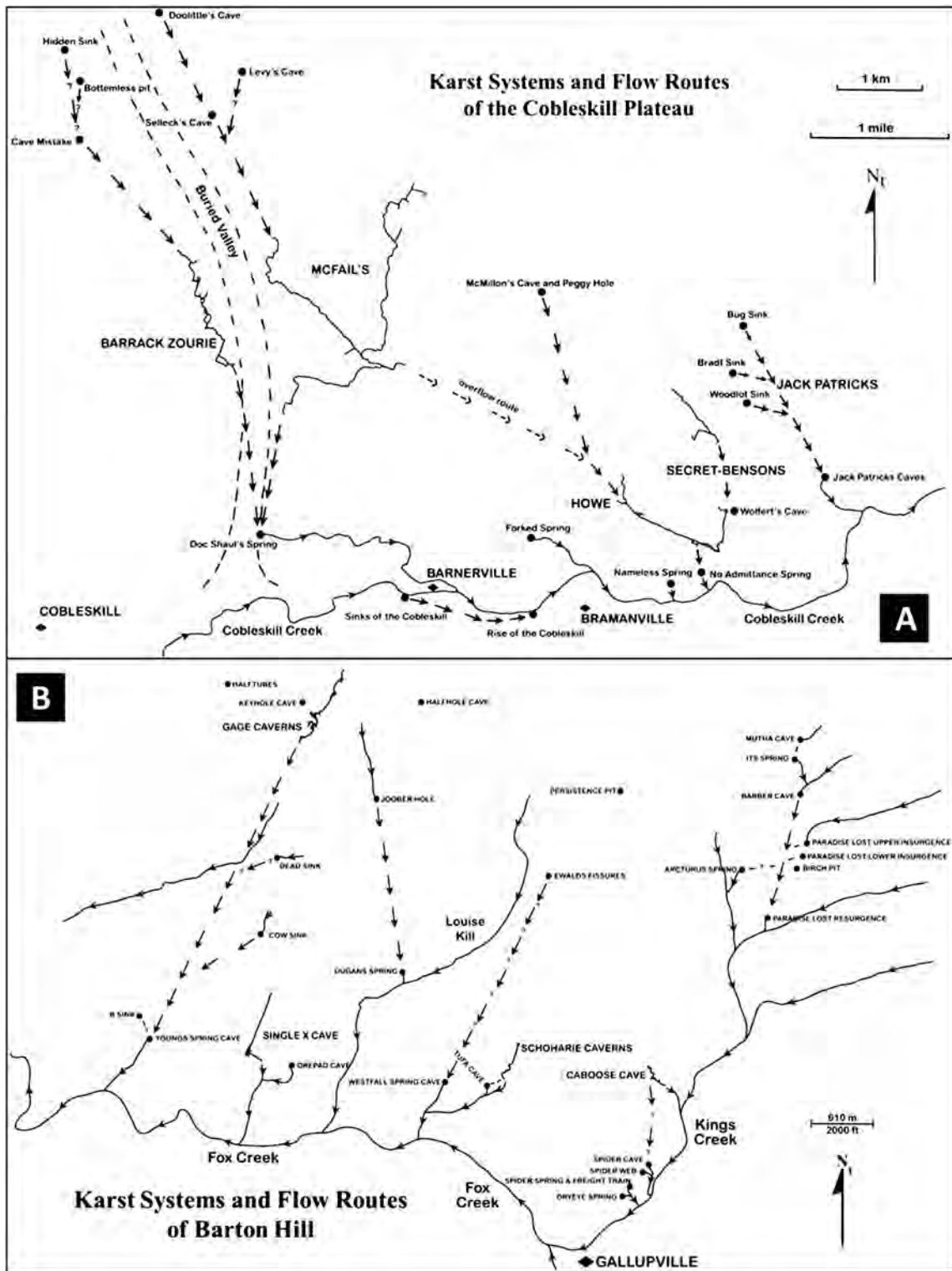
Figure 2. A: Map of the karst systems and flow routes of the Cobleskill Plateau. The buried valley is located between Barrack Zourie Cave and McFail's Cave (re-drawn from Dumont, 1995). B: Map of the karst systems and flow routes of Barton Hill (re-drawn from Mylroie, 1977).
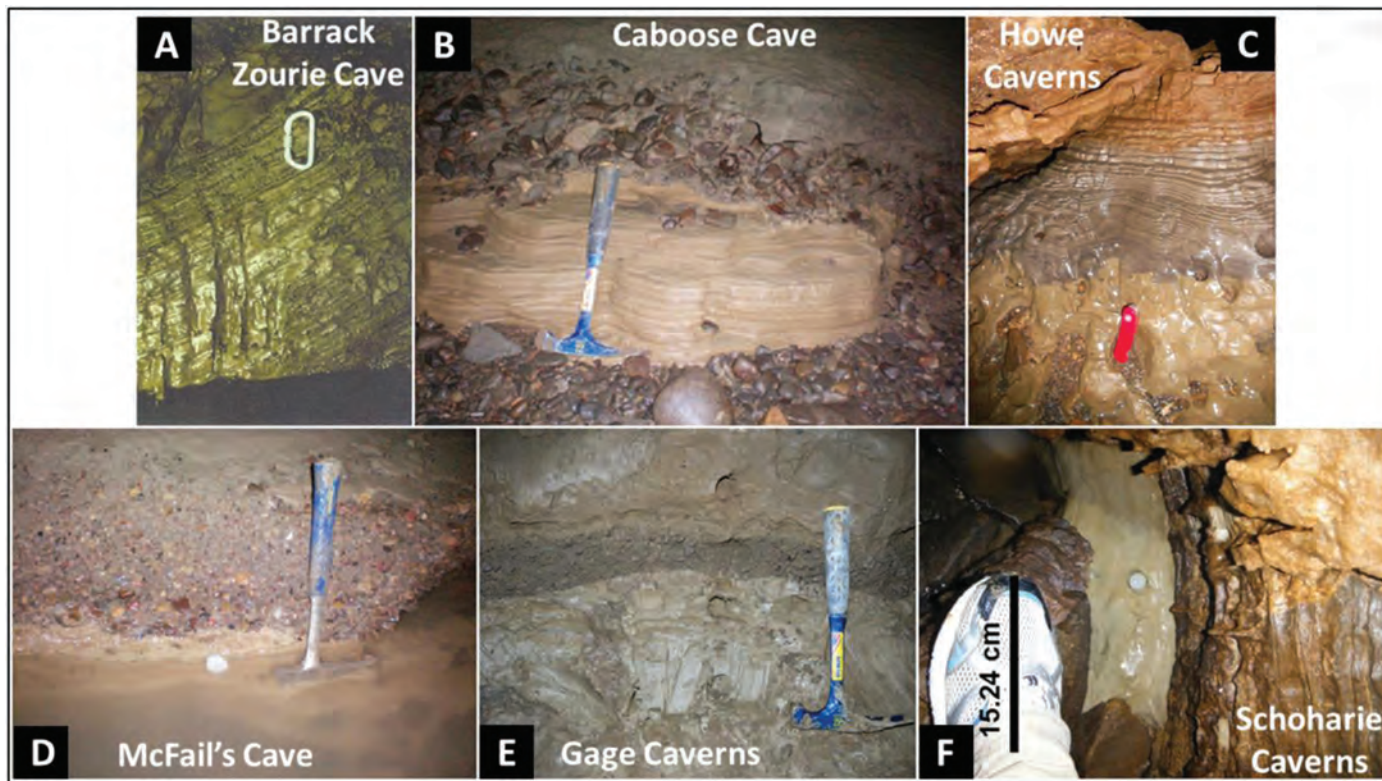
Figure 3. Distinct "white" clay was found to exist in multiple caves selected for this study. Note in B, D, and E the abrupt transition from the finely laminated light-colored material at the bottom of the section to the very coarse gravelly layer above. The darker colored fine-grained deposit that commonly caps the sequence is best seen in B.

this interpretation (e.g., Palmer et al., 2003), but it was recognized that caves in other areas of the state lacked these glacial sediments. The question became, what was unique about the caves in the Schoharie Valley. The presence of a glacial lake could create the same stagnant-water conditions in the underlying caves, and the lake's footprint would explain the unique cluster of caves containing the glacial sediment.

CAVES OF THE HELDERBERG PLATEAU

The caves located in the Helderberg Plateau formed in the Upper Silurian and Lower Devonian limestones of the Helderberg Group. The major caves and cave systems within the plateau, including the caves mentioned in this study, primarily formed within the thick-bedded Coeymans Limestone and the thinly bedded Manlius Limestone (Fig. 5). There has also been some cavern development within the Rondout Dolomite, as at Knox Cave and Baryte's Cave (Mylroie, 1977; Palmer, 2009), but cavern development within this particular unit is usually limited to conduits with small cross-sectional areas.

The caves and karst features of the Helderberg Plateau were created by epigenic processes providing surface runoff water an alternative to over-land flow paths, allowing water to travel more directly. The karst features of the

Helderberg Plateau have been described as "one of the finest examples of glaciated karst in the country" (Palmer et al., 1991, p. 161).

There has been extensive published work regarding the caves located in the Cobleskill Plateau and adjoining areas, such as that of Dumont (1995), Kastning (1975), Mylroie (1977), and Palmer et al. (2003). The glacial deposits within the caves were discussed by these authors, but the link of these sediments to a postulated glacial lake in this area had not been thoroughly investigated.

Westfall Spring Cave was included in this study because its geologic context suggested it was post-glacial in origin; and therefore, it should not have a glacial sediment signature. Knox Cave was included because it is outside the footprint of Glacial Lake Schoharie. These two caves acted as controls for the sediment study.

THE WISCONSIN GLACIATION IN THE HELDERBERG PLATEAU

The last major Pleistocene glaciation to occur in New York was the Late Wisconsin glaciation. The Helderberg Plateau was covered by three lobes of glacial ice, the Mohawk lobe, the Hudson lobe, and the Schoharie sub-lobe, during the onset of the Late Wisconsin glaciation (Dineen, 1986). The lobes that covered the plateau entered
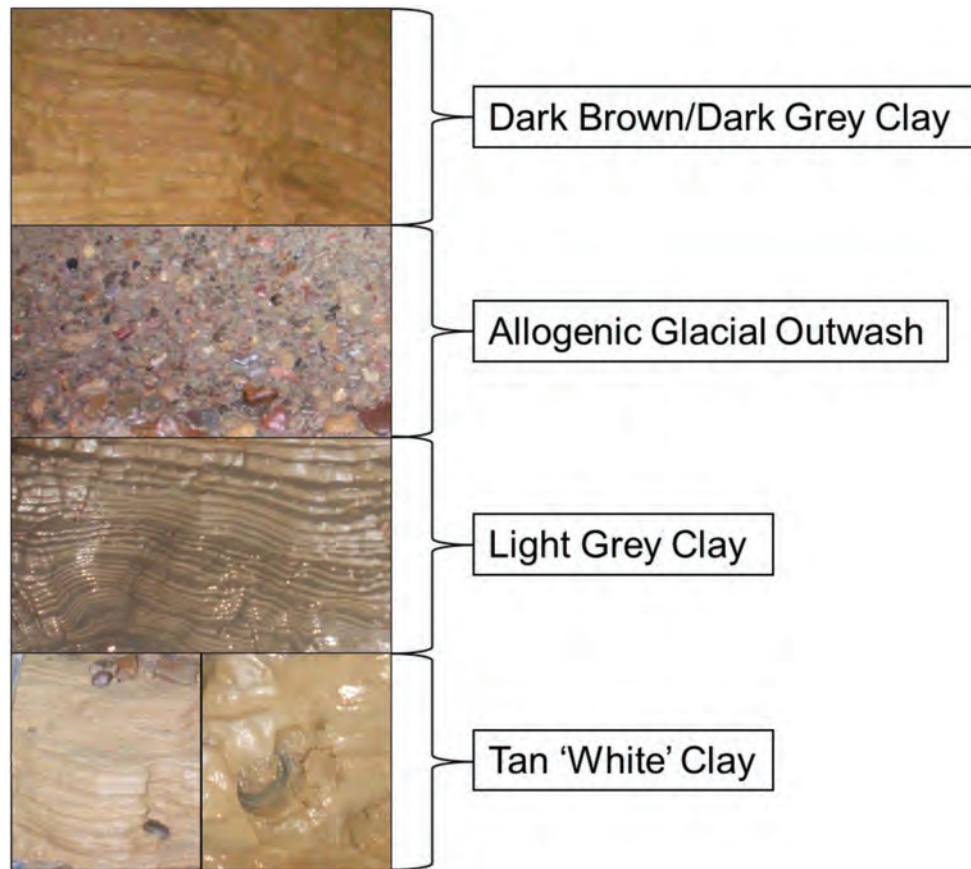
Figure 4. Examples of the sediment layers, in stratigraphic order, encountered within the caves in this study.

the region from the northeast, as shown by drumlins and bedrock striations found in the study area that have a clear northeast-southwest trend (Mylroie and Mylroie, 2004).

The glacial lobes deranged the landscape, altering it greatly. The landscape seen today is covered by drumlins, kames, glaciokarst, and buried glacial drainage basins, as well as other paleoglacial landforms. Dineen and Hanson (1985) proposed the Late Wisconsin glaciation ended in the region approximately 12,300 years ago, but the exact date is still highly debated. According to Muller and Calkin (1993), the Wisconsin is broken up into Early (~117.0–64.0 ka), Middle (~64.0–23.0 ka), and Late (~23.0–11.9 ka) episodes.

Glacial Lake Schoharie

A glacial lake is a body of fresh water that is confined partly or entirely by a glacier or a geomorphic feature produced by a glacier (LaFleur, 1976). As mentioned earlier, there were a number of advance, retreat, and readvance phases associated with the Late Wisconsin glaciation in New York, resulting in the formation of multiple glacial lakes.

The instability of glacial ice caused Glacial Lake Schoharie to have shorelines at varying elevations through-

out the Late Wisconsin glaciation. The Woodstock ice margin was established by a halt in ice retreat from 18.2–17.4 ka, according to Ridge (2004). Following the establishment of the ice margin, glacial meltwater began to flood the Schoharie Valley. As the stagnated glacial ice continued to melt and retreat toward the northeast, water levels continued to rise until a glacial lake was established with a shoreline at an elevation of 213 m (700 ft) above sea level (Dineen, 1986) (Fig. 6). The establishment of Glacial Lake Schoharie will be called *stage one* of three known stages of the glacial lake's development.

With the onset of the Middleburg readvancement at ~17.4 ka, based on Ridge (2004), advancing ice re-entered the Schoharie Valley and the greater Helderberg area until the ice reached the Catskill Front (Catskill Mountains). After reaching the Catskill Front, the glacier stagnated and once again began to retreat northward. While retreating, the glacier produced a vast amount of meltwater, resulting in the enlargement of several proglacial lakes (Dineen, 1986). Glacial Lake Schoharie enlarged considerably and established a shoreline between 354 and 366 m (1,160 and 1,200 ft) above sea level (Fig. 7), reaching *stage two*.

With the establishment of the Delmar ice margin at ~16.2 ka (Ridge, 2004), water from Glacial Lake Schoharie drained to the northeast, through what is known
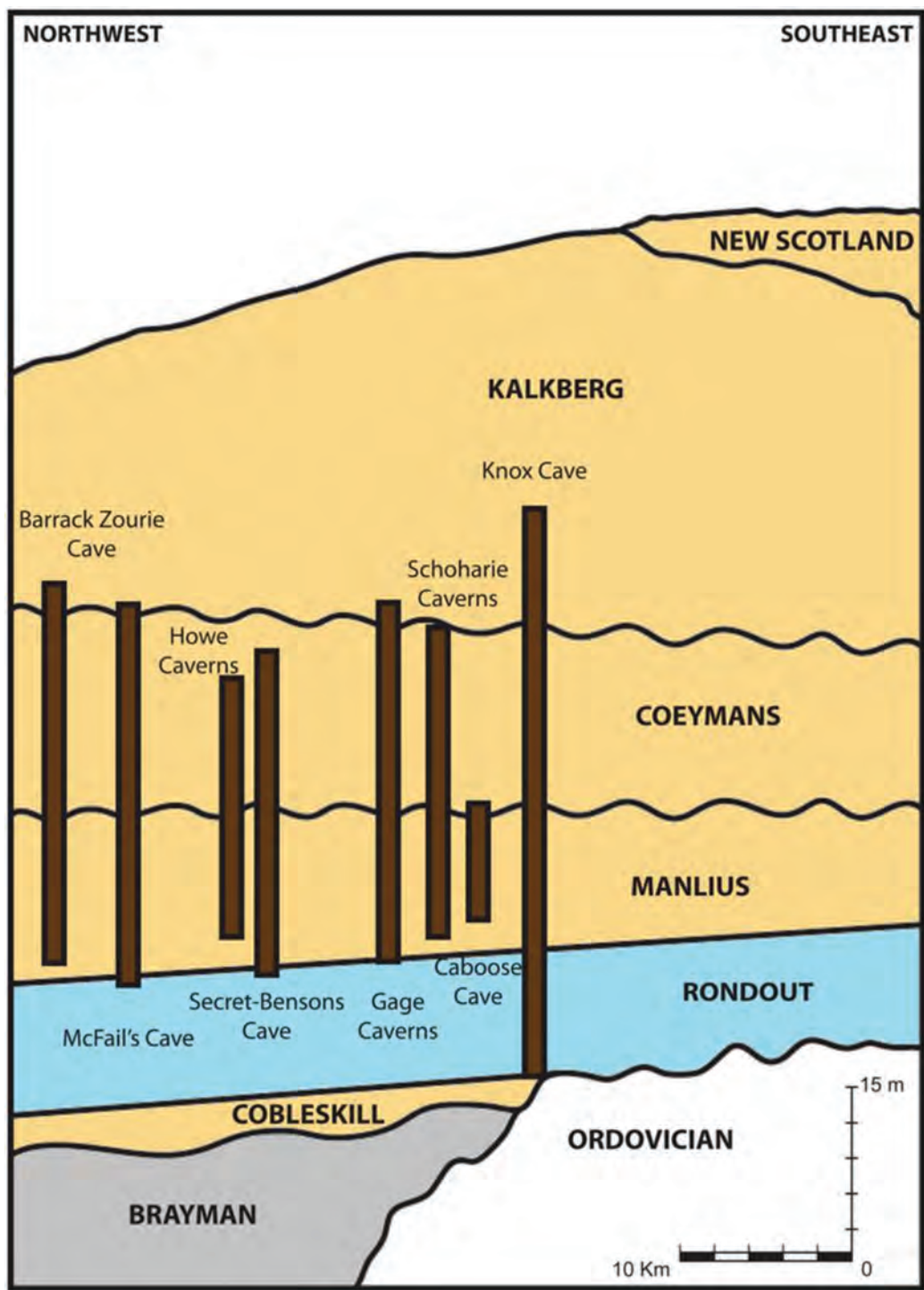
Figure 5. Generalized diagram depicting the Silurian and Devonian rocks in which the caves of this study formed. The grey unit is shale, blue unit is dolomite, and the tan units are limestone.

as the Delanson spillway (LaFleur, 1969). The spillway fed the Delanson River, which eventually emptied into Glacial Lake Albany (LaFleur, 1976). The *stage three* shoreline of Glacial Lake Schoharie was established at 256 to 213 m (840 to 700 ft) above sea level (LaFleur, 1969; Dineen and Hanson, 1985) (Fig. 8).

METHODS

A total of 63 samples were collected and stored in sterilized plastic 35 mm film canisters for this study; three additional samples were collected from Barrack Zourie Cave by Kevin Dumont in 1995. Each sample was labeled
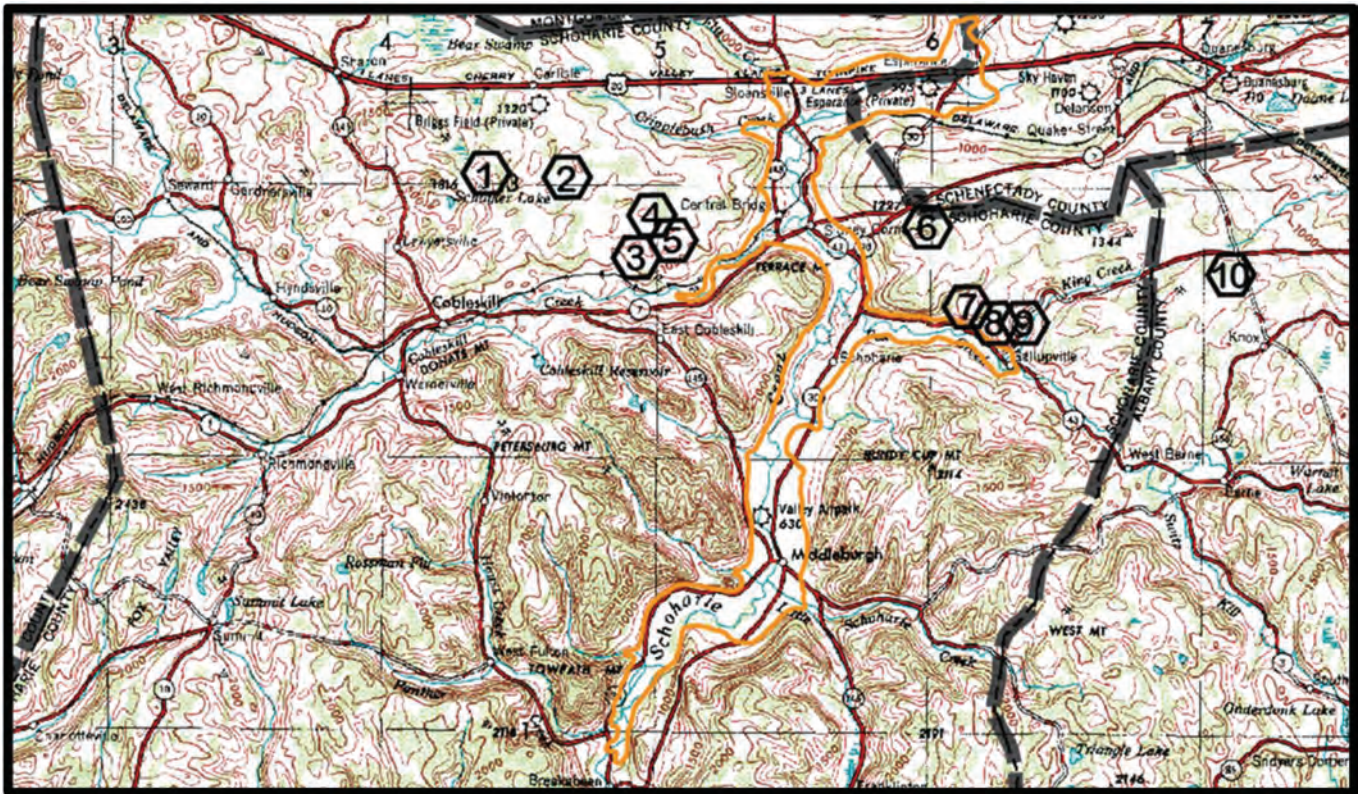
Figure 6. Topographic map showing the location of the caves in relation to the 213 m (700 ft or stage one) shoreline of Glacial Lake Schoharie outlined in orange, created using information provided by Dineen (1986). Caves are numbered as in Figure 1. The grid is 6.4 by 6.4 km (4 by 4 miles.)

with the cave, the location in the cave, and the stratum in the outcrop at that location.

The samples collected for this study come from a wider suite of caves than those used in Mylroie (1984), and more sophisticated analysis techniques were conducted to determine how reliable Mylroie's results were and how the samples compare to his data from Caboose Cave. The sample analyses were not intended to be diagnostic, but to provide a reconnaissance baseline to guide further research.

To determine a general mineralogical content of the samples collected, x-ray diffraction (XRD) was utilized because of its ability to provide qualitative results in a cost-effective and time-efficient manner. All XRD analyses of powdered samples were conducted using the Rigaku Ultima III X-ray diffractometer and were interpreted using the MDI Jade 8 program. The XRD pattern for each sample was obtained using CuKα radiation with a wavelength of 1.541867 Å. Scan speed was set for 2 degrees a minute with a scan step of 0.02 degrees, a scan axis of 2-theta/theta, and an effective scan range of 3.00–70.00 degrees.

RESULTS

The laboratory analyses of samples to determine the mass of water in each sample, the mass of carbonates, and the mass of organics with the purpose of discerning a pattern among individual clastic units recovered from the ten caves in this study was inconclusive in terms of a recognizable pattern and can be seen in Weremeichik (2013).

Although the laboratory results were inconclusive, X-ray diffraction yielded more conclusive information. The XRD data were not used to determine actual amounts of materials in a given sample; it was an assay of presence or absence. Table 1 shows the frequency of mineral content found to exist in each type of sample. Figure 4 shows typical examples of the vertical sequence of the sediment types found in the caves and used in Table 1. For example, the dark-grey/dark-brown clay unit had calcite in 62% of the samples, and the allogenic outwash unit had calcite in 40% of the samples. Together, these post-glacial lake sediments had 56% calcite occurrence. The light-grey clay unit had calcite in 100% of the samples, and the tan "white" clay unit had calcite in 75% of the samples. Together, the supposed glacial lake sediments had calcite in 81% of the samples. The Knox Cave and Westfall Cave sediment control samples, because those cave did not lie under the lake or postdated it, had calcite in only 33% of the samples. Brushite shows a different trend, being more common in the post-glacial sediments.

Figure 7. Glacial Lake Schoharie shoreline at 354–366 m (1,160–1,200 ft or stage two) above sea level outlined in purple. Note the reduction of scale to portray a much larger lake and the lake's extension eastward into Schenectady and Albany Counties. Caves are numbered as in Figure 1. The grid is 6.4 by 6.4 km (4 by 4 mi).

DISCUSSION

During *stage one* of Glacial Lake Schoharie's development, there would not have been any outlet for the water to escape by way of the Schoharie Valley. However, it would have been possible for the water in Glacial Lake Schoharie to drain north toward what is known today as the Mohawk Valley. But there is a problem with this idea, because during the Late Wisconsin the Mohawk Valley was occupied by the active Mohawk glacial lobe. The Mohawk glacial lobe, also referred to locally as the Mohawk Ice

Block, filled the area between the neighboring Cobleskill and Barton Hill plateaus and acted as a plug, trapping glacial meltwater in the Schoharie Valley (LaFleur, 1969). Near the close of the Wisconsin glaciation, at least 50% of Glacial Lake Schoharie would have been covered by active glacial ice belonging to the Schoharie glacial sub-lobe (Dineen, 1986). As seen in Figures 6 and 9, during *stage one* (213 m) there would not have been a sufficient amount of water in Glacial Lake Schoharie to even partially inundate the caves of the Cobleskill Plateau and Barton Hill included in this study.
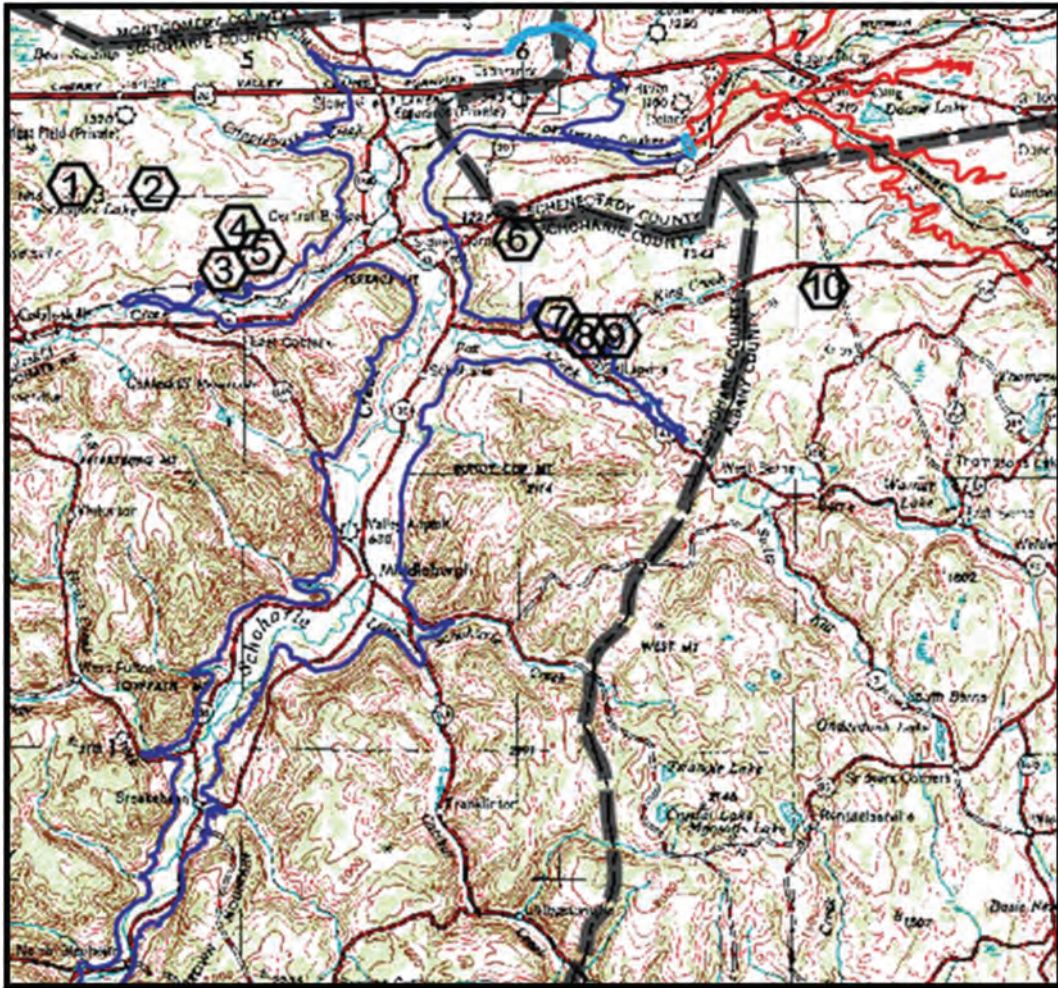
Figure 8. Glacial Lake Schoharie with a shoreline, outlined in dark blue, at 256 m (840 ft or stage three) above sea level, created using information provided by LaFleur (1969) and Dineen and Hanson (1985). The red lines indicate a spillway, and the light-blue lines indicate the boundary between glacial lake water and active glacial ice. Caves are numbered as in Figure 1. The grid is 6.4 by 6.4 km (4 by 4 mi).

In Figures 7 and 9 it can be seen that nearly all of the caves in the Cobleskill Plateau and Barton Hill are completely inundated by water from Glacial lake Schoharie during *stage two* (~360 m). Note that although the entrances to both McFail's Cave and Gage Caverns were not inundated, the majority of the cave passages are over 30 m below the surface and would have been inundated based on their elevation relative to sea level and the *stage two* lake level. This would include inundation of locations where samples were collected for the study. The upper passages where samples were collected in Knox Cave would not have been inundated by glacial lake water due to their elevation, even if the lake had extended that far eastward, and so these samples acted as a control. Westfall Spring Cave, being post-glacial in origin, is not included in Figure 9.

The clay sediments encountered in the caves fit the description of a varved sequence (Fig. 3). Varves are usually couplets of fine and coarse grained material

(Neuendorf et al., 2011). These sediments do not show the alternating coarse-to-fine sequencing; they appear to only contain the fine sediments. A possible reason the sediments that compose the units are so uniform is that the insurgences and resurgences of the caves were most likely choked with glacially transported material, so only the smallest of sediments would be able to slowly percolate through the debris. These deposits are consistent with a laminar-flow regime expected for deposition deep in cave passages below a glacial lake. The white to tan clay deposits have an abrupt contact with overlying sand and gravel deposits (Fig. 3). Mylroie (1984) interpreted these coarse-grained sediments to be the result of ice retreat and re-establishment of the epigenic turbulent flow system in these caves. The same thing would have occurred during the draining of Glacial Lake Schoharie. The dark-brown clay was hypothesized by Mylroie (1984) to represent a surge of incoming sediment associated with clear-cutting

Table 1. X-ray diffraction results. The figures are the percentages of samples of the given strata that showed qualitatively the presence of the mineral. The totals are not numerical averages of the values to their left because there were not equal numbers of samples of each type. The control samples were from caves not under Glacial Lake Schoharie.

Mineral, %	Glacial Lake Sediment, %			Post Glacial Sediment, %			Control Samples, %
	Light Grey Clay	Tan "White" Clay	Total	Dark Brown Clay	Allogenic Glacial Outwash	Total	
Calcite	100	75	81	62	40	56	33
Dolomite ?	0	0	0	4	0	3	0
Quartz	100	100	100	100	100	100	100
Muscovite	60	69	67	73	80	75	83
Phlogopite	40	19	24	31	40	33	67
Chlorite	0	0	0	0	0	0	0
Montmorillonite	0	0	0	0	0	0	0
Albite (low temp)	20	44	38	58	50	56	67
Enstatite ?	0	6	5	0	0	0	0
Brushite	40	31	33	65	40	58	83
Nacrite	20	0	5	15	0	11	17
Carbon	0	25	19	8	30	14	67

following European settlement in the 1700s. The results here can neither prove nor disprove that speculation, but the dark-brown clays do represent what is being deposited in the caves today during flood cycles. The sequence of

events that produced the sediment column of Figure 4 is presented in Figure 10.

The Howe Caverns sediment section is especially instructive and is the thickest of all such sequences. While
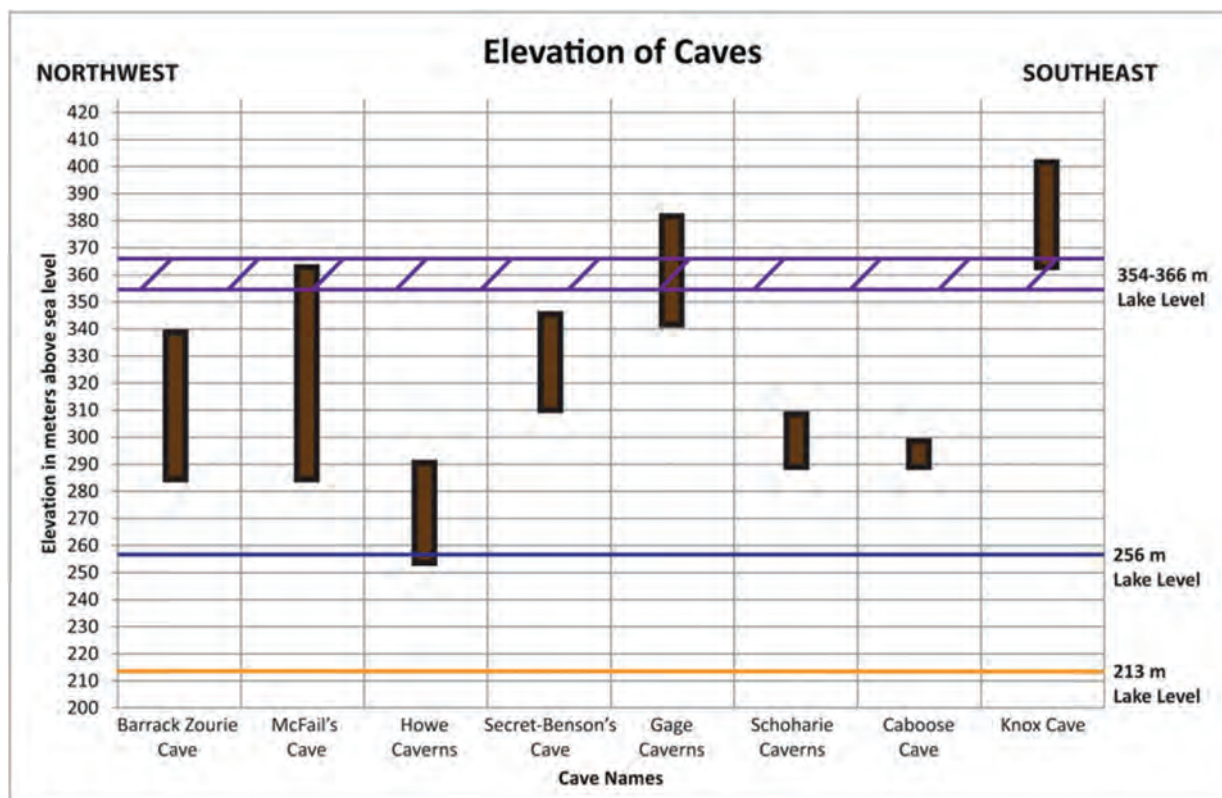

Figure 9. The elevations occupied by each cave in relation to the shoreline elevations of Glacial Lake Schoharie during stage one (213 m, Fig. 6), stage 2 (~360 m, Fig. 7), and stage 3 (256 m, Fig. 8).
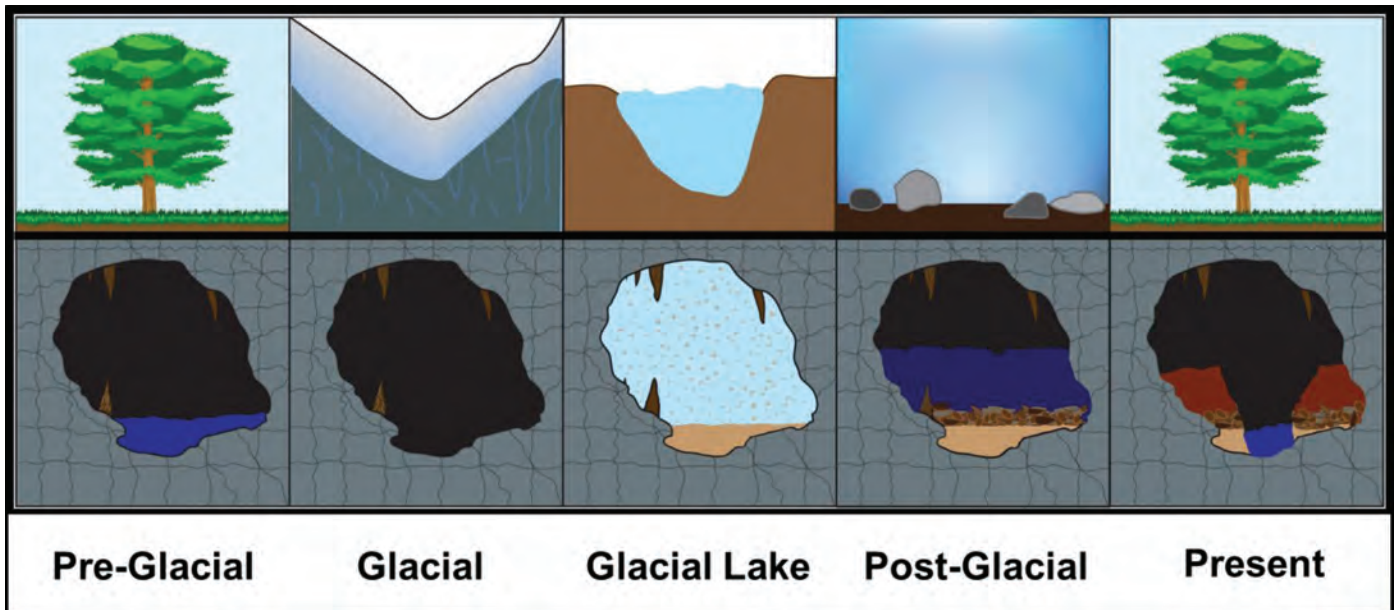
Figure 10. Cartoon depicting the caves' history during a glacial cycle, with time progressing from left to right.

most caves have less than or equal to 1 m of the light-grey and tan ''white'' clay, Howe Caverns has over 2 m of section. This greater thickness is the result of Howe Caverns' main stream passage being the lowest in elevation of all the cave passages studied, by approximately 30 meters (Fig. 9). Therefore, while lake surface elevations shifted vertically, Howe Caverns spent more time under Glacial Lake Schoharie than any other cave in the study, being inundated even during *stage three*. In addition, Figure 3 shows an interesting transition from a very amorphous white clay deposit at the base (next to the knife) to a progressively better layered light-grey clay in which the individual layers get thicker upwards to the contact with more ordinary cave sediments. This transition can be interpreted to indicate initial clay deposition *stage two*, when the Howe Caverns stream passage would have been ~100 m below the lake's surface at ~360 m. Sediment transport by laminar flow into the cave would have been slow and quite isolated from seasonal changes, indicated by the lack of rhythmical layering in the ''white'' clay deposit. As lake level lowered to the 256 m level during *stage three*, the Howe Caverns main stream passage would have been merely meters below the lake's surface and more likely to record the seasonal changes in water and sediment addition to the lake, as demonstrated by the light-grey clay. The upward thickening may record the final transition of Howe Caverns out of the lake footprint as the lake drained away.

The sediment analyses were for the most part inconclusive. Based on the X-ray diffraction results, the glacial sediments are more likely to have calcite in them, which is consistent with the stagnant water conditions proposed by Mylroie (1984). The mass-loss experiments were less convincing, with a great deal of variation within the data

and no consistent pattern. Mylroie (1984) had reported a very high solubles content for the Caboose Cave white clay, and while this study did replicate that result to an extent, the high solubles content was not consistent across the other caves in the study. It is useful to note that Knox Cave, acting as a pre-glacial control cave, has much less variation in its samples than the caves under the Glacial Lake Schoharie footprint. The sediment analysis was done as a reconnaissance, to determine if more work would be worthwhile in the future, and it was not central to the final interpretation of the sediment's glaciolacustrine origin.

Conclusions

The caves suspected to have been inundated by glacial lake water and, therefore, to have collected fine-grained lake sediment do not show any statistical correlation between samples collected (see Weremeichik, 2013). But, as seen in Figure 3, it is apparent that physical similarities between the samples collected exist. These physical similarities can be correlated with their mineral's color and grain size. It was originally hypothesized that the sediment in the caves may have been deposited during a retreat phase of glaciation resulting from stagnant ice-covered conditions (e.g., Mylroie, 1984). This hypothesis was thought to be true because it explains how the fine-grained sediment was deposited in the caves. This could not have happened if there had been turbid or even transitionally laminar flow through the caves. Ice cover would have created the necessary stagnant conditions. The glacial-lake hypothesis presented here also would create stagnant conditions, but in an environment where the associated fine-grained sediment could more easily enter the cave.

Glacial Lake Schoharie endured multiple retreats and readvances of glacial ice, in part, by being insulated and protected by a layer of stagnated glacial ice. During retreat phases of glacial activity, new glacial meltwater carrying glacial-derived sediment must have been delivered to the lake, which subsequently filtered into the caves below.

The analyses of the sediments themselves are consistent with the glacial-lake hypothesis. They are extremely fine-grained, very low in organics (Weremeichik, 2013), and with a measurable soluble content of calcite. They are visually striking when observed in the field and are easily recognized. They are, to date, known only from within the footprint of Glacial Lake Schoharie. This final aspect is important, as the deposits were originally considered by earlier workers (e.g., Mylroie, 1984) to be sub-ice deposits. The failure to find such deposits elsewhere in the Helderberg Plateau or in other glaciated karst regions was very problematic. Everyone who saw the deposits *in situ* agreed with their glacial rock-flour origin (e.g., Palmer et al., 2003). The use of the Glacial Lake Schoharie footprint to explain these deposits as not sub-ice, but sub-lake deposits, explains the failure to find such deposits in other glaciated karst locales in the region.

REFERENCES

Dineen, R.J., 1986, Deglaciation of the Hudson Valley Between Hyde Park and Albany, New York, *in* Cadwell, D.H., ed., The Wisconsinan Stage of the First Geological District, Eastern New York, Albany, New York State Museum Bulletin 455, p. 89–108.

Dineen, R.J., and Hanson, E.L., 1985, Deglaciation of the Middle Mohawk and Sacandaga Valleys, or a tale of two tongues, *in* Lindemann, R.H., ed., Field Trip Guidebook of the New York State Geological Association 57th Annual Meeting, Saratoga Springs, New York, p. 250–256.

Dumont, K.A., 1995, Karst Hydrology and Geomorphology of the Barrack Zourie Cave System, Schoharie County, New York [M.S. thesis]: Mississippi State, Miss., Mississippi State University, reprinted as New York Cave Survey Bulletin 5, 70 p., map plate.

Kastning, E.H., 1975, Cavern Development in the Helderberg Plateau, East-Central New York [M.S. thesis]: Storrs, Conn., University of Connecticut, reprinted as New York Cave Survey Bulletin 1, 194 p. plus map plates.

Lauritzen, S-E., and Mylroie, J.E., 2000, Results of a speleothem U/Th dating reconnaissance from the Helderberg Plateau, New York: Journal of Cave and Karst Studies, v. 62, p. 20–26.

LaFleur, R.G., 1969, Glacial geology of the Schoharie Valley, *in* Bird, J.M., ed., 61st Annual Meeting of the New England Intercollegiate Geological Conference Guidebook for Field Trips in New York, Massachusetts, and Vermont, p. (5-1)–(5-20).

LaFleur, R.G., 1976, Glacial Lake Albany, *in* Rittner, D., ed., The Pine Bush Albany's Last Frontier: Albany, N.Y., Pine Bush Historic Preservation Project, p. 1–10.

Muller, E.H., and Calkin, P.E., 1993, Timing of Pleistocene glacial events in New York State: Canadian Journal of Earth Sciences, v. 30, p. 1829–1845. doi:10.1139/e93-161.

Mylroie, J.E., 1977, Speleogenesis and Karst Geomorphology of the Helderberg Plateau, Schoharie County, New York [Ph.D. dissertation]: Troy, N.Y., Rensselaer Polytechnic Institute, reprinted as New York Cave Survey Bulletin 2, 336 p.

Mylroie, J.E., 1984, Pleistocene climatic variation and cave development: Norsk Geografisk Tidsskrift, v. 38, p. 151–156. doi:10.1080/00291958408552119.

Mylroie, J.E., and Mylroie, J.R., 2004, Glaciated karst: How the Helderberg Plateau revised the geologic perception: Northeastern Geology and Environmental Sciences, v. 26, no. 1–2, p. 82–92.

Neuendorf, K.K.E., Mehl, J.P. Jr., and Jackson, J.A., 2011, ed., Glossary of Geology, 5th revised edition: Alexandria, Virginia, American Geosciences Institute, 800 p.

Palmer, A.N., 2009, Cave exploration as a guide to geologic research in the Appalachians: Journal of Cave and Karst Studies, v. 71, no. 3, p. 180–192.

Palmer, A.N., Rubin, P.A., and Palmer, M.V., 1991, Interaction between karst and glaciation in the Helderberg Plateau, Schoharie and Albany Counties, New York, *in* Ebert, J.R., ed., New York State Geological Association Field Trip Guidebook 63rd Annual Meeting, p. 161–190.

Palmer, A.N., Rubin, P.A., Palmer, M.V., Engel, T.D., and Morgan, B., 2003, Karst of the Schoharie Valley and land use analysis, Schoharie County, New York State, *in* Johnson, E.L., ed., New York State Geological Association Field Trip Guidebook 75th Annual Meeting, p. 141–165.

Ridge, J.C., 2004, The Quaternary glaciation of western New England with correlations to surrounding areas, *in* Ehlers, J., and Gibbard, P.L., eds., Quaternary Glaciations—Extent and Chronology Part II: North America: Amsterdam, Elsevier, Developments in Quaternary Sciences series 2, p. 169–199. doi:10.1016/S1571-0866(04)80196-9.

Weremeichik, J.M., 2013, Paleoenvironmental reconstruction by identification of glacial cave deposits, Helderberg Plateau, Schoharie County, New York [M.S. thesis]: Mississippi State, MS, Mississippi State University, 191 p.

DIET ANALYSIS OF *LEOPOLDAMYS NEILLI*, A CAVE-DWELLING RODENT IN SOUTHEAST ASIA, USING NEXT-GENERATION SEQUENCING FROM FECES

Alice Latinne[1,2], Maxime Galan[3], Surachit Waengsothorn[4], Prateep Rojanadilok[5], Krairat Eiamampai[6], Kriangsak Sribuarod[7], and Johan R. Michaux[1,3]

Abstract: *Leopoldamys neilli* is a Murinae rodent endemic to limestone karst of Thailand and the Lao PDR, but its ecology and the reasons of its endemism to karst are still totally unknown. The aim of this pilot study was to examine the plant composition of the diet of *L. neilli* at the level of order and family using DNA for molecular identification and to compare it with two other forest-dwelling *Leopoldamys* species, *L. herberti* and *L. sabanus*. A 202bp fragment of the *rbc*L gene was amplified and sequenced for twenty-three fecal samples of the three species using 454 pyrosequencing. We successfully identified a total of seventeen orders and twenty-one plant families, corresponding to thirty-three putative species, in the feces of these three *Leopoldamys* species. Solanaceae were the most common plants in the diet of *L.neilli* regardless of the region and sampling season, and they were also present in feces of both *L. herberti* and *L. sabanus*. The Araceae, Fabaceae, and Apocynaceae families were also identified in feces of *L. neilli* collected in various regions of Thailand and at different seasons. Plants of the Oleaceae family are consumed by both *L. herberti* and *L. sabanus* but were not found in the diet of *L. neilli*. Further improvements of the study, such as the use of additional genes, the creation of a reference collection, the microhistological examination of plant fragments to determine which parts of the plant are consumed, and the analysis of the animal diet of *Leopoldamys* are suggested to enhance the quality and accuracy of the results obtained.

INTRODUCTION

Several Murinae rodents endemic to limestone karst have been described in Southeast Asia, but their ecology is still poorly known. *Niviventer hinpoon* (Marshall, 1977) is found in Thailand, *Saxatilomys paulinae* (Musser et al., 2005) in the Lao PDR, and *Tonkinomys daovantieni* (Musser et al., 2006) in Vietnam, while *Leopoldamys neilli* (Marshall, 1977) has been described in Thailand but has also recently been discovered in the Lao PDR (Balakirev et al., 2013; Latinne et al., 2013a). Recent phylogeographic studies of *L. neilli* revealed a deep genealogical divergence among geographically close lineages of this species in Thailand and a high population fragmentation related to the patchy distribution of limestone karst (Latinne et al., 2011; Latinne et al., 2012). Such strong phylogeographic structure is not observed for other Murinae rodents in Thailand that are characterized by lower habitat specialization (Latinne, 2012). These results suggested that the spatial isolation of karst areas prevents migration among lineages of *L. neilli* and indicated a close association of this species with this habitat. However, ecological data on *L. neilli* are lacking, and the reasons of its endemism to limestone karst are still totally unknown. A better knowledge of the ecology of *L. neilli*, notably its feeding habits, is thus necessary for determining if diet contributes to the habitat specialization and distributional limits of this

species, as well as for understanding its functional role in karst ecosystems.

Rodents and other small mammals living in forests of Southeast Asia are generally considered to be omnivorous (Emmons, 2000; Langham, 1983; Lim, 1970), and they play a key role in the food chain, both as consumers of plants and small invertebrates, and as food resources for larger predators. Rodents may also play an important role in the frugivores' community as seed dispersers or seed predators, and it has been suggested that some *Leopoldamys* species might benefit seed recruitment of several tree species by seed hoarding or seed ingestion in Southeast Asia and China (Cheng et al., 2005; Wells et al., 2009; Zhang et al., 2008). However detailed information on the exact diet composition of Southeast Asian rodents remains scarce and should be improved to better understand the trophic

[1] Conservation Genetics Unit, Institut de Botanique, University of Liège, 4000 Liège, Belgium, alice.latinne@gmail.com
[2] Department of Parasitology, Faculty of Veterinary Medicine, Kasetsart University, Bangkok 10900, Thailand
[3] CBGP (Centre de Biologie et de Gestion des Populations), UMR INRA/IRD/ Cirad/Montpellier SupAgro, Campus international de Baillarguet, CS 30016, 34988 Montferrier-sur-Lez cedex France
[4] Environment and Resources Technology Department, Thailand Institute of Scientific and Technological Research, 35 Mu 3 Tambon Khlong Ha, Amphoe Khlong Luang, Changwat Pathum Thani 12120, Thailand
[5] Doi Chiang Dao Wildlife Research Station, Chiang Mai, Thailand
[6] Bung Boraphet Wildlife Research Station, Nakhon Sawan, Thailand
[7] Khlong Saeng Wildlife Research Station, Surat Thani, Thailand

relationships in Southeast Asian ecosystems and the functional role of rodents in these biological communities, as well as the resource partitioning among competing species.

Direct observations of foraging and feeding behaviors are generally time-consuming, and they are particularly difficult to obtain for small nocturnal mammals living in karst habitats. Feces analysis represents an efficient and non-invasive alternative to circumvent this problem. Microhistological examination of plant and invertebrate fragments in fecal samples has been traditionally used, but this method requires a lot of time and training, and its results are often imprecise (Soininen et al., 2009; Emmons, 2000). More recently, molecular techniques using DNA barcoding have been developed to successfully analyze the diet of wild herbivores from feces (Bradley et al., 2007; Kim et al., 2011; Soininen et al., 2009; Valentini et al., 2009). These methods aim to amplify small, but highly variable, DNA fragments contained in the feces with universal primers and use them as barcodes to identify the plant taxa that have been eaten. Several DNA regions have been used for this purpose in the literature, and the choice of the target segment results from a compromise among a minimal size, a maximal genetic distance between species, a minimal genetic diversity within species, and the existence of an adequate reference collection (Bradley et al., 2007). As feces contain only highly degraded DNA, the length of fragments that can be amplified is usually shorter than 200 base pairs (bp).

Using a 202bp short segment of the ribulose-bisphosphate carboxylase (*rbc*L) gene of the chloroplast genome as a barcode region, the present study was designed as a pilot study to assess the performance of this method in analyzing the plant composition of the diet of *L. neilli* at the level of order and family. Another objective of this study was to compare the diet of *L. neilli* with two other forest-dwelling *Leopoldamys* species also found in Thailand but non-endemic to limestone karst, *L. sabanus* and *L. herberti*. (*L. herberti* was previously thought to belong to *L. edwardsi*, but several recent studies have shown that it should be regarded as a distinct species from *L. edwardsi* (Balakirev et al., 2013; Latinne et al., 2013a).

Methods

Twenty-six fecal samples from the three *Leopoldamys* species were collected from nineteen localities (Fig. 1) below traps, baited with ripe banana, where the animals were caught during a survey of the rodent diversity in Thai limestone karst. The samples were preserved in silica gel. Two mitochondrial genes were sequenced for all trapped animals using tissue biopsy from the ear to reliably identify them at the species level (Latinne et al., 2013b). The specific status of these individuals was also confirmed by an independent molecular analysis using a mitochondrial mini-barcode from feces (Galan et al., 2012). DNA was extracted from feces using the QIAamp DNA Stool Kit (Qiagen) and following the protocol designed for the isolation of DNA from human stool.

A 202bp fragment of the *rbc*L gene was amplified for each sample using universal primers Z1aF and hp2R (Hofreiter et al., 2000), modified by the addition of a specific tag on the 5′ end, following the tagging and multiplexing method for the 454 pyrosequencing developed by Galan et al. (2010). This tag consists of a short 7bp sequence to allow the recognition of the sequences after the pyrosequencing where all the PCR products from the different samples are mixed together and a 30bp Titanium adaptor required for the emPCR and 454 GS-FLX pyrosequencing using Lib-L Titanium Series reagents. Six and five different tags were designed for the forward and the reverse primers, respectively. This gives thirty putatively unique combinations of forward and reverse tags, and thus, allows tagging up to thirty different amplicons.

PCRs were carried out in a 10 µL reaction volume using 5 µL of 2x QIAGEN Multiplex Kit (Qiagen), 0.5 µM of each primer, and 2 µl of DNA extract. The PCR started by an initial denaturation step at 95 °C for 15 min, followed by forty cycles of denaturation at 94 °C for 30 s, annealing at 45 °C for 45 s, and extension at 72 °C for 30 s, followed by a final extension step at 72 °C for 10 min.

Positive PCR products were then pooled together for 454 pyrosequencing using 3 µL per strong PCR amplification products or 7 µL per lighter ones. The PCR pool was processed by Beckman Coulter Genomics (Danvers, Massachusetts). Amplicons were sequenced after the emPCR on a 454 Genome Sequencer FLX (Roche) in 1/4th of titanium picotiter plate.

The software SESAME 1.1B (Meglécz et al., 2011) was used to sort the sequences. Thanks to the tag combinations, the sequences were assigned to the fecal sample from which the PCR amplicon was obtained. Artifactual variants due to sequencing errors during PCR, emPCR, and 454 sequencing were discarded as described in Galan et al. (2012).

The validated variants of *rbc*L sequences obtained were compared with published *rbc*L sequences available on GenBank using NCBI's BLASTN program (Zhang et al., 2000) and were assigned to order and family of the closest sequences (with at least 98% of identity and 100% of query coverage) following the APG III classification (Bremer et al., 2009).

Results

Out of the 26 *Leopoldamys* feces analyzed in this study, 23 were successfully amplified (Table 1) and a total of 392 *rbc*L sequences, including 112 distinct variants corresponding to 33 validated variants, were obtained with a mean of 15 sequences per samples. Each variant was assigned unambiguously to one plant family, with the exception of four sequences of the Zingiberales order that could belong
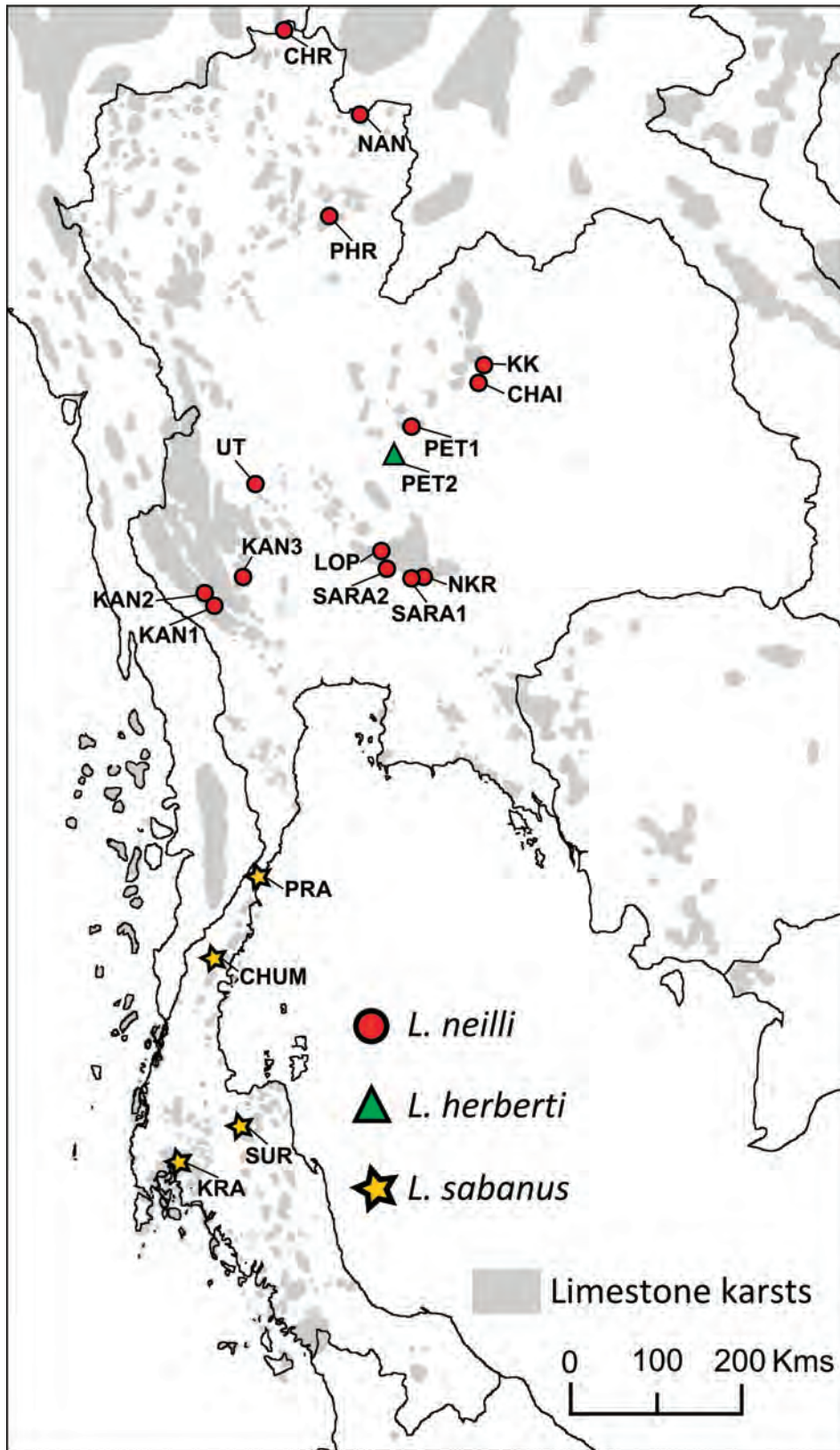
Figure 1. Locations of *Leopoldamys* fecal samples analyzed in this study. The province abbreviations are spelled out in Table 1.

Table 1. Sample locations, regions, and seasons for the *Leopoldamys* fecal samples in this study. See Figure 1 for a map of the locations.

Species	Sample ID	Province (Locality)	Region	Season	PCR Success
Leopoldamys neilli	F161	Kanchanaburi (KAN1)	West	Dry	Yes
	F567	Kanchanaburi (KAN1)	West	Rainy	Yes
	F172	Kanchanaburi (KAN2)	West	Dry	Yes
	F565	Kanchanaburi (KAN2)	West	Rainy	Yes
	F191	Kanchanaburi (KAN3)	West	Dry	Yes
	F577	Kanchanaburi (KAN3)	West	Rainy	Yes
	F554	Uthai Thani (UT)	West	Rainy	Yes
	F313	Chaiyaphum (CHAI)	Northeast	Dry	Yes
	F327	Khon Kaen (KK)	Northeast	Dry	Yes
	F331	Khon Kaen (KK)	Northeast	Dry	Yes
	F418	Petchabun (PET1)	Northeast	Dry	Yes
	F399	Nan (NAN)	North	Dry	Weak
	F406	Nan (NAN)	North	Dry	Weak
	F391	Phrae (PHR)	North	Dry	Yes
	F441	Chiang Rai (CHR)	North	Dry	Yes
	F505	Saraburi (SARA1)	Centre	Rainy	Weak
	F508	Nakhon Ratchasima (NKR)	Centre	Rainy	Weak
	F534	Saraburi (SARA2)	Centre	Rainy	Weak
	F538	Lopburi (LOP)	Centre	Rainy	Yes
Leopoldamys herberti	F420	Petchabun (PET2)	Northeast	Dry	Yes
	F424	Petchabun (PET2)	Northeast	Dry	No
	F430	Petchabun (PET2)	Northeast	Dry	Yes
Leopoldamys sabanus	F254	Krabi (KRA)	South	Rainy	Yes
	F298	Surat Thani (SUR)	South	Rainy	No
	F445	Prachuap Khiri Khan (PRA)	South	Rainy	Yes
	F477	Chumphon (CHUM)	South	Rainy	No

either to Marantaceae or Musaceae families (Table 2). Several *rbc*L variants were assigned to the same family and could represent different plant species if each variant belongs to a different species, but this assumption should be confirmed by further analyses. A total of 17 orders and 21 plant families, corresponding to 33 putative species, were identified in the feces of the *Leopoldamys* species (Table 2).

The diet of *Leopoldamys neilli* is quite diversified, with seventeen orders and nineteen families identified within feces of this species. Plants belonging to Solanaceae (corresponding to a single validated variant) and Marantaceae/Musaceae (corresponding to four validated variants) were identified in ten out of the nineteen feces of *L. neilli* analyzed (53%). Solanaceae are also identified in the two feces of *L. sabanus* (100%) and one of the two feces of *L. herberti* (50%). Plants of the Oleaceae family are consumed by both *L. herberti* and *L. sabanus* but were not found to be consumed by *L. neilli*.

Solanaceae and Marantaceae/Musaceae were highly common in the diet of *Leopoldamys neilli* as they were eaten by specimens in all sampled regions (Fig. 2). Most of the plant families identified in this study (14/19) were encountered in only one *L. neilli* sample, but the Araceae, Fabaceae, and

Apocynaceae families were identified in samples collected in various regions of Thailand and at different seasons.

DISCUSSION

This pilot study is the first study of the diet composition of *Leopoldamys neilli* that remained totally unknown up to now. We successfully identified a total of seventeen orders and nineteen plant families, corresponding to thirty putative species, in the feces of this long-tailed giant rat endemic to limestone karst of Thailand and the Lao PDR. The plant diversity observed in the *L. neilli* feces is high and similar to the one described for large herbivores species using similar methods of molecular identification (Bradley et al., 2007; Kim et al., 2011; Valentini et al., 2009). Plants identified in the diet of *Leopoldamys* species are all flowering plants (angiosperms), and most of these plant families have been observed in the flora of limestone karst in southern Vietnam (International Finance Corporation, 2002). Even though a recent study showed that the primers Z1aF and hp2R used in our study also allow the amplification of sequences belonging to ferns or mosses (Kim et al., 2011), no fern or moss was detected in the feces of the three studied *Leopoldamys* species.

Table 2. Plant families identified in the feces of three *Leopoldamys* species in Thailand, with number and frequency of occurrence.

Order	Family	Number of Validated Variants	Frequency		
			L. neilli (n = 19)	*L. herberti* (n = 2)	*L. sabanus* (n = 2)
Alismatales	Araceae	2	3 (16%)		
Brassicales	Brassicaceae	1	1 (5%)		
Commelinales	Commelinaceae	1	1 (5%)		
Cucurbitales	Cucurbitaceae	1	1 (5%)		
Dioscoreales	Dioscoreaceae	1	1 (5%)		
Fabales	Fabaceae	5	4 (21%)		
Fagales	Fagaceae	1	1 (5%)		
Gentianales	Apocynaceae	3	3 (16%)		
Lamiales	Lamiaceae	1	1 (5%)		
	Oleaceae	2		1 (50%)	1 (50%)
Malpighiales	Phyllanthaceae	1	1 (5%)		
	Putranjivaceae	1			1 (50%)
Malvales	Malvaceae	1	1 (5%)		
Poales	Poaceae	1	1 (5%)		
Piperales	Aristolochiaceae	1	1 (5%)		
Rosales	Rhamnaceae	1	1 (5%)		
Sapindales	Burseraceae	1	1 (5%)		
	Sapindaceae	2	1 (5%)		1 (50%)
Solanales	Convolvulaceae	1	2 (10%)		
	Solanaceae	1	10 (53%)	1 (50%)	2 (100%)
Zingiberales	Marantaceae or Musaceae[a]	4	10 (53%)	2 (100%)	

[a] Possible contamination by the bait.

Species of the Solanaceae and Marantaceae/Musaceae families are the most common plants identified in the diet of *Leopoldamys neilli* regardless of the region and season. However, traps used in this study were baited with ripe banana (*Musa* sp., a genus of the Musaceae family), and these bananas were probably eaten by trapped rats several hours before the collection of feces, because the feces were collected at least twelve hours after trap setup. Direct contact of fecal samples with banana was also possible in the trap. The frequent presence of Musaceae in the feces of *L. neilli* could thus represent a bias due to the bait used, rather than the real diet of this species. Therefore the Marantaceae/Musaceae families should not be included positively in the diet of *L. neilli* without further verification.

As the number of fecal samples analyzed successfully for *Leopoldamys herberti* and *L. sabanus* was much lower than for *L. neilli*, it is not possible to compare rigorously the diet composition of these three species. Despite the small number of samples, Solanaceae were also identified in feces of both *L. herberti* and *L. sabanus*. Therefore this plant family seems to be very common in the diet of all the *Leopoldamys* species in Thailand. Solanaceae are represented in Southeast Asia by the Solanoideae subfamily and may take the form of herbs, shrubs, or small trees in this region, but the lack of resolution at the species level of the

*rbc*L fragment that we used does not allow us to get more information on the type of Solanaceae consumed by the *Leopoldamys* species.

Conclusion

Despite the limitations and small sample size of this pilot study, these preliminary results confirm that DNA barcoding from feces is a promising tool to better understand the feeding habits of *Leopoldamys neilli*. We suggest some improvements for future studies to enhance the quality and accuracy of the results.

First, a better knowledge of the flora of Thai limestone karst is absolutely needed to allow plant identification at lower taxonomic level than order and family. The creation of a reference collection by sampling, identification, and DNA sequencing of the most common plants of Thai limestone karst would help to assess more accurately the diet of these species and allow more precise identifications of the sequences obtained from feces than data now in public databases such as GenBank (Valentini et al., 2009). We also suggest using other highly variable DNA regions such as *trnH, psbA* (Kress and Erickson, 2007), *matK* (Hollingsworth et al., 2009), *trn*L (Taberlet et al., 2007; Valentini et al., 2009), or *ITS-2* (Bradley et al., 2007) as DNA barcodes in association with *rbc*L to obtain more
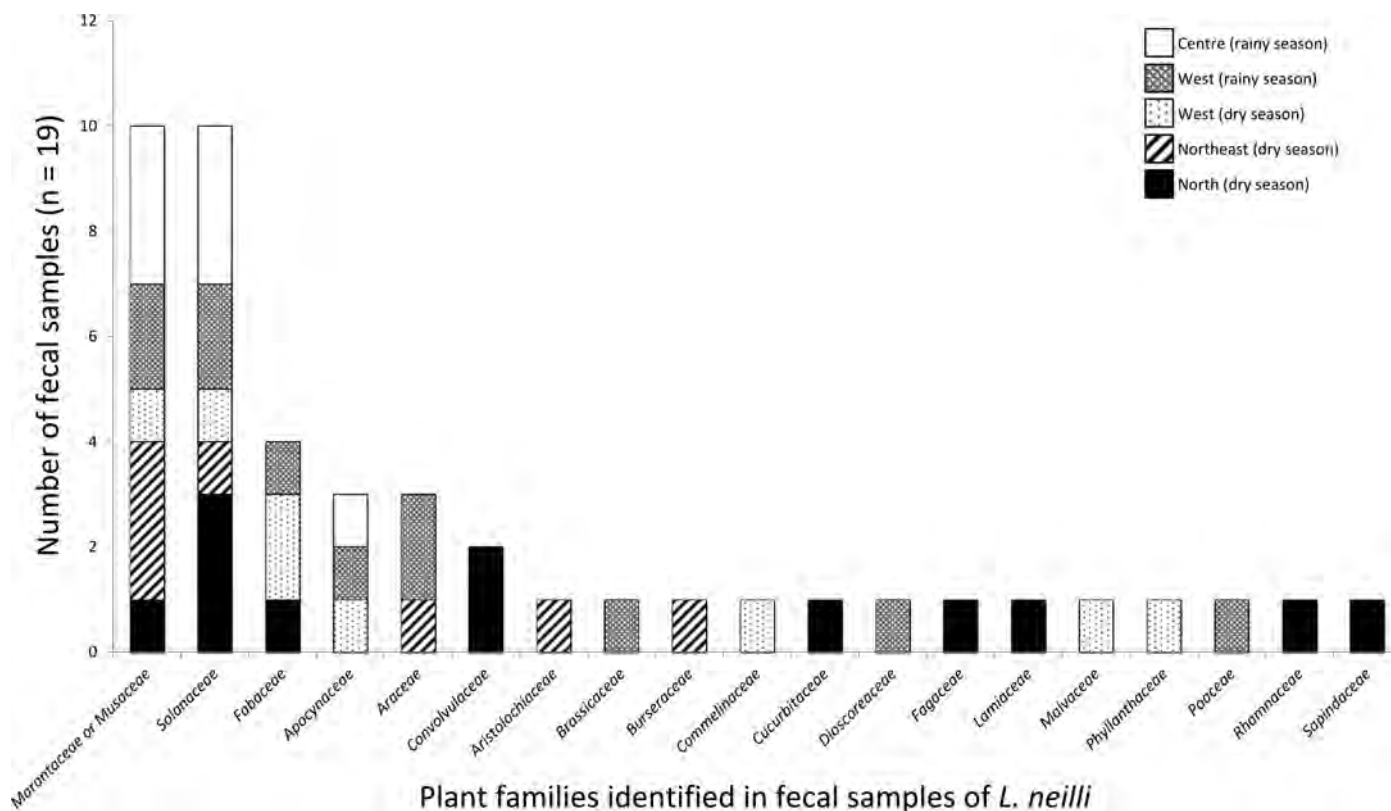
Figure 2. Numbers of samples of feces of *Leopoldamys neilli* out of total of nineteen showing plant families, with samples coded for season and region.

precise results. Checking traps for captures more frequently and collecting feces more rapidly after trap setup would prevent bait contamination of the feces. The use of different baits or baits distinct from all plant species known to occur in the studied region will also help to determine whether Musaceae is part of the natural diet of *Leopoldamys neilli* or not.

Moreover, combining DNA-based analysis of feces with microhistological examination of plant fragments in fecal samples would help to determine which parts of the plant are consumed by *L. neilli* and other *Leopoldamys* species, as this information remains unknown when using DNA barcoding. In particular, the study of the diversity, quantity, and viability of seeds defecated by these long-tailed giant rats is needed to better assess their potential role as seed dispersers in Southeast Asian ecosystems via seed ingestion and subsequent defecation, as already suggested for *L. sabanus* by Wells et al. (2009).

It could also be very interesting to perform such DNA barcoding analysis using universal primers designed to amplify animal DNA, because the *Leopoldamys* species also eat small preys such as insects or snails (Langham, 1983; Lim, 1970). A small fragment of the cytochrome *c* oxidase I gene (Hajibabaei et al., 2011) could be the ideal marker for this purpose.

Finally, most of the plant families identified within our dataset were encountered in only one sample. This observation strengthens the importance of studying a large number of samples to obtain an exhaustive list of the plant composition of the *Leopoldamys* diet to better comprehend the whole diversity of food resources consumed by these long-tailed giant rats and how it may vary in space and time and among species.

References

Balakirev, A.E., Abramov, A.V., and Rozhnov, V.V., 2013, Revision of the genus *Leopoldamys* (Rodentia, Muridae) as inferred from morphological and molecular data, with a special emphasis on the species composition in continental Indochina: Zootaxa, v. 3640, no. 4, p. 521–549. doi:10.11646/zootaxa.3640.4.2.

Bradley, B.J., Stiller, M., Doran-Sheehy, D.M., Harris, T., Chapman, C.A., Vigilant, L., and Poinar, H., 2007, Plant DNA sequences from feces: Potential means for assessing diets of wild primates: American Journal of Primatology, v. 69, no. 6, p. 699–705. doi:10.1002/ajp.20384.

Bremer, B., Bremer, K., Chase, M.W., Fay, M.F., Reveal, J.L., Soltis, D.E., Soltis, P.S., and Stevens, P.F., 2009, An update of the Angiosperm Phylogeny Group classification for the orders and families of flowering plants: APG III: Botanical Journal of the Linnean Society, v. 161, no. 2, p. 105–121. doi:10.1111/j.1095-8339.2009.00996.x.

Cheng, Jinrui, Xiao, Zhishu, and Zhang, Zhibin, 2005, Seed consumption and caching on seeds of three sympatric tree species by four sympatric rodent species in a subtropical forest, China: Forest Ecology and Management, v. 216, no. 1–3, p. 331–341. doi:10.1016/j.foreco.2005.05.045.

Emmons, L.H., 2000, Tupai: A Field Study of Bornean Treeshrews, Berkeley, University of California Press, Organisms and Environments Series 2, 280 p.

Galan, M., Guivier, E., Caraux, G., Charbonnel, N., and Cosson, J.-F., 2010, A 454 multiplex sequencing method for rapid and reliable genotyping of highly polymorphic genes in large-scale studies: BMC Genomics, v. 11, article 296, 15 p. doi:10.1186/1471-2164-11-296.

Galan, M., Pagès, M., and Cosson, J.-F., 2012, Next-Generation Sequencing for Rodent Barcoding: Species Identification from Fresh, Degraded and Environmental Samples: PLoS ONE, v. 7, no. 11, e48374 p.

Hajibabaei, M., Shokralla, S., Zhou, Xin, Singer, G.A.C., and Baird, D.J., 2011, Environmental barcoding: a next-generation sequencing approach for biomonitoring applications using river benthos: PLoS ONE, v. 6, article e17497, 7 p. doi:10.1371/journal.pone.0017497.

Hofreiter, M., Poinar, H.N., Spaulding, W.G., Bauer, K., Martin, P.S., Possnert, G., and Pääbo, S., 2000, A molecular analysis of ground sloth diet through the last glaciation: Molecular Ecology, v. 9, no. 12, p. 1975–1984. doi:10.1046/j.1365-294X.2000.01106.x.

Hollingsworth, M.L., Clark, A.A., Forrest, L.L., Richardson, J., Pennington, R.T., Long, D.G., Cowan, R., Chase, M.W., Gaudeul, M., and Hollingsworth, P.M., 2009, Selecting barcoding loci for plants: evaluation of seven candidate loci with species-level sampling in three divergent groups of land plants: Molecular Ecology Resources, v. 9, p. 439–457. doi:10.1111/j.1755-0998.2008.02439.x.

International Finance Corporation, World Bank Group, 2002, Limestone Biodiversity Study, Hon Chong, Executive summary.

Kim, Baek Jun, Lee, Nam Sook, and Lee, Sang Don, 2011, Feeding diets of the Korean water deer (*Hydropotes inermis argyropus*) based on a 202 bp *rbc*L sequence analysis: Conservation Genetics, v. 12, no. 3, p. 851–856. doi:10.1007/s10592-011-0192-2.

Kress, W.J., and Erickson, D.L., 2007, A two-locus global DNA barcode for land plants: The coding *rbc*L gene complements the non-coding *trnH-psbA* spacer region: PLoS ONE, v. 2, article e508, 10 p. doi:10.1371/journal.pone.0000508.

Langham, N., 1983, Distribution and ecology of small mammals in three rain forest localities of Peninsula Malaysia with particular reference to Kedah Peak: Biotropica, v. 15, no. 3, p. 199–206.

Latinne, A., 2012, Diversity and endemism of Murinae rodents in Thai limestone karsts: a genetic approach [PhD dissertation], University of Liège, 254 p.

Latinne, A., Waengsothorn, S., Herbreteau, V., and Michaux, J.R., 2011, Evidence of complex phylogeographic structure for the threatened rodent *Leopoldamys neilli*, in Southeast Asia: Conservation Genetics, v. 12, no. 6, p. 1495–1511doi:10.1007/s10592-011-0248-3.

Latinne, A., Chaval, Y., Waengsothorn, S., Rojanadilok, P., Eiamampai, K., Sribuarod, K., Herbreteau, V., Morand, S., and Michaux, J.R., 2013a, Is *Leopoldamys neilli* (Rodentia, Muridae) a synonym of *Leopoldamys herberti*? A reply to Balakirev et al. (2013): Zootaxa, v. 3731, no. 4, p. 589–598. doi:10.11646/zootaxa.3731.4.10.

Latinne, A., Waengsothorn, S., Rojanadilok, P., Eiamampai, K., Sribuarod, K., and Michaux, J.R., 2012, Combined mitochondrial and nuclear markers revealed a deep vicariant history for *Leopolda-mys neilli*, a cave-dwelling rodent of Thailand: PLoS ONE, v. 7, no. 10, article e47670, 17 p. doi:10.1371/journal.pone.0047670.

Latinne, A., Waengsothorn, S., Rojanadilok, P., Eiamampai, K., Sribuarod, K., and Michaux, J.R., 2013b, Diversity and endemism of Murinae rodents in Thai limestone karsts: Systematics and Biodiversity, v. 11, no. 3, p. 323–344. doi:10.1080/14772000.2013.818587.

Lim, Boo-Liat, 1970, Distribution, relative abundance, food habits, and parasite patterns of giant rats (*Rattus*) in West Malaysia: Journal of Mammalogy, v. 51, no. 4, p. 730–740.

Marshall, J.D., 1977, Rats and mice of Thailand, *in* Lekagul, B., and McNeely, J.A., eds., Mammals of Thailand, Bangkok, Thailand, Saha Karn Bhaet, p. 395–490.

Meglécz, E., Piry, S., Desmarais, E., Galan, M., Gilles, A., Guivier, E., Pech, N., and Martin, J.-F., 2011, SESAME (SEquence Sorter & AMplicon Explorer): Genotyping based on high-throughput multiplex amplicon sequencing: Bioinformatics, v. 27, no. 2, p. 277–278. doi:10.1093/bioinformatics/btq641.

Musser, G.G., Smith, A.L., Robinson, M.F., and Lunde, D.P., 2005, Description of a New Genus and Species of Rodent (Murinae, Muridae, Rodentia) from Khammouan Limestone National Biodiversity Conservation Area in Lao PDR, American Museum Novitates, no. 3497, 31 p.

Musser, G.G., Lunde, D.P., and Son, N.T., 2006, Description of a New Genus and Species of Rodent (Murinae, Muridae, Rodentia) from the Tower Karst Region of Northeastern Vietnam, American Museum Novitates, no. 3517, 41 p.

Soininen, E.M., Valentini, A., Coissac, E., Miquel, C., Gielly, L., Brochmann, C., Brysting, A.K., Sønstebø, J.H., Ims, R.A., Yoccoz, N.G., and Taberlet, P., 2009, Analysing diet of small herbivores: the efficiency of DNA barcoding coupled with high-throughput pyrosequencing for deciphering the composition of complex plant mixtures: Frontiers in Zoology, v. 6, article 16, 9 p. doi:10.1186/1742-9994-6-16.

Taberlet, P., Coissac, E., Pompanon, F., Gielly, L., Miquel, C., Valentini, A., Vermat, T., Corthier, G., Brochmann, C., and Willerslev, E., 2007, Power and limitations of the chloroplast *trn*L (UAA) intron for plant barcoding: Nucleic Acids Research, v. 35, no. 3, article e14, 8 p. doi:10.1093/nar/gkl938.

Valentini, A., Miquel, C., Nawaz, M.A., Bellemain, E., Coissac, E., Pompanon, F., Gielly, L., Cruaud, C., Nascetti, G., Wincker, P., Swenson, J.E., and Taberlet, P., 2009, New perspectives in diet analysis based on DNA barcoding and parallel pyrosequencing: the *trn*L approach: Molecular Ecology Resources, v. 9, no. 1, p. 51–60. doi:10.1111/j.1755-0998.2008.02352.x.

Wells, K., Corlett, R.T., Lakim, M.B., Kalko, E.K.V., and Pfeiffer, M., 2009, Seed consumption by small mammals from Borneo: Journal of Tropical Ecology, v. 25, no. 5, p. 555–558. doi:10.1017/S0266467409990058.

Zhang, Hongmao, Cheng, Jinrui, Xiao, Zhishu, and Zhang, Zhibin, 2008, Effects of seed abundance on seed scatter-hoarding of Edward's rat (*Leopoldamys edwardsi* Muridae) at the individual level: Oecologia, v. 158, no. 1, p. 57–63. doi:10.1007/s00442-008-1114-y.

Zhang, Zheng, Schwartz, S., Wagner, L., and Miller, W., 2000, A greedy algorithm for aligning DNA sequences: Journal of Computational Biology, v. 7, no. 1–2, p. 203–214. doi:10.1089/10665270050081478.

MICROCLIMATE EFFECTS ON NUMBER AND DISTRIBUTION OF FUNGI IN THE WŁODARZ UNDERGROUND COMPLEX IN THE OWL MOUNTAINS (GÓRY SOWIE), POLAND

Rafał Ogórek[1], Wojciech Pusz[1*], Agnieszka Lejman[2], and Cecylia Uklańska-Pusz[3]

Abstract: In July 2013 we studied the occurrence of fungi in an underground complex named Włodarz, located inside the massif of Włodarz, within the Owl Mountains, Lower Silesia, Poland. The study is the first mycological evaluation of the rocks in the Włodarz underground complex and the air inside and outside of it. To examine the air, the Air Ideal 3P sampler and PDA medium were used. Microbiological evaluation of the rocks inside the adit was performed using two methods, swab sampling and rinse sampling. The results were analyzed by ANOVA, and means were compared using Fisher's least significant difference (LSD) test at $\alpha \leq 0.05$. Eleven taxa of filamentous fungi were isolated from the air sampled outside the Włodarz adit, and fifteen from the air inside. Between 65.5 and 1003 colony-forming units of fungi per m^3 of air were isolated from the air sampled in the adit and about 1115 CFU from the air sampled outside of it; the differences are statistically significant. The majority of the airborne fungi were isolated from outside the adit and from the ventilation shaft containing a waterfall, probably due to air movement. From the rock walls of the shafts seven taxa of fungi were isolated, whereas from the rock debris on the adit's floor, only six taxa. The densities of fungi obtained from the research locations are statistically significant, and the most dense fungus isolated from the air outside and inside the adit was *Cladosporium cladosporioides*, followed by *C. herbarum* at one locations in the adit. Taxa of the *Aspergillus niger* group were most common on the rock debris and wall rocks except for one location where *Penicillium chrysogenum* was most common on the rock debris and one location where *Cladosporium cladosporioides* was most common from the rocks walls.

Introduction

The Włodarz underground complex is a system of adits and shafts constructed inside the upper part of the massif of Włodarz (in German, Wolfsberg), part of the Owl Mountains (Góry Sowie) in Central Sudetes, Lower Silesia, Poland. The complex is located within the northeastern slope of the massif. The mountain range extends in the Central Sudetes along a northwest-southeast axis, but from the point of view of geology and tectonics, the material is distinct and described as the Owl Mountains gneiss.

The Włodarz complex is one of the components of a tunnel complex code-named Riese constructed by the Nazis beginning in 1943. The location had been chosen for two main reasons. The area was located away from the front lines, and the strength of the rock and the stability of the mountains was adequate protection against possible air strikes. The tunnels were drilled using mining techniques; prisoners bored holes into the rock substrate that were then loaded with explosives. The workforce used were prisoners from the Nazi concentration camp Gross-Rosen. Currently the interior of the complex can only be accessed by one of the four existing tunnels. Of the remaining three, two tunnels are now flooded and collapsed (Fig. 1). It is

assumed that the target number of tunnels was six, but no previous studies have confirmed the assumption. The entrances to the tunnels are located at an altitude between 585 and 590 m msl, and the tunnels run in the northeast-southwest direction inside the top-most part of Włodarz Massif. The total length of the known and mapped excavations is about 3100 m, with a total floor surface of approximately 10,710 m^2 and a volume of 42,000 m^3 (Kasza 2012). The Włodarz complex was opened for tourists beginning in 2004, with about forty thousand visitors a year, making it one of the most popular site for tourist visits in Lower Silesia.

The presence of tourists in caves and in other underground places is capable of changing the microclimate, the biogeochemistry, and the balance of organic matter in them. It may hence indirectly impact autochthonous microbial

* Corresponding Author: wojciech.pusz@up.wroc.pl
[1] Wrocław University of Environmental and Life Sciences, Department of Plant Protection, Division of Phytopathology and Mycology, pl. Grunwaldzki 24a, 50-363 Wrocław, Poland
[2] Wrocław University of Environmental and Life Sciences, Department of Agroecosystems and Green Areas Management
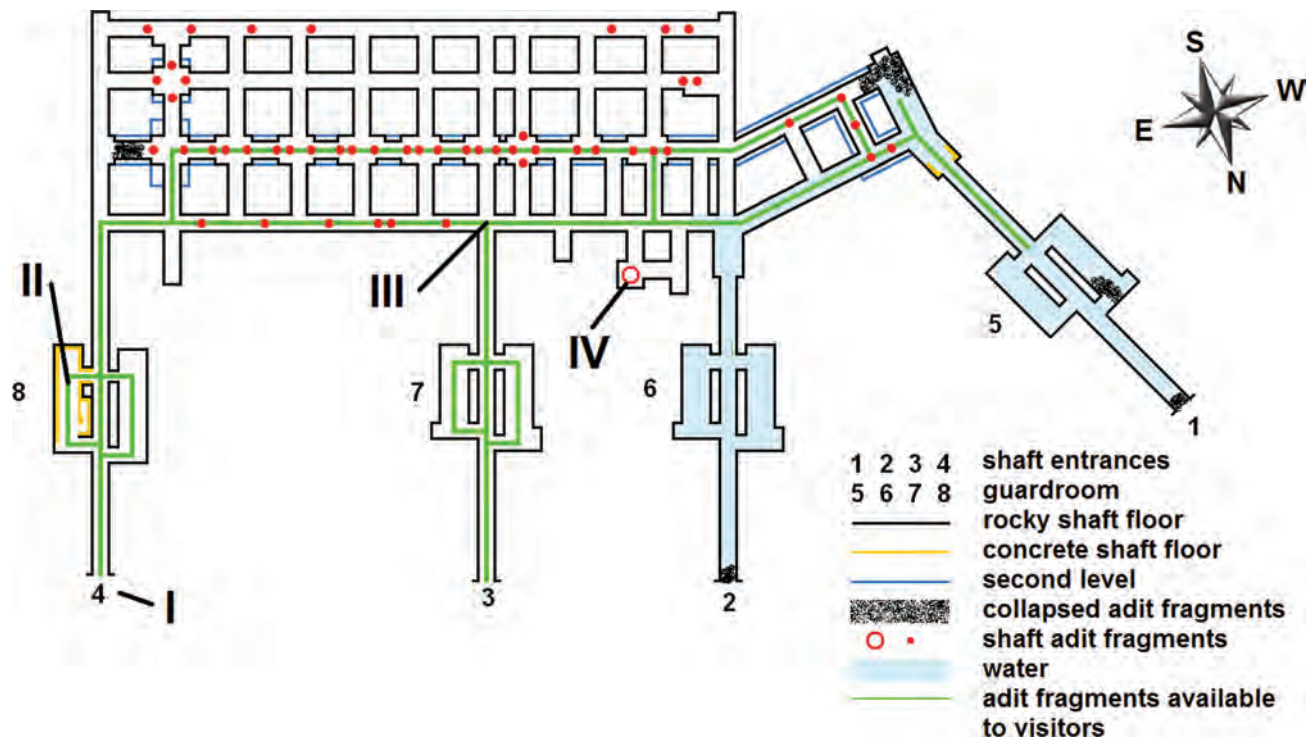[3] Wrocław University of Environmental and Life Sciences, Department of Horticulture

Figure 1. The plan, based on Kasra (2012), of the Włodarz underground complex of tunnels, with the sample locations indicated. I, the entrance; II, the guard house; III, the crossroads; and IV the ventilation shaft.

communities, such as those of fungi. Seen from that perspective, the visits are always undesirable, and therefore, the presence of microorganisms should be monitored in all cave and underground ecosystems. The identification of reservoirs of potentially pathogenic fungi and the elucidation of the distribution of these communities and their components are important not only in preventing potential health problems in tourists (Fernández-Cortés et al., 2011; Saíz-Jiménez, 2012), but also in maintaining the stability of any underground ecosystem. Fungi can be dangerous for humans and also affect the walls of caves and adits. In humans, they can cause infections and allergies. For example, *Aspergillus* spp. can cause aspergillosis of the lungs, sinuses, cornea, orbit, skin, nails, and ear canal. *Rhizopus* spp. can cause generalized mucormycosis, as well as infections of lungs and sinuses. Infection by *Fusarium* spp. can result in generalized fusariosis (Adamski et al., 2008). Fungi such as *Fusarium* spp. in caves and adits may cause biodeterioration of natural stones (Gu et al., 1998), and fungi such as *Epicoccum* spp. can contaminate stones with pigments (Li et al., 2008).

Our research focused on two goals: 1) the mycological analysis of the species composition of the fungi found in the air inside and outside of the underground Włodarz complex and on rocks in it, and 2) to quantify their concentrations.

Materials and Methods

The air samples were taken on July 5, 2013 from one location outside the adit (near entrance 4, sample location I in Fig. 1) and from three locations inside it, the guard house (II), the crossing (III), and the ventilation shaft (IV). The air temperature and relative humidity were measured using a thermohygrometer LB-522 (LAB-EL). The carbon dioxide concentration was measured using a CO_2 meter pSense RH (Gazex). Moisture content of rocks was measured with the Testo 606-1 (Testo) hygrometer, and the wind speed by aerometer Testo 410-1 (Testo).

Media

The following growth media were used: Potato Dextrose Agar (PDA, Biocorp), Czapek-Dox Agar (1.2% agar, Biocorp) and Malt Extract Agar (MEA, Biocorp). PDA medium was used for the isolation of fungi from the air and the rocks and for the identification of some species. Czapek-Dox agar medium and MEA medium were used for identification of the fungi of *Penicillium* and *Aspergillus* genera.

Fungal Identification

The fungal colonies grown on all the Petri dishes were counted and identified. The specific identification of the sampled fungi was performed using macro- and microscopic

Table 1. Microclimate conditions in the Włodarz underground complex on July 5, 2013.

Measurement Location	Air				Moisture Content, %	
	Temperature, °C	Relative Humitidy, %	Wind Speed, m s^{-1}	CO_2, ppm	Rock Wall	Rock Debris
Near the entrance (Site I)	24.6	50.2	0.8	390.0	···	···
Guard-house (Site II)	11.0	61.4	0.0	560.0	39.4	21.2
Crossroads (Site III)	10.6	67.4	0.0	608.0	36.0	21.0
Ventilation shaft with waterfall (Site IV)	12.8	98.0	0.2	400.0	39.9	32.1

observations of hyphae, conidia, and sporangia and colony morphology according to the commonly accepted methods used in mycological laboratories. The fungi were identified using diagnostic keys (Raper and Fennell 1965; Raper and Thom 1968; Ellis 1971; Zycha and Siepmann 1973; Arx 1974).

MYCOLOGICAL EVALUATION OF THE AIR

We used PDA medium to examine the fungal load of air. The sampler (Air Ideal 3P) was programmed for air sample volumes of 50 L, 100 L, and 150 L. Measurements in each location were performed in six replicates for each volume. The sampler was positioned 1.5 m above the level of the cave floor. The incubation of the cultures was carried out at room temperature (22 °C) for 2 to 7 days, in darkness. After the incubation, the fungi were identified and the numbers of colony forming units per m^3 of air were calculated.

MYCOLOGICAL EVALUATION OF THE ROCKS

Mycological evaluation of the rocks inside the adits was performed using two methods, swabbing of the wall and rinsing of rock debris.

At sample locations II, III, and IV inside the complex (Fig. 1) swabs of the wall were made using sterile swabs in transport tubes (sterile 15 cm viscose swab). Material from every location was sampled with three swabs from a surface area of 1 cm^2. The samples were taken from the cave walls at the height of 1.5 m above the floor. On the same day, the collected samples were shaken for 20 minutes in 50-ml Erlenmayer flasks containing 10 ml of sterile water. After shaking, the samples were placed in Petri dishes onto the PDA agar using serial dilution. The incubation of cultures was at room temperature (22 °C) in darkness, for 2 to 7 days. After incubation, the fungi were identified and the numbers of CFU per cm^2 of rock surface were calculated.

At sampling locations II, III, and IV (Fig. 1), four samples of rock debris from the floor were collected in sterile sampling bags (114 by 229 mm). On the same day, each sample (ca. 50 g) was shaken for 20 minutes in a 250-mL Erlenmeyer flask containing 100 mL of sterile water. After shaking, the samples were plated onto PDA agar using serial dilution. The incubation of cultures was for 2

to 7 days. After the incubation, the fungal taxa were identified and the numbers of CFU per 50 g of rock debris were calculated.

STATISTICAL ANALYSIS

The results were analyzed by ANOVA, using Statistica 9.0 package. Means were compared using Fisher's least-significant-difference test at $\alpha \leq 0.05$.

RESULTS

The results of the environmental measurements are in Table 1. The air temperature during the study in Włodarz complex was 24.6 °C outside the adit and approximately 11 °C inside it. The wind at the entrance (Site I) was 0.8 m s^{-1}. Inside air movement was only observed at the ventilation shaft with the waterfall (Site IV), and there it was only 0.2 m s^{-1}. The highest concentration of carbon dioxide was observed inside the adit at Site III, and the lowest was at the entrance. Rock moisture was higher in wall rock than in debris on the adit's floor.

Eleven taxa of filamentous fungi were cultured from the air sampled outside the Włodarz complex and fifteen from the inside air. From the rock walls we cultured seven taxa of fungi, but only six taxa from the floor debris. *Aspergillus niger* group and *Mucor* spp. were present only on the rock, whereas *Acremonium strictum*, *Alternaria alternata*, *Botrytis cinerea*, *Cladosporium herbarum*, *Epicoccum nigrum*, *Fusarium avenaceum*, *Fusarium equiseti*, *Penicillium citrinum*, *Penicillium waksmanii*, *Sordaria fimicola*, and *Ulocladium alternariae* were found exclusively in the air (Table 2).

The quantities of filamentous fungi taxa isolated from the air inside and outside the Włodarz adit ranged between 65.5 to 1115.9 colony forming units per m^3 of air (Table 3). The most taxa of filamentous fungi were isolated from the air outside the complex, whereas from the air inside, the highest number of species were isolated from the ventilation shaft with waterfall (Site IV) and the smallest number of species from this group was observed in the guard house (Table 3). The highest density of colonies, both from the rock walls and from the rock debris on the adit's floor, were cultured from the ventilation shaft with waterfall (Tables 4 and 5). The smallest number of CFU was

Table 2. Species of filamentous fungi cultured from the outside and inside air and from the rocks in the Włodarz complex. A + indicates the species was found.

Taxa		Air		Rock	
		Outside	Inside	Wall	Debris
1	*Aspergillus niger* group	−	−	+	+
2	*Acremonium strictum*	+	−	−	−
3	*Alternaria alternata*	+	−	−	−
4	*Botrytis cinerea*	−	+	−	−
5	*Cladosporium cladosporioides*	+	+	+	+
6	*Cladosporium herbarum*	+	+	−	−
7	*Epicoccum nigrum*	+	+	−	−
8	*Fusarium avenaceum*	−	+	−	−
9	*Fusarium culmorum*	−	+	+	−
10	*Fusarium equiseti*	+	−	−	−
11	*Fusarium oxysporum*	+	+	+	−
12	*Mucor* spp.	−	−	+	+
13	*Penicillium chrysogenum*	−	+	−	+
14	*Penicillium citrinum*	+	+	−	−
15	*Penicillium expansum*	−	+	+	−
16	*Penicillium waksmanii*	−	+	−	−
17	*Rhizopus* spp.	+	+	+	+
18	*Sclerotinia sclerotiorum*	−	+	−	+
19	*Sordaria fimicola*	+	+	−	−
20	*Ulocladium alternariae*	+	+	−	−
Σ species		11	15	7	6

observed in the guard house for rock debris, while for rock wall both the guard house and the crossroads sites were smallest and statistically similar. (Tables 4 and 5).

The fungus most frequently cultured from the air outside and inside the adit was *Cladosporium cladosporioides*, except in the guard house, where *C. herbarum* was most common. The least common fungus species in the outside air was *Acremonium strictum*, but the abundance of this species do not differ significantly from that of six other species. The species *Epicoccum nigrum*, *Fusarium culmorum*, *Penicillium citrinum*, *Sclerotinia sclerotiorum*, and *Ulocladium alternariae* were the least common in the guard house, *F. culmorum* was least common in the crossroads samples, and *F. culmorum* and *F. oxysporum* were least common at the ventilation shaft site (Table 3).

The species most common in cultured from the rock walls and the rocky debris was the *Aspergillus niger* group in the guard house and crossroads locations, while at the ventilation shaft *Cladosporium cladosporioides* was most common on the rock walls and *Penicillium chrysogenum* in rocky floor debris (Tables 4 and 5).

Discussion

The total numbers of fungi cultured from the air at the various sampling sites differed significantly (Table 3). The most airborne fungi were found outside the complex (Site I

in Fig. 1) and in the ventilation shaft with waterfall (Site IV). The situation is probably due to the air movement at those locations (Table 1). Moreover, the complex is populated by bat colonies and accessible to tourism (Martini, 1963; Shapiro and Pringle, 2010; Porca et al., 2011; Ogórek et al., 2013). Mulec (2008) reported that microbes are passively transported by airflows, which depend on the season and represent an important mode of spreading inoculum to different parts of caves. Dripping and seeping water, as in the Włodarz complex at the ventilation shaft, may be another carrier of microbes. Hsu and Agoramoorthy (2001), Kuzmina et al. (2012), and Mulec et al. (2012) noted that microorganisms show decreasing biodiversity and biomass starting from the entrance towards the deep zones in caves, a gradient that they found very important for survival and development of fungi.

According to Nieves-Rivera (2003), Nováková (2009), and Vanderwolf et al. (2013), the most abundant fungi in caves are *Aspergillus*, *Penicillium*, *Mucor*, *Fusarium*, *Trichoderma*, and those of *Cladosporium* genus. Our results agree with theirs. The most common airborne fungi in the Włodarz complex were *Cladosporium* from air, *Aspergillus* and *Cladosporium* from rock walls, and *Aspergillus* and *Penicillium* from rocky debris. These results were statistically significant. The work of other researchers surveying caves with respect to fungal spores supports these findings.

Table 3. Filamentous fungi cultured from the air at the Włodarz underground complex, with means of colony forming units per m^3 for six replicated air samples.

Sampling Location	Taxa		Air (CFU/m^3)	
	Name	Percent		
Near Entrance (Site I)	*Alternaria alternata*	0.3	3.3	d
	Acremonium strictum	0.3	3.1	d
	Botrytis cinerea	29.8	333.0	b
	Cladosporium cladosporioides	58.2	650.0	a
	Cladosporium herbarum	3.6	40.0	c
	Epicoccum nigrum	0.6	6.7	d
	Fusarium equiseti	0.3	3.0	d
	Fusarium oxysporum	0.6	6.7	d
	Penicillium citrinum	2.1	23.3	cd
	Rhizopus spp.	3.0	33.0	c
	Sclerotinia sclerotiorum	0.6	6.7	d
	Ulocladium alternariae	0.6	7.1	d
			1115.9	A
Guard House (Site II)	*Cladosporium cladosporioides*	8.1	5.3	d
	Cladosporium herbarum	42.6	28.0	a
	Epicoccum nigrum	2.3	1.5	e
	Fusarium culmorum	2.0	1.3	e
	Penicillium chrysogenum	12.2	8.0	b
	Penicillium citrinum	1.7	1.1	e
	Penicillium expansum	8.1	5.3	d
	Penicillium waksmanii	10.2	6.7	c
	Rhizopus spp.	8.4	5.5	cd
	Sclerotinia sclerotiorum	2.0	1.3	e
	Ulocladium alternariae	2.4	1.6	e
			65.5	D
Crossroads (Site III)	*Cladosporium cladosporioides*	33.8	25.0	a
	Cladosporium herbarum	19.6	14.4	c
	Fusarium culmorum	1.5	1.1	f
	Penicillium chrysogenum	6.8	5.0	e
	Penicillium citrinum	7.5	5.6	e
	Penicillium expansum	21.8	16.1	b
	Sclerotinia sclerotiorum	9.0	6.7	d
			73.9	B
Ventilation Shaft with Waterfall (Site IV)	*Botrytis cinerea*	1.1	11.0	e
	Cladosporium cladosporioides	84.8	851.0	a
	Cladosporium herbarum	6.0	60.0	b
	Epicoccum nigrum	0.7	6.7	fg
	Fusarium avenaceum	0.5	5.1	gh
	Fusarium culmorum	0.3	3.0	h
	Fusarium oxysporum	0.3	3.3	h
	Penicillium expansum	2.0	20.0	d
	Sclerotinia sclerotiorum	3.3	33.3	c
	Sordaria fimicola	1.0	9.6	ef
			1003.0	C

For each location, concentrations followed by the same letter are not statistically different at the $\alpha \leq 0.05$ level according to Fisher's least-significant-difference test; others are. Small letters mark the effect of locations on isolates taxa fungi. Capital letters mark the effect of a particular location on total fungal isolates.

Table 4. Filamentous fungi cultured from swab sampling the wall rock in the Włodarz undergound complex, means of three replicate samples.

| Sampling Location | Taxa | | Rock Surface (CFU/cm^3) | |
	Name	Percent		
Guard-House (Site II)	*Aspergillus niger* group	42.8	43.7	a
	Cladosporium cladosporioides	9.2	9.4	d
	Mucor spp.	22.9	23.4	b
	Penicillium chrysogenum	5.5	5.6	e
	Rhizopus spp.	19.7	20.1	c
			102.2 B	B
Crossroads (Site III)	*Aspergillus niger* group	55.4	57.3	a
	Mucor spp.	20.7	21.4	c
	Rhizopus spp.	23.9	24.7	b
			103.4	B
Ventilation Shaft with Waterfall (Site IV)	*Aspergillus niger* group	14.0	25.0	c
	Cladosporium cladosporioides	37.1	66.0	a
	Fusarium culmorum	6.2	11.0	f
	Fusarium oxysporum	4.5	8.0	g
	Mucor spp.	16.3	29.0	b
	Penicillium expansum	9.6	17.0	e
	Rhizopus spp.	12.4	22.0	d
			178.0	A

For each location, concentrations followed by the same letter are not statistically different at the α ≤ 0.05 level according to Fisher's least-significant-difference test; others are. Small letters mark the effect of locations on isolates taxa fungi. Capital letters mark the effect of a particular location on total fungal isolates.

A cave in Spain examined by Docampo et al. (2011) turned out to host several fungal species, with *Penicillium* and *Cladosporium* genera being the most numerous. Interestingly, in our air sampling both near the entrance and inside we found mostly the spores of *Cladosporium* at the Włodarz complex. Our results generally agree with those of Porca et al. (2011) and Fernández-Cortés et al. (2011). They claimed that the most abundant type of spore in the

Table 5. Filamentous fungi cultured from rinse sampling the floor rock debris in the Włodarz undergound complex, means of four replicate samples.

| Sampling Location | Taxa | | Rock (CFU / 50 g) | |
	Name	Percent		
Guard-House (Site II)	*Aspergillus niger* group	55.7	76.0	a
	Mucor spp.	28.6	39.0	b
	Penicillium chrysogenum	7.5	10.2	c
	Sclerotinia sclerotiorum	8.3	11.3	c
			136.5	C
Crossroads (Site III)	*Aspergillus niger* group	62.8	104.2	a
	Cladosporium cladosporioides	3.1	5.1	d
	Mucor spp.	24.1	40.0	b
	Rhizopus spp.	10.0	16.5	c
			165.8	B
Ventilation Shaft with Waterfall (Site IV)	*Aspergillus niger* group	4.3	16.3	d
	Cladosporium cladosporioides	17.3	66.0	c
	Mucor spp.	26.2	100.0	b
	Penicillium chrysogenum	52.3	200.0	a
			382.3	A

For each location, concentrations followed by the same letter are not statistically different at the α ≤ 0.05 level according to Fisher's least-significant-difference test; others are. Small letters mark the effect of locations on isolates taxa fungi. Capital letters mark the effect of a particular location on total fungal isolates.

external environment was *Cladosporium*, whereas the spores most widely represented inside the cave belonged to *Aspergillus* and *Penicillium*. According to other authors, the most abundant fungal taxa isolated from rocks, especially from granite, were from the family *Mucorales*, and the genera *Penicillium*, *Phoma*, *Auerobasidium*, and *Trichoderma* (Hirsch et al., 1995; Burford et al., 2003 a,b; Brunner et al., 2011). Our results show statistical differences in the numbers of fungi isolated from the rocks, and the most abundant fungi cultured from granite inside the Włodarz complex were the *Aspergillus niger* group from Sites I and II and *Cladosporium cladosporioides* from rock walls and *Penicillium chrysogenum* from rock debris from Site IV. High concentrations of *Cladosporium* spp. on the walls at the ventilation shaft are probably caused by the movements of air and water from the outside into the complex there. The ventilation shaft provides a constant bidirectional exchange of air from the external environment that was dominated fungi of the genus *Cladosporium*.

During the present study, the humidity of the air and the rock moisture inside and outside the complex were conducive for the survival and development of fungi. The air temperature outside, but not inside, was favorable to their development. Krzysztofik (1992) reported that the most important factors affecting the survival of fungi in the environment are temperature and humidity. Nevertheless, that author had observed that the incidence of fungi in the investigated shafts had been dependent on airflow. This is consistent with the numbers of fungi cultured from the air inside our complex and from rocks there. The most fungi were isolated from locations with air movement, including an interior one connected with the external environment.

The high concentrations of carbon dioxide inside the complex may be brought about by tourists or bats or by fungi that decompose organic matter. Hoyos et al. (1998) reported that opening a cave to tourists can result in changes in its microclimatic conditions and the food web, as the mass of visitors increases the cave temperature, CO_2 concentration, and the amount of water vapor in the cave's atmosphere. As the Włodarz underground complex is fairly popular for tourist visits, the possible influence of visitors on the conditions in the cave seems quite likely to affect the fungal populations hosted by it. Although Wells and Uota (1970) report that some fungi species decrease in abundance where the highest values of carbon dioxide are observed, it appears that in some situations higher carbon dioxide concentrations may stimulate fungi to more intensive growth.

Conclusions

Mycobiota of the artificial underground are generally similar to those of natural caves. The internal microclimate and the air flow in adits produce statistically distinct concentrations and species compositions of filamentous fungi in them. Most fungi in the Włodarz underground complex occur in places where they may have migrated from the external environment due to air flow. The most frequently cultured fungi from the air outside and inside the complex were *Cladosporium* spp. The *Aspergillus niger* group were most commonly found on the rocks walls and rock debris except for one location, where *Penicillium chrysogenum* was the species most often isolated from the bottom substrate rocks and *C. cladosporioides* from the rock walls. The incidence level of the fungi isolated from internal air of the adit constitutes no threat to the health of the visiting tourists, though it may be problematic due to possible effects on historical objects like mining trolleys or uniforms. Therefore, it seems that speleomycological research and monitoring are not only important for the underground ecosystems themselves, but also for protection of historical memorabilia.

References

Adamski, Z., Henke, K., Zawirska, A., and Kubisiak-Rzepczyk, H., 2008, Grzybice narządowe (Fungal infections of the organs), *in* Baran, E., ed., Mykologia – co nowego? (Mycology—What's New?), Wrocław, Cornetis, p. 189–202.

Arx, J.A. von., 1974, The Genera of Fungi Sporulating in Pure Culture, Berlin, J. Cramer, 315 p.

Brunner, I., Plötze, M., Rieder, S., Zumsteg, A., Furrer, G., and Frey, B., 2011, Pioneering fungi from the Damma glacier forefield in the Swiss Alps can promote granite weathering: Geobiology, v. 9, p. 266–279. doi:10.1111/j.1472-4669.2011.00274.x.

Burford, E.P., Fomina, M., and Gadd, G.M., 2003a, Fungal involvement in bioweathering and biotransformation of rocks and minerals: Mineralogical Magazine, v. 67, p. 1127–1155. doi:10.1180/0026461036760154.

Burford, E.P., Kierans, M., and Gadd, G.M., 2003b, Geomycology: fungi in mineral substrata: Mycologist, v. 17, no. 3, p. 98–107. doi:10.1017/S0269915X03003112.

Docampo, S., Trigo, M.M., Recio, M., Melgar, M., García-Sanchez, J., and Cabezudo, B., 2011, Fungal spore content of the atmosphere of the Cave of Nerja (southern Spain): diversity and origin: Science of the Total Environment, v. 409, p. 835–843. doi:10.1016/j.scitotenv.2010.10.048.

Ellis, M.B., 1971, Dematiaceous Hyphomycetes: Kew, Surrey, Commonwealth Mycological Institute, 608 p.

Fernández-Cortés, A., Cuezva, S., Sánchez-Moral, S., Cañaveras, J.C., Porca, E., Jurado, V., Martin-Sánchez, P.M., and Saíz-Jiménez, C., 2011, Detection of human-induced environmental disturbances in a show cave: Environmental Science and Pollution Research, v. 18, p. 1037–1045. doi:10.1007/s11356-011-0513-5.

Gu, Ji-Dong, Ford, T.E., Berke, N.S., and Mitchell, R., 1998, Biodeterioration of concrete by the fungus *Fusarium*: International Biodeterioration and Biodegradation, v. 41, p. 101–109. doi:10.1016/S0964-8305(98)00034-1.

Hirsch, P., Eckhardt, F.E.W., and Palmer, R.J. Jr., 1995, Fungi active in weathering of rock and stone monuments: Canadian Journal of Botany, v. 72, no. S1, p. 1384–1390. doi:10.1139/b95-401.

Hoyos, M., Soler, V., Cañaveras, J.C., Sánchez-Moral, S., and Sanz-Rubio, E., 1998, Microclimatic characterization of a karstic cave: human impact on microenvironmental parameters of a prehistoric rock art cave (Candamo Cave, northern Spain): Environmental Geology, v. 33, p. 231–242. doi:10.1007/s002540050242.

Hsu, Minna J., and Agoramoorthy, G., 2001, Occurrence and diversity of thermophilous soil microfungi in forest and cave ecosystems of Taiwan: Fungal Diversity, v. 7, p. 27–33.

Kasza, D., 2012, Możliwosci wykorzystania aplikacji GIS do prac związanych z kartowaniem geologicznym na przykładzie podziemnego obiektu "Włodarz" w Górach Sowich: Prace Naukowe Instytutu Górnictwa Politechniki Wrocławskiej, no. 135, p. 23–35. doi:10.5277/gig121802.

Krzysztofik, B., 1992, Mikrobiologia powietrza, Warsaw, Wydawnictwa Politechniki Warszawskiej, Warsaw, 198 p.

Kuzmina, L.Y., Galimzianova, N.F., Abdullin, S.R., and Ryabova, A.S., 2012, Microbiota of the Kinderlinskaya Cave (South Urals, Russia): Microbiology, v. 81, no. 2, p. 251–258. doi:10.1134/S0026261712010109.

Li, Xianshu, Arai, H., Shimoda, I., Kuraishi, H., and Katayama, Y., 2008, Enumeration of sulfur-oxidizing microorganisms on deteriorating stone of the Angkor monuments Cambodia: Microbes and Environments, v. 23, p. 293–298. doi:10.1064/jsme2.ME08521.

Martini, A., 1963, Yeasts in cavern environments: Archiv für Mikrobiologie, v. 45, p. 111–114. doi:10.1007/BF00408431.

Mulec, J., 2008, Microorganisms in hypogeon: examples from Slovenian karst caves: Acta Carsologica, v. 37, no. 1, p. 153–160.

Mulec, J., Vaupotič, J., and Walochnik, J., 2012, Prokaryotic and eukaryotic airborne micoorganisms as tracers of microclimatic changes in the underground (Postojna Cave, Slovenia): Microbial Ecology, v. 64, p. 654–667. doi:10.1007/s00248-012-0059-1.

Nieves-Rivera, Á.M., 2003, Mycological survey of Rio Camuy Caves Park, Puerto Rico: Journal of Cave and Karst Studies, v. 65, no. 1, p. 23–28.

Nováková, A., 2009, Microscopic fungi isolated from the Domica Cave system (Slovak Karst National Park, Slovakia). A review: International Journal of Speleology, v. 38, p. 71–82. doi:10.5038/1827-806X.38.1.8.

Ogórek, R., Lejman, A., and Matkowski, K., 2013, Fungi isolated from Niedźwiedzia Cave in Kletno (Lower Silesia, Poland): International Journal of Speleology, v. 42, p. 161–166. doi:10.5038/1827-806X.42.2.9.

Porca, E., Jurado, V., Martin-Sanchez, P.M., Hermosin, B., Bastian, F., Alabouvette, C., and Saiz-Jimenez, C., 2011, Aerobiology: an ecological indicator for early detection and control of fungal outbreaks in caves: Ecological Indicators, v. 11, p. 1594–1598. doi:10.1016/j.ecolind.2011.04.003.

Raper, K.B., and Fennell, D.I., 1965, The Genus Aspergillus: Baltimore, Williams and Wilkins Company, 686 p.

Raper, K.B., and Thom, C., 1968, A Manual of the Penicillia: New York, Hafner Publishing Company, 876 p.

Saíz-Jiménez, C., 2012, Microbiological and environmental issues in show caves: World Journal of Microbiology and Biotechnology, v. 28, no. 7, p. 2453–2464. doi:10.1007/s11274-012-1070-x.

Shapiro, J., and Pringle, A., 2010, Anthropogenic influences on the diversity of fungi isolated from caves in Kentucky and Tennessee: American Midland Naturalist, v. 163, no. 1, p. 76–86. doi:10.1674/0003-0031-163.1.76.

Vanderwolf, K.J., Malloch, D., McAlpine, D.F., and Forbes, G.J., 2013, A world review of fungi, yeasts, and slime molds in caves: International Journal of Speleology, v. 42, no. 1, p. 77–96. doi:10.5038/1827-806X.42.1.9.

Wells, J.M., and Uota, M., 1970, Germination and growth of five fungi in low-oxygen and high-carbon dioxide atmospheres: Phytopathology, v. 60, no. 1, p. 50–53. doi:10.1094/Phyto-60-50.

Zycha, H., Siepmann, R., and Linnemann, G., 1973, Keys to the Families, Genera and Species of the Mucorales: Berlin, J. Cramer, 49 p.

BOOK REVIEW

Sources et Sites des Eaux Karstiques
(Karst springs and their settings)

Jean Nicod, 2012, Méditerranée (Geographical revue of Mediterranean countries), Special edition, Presses Universitaires de Provence, 29 ave. Robert Schuman, 13621 Aix-en-Provence, Cedes 01, France, 277 p., 8.2 × 11.5 in., ISBN 978-2-85399-810-9, soft-cover, €30 (~$40).

Few readers of this journal are fluent in French, but when this book arrived for review it showed promise beyond its immediate goal of summarizing the significant karst in the countries bordering the Mediterranean. Prof. Nicod, one of the world's premier karst researchers, has assembled a lifetime of information about this important region. In condensed fashion, he summarizes his own research and that of many others. It is purposely not comprehensive, but contains the most representative and instructive examples.

Karst geomorphology and land use are the major topics. The author admits to an ''old-school'' approach, with much attention to the physical setting and how people have adapted to it. Most of the emphasis is on the southern European countries, less so on the Levant and northern Africa, but the geographic range extends outward as far as Germany. Many observations span several decades, giving a historical perspective. Surface features receive more emphasis than caves.

The book contains four major sections: (1) karst springs and their geographic context, (2) karst lakes, (3) water supply, dams, and aqueducts in karst, and (4) travertine sites. These are divided into a total of eighteen chapters, each containing numerous individual topics. There are many sidebars with special examples and case histories, many of them classics. In the rear are fifteen pages of color photos and maps, including a detailed two-page spread of the region covered.

Descriptions are short and to the point, but with room for instructive anecdotes. More than half the space is devoted to monochrome photos, diagrams, maps, sketches, and tables. Geologic maps and cross sections are detailed, but many of the cave profiles are simplified. Many show their age by their informal but personalized hand-drawn style. Each chapter ends with a list of pertinent references.

Case histories provide examples and odd anecdotes of the use (and misuse) of karst water, such as vanishing lakes, reservoirs that never filled, and pollution. For example, one learns that much of the upper part of the Danube River disappears underground and emerges in a distant karst spring in the Rhine basin, to reach the ocean at the opposite end of Europe from where it was originally headed. Have you heard of the accidental water-trace with absinthe? Or the deep springs that are the indirect result of the Messinian Crisis when the Mediterranean Sea dried up a few million years ago? Or what life is like in a home carved out of travertine deposited by karst springs? Or St. John of Tufa?

What if you don't read French? First find an interesting map or diagram or exclamation points in the text and enter the accompanying sentences into one of the free on-line translation sites. Optical character recognition on your scanner can even bypass the need for typing. The translation will not be poetic, but anyone familiar with karst will understand it.

Prof. Nicod dedicates this book as a tribute to his colleagues, past and present. He recognizes that their original material is scattered and increasingly difficult to find, and that modern researchers rarely probe the older literature. These statements can be read as an invitation: Researchers with a life-long passion have much to say, and they are encouraged to summarize the developments they have witnessed in their fields so that the record is preserved.

Reviewed by Arthur N. Palmer, Dept. of Earth and Atmospheric Sciences, State University of New York, Oneonta, NY 13820-4015, (palmeran@oneonta.edu).

GUIDE TO AUTHORS

The *Journal of Cave and Karst Studies* is a multidisciplinary journal devoted to cave and karst research. The *Journal* is seeking original, unpublished manuscripts concerning the scientific study of caves or other karst features. Authors do not need to be members of the National Speleological Society, but preference is given to manuscripts of importance to North American speleology.

LANGUAGES: The *Journal of Cave and Karst Studies* uses American-style English as its standard language and spelling style, with the exception of allowing a second abstract in another language when room allows. In the case of proper names, the *Journal* tries to accommodate other spellings and punctuation styles. In cases where the Editor-in-Chief finds it appropriate to use non-English words outside of proper names (generally where no equivalent English word exists), the *Journal* italicizes them. However, the common abbreviations i.e., e.g., et al., and etc. should appear in roman text. Authors are encouraged to write for our combined professional and amateur readerships.

CONTENT: Each paper will contain a title with the authors' names and addresses, an abstract, and the text of the paper, including a summary or conclusions section. Acknowledgments and references follow the text.

ABSTRACTS: An abstract stating the essential points and results must accompany all articles. An abstract is a summary, not a promise of what topics are covered in the paper.

STYLE: The *Journal* consults The Chicago Manual of Style on most general style issues.

REFERENCES: In the text, references to previously published work should be followed by the relevant author's name and date (and page number, when appropriate) in parentheses. All cited references are alphabetical at the end of the manuscript with senior author's last name first, followed by date of publication, title, publisher, volume, and page numbers. Geological Society of America format should be used (see http://www.geosociety.org/pubs/geoguid5. htm). Please do not abbreviate periodical titles. Web references are acceptable when deemed appropriate. The references should follow the style of: Author (or publisher), year, Webpage title: Publisher (if a specific author is available), full URL (e.g., http://www. usgs.gov/citguide.html) and date when the web site was accessed in brackets; for example [accessed July 16, 2002]. If there are specific authors given, use their name and list the responsible organization as publisher. Because of the ephemeral nature of websites, please provide the specific date. Citations within the text should read: (Author, Year).

SUBMISSION: Effective February 2011, all manuscripts are to be submitted via Peertrack, a web-based system for online submission. The web address is http://www.edmgr.com/jcks. Instructions are provided at that address. At your first visit, you will be prompted to establish a login and password, after which you will enter information about your manuscript (e.g., authors and addresses, manuscript title, abstract, etc.). You will then enter your manuscript, tables, and figure files separately or all together as part of the manuscript. Manuscript files can be uploaded as DOC, WPD, RTF, TXT, or LaTeX. A DOC template with additional manuscript specifications may be downloaded. (Note: LaTeX files should not use any unusual style files; a LaTeX template and BiBTeX file for the *Journal* may be downloaded or obtained from the Editor-in-Chief.) Table files can be uploaded as DOC, WPD, RTF, TXT, or LaTeX files, and figure files can be uploaded as TIFF, EPS, AI, or CDR files. Alternatively, authors may submit manuscripts as PDF or HTML files, but if the manuscript is accepted for publication, the manuscript will need to be submitted as one of the accepted file types listed above. Manuscripts must be typed, double spaced, and single-sided. Manuscripts should be no longer than 6,000 words plus tables and figures, but exceptions are permitted on a case-by-case basis. Authors of accepted papers exceeding this limit may have to pay a current page charge for the extra pages unless decided otherwise by the Editor-in-Chief. Extensive supporting data will be placed on the *Journal*'s website with a paper copy placed in the NSS archives and library. The data that are used within a paper must be made available. Authors may be required to provide supporting data in a fundamental format, such as ASCII for text data or comma-delimited ASCII for tabular data.

DISCUSSIONS: Critical discussions of papers previously published in the *Journal* are welcome. Authors will be given an opportunity to reply. Discussions and replies must be limited to a maximum of 1000 words and discussions will be subject to review before publication. Discussions must be within 6 months after the original article appears.

MEASUREMENTS: All measurements will be in Systeme Internationale (metric) except when quoting historical references. Other units will be allowed where necessary if placed in parentheses and following the SI units.

FIGURES: Figures and lettering must be neat and legible. Figure captions should be on a separate sheet of paper and not within the figure. Figures should be numbered in sequence and referred to in the text by inserting (Fig. x). Most figures will be reduced, hence the lettering should be large. Photographs must be sharp and high contrast. Color will generally only be printed at author's expense.

TABLES: See http://www.caves.org/pub/journal/PDF/Tables. pdf to get guidelines for table layout.

COPYRIGHT AND AUTHOR'S RESPONSIBILITIES: It is the author's responsibility to clear any copyright or acknowledgement matters concerning text, tables, or figures used. Authors should also ensure adequate attention to sensitive or legal issues such as land owner and land manager concerns or policies.

PROCESS: All submitted manuscripts are sent out to at least two experts in the field. Reviewed manuscripts are then returned to the author for consideration of the referees' remarks and revision, where appropriate. Revised manuscripts are returned to the appropriate Associate Editor who then recommends acceptance or rejection. The Editor-in-Chief makes final decisions regarding publication. Upon acceptance, the senior author will be sent one set of PDF proofs for review. Examine the current issue for more information about the format used.

ELECTRONIC FILES: The *Journal* is printed at high resolution. Illustrations must be a minimum of 300 dpi for acceptance.

Journal of Cave and Karst Studies

Volume 76   Number 2   August 2014